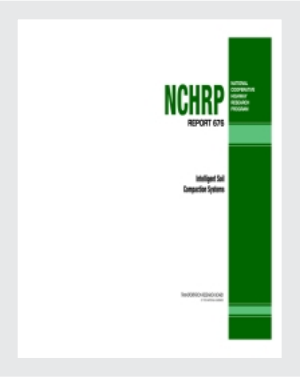

Intelligent Soil Compaction Systems

DETAILS

165 pages | | PAPERBACK
ISBN 978-0-309-15519-9 | DOI 10.17226/22922

AUTHORS

NATIONAL COOPERATIVE HIGHWAY RESEARCH PROGRAM

NCHRP REPORT 676

Intelligent Soil Compaction Systems

Michael A. Mooney
Robert V. Rinehart
Norman W. Facas
Odon M. Musimbi
Colorado School of Mines
Golden, CO

David J. White
Pavana K. R. Vennapusa
Iowa State University
Ames, IA

Subscriber Categories
Construction • Geotechnology • Pavements

Research sponsored by the American Association of State Highway and Transportation Officials
in cooperation with the Federal Highway Administration

TRANSPORTATION RESEARCH BOARD

WASHINGTON, D.C.
2010
www.TRB.org

NATIONAL COOPERATIVE HIGHWAY RESEARCH PROGRAM

Systematic, well-designed research provides the most effective approach to the solution of many problems facing highway administrators and engineers. Often, highway problems are of local interest and can best be studied by highway departments individually or in cooperation with their state universities and others. However, the accelerating growth of highway transportation develops increasingly complex problems of wide interest to highway authorities. These problems are best studied through a coordinated program of cooperative research.

In recognition of these needs, the highway administrators of the American Association of State Highway and Transportation Officials initiated in 1962 an objective national highway research program employing modern scientific techniques. This program is supported on a continuing basis by funds from participating member states of the Association and it receives the full cooperation and support of the Federal Highway Administration, United States Department of Transportation.

The Transportation Research Board of the National Academies was requested by the Association to administer the research program because of the Board's recognized objectivity and understanding of modern research practices. The Board is uniquely suited for this purpose as it maintains an extensive committee structure from which authorities on any highway transportation subject may be drawn; it possesses avenues of communications and cooperation with federal, state and local governmental agencies, universities, and industry; its relationship to the National Research Council is an insurance of objectivity; it maintains a full-time research correlation staff of specialists in highway transportation matters to bring the findings of research directly to those who are in a position to use them.

The program is developed on the basis of research needs identified by chief administrators of the highway and transportation departments and by committees of AASHTO. Each year, specific areas of research needs to be included in the program are proposed to the National Research Council and the Board by the American Association of State Highway and Transportation Officials. Research projects to fulfill these needs are defined by the Board, and qualified research agencies are selected from those that have submitted proposals. Administration and surveillance of research contracts are the responsibilities of the National Research Council and the Transportation Research Board.

The needs for highway research are many, and the National Cooperative Highway Research Program can make significant contributions to the solution of highway transportation problems of mutual concern to many responsible groups. The program, however, is intended to complement rather than to substitute for or duplicate other highway research programs.

NCHRP REPORT 676

Project 21-09
ISSN 0077-5614
ISBN 978-0-309-15519-9
Library of Congress Control Number 2010939000

COPYRIGHT INFORMATION

NOTICE

The project that is the subject of this report was a part of the National Cooperative Highway Research Program, conducted by the Transportation Research Board with the approval of the Governing Board of the National Research Council.

The members of the technical panel selected to monitor this project and to review this report were chosen for their special competencies and with regard for appropriate balance. The report was reviewed by the technical panel and accepted for publication according to procedures established and overseen by the Transportation Research Board and approved by the Governing Board of the National Research Council.

The opinions and conclusions expressed or implied in this report are those of the researchers who performed the research and are not necessarily those of the Transportation Research Board, the National Research Council, or the program sponsors.

The Transportation Research Board of the National Academies, the National Research Council, and the sponsors of the National Cooperative Highway Research Program do not endorse products or manufacturers. Trade or manufacturers' names appear herein solely because they are considered essential to the object of the report.

Published reports of the

NATIONAL COOPERATIVE HIGHWAY RESEARCH PROGRAM

are available from:

Transportation Research Board
Business Office
500 Fifth Street, NW
Washington, DC 20001

and can be ordered through the Internet at:

http://www.national-academies.org/trb/bookstore

Printed in the United States of America

THE NATIONAL ACADEMIES

Advisers to the Nation on Science, Engineering, and Medicine

The **National Academy of Sciences** is a private, nonprofit, self-perpetuating society of distinguished scholars engaged in scientific and engineering research, dedicated to the furtherance of science and technology and to their use for the general welfare. On the authority of the charter granted to it by the Congress in 1863, the Academy has a mandate that requires it to advise the federal government on scientific and technical matters. Dr. Ralph J. Cicerone is president of the National Academy of Sciences.

The **National Academy of Engineering** was established in 1964, under the charter of the National Academy of Sciences, as a parallel organization of outstanding engineers. It is autonomous in its administration and in the selection of its members, sharing with the National Academy of Sciences the responsibility for advising the federal government. The National Academy of Engineering also sponsors engineering programs aimed at meeting national needs, encourages education and research, and recognizes the superior achievements of engineers. Dr. Charles M. Vest is president of the National Academy of Engineering.

The **Institute of Medicine** was established in 1970 by the National Academy of Sciences to secure the services of eminent members of appropriate professions in the examination of policy matters pertaining to the health of the public. The Institute acts under the responsibility given to the National Academy of Sciences by its congressional charter to be an adviser to the federal government and, on its own initiative, to identify issues of medical care, research, and education. Dr. Harvey V. Fineberg is president of the Institute of Medicine.

The **National Research Council** was organized by the National Academy of Sciences in 1916 to associate the broad community of science and technology with the Academy's purposes of furthering knowledge and advising the federal government. Functioning in accordance with general policies determined by the Academy, the Council has become the principal operating agency of both the National Academy of Sciences and the National Academy of Engineering in providing services to the government, the public, and the scientific and engineering communities. The Council is administered jointly by both the Academies and the Institute of Medicine. Dr. Ralph J. Cicerone and Dr. Charles M. Vest are chair and vice chair, respectively, of the National Research Council.

The **Transportation Research Board** is one of six major divisions of the National Research Council. The mission of the Transportation Research Board is to provide leadership in transportation innovation and progress through research and information exchange, conducted within a setting that is objective, interdisciplinary, and multimodal. The Board's varied activities annually engage about 7,000 engineers, scientists, and other transportation researchers and practitioners from the public and private sectors and academia, all of whom contribute their expertise in the public interest. The program is supported by state transportation departments, federal agencies including the component administrations of the U.S. Department of Transportation, and other organizations and individuals interested in the development of transportation. **www.TRB.org**

www.national-academies.org

COOPERATIVE RESEARCH PROGRAMS

CRP STAFF FOR NCHRP REPORT 676

Christopher W. Jenks, *Director, Cooperative Research Programs*
Crawford F. Jencks, *Deputy Director, Cooperative Research Programs*
David A. Reynaud, *Senior Program Officer*
Megan A. Chamberlain, *Senior Program Assistant*
Eileen P. Delaney, *Director of Publications*
Ellen M. Chafee, *Editor*

NCHRP PROJECT 21-09 PANEL
Field of Soils and Geology—Area of Testing and Implementation

Ahmad A. Ardani, *FHWA Turner-Fairbank, McLean, VA (Chair)*
Steve W. Perkins, *Montana State University, Bozeman, MT*
Sastry P. Putcha, *Florida DOT, Tallahassee, FL*
Danesh Sajedi, *Maryland State Highway Administration, Hanover, MD*
David P. Shiells, *Virginia DOT, Chantilly, VA*
John A. Siekmeier, *Minnesota DOT, Maplewood, MN*
Chun-Kun Su, *North Carolina DOT, Raleigh, NC*
Michael Adams, *FHWA Liaison*
G. P. Jayaprakash, *TRB Liaison*

AUTHOR ACKNOWLEDGMENTS

The authors are grateful to the NCHRP for funding the study and to the technical review panel members: Mr. Ahmad Ardani (chair), FHWA Turner-Fairbank; Mr. John Siekmeier, Minnesota Department of Transportation; Dr. Steve Perkins, Montana State University; Dr. Sastry Putcha, Florida Department of Transportation; Mr. Dan Sajedi, Maryland State Highway Administration; Mr. David Shiells, Virginia Department of Transportation; and Mr. Chun-Kun Su, North Carolina Department of Transportation.

The authors wish to thank a number of individuals who provided invaluable assistance throughout the project, including Geoffrey Bee and Kyle Jackson, Colorado School of Mines; Heath Gieselman, Mike Kruse, Amy Heurung, Eddy Blahut, and Allison Moyer, Iowa State University; Dr. Reinhard Furrer, University of Zurich; Dr. Nils Ryden, Peab AB Sweden and Lund University; Patrick Miller, Olson Engineering, Inc.; Dr. Mark Thompson, CH2MHill; Dr. Dietmar Adam, Technical University of Vienna; and Dr. Gerhard Bräu, Technical University of Munich.

The authors are grateful for the assistance and cooperation of the state departments of transportation/highway authorities and project contractors at the five field sites where testing was conducted:

- John Siekmeier of the Minnesota Department of Transportation; Tim Clyne, Ruth Roberson, and Jack Herndon at the Minnesota ROAD Research Facility; Hard Drives of Minnesota
- Aziz Khan, Naser Abu-Hejleh, Jake Kononov, and Chris Boespflug of the Colorado Department of Transportation; Flatiron Constructors, Inc., Intermountain Division
- Dan Sajedi of the Maryland State Highway Administration; Devin Miller and colleagues at Dewey Jordan Construction of Maryland
- Sastry Putcha of the Florida Department of Transportation; Tom Woods and colleagues at JEA Construction Engineering Services; Wade Henderson and colleagues at Keith & Schnars, P.A.
- C. K. Su and Brian Smith of the North Carolina Department of Transportation, David Teal and colleagues at Blythe Construction of North Carolina

The authors are very grateful to Ammann, Bomag, Caterpillar, Case, Dynapac, and Sakai for providing rollers and to the representatives from these roller manufacturers for providing information about their current continuous compaction control and intelligent control equipment. The authors also thank Bob Horan for assisting in coordinating field project sites. Equipment and expertise provided by Arthur Taylor, Jeff Drake, and Geoffrey Kirk of Trimble Navigation Limited (3D Machine Control Construction Division) greatly increased the effectiveness of the research team and improved the quality of results and is very much appreciated. In addition, equipment provided by Olson Engineering, Inc., allowed for more efficient field testing and is appreciated.

FOREWORD

By David A. Reynaud
Staff Officer
Transportation Research Board

This report describes intelligent compaction, a new method of achieving and documenting compaction requirements through continuous compaction-roller vibration monitoring to assess mechanistic soil properties (e.g., stiffness, modulus), continuous modification/adaptation of roller vibration amplitude and frequency to ensure optimum compaction, and full-time monitoring by an integrated global positioning system (GPS) to provide a complete GPS-based record of the compacted area. This report will interest state and local highway agency construction managers and geotechnical engineers and contractors, particularly excavation superintendants. Implementation of this system has the potential to improve infrastructure performance, reduce costs, reduce construction duration, and improve safety.

Compaction of embankment, subgrade, and base materials is a significant portion of state highway construction budgets and is critical to the performance of highway pavements. Heterogeneity of earth materials, variability in equipment and operators, and difficulty in maintaining uniform lift thickness and prescribed moisture content combine to make desired earthwork compaction difficult to achieve. Current quality-control and quality-assurance testing devices are typically used to assess less than 1% of the actual compacted area.

Research findings in Europe and in the United States have shown that soil stiffness and modulus can be assessed through monitoring vibration of the compaction roller drum and that continuous monitoring, feedback, and automatic adjustment of the compaction equipment can significantly improve the quality of the compaction process. Standard specifications for intelligent compaction systems in the United States are needed, much as they exist overseas.

Under NCHRP Project 21-09, the Colorado School of Mines and Iowa State University conducted research to determine the reliability of intelligent compaction systems and to develop recommended construction specifications for the application of intelligent compaction systems in soils and aggregate base materials. For the purposes of this project, intelligent compaction is defined as involving the use of vibratory rollers that are equipped with a control system that can automatically adjust compactive effort in response to real-time feedback of changes in material modulus during the compaction process.

To achieve the project objectives, the researchers conducted a review of domestic and international literature and determined the current state of practice of intelligent compaction. Interviews with compaction equipment manufacturers and European researchers provided information on equipment capabilities and the current state of practice abroad. The investigators identified five active state department of transportation construction

projects for the collection and comparison of intelligent and traditional compaction data. They formulated a data collection plan for roller data (from a minimum of three different manufacturers), instrumentation data, and in situ testing data. The researchers' analysis of the data allowed validation of the roller data with the instrumentation data and correlation of the roller data with the in situ data. Additional analysis confirmed the importance of determining moisture, layer depth, and the foundation layer in the accuracy of intelligent compaction systems. Based on further analysis of the acquired data, target values for the modulus of different soil types have also been provided. Preliminary recommended construction specifications are included for the application of intelligent compaction systems in soils and aggregate base materials. The final report addresses the reliability and effectiveness of intelligent compaction technology in different soil types. Appendixes A through D, which provide supplemental information, are available on the TRB website (www.trb.org) at http://www.trb.org/Main/Blurbs/164279.aspx.

CONTENTS

Note: Many of the figures in this report have been converted from color to grayscale for printing. The electronic version of the report (posted on the Web at www.trb.org) retains the color versions.

SUMMARY

Intelligent Soil Compaction Systems

This report details the findings of NCHRP Project 21-09, "Intelligent Soil Compaction Systems," undertaken to investigate intelligent soil compaction (IC) systems and to develop generic specifications for the application of IC in quality assurance (QA) of soil and aggregate base material compaction. The term *intelligent soil compaction systems* was defined (in the NCHRP Project 21-09 request for proposals) to include (1) continuous assessment of mechanistic soil properties (e.g., stiffness, modulus) through roller vibration monitoring; (2) automatic feedback control of vibration amplitude and frequency; and (3) an integrated global positioning system to provide a complete geographic information system-based record of the earthwork site. An equally important term is *roller-integrated continuous compaction control*—defined by IC components (1) and (3).

Roller-integrated continuous compaction control (CCC) technology was initiated in Europe in the 1970s and has been used in European practice for nearly 20 years. The first European specification for roller-integrated CCC was developed in Austria in 1990. Today, four European countries have soil compaction QA specifications using roller-integrated CCC (Austria, Germany, Sweden, and Switzerland) and U.S. states are beginning to implement pilot specifications (e.g., Minnesota). In European specifications the use of automatic feedback control IC rollers is permitted during compaction but not during QA because the roller measurement values (MVs) can be strongly influenced by varying amplitude and frequency. The dependence of roller MVs on frequency and amplitude in particular was verified in this study (summarized below) and further determined to be quite complex and difficult to predict. Accordingly, the recommended specifications developed here allow IC during compaction but do not permit the use of automatic feedback control IC during roller-based QA.

Recommended Specifications for Roller-Integrated CCC in Earthwork QA

Six options for QA of earthwork compaction using roller-integrated CCC were developed as a result of this study to accommodate the diversity of earthwork site conditions, earthwork and QA practice, and agency needs observed throughout the United States. The six recommended specification options are distinguished into three principal categories. In Option 1, CCC is used to assist in QA, but acceptance is based on spot-test measurements. Options 2a and 2b acceptance is based on roller MVs, but no initial calibration of roller MV is required. Options 3a, 3b, and 3c acceptance is based on achieving a target roller MV over a specified proportion of an evaluation area. Target MVs are determined via various initial calibration techniques. Technically, the proposed specifications are end product based with methodological aspects that must be followed. None of the recommended options constitute performance-based specifications. Each specification option can be adopted as the sole

method for QA; alternatively, two or more options can be combined to increase reliability. Option 1 is recommended as a beginning approach. Once personnel are comfortable with CCC technology, states can advance to more complex options.

The recommended specifications were developed and pilot tested through field testing on active earthwork construction projects in Minnesota, Colorado, Maryland, Florida, and North Carolina. Extensive testing with IC and CCC rollers was conducted on granular soils, fine-grained soils, and aggregate base materials commonly used in subgrade, subbase, and base course construction. Smooth drum and pad foot drum IC and CCC roller compactors from Ammann, Ammann/Case, Bomag, Caterpillar, Dynapac, and Sakai were used throughout the study. Field investigations were conducted on more than 200 test beds across the five sites. Test beds involved single lifts of subgrade, subbase, and base course materials ranging in thickness from 150 to 300 mm (6 to 12 in) and, in some cases, multiple lifts and layered systems to depths greater than 1.5 m (4.9 ft). Single-lane test beds were constructed to conduct detailed investigations of the relationship between roller MVs and measurements from commonly used spot tests (e.g., nuclear gauge, lightweight deflectometer, dynamic cone penetrometer). Full-width test beds were constructed to calibrate roller MVs to spot-test measurements and to examine the implementation of recommended specifications. Multiple lift and layered test beds were constructed with embedded instrumentation to investigate the relationship between roller MVs and in situ stress-strain-modulus, the measurement depth of roller MVs, and the influence of layered structures on roller MVs.

Fundamentals of Roller Measurement Systems

Each vibration-based roller MV investigated provides a measure of soil or foundation stiffness for an area the width of the roller [2.1 m (6.9 ft)] by a spatial distance in the direction of roller travel that varies [0.06 to 1.0 m (0.2 to 3.3 ft)] across the different MVs. The reporting spatial resolution of roller MVs varied from 0.2 to 1.0 m (0.7 to 3.3 ft), and the resulting records provide complete coverage of the earthwork. For best results, real-time kinematic differential global positioning system (GPS) with an accuracy of 1 to 2 cm (0.4 to 0.8 in) is recommended. The position reporting accuracy of the roller-mounted GPS should be verified regularly. Repeatability testing of properly working CCC/IC rollers and roller measurement systems revealed a pass-to-pass roller MV uncertainty of ±10% (one standard deviation). Repeatability testing of vibratory pad foot measurement systems revealed pass-to-pass MV uncertainties in excess of 25%. A repeatability testing procedure was developed and is recommended for CCC specifications.

Four vibration-based roller MVs were investigated—Ammann and Case/Ammann k_s, Bomag E_{vib}, Dynapac CMV_D, and Sakai continuous compaction value (CCV). The various MVs correlated well with each other over a range of soft to stiff soil conditions. CCV and compaction meter value (CMV) were found to be insensitive to changes in soil stiffness below values of approximately 10. Many of the roller MVs employed by manufacturers were validated using independent instrumentation and implementation of published roller MV algorithms. This dispels the "black box" mentality that would inhibit implementation by the engineering community.

Field testing revealed that vibration-based roller MVs vary with operating parameters such as excitation force amplitude and frequency, roller speed, and travel mode (forward/reverse). The amplitude dependence of roller MVs was not predictable; MVs were found to increase, decrease, or remain the same with increasing amplitude depending on the soil and layering conditions. The complex variation of roller MVs with operational parameters indicates that operational parameters must be held constant when using roller-integrated CCC for QA. Local soil heterogeneity transverse to the direction of roller travel has a significant influence on roller MVs. Due to the nature of drum instrumentation, roller MVs are direc-

tionally dependent on heterogeneous soil. Bidirectional roller MVs were found to vary by 100% due to transverse soil stiffness variability. Spot testing should be conducted across the drum lane when correlating to roller MVs, and great care should be used when performing spatial statistical analysis of pass-to-pass data maps in the presence of heterogeneity.

Relationship Between Roller-Measured Stiffness and In Situ Stress-Strain-Modulus Behavior

Roller MVs measure to depths considerably greater than typical compaction lifts. For vertically homogeneous embankment conditions and the 11- to 15-ton smooth drum vibratory rollers used in this study, the volume of soil reflected in a roller MV is cylindrical in shape and extends to 0.8 to 1.2 m (2.6 to 3.9 ft) deep and 0.2 to 0.3 m (0.7 to 1.0 ft) in front of and behind the drum. The measurement depth of roller MVs was mildly influenced by vibration amplitude; that is, a 0.1-mm (0.004-in) increase in amplitude (A) yielded a 3-cm (1.2-in) increase in measurement depth.

In situ stress-strain-modulus measurements at depths to 1 m revealed highly nonlinear modulus behavior within the bulb of soil reflected in roller MVs. In base, subbase, and subgrade structures, modulus varies widely from layer to layer and within layers. Modulus values increased by a factor of 2 with depth in vertically homogeneous embankment test beds. A change in vibration amplitude from low to high created a twofold change in modulus. Plane strain conditions exist under the center of the drum and do not exist under the drum edges. As a result, the soil under the drum center responds stiffer than the soil under the edge.

Roller MVs are a composite reflection of typical base, subbase, and subgrade structures with a surface to top-of-subgrade thickness of less than approximately 1 m (3.3 ft). The contribution of each layer to roller MV is influenced by layer thickness, relative stiffness of the layers, vibration amplitude, and drum/soil interaction issues (contact area, dynamics). The contribution of sublift materials to roller MVs can be significant. The amplitude dependence of roller MVs—particularly stiffness measures such as E_{vib} and k_s—is a result of stress-dependent soil modulus, layer interaction, and drum/soil contact mechanics. For vertically homogeneous embankment conditions, granular soils that are governed by mean effective stress-induced hardening may exhibit a positive roller MV-A dependence (i.e., increase in A yields an increase in roller MV). Conversely, cohesive soils governed by shear stress–induced softening may exhibit a negative roller MV-A dependence (i.e., an increase in A yields a decrease in roller MV). The roller MV-A dependence of layered structures is more complex and is influenced by stress-dependent soil modulus (modulus function parameters), layer thickness, relative stiffness of layers, and drum/soil interaction issues. Both positive and negative roller MV-A dependence is possible, even within the same material. The roller MV-A relationship is site dependent.

Roller MVs were found to be insensitive to the compaction of thin lifts [15 cm (6 in)] of stiff base material placed directly over a soft subsurface. Roller MVs were sensitive to compaction of 30-cm (12-in) lifts of the same stiff material over soft subgrade. The sensitivity of roller MVs to compaction of thin lifts improves as the modulus ratio of the overlying to underlying layers decreases.

The extraction of mechanistic material parameters using roller-based measurements for performance-based specifications consistent with mechanistic-empirical–based design (e.g., AASHTO 2007 Pavement Design Guide) is possible. However, the extraction of appropriate parameters must account for the three-dimensional nature of the roller/soil interaction, the influence of layers, the nonlinear modulus of each involved material, and the dynamics of the drum/soil interaction.

Evaluation of Automatic Feedback Control-Based Intelligent Compaction

The current technology for IC involves automatic feedback control (AFC) of excitation force amplitude (Ammann, Bomag, Case/Ammann, Dynapac) and in some cases excitation frequency (Ammann, Case/Ammann). At a minimum level, each manufacturer controls the vertical excitation force amplitude to prevent unstable "jump" mode vibration of the roller. Bomag, Ammann, and Case/Ammann employ additional AFC in an attempt to improve compaction and uniformity. The influence of AFC-based IC on compaction efficiency and uniformity was investigated on granular base material. AFC-based IC did not produce increased compaction or improved uniformity compared to constant amplitude mode compaction during this test case. The response distance of AFC was found to be approximately 1 m (3.3 ft), indicating that rollers in AFC mode can respond to relatively local changes in soil conditions. The dependence of roller MVs on *A* can provide a misleading record of soil stiffness when operating in AFC mode. Both positive and negative MV-*A* dependence were observed during testing and resulted in an artificial and misleading level of variability in soil stiffness. In addition, roller MV-*A* dependence can trigger AFC changes in *A*. This is particularly problematic when roller MVs hover around a target or limit MV. The current AFC-based method to IC is a first-generation approach. As the influence of vibration force, frequency, roller speed, and so forth on soil compaction is further developed, IC approaches will likely improve and advance the compaction process.

Correlation of Roller Measurement Values to Spot-Test Measurements

Field testing was performed with five roller MVs from smooth and pad foot rollers and spot-test measurements from 17 different nongranular subgrade, granular subgrade, and granular subbase/base materials. The results indicated that correlations are possible to dry unit weight, modulus, and California bearing ratio (CBR) with simple linear regression analysis for test conditions with homogeneous and relatively stiff underlying layer support conditions and MVs obtained under constant operation settings. A wide range of resulting R^2 values is attributed to various factors, including sublift heterogeneity, moisture content variation, limited measurement range, transverse heterogeneity, and variation in machine operating parameters. High variability in soil properties across the drum width and soil moisture content contributes to scatter in relationships. Averaging measurements across the drum width and incorporating moisture content into multiple regression analysis, when statistically significant, helped mitigate the scatter to some extent. Correlations are generally better for low-amplitude vibration settings [e.g., $A = 0.7$ to 1.1 mm (0.028 to 0.043 in)].

The influence of soil moisture content, compaction layer lift thickness, underlying layer properties, and machine operation settings was statistically analyzed using multiple regression analysis. Where heterogeneous conditions were evident below the compaction layer, the underlying layer properties (MVs and spot-test measurements) were often statistically significant in the multiple regression model. Regression relationships improved by incorporating the underlying layer properties. Where compaction layer properties were strongly correlated with the underlying layer properties, compaction layer spot-test measurements were statistically not significant in the analysis.

Moisture content was significant for two nongranular subgrade layer test beds and one granular base layer test bed, although generally moisture content was not statistically significant in the regression analysis for most of the test bed studies. Factors contributing to this observation were (1) moisture content did not vary enough over the length of the test

strip; (2) spot-test measurements typically only measured moisture content to about 3 in below the surface, while the measurement depth of the roller is much greater; and (3) when correlating with elastic modulus–based spot-test measurements using multiple regression analysis, moisture content is co-linear (i.e., highly correlated to in situ measurement). Amplitude variation was statistically significant for all cases in which a minimum amplitude variation of ±0.30 mm (0.012 in) was present in the data.

An approach to empirically relate laboratory-determined M_r and roller MVs was possible for compaction layer material underlain by homogeneous and relatively stiff support conditions. Heterogeneous supporting layer conditions affected these relationships. The relationships improved by including parameter values that represented the underlying layer conditions through multiple regression analysis.

Case Study Implementations of Recommended Specifications

Implementation of the recommended specifications allowed a direct comparison of roller-based CCC options with each other and with existing (i.e., random spot-test-driven) QA practice. Specification Option 1—using roller-integrated CCC to identify the weakest area(s) for spot testing—requires minimal changes to typical existing QA practices but may be more stringent than current random selection spot testing. Specification Option 2a—based on the percentage change in the mean roller MV from pass to pass—appeared to be less stringent than current practice. Specification Option 2b—based on the percentage change in spatial roller MV data— appeared to be more stringent than current QA practices. One major challenge to successfully implementing specification options that require initial calibration of the roller to spot-test measurements is ensuring that the calibration area is representative of the evaluation section. Calibration-based Options 3a, b, and c require a significant initial investment of time and careful, detailed analysis. QA personnel will require careful training to ensure they are familiar with both the roller MV systems and the analysis required for the various options. For these reasons, Option 1 is recommended as a beginning approach. Once personnel are comfortable with CCC technology, states can advance to more complex options.

Construction traffic poses a challenge to implementing CCC-based QA. All of the options require careful, repeatable rolling patterns. Construction traffic often made it difficult to create uninterrupted and repeatable evaluation area roller MV maps and to perform measurements in the calibration areas. Performing correlation studies in a designated full-width calibration area requires a change in how the earthwork contractor places material. The pace of the production earthwork placement and compaction frequently limited the time the research team was able to spend in the calibration area. Correlations were developed in approximately 3 to 4 hours, though a time frame of 1 to 2 hours or less would be more consistent with production schedules. In typical production compaction practice, roller compactors are used throughout the hauling, placing, and grading operation. Careful planning and cooperation between the contractor and QA personnel, together with modifications in work flow, are critical for successful implementation of CCC-based QA.

The quality of the constructed earthwork is critical to the performance of pavements. Roller-integrated measurement of soil properties holds significant promise in that it provides an effective and efficient tool to comprehensively assess earthwork construction quality. The complete coverage capability of roller-integrated CCC is a significant improvement over current spot-test-based QA. The use of roller-integrated CCC enables departments of transportation to enforce high expectations for earthwork quality. Successful implementation of roller-integrated CCC for earthwork QA requires such high expectations, as well as

the coordination and thus buy-in from departments of transportation and contractors. QA personnel and contractors will need training on the capabilities and proper use of roller-integrated CCC.

Intelligent compaction, currently implemented using automatic feedback control of vibration amplitude and sometimes frequency, is in its infancy and will likely evolve to incorporate numerous ways in which the process of compaction is improved and made more efficient. The capabilities and friendliness of onboard computers and software will also likely improve significantly. Finally, the measurement systems, currently limited by the influence of operating parameters, local heterogeneity, and measurement depths that far exceed lift thickness, will also evolve to account for these factors. True performance-based assessment of earthwork materials using roller-integrated CCC is within reach. The results presented here illustrate reasonably complex but determinable soil behavior within the measurement volume of a vibrating roller.

CHAPTER 1

Introduction

1.1 Impetus and Objectives

NCHRP Project 21-09, "Intelligent Soil Compaction Systems," was initiated in 2006 to investigate intelligent compaction (IC) systems and to develop generic specifications for the application of IC in quality assurance (QA) of soil and aggregate base material compaction. The term "intelligent soil compaction systems" was defined in the NCHRP Project 21-09 Request for Proposals to include:

- Continuous assessment of mechanistic soil properties (e.g., stiffness, modulus) through roller vibration monitoring;
- On-the-fly modification of vibration amplitude and frequency;
- Integrated global positioning system to provide a complete geographic information system–based record of the earthwork site.

Roller-integrated continuous compaction control (CCC)—defined, in essence, above—was developed in Europe in the 1970s and has been used there for nearly 20 years. The first European specification for roller-integrated CCC was developed in Austria in 1990. Today, four European countries have compaction QA specifications using roller-integrated CCC (Austria, Germany, Sweden, and Switzerland), and the International Society for Soil Mechanics and Geotechnical Engineering has endorsed the Austrian CCC specifications (Adam 2007).

As described in this report, roller-integrated measurement of soil stiffness is strongly dependent on machine operating parameters (i.e., excitation force amplitude, frequency, and roller speed). Accordingly, current intelligent compaction technology employing on-the-fly or automatic modification of vibration amplitude and frequency should not be used during QA. IC can be used during compaction. The resulting QA specifications therefore pertain to the use of roller-integrated CCC for QA of earthwork compaction.

1.2 Work Plan Overview

A 24-month, two-phase work plan was carried out to address NCHRP Project 21-09 objectives. Field testing was performed on earthwork construction projects in five states: Minnesota, Colorado, Maryland, Florida, and North Carolina (see Table 1.1 and Figure 1.1). Testing was conducted on granular soils, fine-grained soils, and aggregate base materials commonly used in subgrade, subbase, and base course construction. Roller compactors from Ammann, Ammann/Case, Bomag, Caterpillar, Dynapac, and Sakai were used throughout the study (see Table 1.2). The Ammann, Ammann/Case, Bomag, and Dynapac rollers included measurement systems, a global positioning system (GPS), and automatic feedback control of vibration amplitude and therefore are referred to as IC rollers. The Caterpillar and Sakai rollers included measurement systems and GPS only and therefore are referred to as CCC rollers. The study used both smooth drum and pad foot rollers.

Field investigations were conducted on more than 200 test beds (TBs) across the five sites (see Figures 1.2 through 1.6). TBs ranged in size from single roller lane widths [i.e., 2.1 m (6.9 ft) by 20 m (65.6 ft) long] to multiple roller lane widths [i.e., 20 m (65.6 ft) by hundreds of meters long], more consistent with typical production earthwork compaction sections. TBs involved single lifts of subgrade, subbase, and base course materials ranging in thickness from 150 to 300 mm (6 to 12 in) and, in some cases, multiple lifts and layered systems to depths greater than 1.5 m (4.9 ft). Detailed information about the five sites, the soils tested, and individual TBs is provided in Appendix A.

Single lane TBs were constructed to conduct detailed investigations of the relationship between roller measurement values (MVs) and measurements from commonly used spot tests (see Figure 1.7). In these cases, soil mixers or reclaimers were often used to prepare the TB as homogeneously as possible (e.g., see Figures 1.2 and 1.5). Descriptions of the spot-

Table 1.1. Summary of field research sites.

State	Project	Dates	Rollers[a]	Soils[b]
MN	Mn/ROAD research site	July 2006	Ammann SD Bomag SD, PD Caterpillar SD, PD	Subgrade: A-6(5), A-4(3), A-2-6 Base: A-1-b, A-1-a
CO	I-25 reconstruction	Aug.–Oct. 2007	Bomag SD Caterpillar SD Dynapac SD	Subgrade: A-6(7), A-4, A-4(3) Subbase: A-1-a Base: A-1-a
MD	I-70 interchange	Nov. 2007	Bomag SD Dynapac SD, PD Sakai SD	Subgrade: A-2-4, A-4 Base: A-1-a, A-1-b
FL	Branan Field Chaffe/ I-10 interchange	April 2008	Case/Ammann SD Dynapac SD Sakai SD	Subgrade: A-3, A-2-4 Base: A-1-b
NC	NC311/I-85 divided highway	May–June 2008	Bomag SD Case/Ammann SD Sakai SD	Subgrade: A-2-4, A-4, A-1-b Base: A-1-a

[a]SD = smooth drum, PD = pad foot drum.
[b]American Association of State Highway and Transportation Officials classification provided; see Appendix A for more detail.

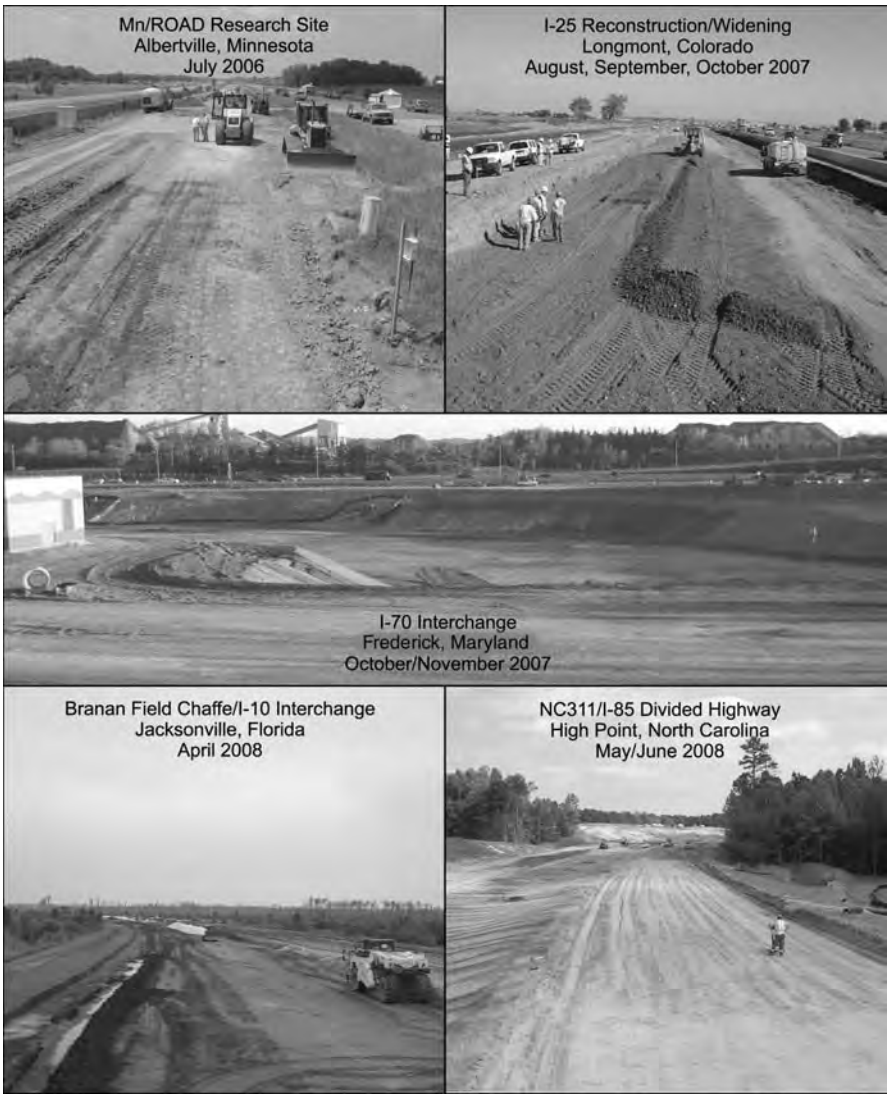

Figure 1.1. Overview of the five NCHRP 21-09 field test sites.

Table 1.2. Summary of rollers used during the study.

Roller	MV	Drum Length, m (ft)	Drum Radius, m (ft)	Static Mass, kg (lb)	Static Linear Load, kN/m (kip/ft)	Excitation Frequency, Hz	Excitation Force, kN (kip)
Ammann/Case AC110/SV212	k_s	2.20 (7.22)	0.75 (2.46)	11,500 (25,350)	31.5 (2.2)	20–34	0–277 (0–62)
Bomag BW113-BVC	E_{vib}	2.13 (7.00)	0.75 (2.46)	14,900 (32,850)	42.4 (2.9)	28	0–365 (0–82)
Caterpillar CS563	CMV_C MDP	2.13 (7.00)	0.76 (2.49)	11,100 (24,500)	26.9 (1.8)	32	133, 266 (30, 60)
Dynapac CA362	CMV_D	2.13 (7.00)	0.77 (2.53)	13,200 (29,100)	37.3 (2.6)	32	0–260 (0–58)
Sakai SV510	CCV	2.13 (7.00)	0.75 (2.46)	12,500 (27,600)	32.2 (2.2)	37, 28	186, 245 (42, 55)

Figure 1.2. IC/CCC rollers and TBs at the Minnesota work site.

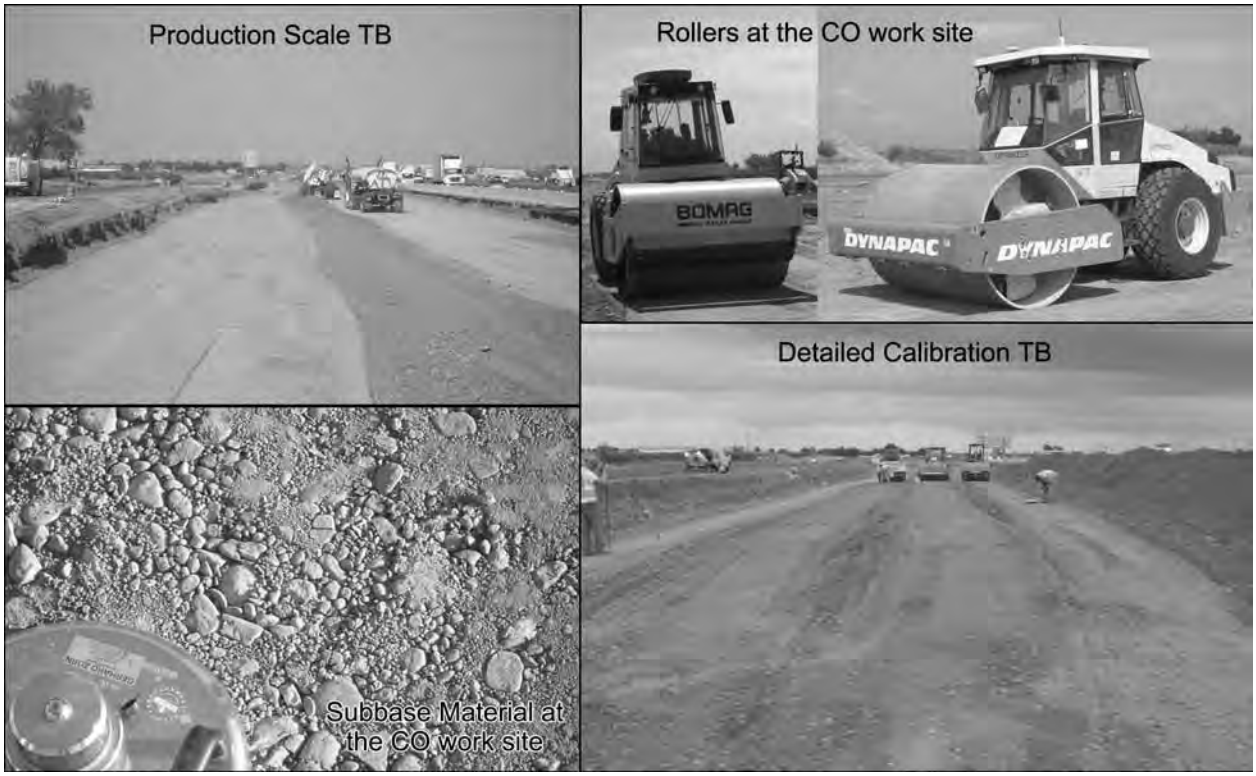

Figure 1.3. IC/CCC rollers and TBs at the Colorado work site.

Figure 1.4. IC/CCC rollers and TBs at the Maryland work site.

Figure 1.5. IC/CCC rollers and TBs at the Florida work site.

Figure 1.6. IC/CCC rollers and TBs at the North Carolina work site.

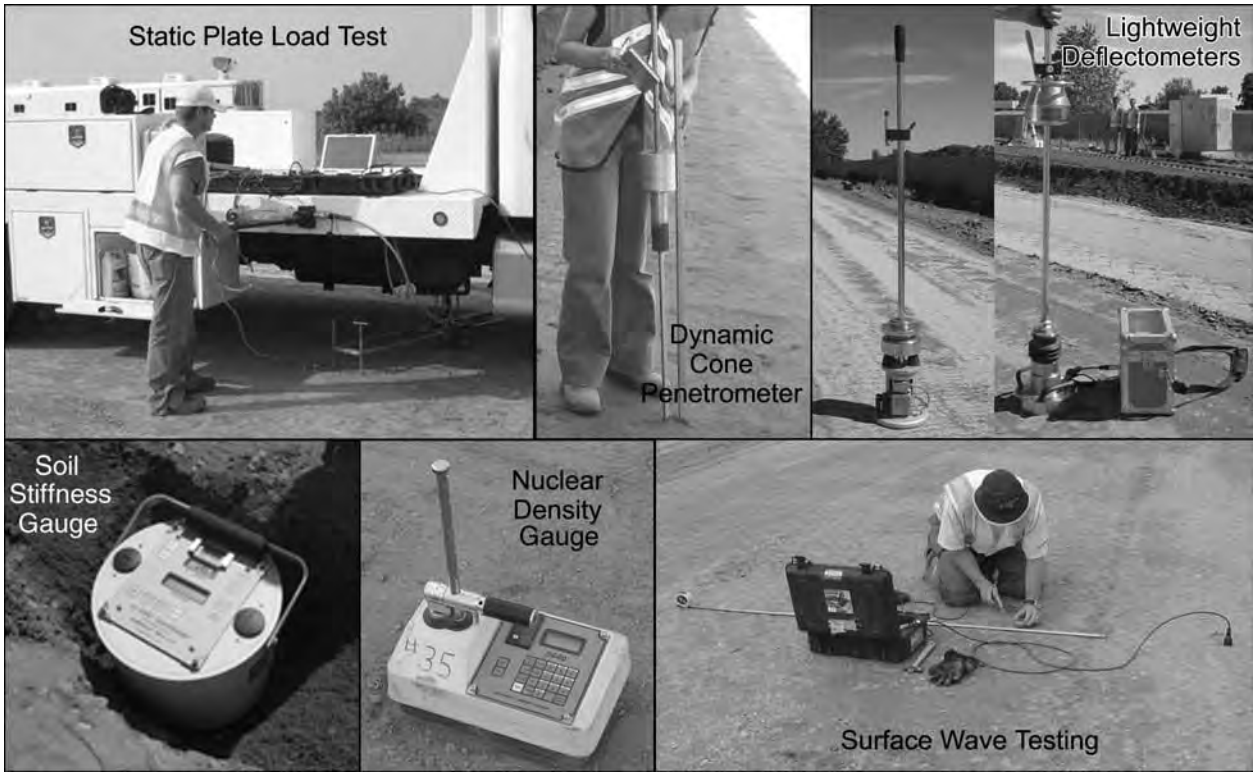

Figure 1.7. Spot-testing devices used in the study.

Figure 1.8. Multilayered TBs.

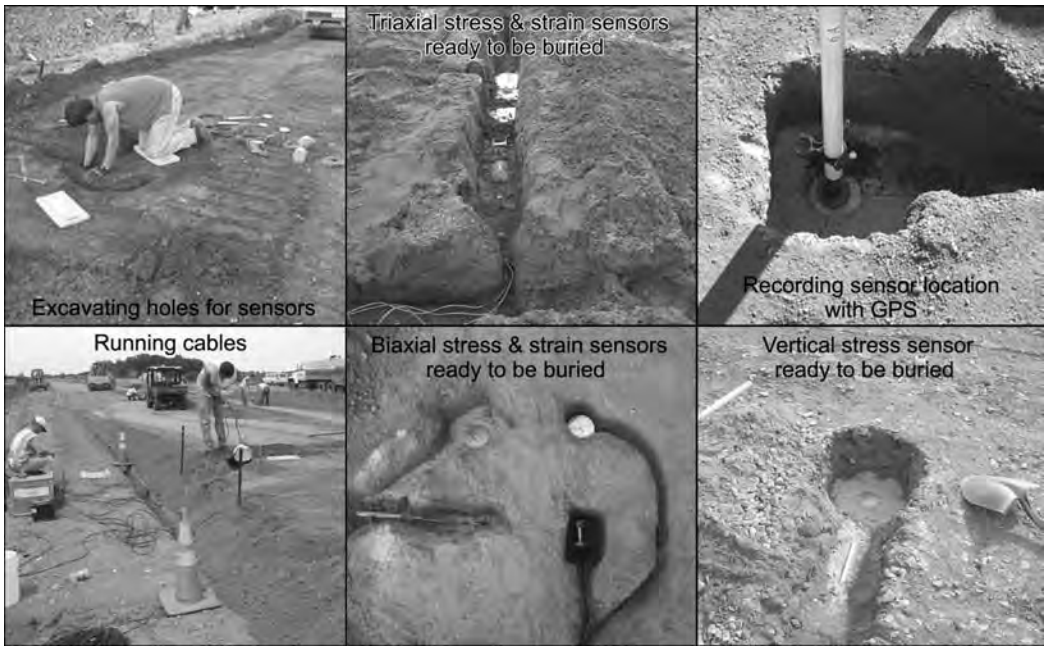

Figure 1.9. Installing in situ stress and strain sensors.

test devices employed are provided in Appendix A. Full-width TBs were constructed to calibrate roller MVs to spot test measurements for evaluation of QA specification options (e.g., see Figures 1.3 and 1.5). These TBs were usually prepared according to typical construction practice. Multiple lift and layered TBs were constructed with embedded instrumentation to investigate the in situ stress-strain field and measurement depth of roller MVs (see Figures 1.8 and 1.9).

1.3 Summary of Report

Following this Introduction, the report contains eight additional chapters, summarized as follows:

- Chapter 2 summarizes the state of practice regarding prior CCC and IC research findings and provides a history of CCC and IC. The chapter also summarizes current CCC/IC equipment and provides a detailed presentation of European CCC specifications.
- Chapter 3 investigates fundamental aspects of roller measurement systems, including MV and GPS position reporting, comparison of roller MVs, MV dependence on machine parameters (i.e., vibration amplitude, frequency, roller speed, direction of travel), and the influence of local heterogeneity on roller MVs.
- Chapter 4 characterizes roller-soil interaction, in-ground soil behavior (stress, strain, modulus) during rolling, and the relationship between roller MVs and in-ground soil behavior. The chapter focuses on the measurement depth of roller MVs, how MVs may relate to in situ soil response, and why MVs vary with excitation parameters (e.g., force amplitude).
- Chapter 5 explores the operation and benefits of automatic feedback control IC.
- Chapter 6 evaluates the relationship between roller MVs and spot-test results (i.e., nuclear density and moisture gauge, lightweight deflectometer, dynamic cone penetrometer, plate load test, and falling weight deflectometer). Through single and multiple variable regression analysis, this chapter addresses the influence of moisture, amplitude, and underlying layer stiffness.
- Chapter 7 presents recommended specifications for the use of roller-integrated CCC for QA of earthwork compaction. Six specification options are recommended.
- Chapter 8 presents six case studies carried out to evaluate the recommended specification options. The case studies are based on field tests in Colorado, Florida, North Carolina, and Minnesota.
- Chapter 9 presents the findings and conclusions from Project 21-09.
- The main body of the report was written with practical implementation in mind. Additional data and detailed information are presented in the appendixes. Appendixes A through D are available on the TRB website (www.trb.com) at http://www.trb.org/Main/Blurbs/164279.aspx.

CHAPTER 2

State of Practice

2.1 Continuous Compaction Control and Intelligent Compaction

Roller-integrated CCC has been used in Europe since the late 1970s, while IC technology has been available since the late 1990s. This section summarizes the history of CCC and IC as well as key results of previous research studies on CCC and IC in both Europe and the United States.

2.1.1 History of Continuous Compaction Control and Intelligent Compaction

The history of CCC and IC is summarized here; the reader is referred to Mooney & Adam (2007) for a more detailed account. The initial research on roller-integrated measurement dates to 1974, when Dr. Heinz Thurner of the Swedish Highway Administration performed field studies with a 5-ton tractor-drawn Dynapac vibratory roller instrumented with an accelerometer. The tests indicated that in the frequency domain the ratio between the amplitude of the first harmonic and the amplitude of the excitation frequency could be correlated to the state of compaction and the stiffness of the soil as measured by the static plate load test. In 1975, Dr. Thurner founded the firm Geodynamik with partner Åke Sandström to continue development of the roller-mounted compaction meter. In cooperation with Dr. Lars Forssblad of Dynapac, Geodynamik developed and introduced the Compactometer and the compaction meter value (CMV) in 1978. The new method was introduced to the technical community at the First International Conference on Compaction held in Paris, France, in 1980 (Thurner & Sandström 1980, Forssblad 1980). Dynapac began offering the CMV-based Compactometer commercially in 1980. A number of roller manufacturers (e.g., Ammann, Caterpillar, Ingersoll Rand) subsequently began offering the Geodynamik CMV Compactometer measurement system. Sakai introduced the compaction control value (CCV) in 2004 (Scherocman et al. 2007). The CCV follows in the footsteps of the CMV by using harmonic content from the measured drum vibration to estimate the compacted state.

Bomag introduced the Omega value and corresponding Terrameter in 1982. The Omega value provided a continuous measure of compaction energy and at the time served as the only alternative to CMV. In the late 1990s, Bomag introduced a vibration modulus E_{vib}, which provides a measure of dynamic soil stiffness (e.g., Kröber et al. 2001). The Omega value was thereafter discontinued for new machines. Ammann followed with the introduction of soil stiffness parameter k_s (also called k_B) in 1999 (Anderegg 1998, Anderegg & Kaufmann 2004). The introduction of E_{vib} and k_s signaled an important evolution toward the measurement of more mechanistic, performance-related soil properties (e.g., soil stiffness/modulus). The current commercially available roller-based measurement values (MVs) are summarized in Table 2.1.

Specifications for quality assurance (QA) of earthwork compaction using roller-integrated CCC were first introduced in Austria (1990), Germany (1994), and Sweden (1994). Revisions to these original specifications have been made in each country. The International Society of Soil Mechanics and Geotechnical Engineering (ISSMGE) recently endorsed the Austrian specifications for CCC (Adam 2007). The Austrian/ISSMGE and German specifications each permit multiple options for using CCC in earthwork compaction QA. The most common and simplest approach uses CCC to identify weak areas for evaluation via a static plate load test (PLT), a lightweight deflectometer (LWD), or density spot testing. Acceptance is based on these weak areas meeting prerequisite PLT modulus, LWD modulus, or density requirements. The most advanced CCC-based QA specifications involve correlating roller MVs to PLT modulus, LWD modulus, or density in a defined calibration area. If a suitable correlation is found,

Table 2.1. Commercially available roller MVs.

Roller MV	Manufacturers	Drum Vibration Parameters Used for Determining Roller MV
Compaction meter value (CMV)	Dynapac, Caterpillar, Hamm, Volvo	In the frequency domain, ratio of vertical drum acceleration amplitudes at fundamental (operating) vibration frequency and its first harmonic
Compaction control value (CCV)	Sakai	In the frequency domain, algebraic relationship of multiple vertical drum vibration amplitudes, including fundamental frequency, and multiple harmonics and subharmonics
Stiffness k_s	Ammann, Case	Vertical drum displacement, drum-soil contact force
Vibration modulus E_{vib}	Bomag	Vertical drum displacement, drum-soil contact force

a target roller MV is determined from the MV versus spot test regression equation. Acceptance is based on comparison of roller MV data collected in a production area to the target roller MV. Based on a survey of European practices, the calibration approach is challenging to implement and requires a high level of on-site knowledge (G. Bräu, personal communication, 2008; D. Adam, personal communication, 2008). A complete description of the European specifications is provided in Section 2.2.

When Geodynamik first introduced the compaction meter and CMV, vibratory drum technology was rudimentary by current standards. Vibration was implemented mechanically via a two-piece "clamshell" eccentric mass assembly within the drum. If rotated in one direction with frequency Ω (rad/s), the two eccentric masses would join together and provide maximum eccentric mass moment $m_o e_o$ and therefore maximum time-varying centrifugal force $F(t)$ per Equation 2.1. If operated in the reverse rotational direction, $m_o e_o$ and $F(t)$ would be a minimum. In the 1990s, vibratory roller technology became much more sophisticated. Bomag introduced the Variocontrol roller with counterrotating eccentric masses and servo-hydraulic control of the vertical component of $F(t)$, referred to as F_{ev} (see Section 2.2.2.2). Ammann introduced the ACE roller with servo-hydraulic two-piece eccentric mass moment and frequency control in 1999 (see Section 2.2.1.2). Dynapac followed suit with variable eccentric mass moment control in 2006 (see Section 2.2.3.2). The remaining roller manufacturers use the traditional two-piece and thus two-amplitude eccentric mass assembly. In the roller community the maximum vertical excitation force F_{ev} is commonly referred to as theoretical amplitude A (see Equation 2.2) and is equal to the peak displacement of the drum (with mass m_d) if suspended in air.

$$F(t) = m_o e_o \Omega^2 \cos(\Omega t) = F_{ev} \cos(\Omega t) \tag{2.1}$$

$$A = \frac{m_o e_o}{m_d} = \frac{F_{ev}}{m_d \Omega^2} \tag{2.2}$$

The introduction of servo-controlled eccentric excitation has catalyzed the term *intelligent compaction*, where the vibratory force amplitude and/or frequency are automatically adjusted in an attempt to improve roller performance and compaction. Currently, the *intelligence* in IC is limited. The Ammann/Case, Bomag, and Dynapac IC rollers automatically decrease the vertical vibration force when undesirable operating conditions are detected (e.g., jump mode). Further, some rollers (e.g., Bomag, Ammann/Case) have the ability to automatically reduce the eccentric force amplitude when a user-defined threshold roller MV has been reached. In a broader sense, however, intelligent compaction is in its infancy. Considerable advances in truly intelligent compaction are anticipated over the next decade.

2.1.2 Prior Investigations of Roller Vibration and Roller-Integrated Measurement Systems

Roller-integrated measurement of soil properties was initiated within the roller manufacturer community, and therefore early literature on the topic is limited. Issues pertaining to roller instrumentation and vibration behavior over a broad range of operating frequencies and amplitudes have only recently been addressed in the literature (Adam 1996, Adam & Kopf 2004, Brandl et al. 2005, Mooney et al. 2005, Rinehart & Mooney 2008). Recent experimental data collected with instrumented roller compactors (Mooney et al. 2003, Anderegg & Kaufman 2004, Adam & Kopf 2004, Mooney & Rinehart 2007, van Susante & Mooney 2008) have revealed fairly complex nonlinear roller vibration behavior, including loss of contact between the drum and soil, drum and frame rocking, and chaotic behavior.

Combined experimental and numerical investigations over the past 30 years have shed considerable light on roller-soil interaction and roller-integrated measurement systems. Early modeling efforts by Yoo & Selig (1979, 1980) employed a two degrees-of-freedom (DOF) model to represent steady state vertical drum and frame kinematics. These early studies were able to demonstrate the sensitivity of roller vibration

to changes in soil stiffness and damping and were used to investigate compaction efficiency (e.g., maximizing transmitted force). Decoupling of the drum from the soil (i.e., loss of contact, partial uplift) was first experimentally shown and predicted through lumped parameter modeling by Quibel (1980), Machet (1980), and Kröber (1988). Adam (1996) and Anderegg (1998) used lumped parameter modeling to characterize the various operational modes of roller vibration, including nonlinear and chaotic vibration. In addition to drum/soil coupled behavior (i.e., full contact throughout), Adam (1996) characterized both partial loss of contact, where the drum decouples from the soil for a portion of each loading cycle, and "jump" mode (also referred to as double jump), wherein the drum loses contact for more than one cycle of vibration at a time (see Figure 2.1). The resulting nonlinear signal in jump mode includes a subharmonic at one-half the excitation frequency (Adam 1996, Adam & Kopf 2004). Anderegg (1998) and Anderegg & Kaufmann (2004) described jump mode and rocking mode vibration as chaotic states. Employing chaos theory, Anderegg showed that rocking and jump mode vibration states occur above a certain centrifugal force and soil stiffness combination (roller parameter specific). In current practice, IC roller compactors use automatic feedback control of the centrifugal force to prevent chaotic motion (e.g., Anderegg & Kaufmann 2004) because these motions are harmful to the machines and dangerous for the operator.

van Susante & Mooney (2008) demonstrated through numerical model fitting to experimental data that soil behaves nonlinearly during roller vibration. The nonlinearity is attributed to partial loss of contact, curved drum surface, and stress-dependent soil modulus. They also demonstrated that rocking mode drum vibration occurs within the operating frequency range of most rollers and that this drum rocking can significantly alter vertical vibration response. In addition, a traveling roller interacting with underlying soil heterogeneity and employing variable excitation frequencies and amplitudes results in transient behavior that in turn influences the measurement systems (van Susante & Mooney 2008).

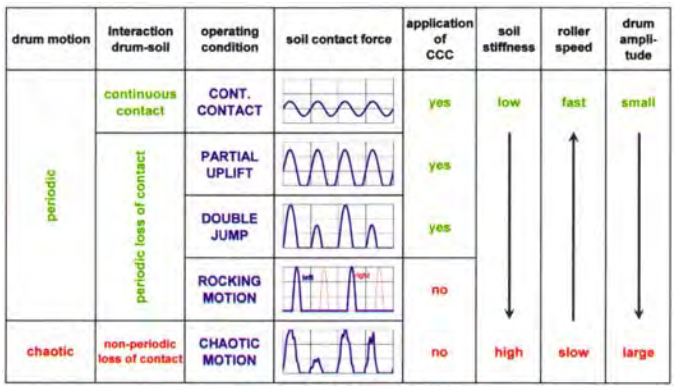

Figure 2.1. Observed modes of vibratory roller operation (from Adam & Kopf 2004).

The coupling of modeling efforts with experimental studies has enabled numerous investigations of roller MVs. Mooney et al. (2003, 2005) presented the findings from a laboratory, field, and numerical modeling investigation into the relationship between roller MVs and soil compaction properties for clay, sand, and crushed rock materials. Here, the frequency content of the drum acceleration signal—akin to CMV and CCV—was explored. Both laboratory and field studies showed that soil stiffness and harmonic content-based MVs are much more sensitive to the compaction process than is measured dry density. Dry density may increase 10% from loose deposition to full compaction, whereas laboratory-measured stiffness and field roller MVs may increase by more than 100% (Mooney et al. 2003). This contributes to the relative difficulty in correlating roller MVs to dry density compared to roller MV versus spot-test modulus. The study also showed that roller MVs exhibit much greater sensitivity to the compaction of a lift if the underlying (sublift) material is stiff. The results of roller-based measurement on soft soil indicated that low CMV is insensitive to changes in soil properties.

Adam & Kopf (2004) investigated the relationship between roller MV, soil modulus, and eccentric force amplitude (see Figure 2.2). Their study revealed how the various operational modes are influenced by eccentric force amplitude (referred to as relative amplitude in Figure 2.4) and soil modulus. More importantly, their study revealed the sensitivity of roller MVs to soil modulus within each operational mode. Figure 2.3 illustrates that Ammann k_s and Bomag E_{vib} increase fairly linearly with soil modulus throughout both continuous contact and partial uplift (the most commonly observed field behaviors). CMV increases linearly with soil modulus during partial uplift but is insensitive to soil modulus during continuous contact (CMV below approximately 10). Figure 2.4 confirms the insensitivity of CMV to soil modulus for CMV <10.

The Adam & Kopf numerical study also showed that roller MVs are amplitude dependent (see Figure 2.2). Experimental investigations by Kröber et al. (2001), Hartmann (2002), and Mooney & Rinehart (2007, 2009) revealed various degrees-of-amplitude dependence on roller-measured soil stiffness. The study by Hartmann also found that E_{vib} decreased with increasing roller speed.

2.1.3 Correlation Studies

A number of studies have been performed over the past 20 years to relate roller MVs to spot-test measurements (e.g., density, PLT modulus, LWD modulus). Floss et al. (1991)

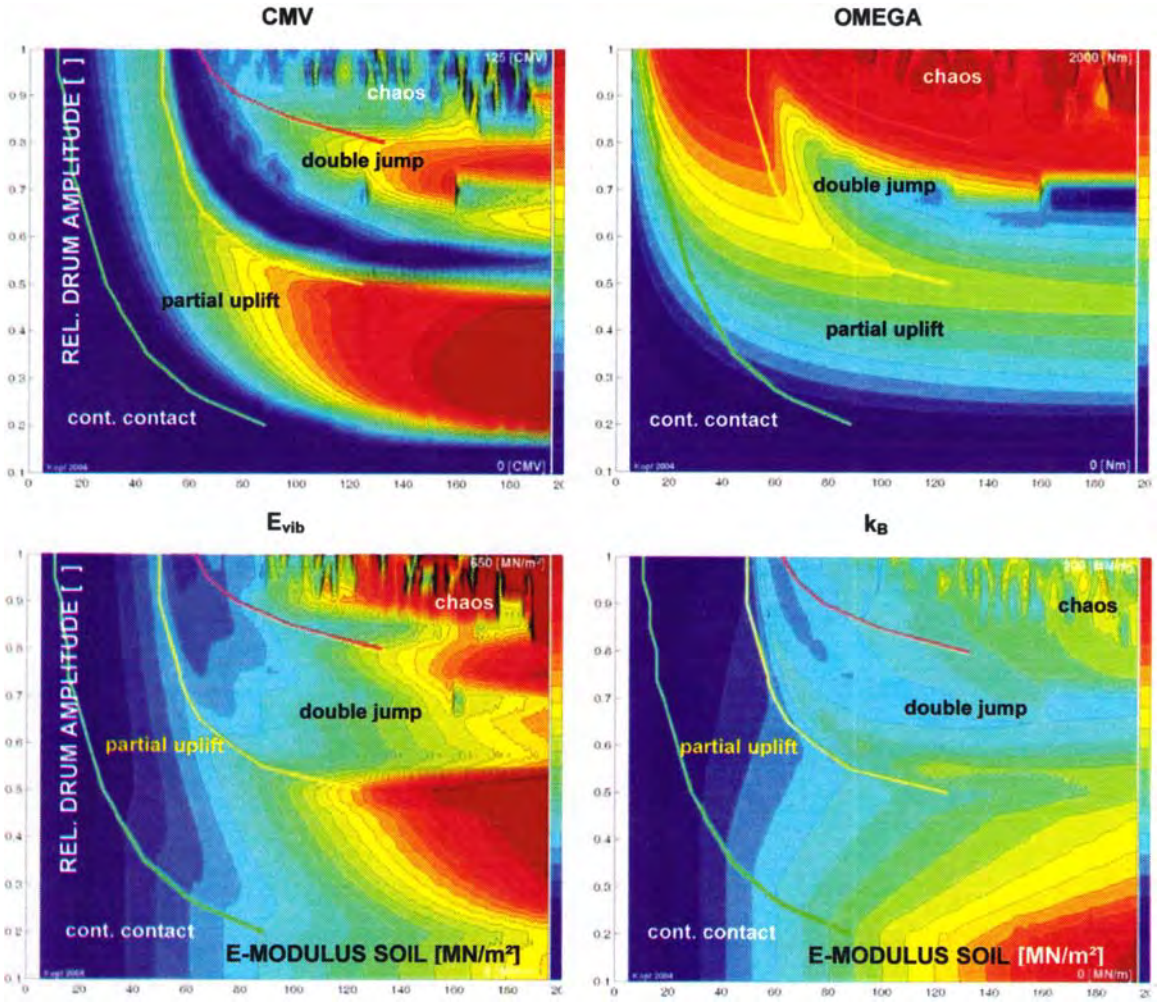

Figure 2.2. Relative roller MVs depending on soil stiffness (from Adam & Kopf 2004).

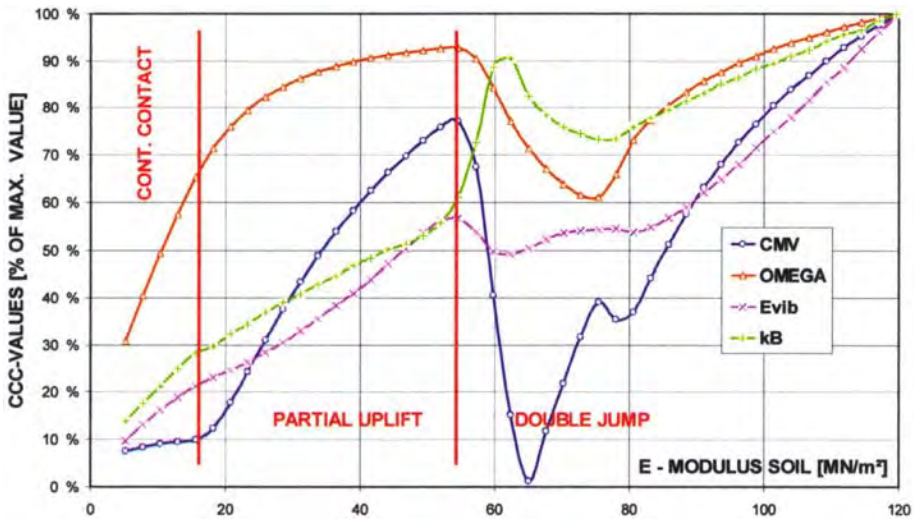

Figure 2.3. Sensitivity of roller MVs to soil modulus (from Adam & Kopf 2004); $k_B = k_s$.

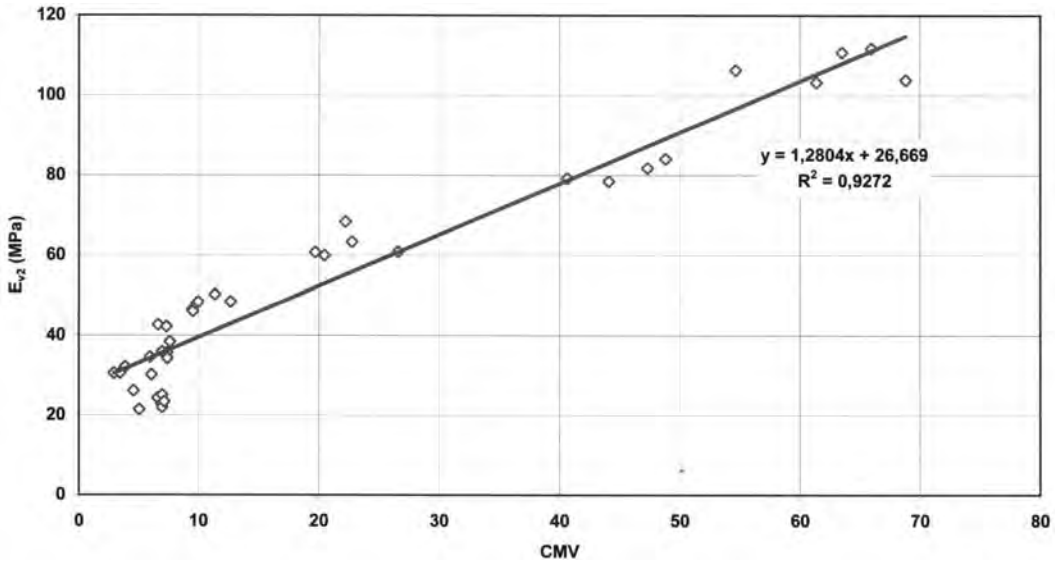

Figure 2.4. Empirical relationship between CMV and E_{v2} illustrating the insensitivity of CMV to E_{v2} for CMV<10 (results and figure courtesy of Dynapac).

reported dozens of correlations between CMV and PLT moduli E_{V1} and E_{V2} as well as between CMV and density (or % compaction) for coarse-grained, mixed, and fine-grained soils. The resulting regressions were found to be linear and sometimes nonlinear. Their results revealed higher correlation coefficients from CMV to PLT modulus correlation than from CMV to density correlation. The reason for this, they concluded, is that the measurement depth of the PLT is closer to that of CMV than is the measurement depth of density tests (sand cone, nuclear gauge). They found that roller MV is influenced by moisture content for fine-grained soils. Specifically, at a constant density, MV was found to increase with decreasing moisture content.

Kröber et al. (2001) investigated the relationship between Bomag E_{vib} and PLT moduli E_{V1} and E_{V2} during field testing on a silty gravel. Their results showed a strong linear correlation between E_{vib} and both E_{V1} and E_{V2} ($R^2 > 0.9$). Their results also showed that E_{vib} was equivalent in magnitude to E_{V1} during early compaction passes and nearly equal to E_{V2} at full compaction. Hartmann (2002) explored the correlation between E_{vib} and PLT moduli E_{V1} and E_{V2} as well as the influence of eccentric amplitude on the correlations. Hartman found no E_{vib} amplitude dependence on a soft silty soil but significant amplitude dependence for a gravelly sand soil.

Preisig et al. (2006) explored the correlation of Ammann k_s to E_{V1} and E_{V2} using more than a dozen data sets from sandy gravels. As shown in Figure 2.5, when the results from eight sandy gravel sites are combined, the resulting k_s versus E_V correlations are quite good. Visually, the correlations for individual soils are not as evident. The research found that if only data near the fully compacted state were used (as defined by $M_{e2}/M_{e1} = E_{V1}/E_{V2} < 3.5$), the correlations improved considerably. Based on these data, they called into question the European calibration approaches that use data from low-, medium-, and full-compacted states. Based on their gravel data sets, Preisig et al. argued that a correlation can be developed by using measurements on fully compacted material and assuming that the linear regression line passes through the origin.

Bräu et al. (2004) attempted to develop universal regression relationships using roller MV and spot-test measurement data from dozens of sites. They divided results by soil type (granular, mixed grain, cohesive), by layered versus homogeneous [i.e., >1.5-m (4.9-ft)-thick] conditions, and by roller vibration amplitude (high and low) used during measurement. Their results revealed significant scatter. Bräu et al. concluded that the approach is possible but that there was too much uncertainty in the variables of the archived data.

Mooney et al. (2003, 2005) performed a study to correlate harmonics-based roller MVs (CMV, CCV) to spot-test measurements (dry density, dynamic cone penetrometer) for sand subgrade soil and crushed rock base material. Their work showed that strength of the correlation and sensitivity of the roller MV improved significantly if the sublift material was stiffer. Petersen (2005) found poor correlations between E_{vib} and spot-test measurements and attributed the results to stress dependency of soil modulus and inherent soil heterogeneity that affects roller MVs differently than in situ tests. White & Thompson (2008) performed a study to correlate CMV to spot test measurements—dry unit weight, dynamic cone penetrometer (DCP) index, Clegg impact value (CIV), and LWD modulus—for five cohesionless base materials

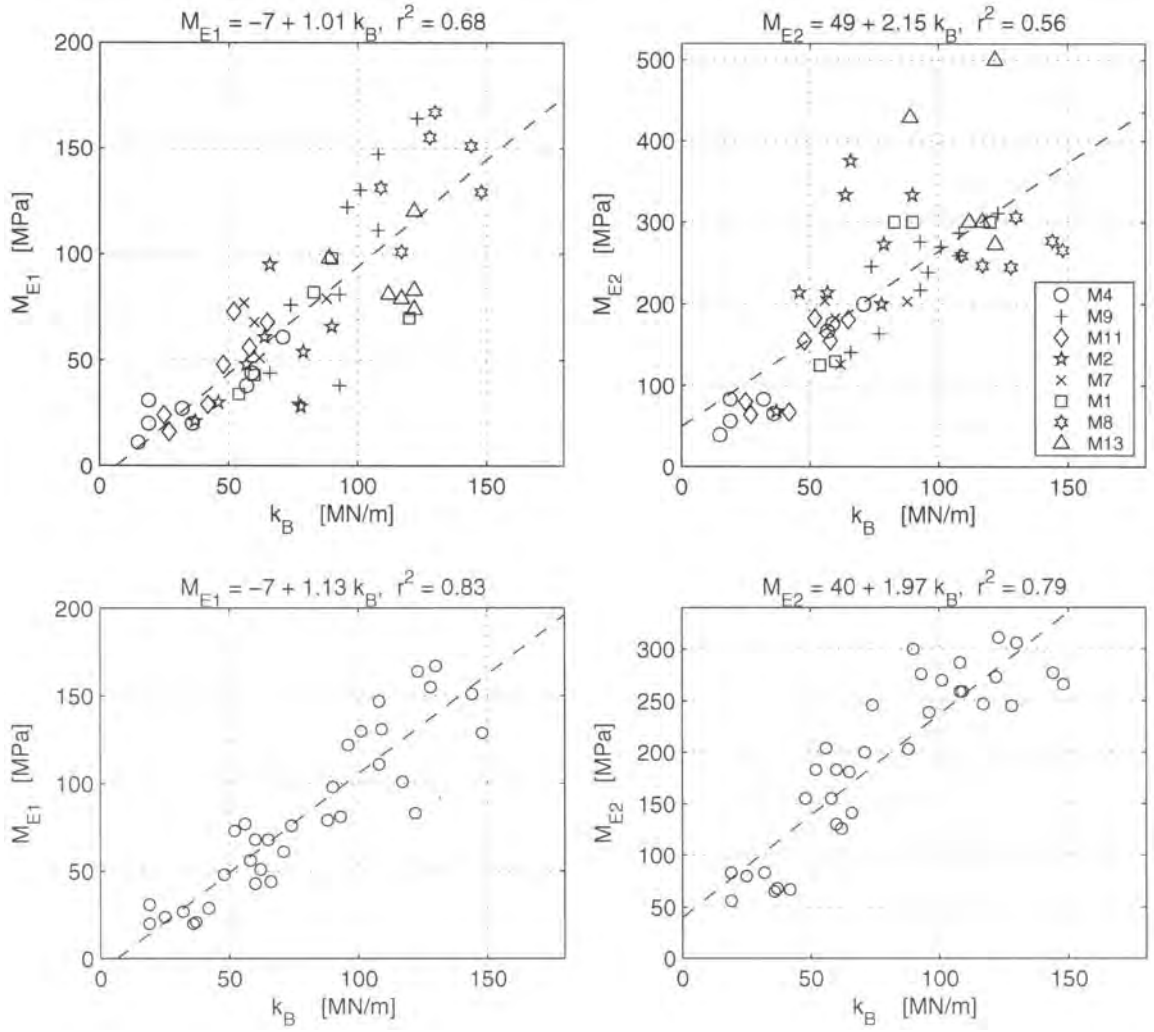

Figure 2.5. Correlations between Ammann ks and PLT moduli. Note: $M_{e1} = E_{V1}$, $M_{e2} = E_{V2}$. Top plots show all data; bottom plots show data for $M_{e2}/M_{e1} = E_{V1}/E_{V2} < 3.5$ (from Preisig et al. 2006).

through linear regression analysis. Data were collected over the entire compaction range for each base material. By averaging the data over a uniform area for each compaction state, high correlation was observed ($R^2 > 0.90$ for 20 of 28 correlations).

The relationships between Ammann k_s and spot-test measurements were investigated by White et al. (2007). The correlations observed for subgrade and subbase soils were found to depend heavily on the range of compaction states over which the soil was tested. For subgrade soil, k_s was found to be linearly proportional to LWD modulus E_{LWD} and CIV and showed a power-function relationship with DCP index. For one test area comprised of subgrade material, a test roller was used to evaluate k_s output and in situ test results. k_s was related to rut depth through a linear relationship for k_s ranging from 10 to 35 MN/m and rut depths ranging from 10 to 60 mm (0.4 to 2.4 in). Thompson & White (2007) performed multiple linear regression analyses between MVs (CMV or MDP, both from a Caterpillar roller), moisture content, and spot test measurements (density, DCP index, CIV, or E_{LWD}). Testing was performed on an A-1-b soil. Spot testing was performed after passes 1, 2, 4, 8, and 12 on three lanes. Regression relationships between both MVs and DCP index, CIV and E_{LWD} each exhibited R^2 between 0.85 and 0.95. The R^2 for the regression relationship for density varied between the two different MVs, with CMV having $R^2 = 0.68$ and MDP having $R^2 = 0.92$.

White et al. (2008a) conducted a field investigation to correlate Caterpillar CMV to spot test measurements. Acceptable correlations were found between CMV and DCP index and between CMV and dry unit weight. No correlation was found between CMV and E_{LWD}. Thompson et al. (2008) performed correlation analysis between Ammann k_s and measurements from various spot-test methods. R^2 values were between 0.3

and 0.8, depending on the spot test being correlated (dry unit weight, E_{V1}, E_{LWD}, $CIV_{4.5\text{-kg}}$, DCP index) on A-6(9) subgrade material. It was found that k_s was dependent on the moisture content of the subgrade soil ($R^2 = 0.61$). Correlations were also examined on A-1-b soil but were not found. This was attributed to the small range of k_s values (30 to 40 MN/m) observed in this test area.

Rahman et al. (2008) investigated the relationship between Bomag E_{vib} and spot-test measurements. For two sandy soils, they concluded there was no clear correlation between E_{vib} and modulus determined from LWD, FWD, Geogage, or DCP. The authors attributed the poor correlations to differences in measurement depth. Though not mentioned as a reason for the poor correlations, these investigators used variable control IC to gather E_{vib} data. As described above and herein, roller MVs can be strongly amplitude dependent. Rahman et al. found that E_{vib} was sensitive to moisture.

2.1.4 Prior Investigations of Measurement Depth of IC/CCC Rollers

A review of the literature reveals limited results regarding the measurement depth of an IC or CCC roller (i.e., the depth to which an MV is representative). Two experimental studies and one numerical study provide some insight. Several other general statements are made about measurement depth but are not substantiated with theory, experimental results, or references to other literature. Floss et al. (1991) present the results of a study in which soft mattresses were buried in granular soil at four depths to 1.2 m (3.9 ft). Once the excavations were refilled and fully compacted, several different rollers were operated along the track containing the mattresses. The study concluded that measurement depth for low- versus high-vibration amplitudes was difficult to interpret but that measurement depth increased with increasing roller static weight. The following guidelines were proposed as a result of this study and now appear in the ISSMGE-recommended CCC specifications (Adam 2007; see Section 2.3.2 below):

- For 2-ton rollers the approximate measurement depth is 0.4 to 0.6 m (1.3 to 2.0 ft),
- For 10-ton rollers the approximate measurement depth is 0.6 to 1.0 m (2.0 to 3.3 ft),
- For 17-ton rollers the measurement depth is greater than 1 m (3.3 ft).

For reference, common highway construction smooth drum and pad foot vibratory rollers—those used in this study—are 11- to 15-ton rollers. In addition to the mattress study, Floss et al. (1991) describe a two-layer study in which a layer of sandy gravel material was compacted above a stepped embankment of sandy silt material, resulting in three discrete layers of thickness for the sandy gravel (stiff) above the sandy silt (soft). They conclude that the results agree with those from the mattress study.

Brandl & Adam (2000) do not present any results of theoretical or experimental investigations regarding measurement depth but do state that "measurement depth depends on static load of the drum, vibration amplitude and frequency and also the soil." The following standardized values for measurement depth are recommended in Brandl & Adam:

- For 2-ton rollers the measurement depth is approximately 0.4 to 0.6 m (1.3 to 2.0 ft),
- For 10-ton rollers the measurement depth is approximately 0.6 to 0.8 m (2.0 to 2.6 ft),
- For 12-ton rollers the measurement depth is approximately 0.8 to 1.5 m (2.6 to 4.9 ft).

Anderegg & Kaufmann (2004) state that it is commonly accepted that 0.1 mm (0.004 in) of vertical drum vibration amplitude equates to 0.1 m (0.33 ft) of measurement depth; however, no theoretical or experimental justification is given. Classical foundation settlement analysis forms the underpinnings for this rule of thumb, but it has not been rigorously analyzed or validated experimentally (R. Anderegg, personal communication, 2008).

Brandl et al. (2005) present the results of another study involving rolling over buried mattresses. Mattresses were placed on an existing grade, and layers of sandy gravel material were placed and compacted above the mattresses with a 13-ton vibratory roller, eventually to a height of 1.05 m (3.40 ft). The authors conclude that the measurement depth of the roller at medium amplitude was 2.1 m (6.9 ft) in the sandy gravel material. Kopf & Erdmann (2005) performed finite element analysis of a 13-ton vibratory roller on stratigraphies of soft over stiff soil and stiff over soft soil. Their results indicate that measurement depth increased from about 0.7 to 1.4 m (2.3 to 4.6 ft) for stiff soil over soft soil and from about 0.6 to 1.2 m (3.9 ft) for soft soil over stiff soil, as the vibration force amplitude increased from low to high, 95 to 365 kN (21 to 82 kip).

2.1.5 Studies Utilizing In Situ Stress-Strain Instrumentation

A review of the literature regarding the use of in-ground instrumentation to monitor the response and behavior of soil due to vibratory compaction yielded limited results, possibly due to the difficulties and costs associated with installing and securing accurate results from in-ground instrumentation. Brandl & Adam (2000) measured vertical stress and displacement induced by a 13-ton vibratory roller at three depths—15, 50, and 85 cm (6, 20, and 33 in)—in a granular material. No discussion of in-ground sensor calibration or

placement procedures is presented. Values for vertical stress are not given; rather the results are presented as a percentage of the maximum measured value, which occurred at a depth of 15 cm (6 in) under high-vibration amplitude. For the high-amplitude pass, the roller operated in jump mode, and the peak stresses at 50 and 85 cm (20 and 33 in) were observed to be about 75% and 25% of the maximum, respectively. For the low-amplitude pass the roller operated in contact mode and the peak stresses at 15, 50, and 85 cm (6, 20, and 33 in) were observed to be about 70%, 30%, and 10% of the maximum, respectively. For the low-amplitude pass, the displacements at 15, 50, and 85 cm (6, 20, and 33 in) were observed to be about 8, 1.75, and 0.4 mm (0.31, 0.07, and 0.02 in), respectively. For the high-amplitude pass, the displacements at 15, 50, and 85 cm (6, 20, and 33 in) were 13, 2.5, and 0.7 mm (0.51, 0.10, and 0.03 in), respectively. A phenomenon called the bow-wave effect, in which the soil in front of the drum experiences vertical extension before being compressed as the drum traverses over it, is observed at all three depths during both high- and low-amplitude passes. It is also shown that some roller passes result in permanent compressive displacements (i.e., compaction), whereas other passes result in permanent extension (i.e., loosening).

Brandl et al. (2005) present the results of a similar study designed to measure stress and displacement at several depths. Two different rollers were used. No discussion of in-ground sensor calibration or placement procedures is presented. Roller-induced vertical stress is presented at a depth of 0.4 m (16 in) in a sandy gravel and at a depth of 0.35 m (14 in) in a clayey silt. Vertical displacement is presented at 0.1 m (4 in) in both the sandy gravel and clayey silt. Peak vertical stresses at 0.4 m (16 in) in the sandy gravel varied from 225 to 650 kPa (32.6 to 94.3 psi) across the range of amplitudes tested. The roller operated in contact mode for low-amplitude settings, partial loss of contact mode for medium-amplitude settings, and jump and rocking modes for high-amplitude settings. The peak vertical displacements at a depth of 0.1 m (4 in) in the sandy gravel were 1.7 and 3.25 mm (0.07 and 0.13 in) for low- and high-amplitude settings, respectively. In the clayey silt material, peak stresses at a depth of 0.35 m (14 in) were observed to range between 120 and 200 kPa (17.4 to 29.0 psi) for the range of low to high amplitudes. The roller operated in contact mode for all amplitudes. The peak vertical displacements at a depth of 0.1 m (4 in) in the clayey silt were about 10.5 and 19 mm (0.41 and 0.75 in) for low- and high-amplitude settings, respectively. It is noteworthy that the clayey silt TB was built in one day and that all testing was done on the following day. Even though the TB was fully compacted the first day, the first roller pass of the second day resulted in a permanent displacement of nearly 5 mm (0.20 in). Permanent settlements were very small or nonexistent after this first pass.

Ping et al. (2002) present roller-induced vertical stress data at three depths in a fine sand material. The study used 230-mm (9-in)-diameter Geokon earth pressure cells (EPCs), but no discussion of the calibration or placement procedures is provided. The results show peak stresses during compaction by a typical vibratory soil roller operating at 1.7 mm (0.07 in), with a theoretical vibration amplitude of 330 and 170 kPa (47.9 and 24.7 psi) at a depth of 0.23 and 0.4 m (9 and 16 in), respectively. For 0.8-mm (0.03-in) theoretical vibration amplitude by the same roller, the peak stresses were 190 and 110 kPa (27.6 and 16.0 psi) at a depth of 0.28 and 0.56 m (11 and 22 in), respectively. The study also showed a decrease in vertical stress with increasing roller forward velocity and little to no change in vertical stress with increasing number of roller passes. It should be noted that in-ground sensor data could be unreliable before the soil is fully compacted as the sensor calibration depends on the density of the surrounding material (see Chapter 4 and Appendix D).

D'Appolonia et al. (1969) installed vertical stress cells at depths of 0.3, 0.45, 0.6, 1.2, and 1.8 m (12, 18, 24, 47, and 71 in) and horizontal stress cells at a depth of 0.6 m (24 in) in a poorly graded dune sand. Two towed (usually towed by a dozer) roller compactors were used, weighing 6.25 and 3.15 tons and operating at 27.5 and 19 to 30 Hz, respectively. Maximum dynamic vertical stresses (i.e., static component removed) under the 6.25-ton roller at depths of 0.3, 0.45 0.6, 1.2, and 1.8 m (12, 18, 24, 47, and 71 in) were observed to be 103, 76, 62, 28, and 21 kPa (14.9, 11.0, 9.0, 4.1 and 3.1 psi), respectively, and were observed to be independent of the number of roller passes. Dynamic horizontal stress data are not presented; however, these data are said to be independent of the number of roller passes. Static horizontal stress (i.e., due to overburden and residual stresses due to compaction) data are presented in terms of the coefficient of horizontal earth pressure K_o defined as the ratio of horizontal to vertical stress. K_o values at a depth of 0.6 m (24 in) for a TB compacted with the 6.25-ton roller in the direction parallel to the roller path range from about 0.8 to 1.1 and tend to increase with the number of roller passes. K_o values for a TB compacted with the 6.25-ton roller at a depth of 0.6 m (24 in) in the direction perpendicular to the roller path range from about 0.8 to 2.75 and also tend to increase with the number of roller passes. K_o values are generally lower for TBs compacted with the 3.15-ton roller and tend to increase with both number of roller passes and increasing frequency of vibration.

2.1.6 Geostatistical Studies

Grabe (1994) performed spatial analysis of CMV maps using a spectral density approach. Aside from a dominant wavelength in the data at a distance equal to the circumference of the drum that he attributed to soil sticking to the drum,

Grabe concluded that there were no patterns in the roller MV data maps. Grabe found that CMV values at close distances were correlated, and he concluded that the data had an infinite correlation length (limited by the sample size of the data).

Petersen et al. (2007) examined why and how geostatistics could be used with CCC rollers. They concluded that the variogram parameters could be very useful. Peterson et al. found the variogram of roller MV data to be directionally dependent (i.e., anisotropic) and only used data in the driving direction. They proposed that roller MVs that change by more than the nugget over short distances suggest possible problem areas. White et al. (2008b) further examined variogram properties and how they could be used for earthwork compaction QA. They concluded that the range could be used as a window size for QA analysis and that the sill could be used as a target for uniformity of the data. They concluded there was anisotropy but that it can be ignored due to the high density of the data.

2.2 State of Current and Emerging IC Equipment

The primary manufacturers of CCC and/or IC soil rollers include Ammann (offered under the Case name in the United States and referred to hereafter as Ammann/Case), Bomag, Caterpillar, Dynapac, Volvo (formerly Ingersoll Rand), Sakai, and Hamm. Ammann/Case, Bomag, Caterpillar, Dynapac, and Sakai rollers were in this study and are described further here. As summarized in Table 2.2, all manufacturers offer roller-integrated measurement systems. The six roller MVs used in practice include (1) CMV, developed by Geodynamik and used by Dynapac, Caterpillar, and Volvo; (2) CCV, a derivative of CMV developed by Sakai; (3) stiffness E_{vib}, developed and used by Bomag; (4) stiffness k_s, developed and used by Ammann/Case; and (5) machine drive power (MDP), developed and used by Caterpillar. CMV, CCV, k_s, and E_{vib} require vibration and thus are applicable only on vibratory rollers. MDP does not require vibration but can be employed on vibratory rollers. The roller-integrated measurement systems, feedback control, and GPS-based documentation for each manufacturer's IC rollers are described in the following sections.

2.2.1 Ammann/Case

2.2.1.1 Measurement Value

The Ammann ACE Plus system calculates soil stiffness k_s once per cycle of vibration. The measurement system is thoroughly described in Anderegg (1998) and Anderegg & Kaufmann (2004) and is briefly described here. To best understand k_s the basic vibration of the drum/soil system must be considered. Figure 2.6 shows a schematic of a roller and a two DOF model representing the vertical kinematics of the drum-frame system (Figure 2.6b), where m_d and m_f are the drum and frame masses, respectively; z_d and $\ddot{z}_d$ are the drum displacement and acceleration, respectively; $m_o e_o$ is the eccentric mass moment; and Ω is the excitation frequency. Here, the soil is represented with a spring-dashpot Kelvin-Voigt model.

The resulting free body diagram (Figure 2.6c) shows the drum/soil contact force F_s comprised of four elements: drum inertia, frame inertia, eccentric force, and machine weight. Ammann determines drum inertia and eccentric force via measurement of vertical drum acceleration and eccentric position (frame inertia is neglected).

The resulting equation of motion is a second-order differential equation. The vertical drum displacement amplitude z_d is determined via spectral decomposition and integration of the measured peak drum accelerations (Anderegg & Kaufmann 2004). Solving this equation for k_s when the drum velocity is zero (i.e., down-most position) yields Equation

Table 2.2. Summary of CCC and IC equipment investigated (as of August 2008).

	Intelligent Compaction Features		
Roller Manufacturer	**Roller-Integrated Measurement**	**Automatic Feedback Control of:**	**GPS-Based Documentation**
Ammann/Case	Stiffness k_s	Eccentric force, amplitude, and frequency	Yes
Bomag	Stiffness E_{vib}	Vertical eccentric force amplitude	Yes
Caterpillar	MDP, CMV_C	None	Yes
Dynapac US	CMV_D	Eccentric force amplitude	Yes
Volvo	CMV_V	None	No
Sakai America	CCV	None	Yes

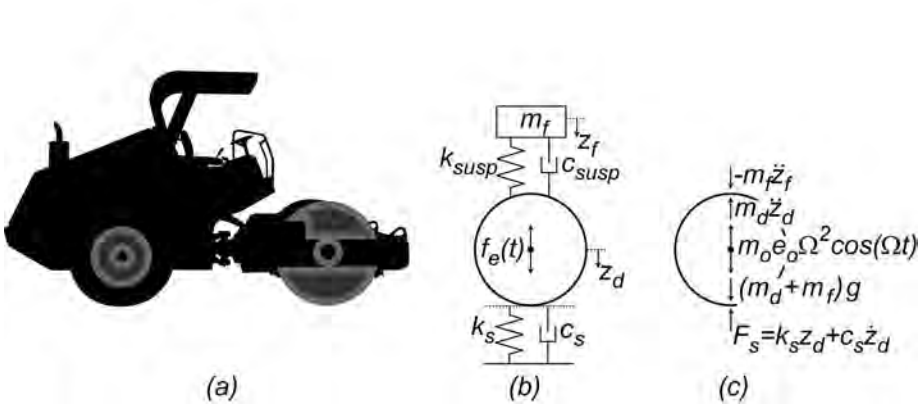

Figure 2.6. (a) vibratory compactor schematic; (b) two DOF model representation of vibratory compactor; (c) free body diagram of forces acting on the drum.

2.3, where ϕ is the phase lag between the eccentric force and drum displacement. The Ammann k_s is effectively the ratio of F_s to maximum vertical drum displacement $z_{d(max)}$ and occurs when the velocity equals zero (see Figure 2.7).

$$k_s = \Omega^2 \left[m_d + \frac{m_o e_o \cos(\phi)}{z_d} \right] \tag{2.3}$$

Accordingly, k_s can be determined from measured drum acceleration and phase lag. The accuracy of Ammann measurement data is as follows: $\Delta z_d = 0.001$ mm (0.00004 in); $\Delta\phi = 0.5°$; $\Delta\Omega = 0.31$ rad/s ($\Delta f = 0.05$ Hz) (R. Anderegg, personal communication, 2007).

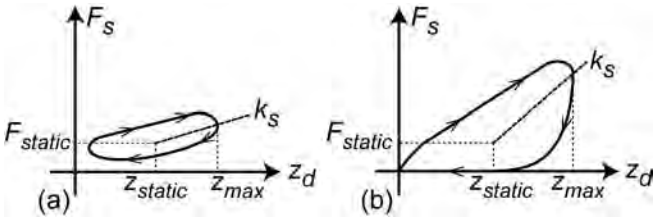

Figure 2.7. Illustration of k_s during (a) contact and (b) partial loss of contact.

2.2.1.2 Feedback Control

The Ammann ACE Plus eccentric assembly (shown in Figure 2.8) is comprised of outer and inner masses. The angle between the two masses, θ, is computer controlled and can be adjusted through a differential gear to provide maximum eccentric force ($\theta = 0°$), zero eccentric force ($\theta = 180°$), and any eccentric force in between ($0° < \theta < 180°$). The maximum eccentric mass moment $m_o e_o$ and associated theoretical drum displacement amplitude A for the Ammann model ASC 110/130 are 8.8 kg-m (63.7 lb-ft) and 2.2 mm (0.09 in), respectively. The ACE Plus system performs closed-loop feedback control of drum/soil contact force F_s. Three operator-selected levels of F_s are possible:

- Low force: $F_{s(max)}$ = 14 kN (3.1 kip), leading to measured z_d = 0.4 to 1.5 mm (0.02 to 0.06 in);
- Medium force: $F_{s(max)}$ = 20 kN (4.5 kip), leading to measured z_d = 1.0 to 2.0 mm (0.04 to 0.08 in);
- High force: $F_{s(max)}$ = unlimited, leading to measured z_d = 2.0 to 3.0 mm (0.08 to 0.12 in).

With a selected force level, the roller adjusts the eccentric mass moment to maintain the $F_{s(max)}$. The excitation frequency is adjusted to maintain a phase lag ϕ between 140° and 160°. For high-force levels, the frequency required to maintain the appropriate ϕ is 23 to 25 Hz. As the amplitude decreases, the frequency required to maintain the appropriate ϕ is higher—up to 35 Hz.

The ACE Plus system can also use a user-specified k_s value as the control parameter. In the so-called plate modulus measurement mode, a limit value for k_s is selected. When the pre-

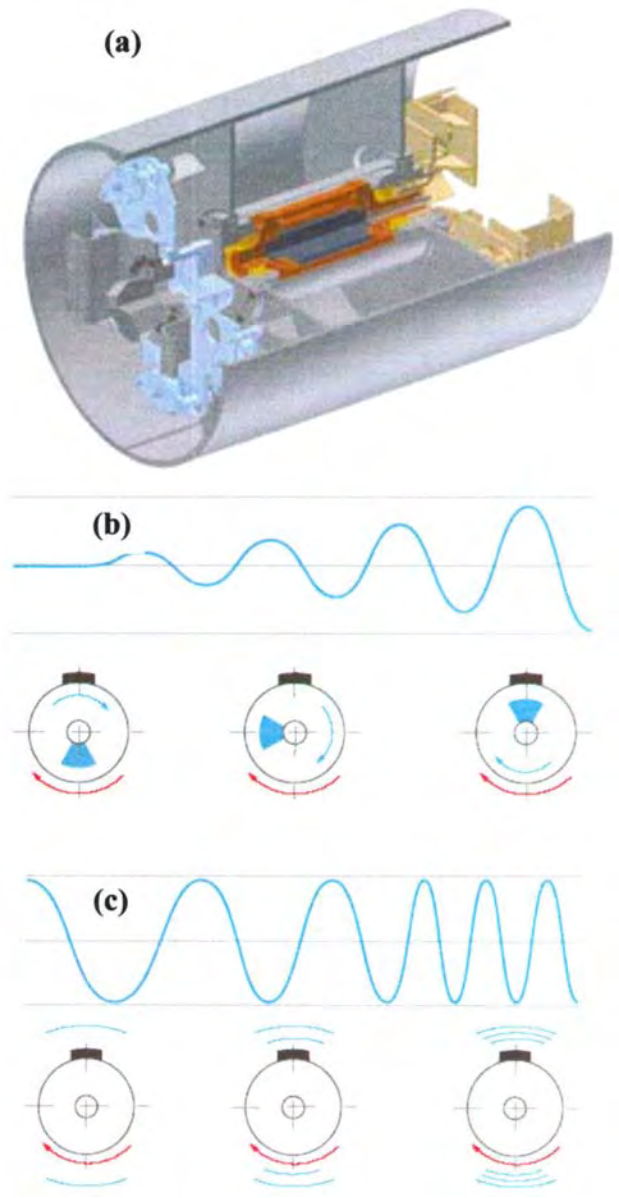

Figure 2.8. Two mass eccentric assembly (courtesy of Ammann).

determined value of k_s is reached, the ACE Plus system automatically decreases the eccentric mass moment to 0.5 $F_{s(max)}$ for the range chosen. In addition, the ACE Plus system calculates an optimal speed based on a desired impact spacing of 2 to 4 cm (0.8 to 1.6 in). The operator can use a gauge in the roller cab to perform open-loop control of speed. Finally, the ACE Plus system monitors for unstable rocking or jumping (primarily through analysis of subharmonics) and automatically decreases the eccentric mass moment until stable operation is restored.

2.2.1.3 GPS-Based Mapping and Documentation Software

The ACE Plus software (see Figure 2.9) marries k_s data with x, y, and z coordinates collected via onboard GPS equipment. Using differential GPS with real-time kinematic (RTK), Ammann indicates accuracies are ±10 cm (3.9 in). Without a reference signal (e.g., base station), the system has an accuracy within a few meters. Though k_s is determined for each vibration cycle (and with an x-direction resolution of 2 to 4 cm [0.8 to 1.6 in]), GPS coordinates are acquired once per second (once per 1 to 3 m [3.3 to 9.9 ft]). Currently, the ACE Plus system collects k_s data each cycle and reports an average k_s with GPS data at a frequency of 1 Hz. Ammann indicates that the time resolution in seconds is inversely proportional to the number of GPS receivers (e.g., three receivers will give a time resolution of 0.33 s). Roller MV reporting is discussed in more detail in Section 3.1.

Housed within a tablet PC onboard computer, the ACE Plus software maps a number of roller parameters in graphical view, as shown in Figure 2.9a. Data are downloaded from the onboard PC in text file format via USB memory stick. The data can be evaluated with any program. Ammann also provides PC-based software (Figure 2.9b).

2.2.2 Bomag Variocontrol System

2.2.2.1 Measurement Value

The Bomag Variocontrol system calculates a "vibration modulus" E_{vib} using lumped parameter vibration theory and cylinder on elastic half-space theory. The principle behind E_{vib} is presented in Kröber et al. (2001) and is briefly described here. To determine E_{vib} the drum/soil assembly is modeled as shown in Figure 2.6. Bomag uses constant frequency compaction, with Ω = 176 rad/s (f = 28 Hz). Bomag uses two accelerometers with measurement axes arranged at ±45° from vertical to measure vertical drum acceleration. Phase lag is calculated (specific method is confidential information), enabling determination of the contact force F_s per equilibrium of forces shown in Figure 2.6. The drum displacement is computed (confidential information). The combination of F_s and z_d data yield force-deflection curves from which soil stiffness can be extracted (Figure 2.10).

Along the way to determining E_{vib}, Bomag calculates a secant stiffness k from the compression portion of each F_s versus z_d cycle (Figure 2.10). To relate the measured F_s versus z_d behavior and stiffness k to modulus E, Bomag utilizes a theoretical solution for a rigid cylinder resting on a homogeneous, isotropic, elastic half-space (see Figure 2.11) developed by Lundberg (1939). Lundberg's theory is a static solution and

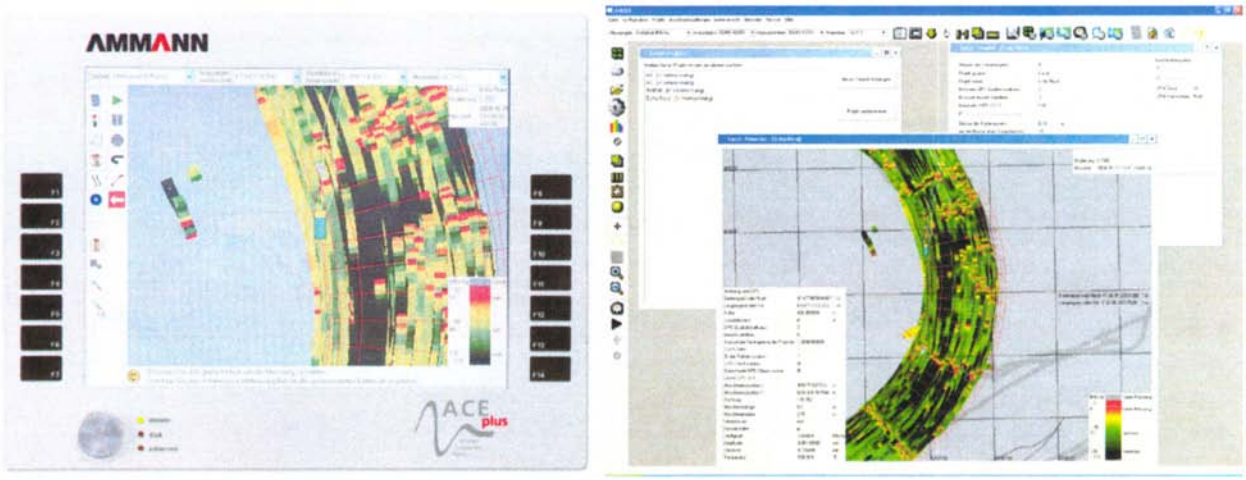

Figure 2.9. (a) Ammann ACE Plus onboard tablet PC and software; (b) office PC software (courtesy of Ammann).

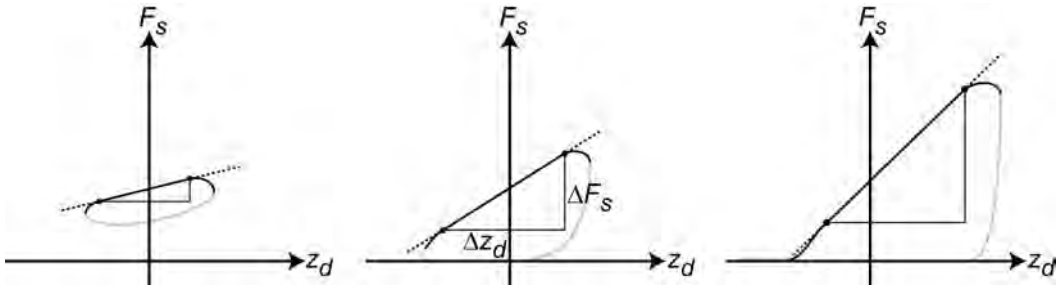

Figure 2.10. Contact force–drum displacement behavior, $F_s = F_B$ (adapted from Kröber et al. 2001).

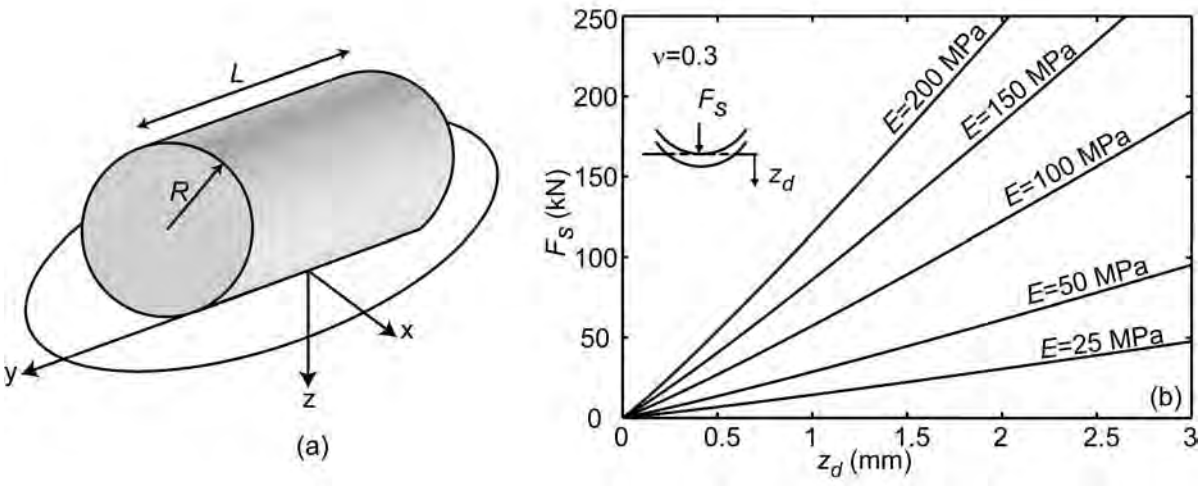

Figure 2.11. Drum on elastic half-space and relationship between stiffness k and modulus E (adapted from van Susante & Mooney 2008).

relates z_d, F_s, drum length L, and radius R to Poisson's ratio ν and Young's modulus E of the half-space as shown in Equation 2.4:

$$z_d = \frac{2\times(1-\nu^2)}{\pi\times E}\times\frac{F_s}{L}\times\left(1.8864+\ln\frac{L}{b}\right) \quad (2.4)$$

where b is the contact width as given by:

$$b=\sqrt{\frac{16\times R\times\left(1-\nu^2\right)}{\pi\times E\times L}\times F_s} \quad (2.5)$$

Bomag uses ν = 0.25 for soil. The nonlinear relationship between stiffness k and E is shown in Figure 2.11. The Variocontrol system determines the appropriate E (referred to as E_{vib}) via a fitting approach.

2.2.2.2 Feedback Control

The Bomag Variocontrol system uses a counterrotating eccentric mass assembly that is directionally vectored to vary the *vertical* excitation force (Figure 2.12). The counterrotating masses each create a centrifugal force. When the masses are opposite each other in their rotation cycles, the centrifugal force and thus the eccentric force are zero. Conversely, when the counterrotating masses pass each other, the eccentric force is maximum. The Variocontrol system rotates the entire counterrotating mass assembly to control the vector angle α at which maximum and minimum eccentric forces occur. Figure 2.12 illustrates this concept. As a result, when the Variocontrol system provides maximum vertical excitation (maximum drum displacement amplitude), the horizontal excitation is zero. Conversely, when the vertical excitation is zero (minimum drum displacement), the horizontal excitation is maximum. Accordingly, when rewritten to account for vectoring, Equation 2.1 appears as Equation 2.6:

$$F(t)=m_o e_o \Omega^2 \sin(\alpha)\cos(\Omega t)=F_{ev}\cos(\Omega t) \quad (2.6)$$

The Variocontrol system allows the operator to preselect from six maximum theoretical drum displacement amplitude options (and corresponding vector angles): 0, 0.6, 1.2, 1.7, 2.1, and 2.5 mm (0, 0.024, 0.047, 0.067, 0.083, and 0.098 in). Within a maximum amplitude setting, the Variocontrol system begins operation at the vector angle α corresponding to maximum amplitude until the target E_{vib} value is reached. Once reached, the vector angle is decreased in the areas where the target E_{vib} has been reached [to a theoretical amplitude = 0.4 mm (0.016 in)]. Figure 2.13 illustrates this principle. The Variocontrol system also allows for manual mode operation

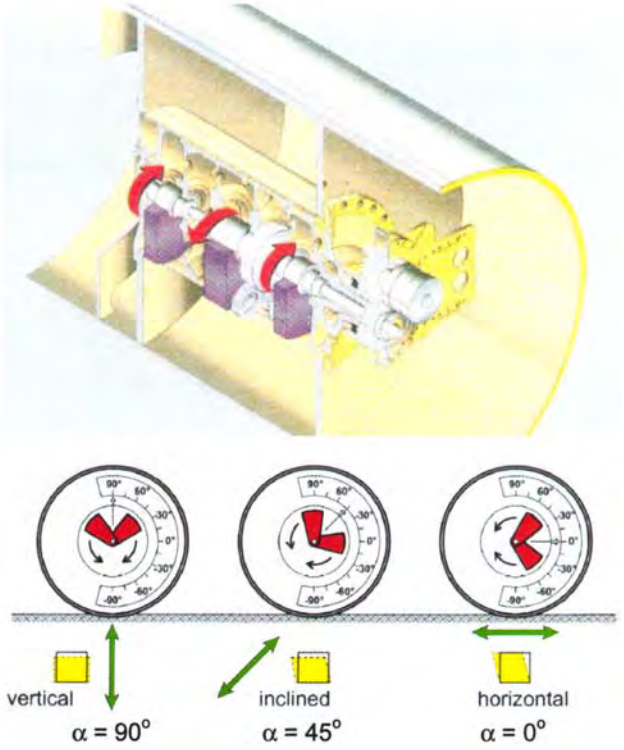

Figure 2.12. Bomag counterrotating eccentric mass assembly and vectoring of assembly to vary vertical eccentric force (courtesy of Bomag).

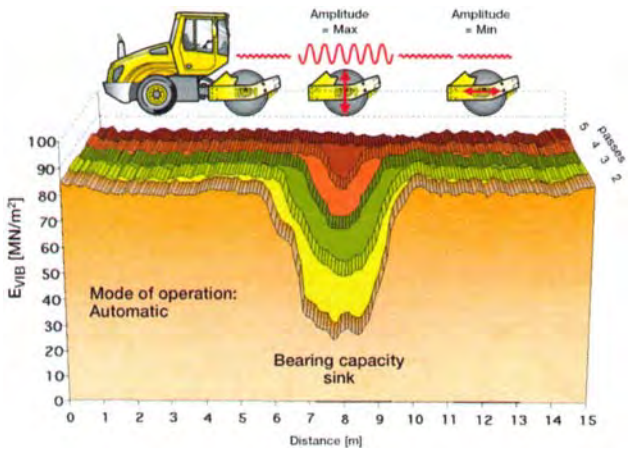

Figure 2.13. Principle of variable-amplitude system (courtesy of Bomag).

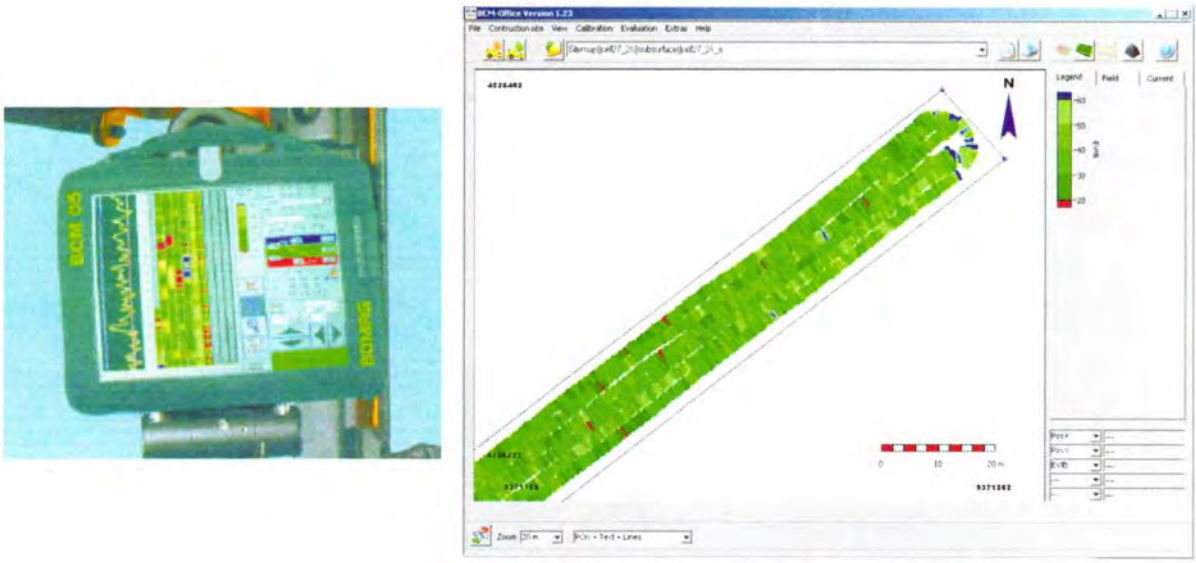

Figure 2.14. Bomag documentation system (images courtesy of Bomag).

in one of the six maximum amplitude settings. In manual mode the vector angle corresponding to the selected maximum amplitude remains constant throughout operation. Because there is theoretically no vertical vibration in setting 1 (amplitude = 0 mm), E_{vib} is not measured. In Variocontrol mode the minimum amplitude for which E_{vib} is reported is 0.4 mm (0.016 in). Finally, the Variocontrol monitors for jumping and automatically decreases F_{ev} until stable operation is restored.

2.2.2.3 GPS-Based Mapping and Documentation Software

Bomag's documentation system (BCM 05) includes a tablet PC, mobile software, and a USB memory stick for data transfer (see Figure 2.14). A screenshot from the Bomag software is also illustrated in Figure 2.14. Bomag can accept any GPS receiver capable of providing GGA or PJK data via RS232 interface. Bomag has also used a correction service (e.g., Omnistar, Starfire) with reported accuracies of ±10 to 50 mm (0.4 to 2 in). Bomag has used 10-Hz GPS receivers. The E_{vib} at the sampled GPS coordinates is reported and stored; additional data averaging is not performed.

2.2.3 Dynapac Compaction Analyzer and Compaction Optimizer

2.2.3.1 Measurement Value

The Dynapac Compaction Meter uses the CMV as a measure of the level of compaction. The CMV was developed by Geodynamik in the 1970s and introduced commercially in 1980. CMV is defined as the ratio of the second harmonic of the vertical drum acceleration frequency domain amplitude $A_{2\Omega}$ (operating frequency Ω) divided by the first harmonic of the vertical drum acceleration frequency domain amplitude A_{Ω} multiplied by a constant c (typically 300; see Equation 2.7).

$$\text{CMV} = c\frac{A_{2\Omega}}{A_{\Omega}} \tag{2.7}$$

A sister parameter called the resonance meter value (RMV) is defined by the ratio of the 0.5Ω subharmonic acceleration amplitude to the first harmonic. Subharmonic content occurs when the drum begins to jump. CMV is determined by first performing spectral analysis of the measured vertical drum acceleration over two cycles of vibration (Figure 2.15). The reported CMV is the average of a number of two-cycle calculations. Geodynamik typically averages over 0.5 s; however, this is customized to meet the manufacturer's needs. For example, the Dynapac Compaction Meter reports CMV every 1.0 s, implying that the reported CMV is an average of approximately 15 two-cycle calculations values. CMV precision is governed by 1% distortion resolution of the accelerometer. Per Equation 2.7, 1% acceleration distortion equates to CMV = 3 or ± 1.5.

2.2.3.2 Feedback Control

The Dynapac Compaction Optimizer (DCO) performs feedback control of the eccentric excitation force (and thus theoretical amplitude) to prevent jumping. As shown in Figure 2.16, a dual-mass eccentric configuration is used to pro-

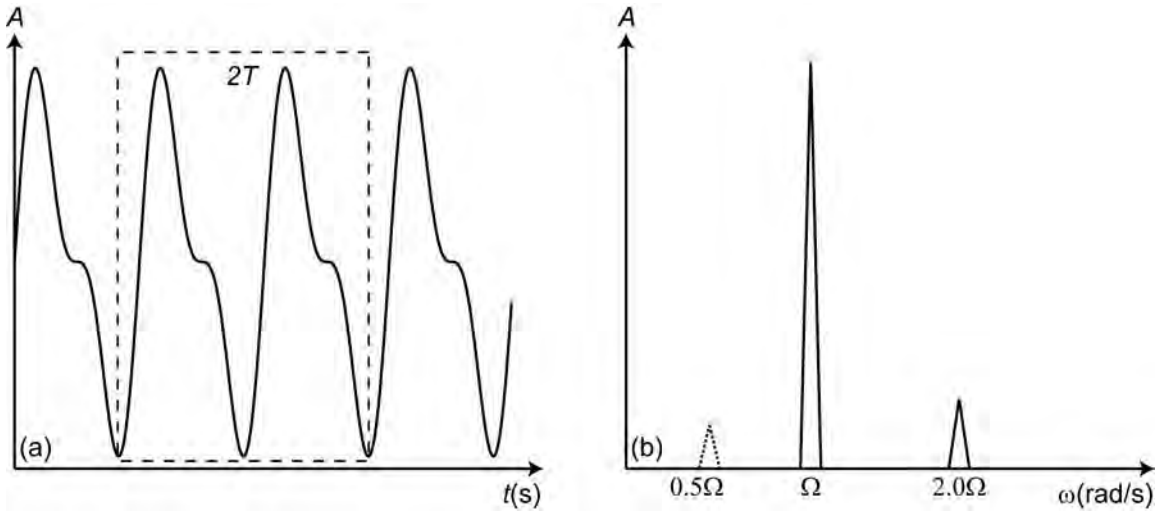

Figure 2.15. Method to determine CMV involves spectral analysis (b) of two cycles of vertical drum acceleration time history data (a).

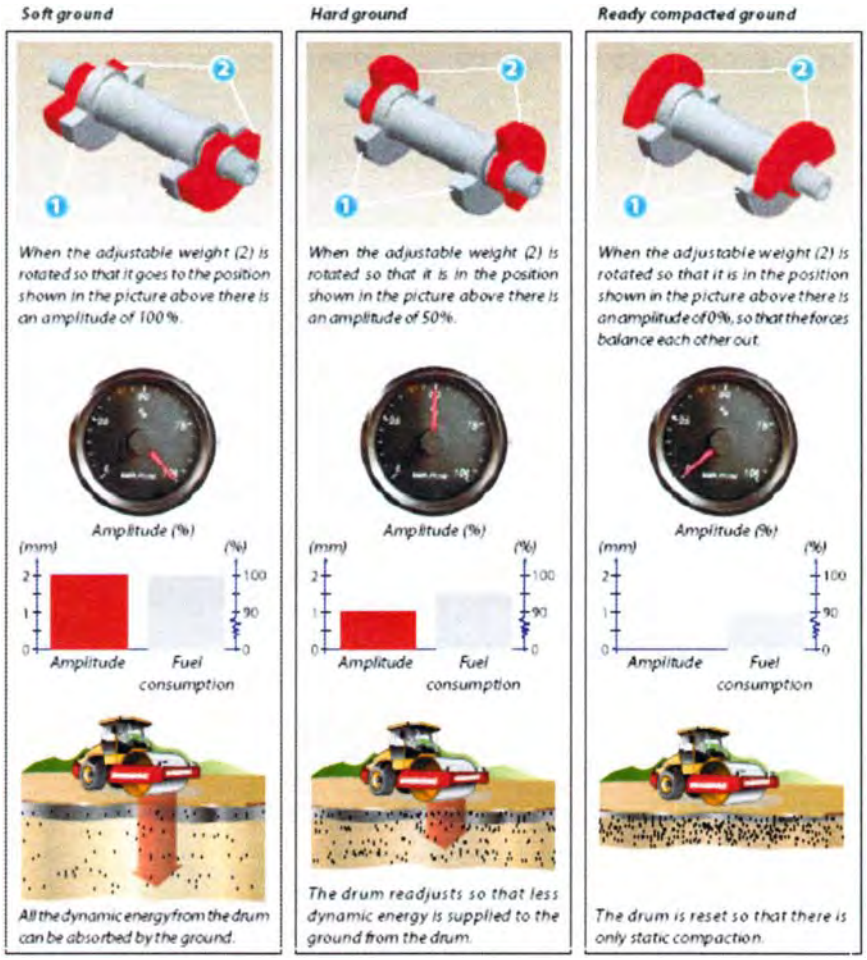

Figure 2.16. Overview of Dynapac's Compaction Optimizer (DCO) (courtesy of Dynapac).

vide any theoretical amplitude between 0 and 2 mm (0 to 0.078 in). The DCO maintains a vibration frequency of 28 Hz. Jumping is prevented by monitoring the RMV. When a threshold RMV is approached, the amplitude is reduced accordingly. The DCO allows operation in one of six automatic settings, with maximum amplitudes of 0.40, 0.65, 0.90, 1.40, 1.80, and 2.00 mm (0.016, 0.026, 0.035, 0.055, 0.071, and 0.079 in). During operation the DCO continuously compares the measured RMV with the threshold RMV. If the measured RMV is less than the threshold RMV, the roller is operated at its maximum amplitude (e.g., 0.40, 0.65 mm). Otherwise, the amplitude is reduced accordingly. Dynapac does not currently use feedback control based on CMV.

2.2.3.3 GPS-Based Mapping and Documentation Software

The Dynapac Compaction Analyzer (DCA) and accompanying field computer registers all pertinent roller data (e.g., CMV, pass number, amplitude, frequency, GPS coordinates) with presentation in graphical format for the operator (Figure 2.17). The DCA is compatible with any GPS receiver brand as long as the correct National Marine Electronics Association (NMEA) messages are available. Dynapac has used differential GPS (DGPS) receivers with submeter accuracy for x and y coordinates. RTK receivers have been used with better results. Dynapac has also used satellite correction via Omnistar. The DCA records the z coordinate; however, with DGPS the accuracy is normally less than the layer thickness and is thus not displayed. The DCA software records all compaction data in local coordinates via local transformation between world geodetic system (WGS 84) and the local grid. The DCA also utilizes the road alignment parameters to show the operator the current position of the machine and to position the measured values.

Since the DCA produces a CMV every 1.0 s, the spatial resolution of recorded data depends on the roller speed used for measurement. Dynapac recommends a speed of approximately 1.0 m/s (3.3 ft/s), which provides an x-direction spatial resolution of 1.0 m (3.3 ft). The y-direction resolution is the width of the drum [typically 2.13 m (7.0 ft)]. Data can be exported from the field computer as a text file to be imported for further analysis. Paper printouts can be created for further documentation. The DCA software is available in an office version, so all preparations can be made and the final data can be analyzed.

2.2.4 Caterpillar

2.2.4.1 Measurement Values

Caterpillar uses the Geodynamic CMV measurement system. In addition, Caterpillar uses MDP. The use of MDP as a measure of soil compaction is a concept originating from study of vehicle-terrain interaction (see Bekker 1969). MDP uses the concepts of rolling resistance and sinkage to determine the stresses acting on the drum and the energy necessary to overcome the resistance to motion (Figure 2.18). MDP is calculated as:

$$\mathrm{MDP} = P_g - WV\left(\sin\theta + \frac{a}{g}\right) - (mV + b) \tag{2.8}$$

where P_g is the gross power needed to move the machine, W is roller weight, a is machine acceleration, g is acceleration of gravity, θ is slope angle (roller pitch), V is roller velocity, and m and b are machine internal loss coefficients specific to a

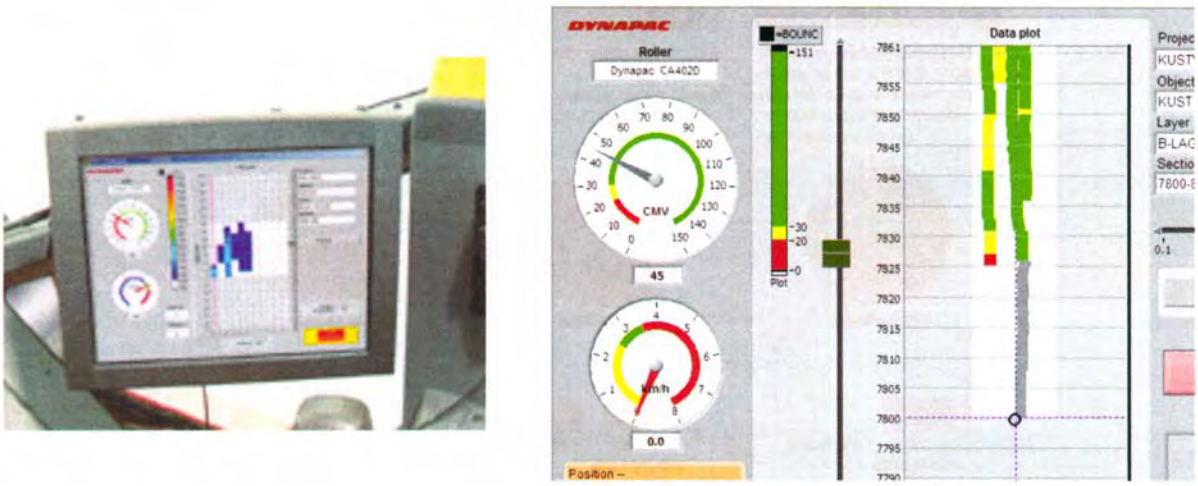

Figure 2.17. Dynapac onboard software and PC (courtesy of Dynapac).

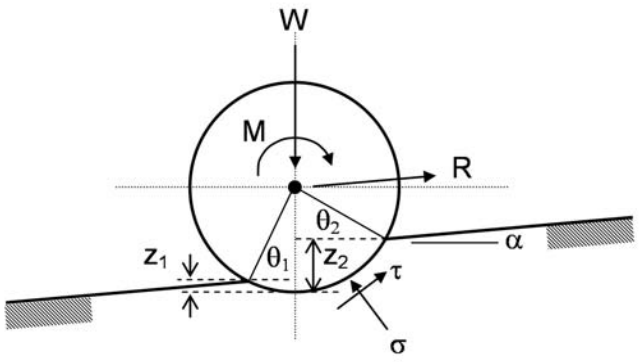

Figure 2.18. Simplified two-dimensional free body diagram of stresses acting on a rigid compaction drum (MDP increases with increasing z_2).

particular machine (White et al. 2006). The second and third terms of Equation 2.7 account for the machine power associated with sloping grade and internal machine loss, respectively. Therefore, MDP represents only the machine power associated with material properties.

Prior to its use, MDP is calibrated for θ, *m*, and *b* (see Equation 2.7). First, the orientation of the roller pitch sensor is found by noting the pitch readings when the roller is parked on the same sloping surface facing uphill and downhill. The average of these two readings is the pitch offset applied to all later sensor readings. The internal loss coefficients *m* and *b* are then found by operating the roller on a relatively uniform, unchanging calibration surface. P_g and slope compensation (i.e., the second term of Equation 2.7) are monitored while operating the roller in both forward and reverse directions at the range of roller speeds anticipated during construction operations, generally 3 to 8 km/h (1.9 to 5.0 mph). At each roller speed the difference between P_g and slope compensation is taken as the internal machine loss. Plots of slope-compensated machine power versus roller speed provide linear relationships from which the internal loss coefficients *m* and *b* are calculated. By incorporating both slope compensation and internal machine loss into Equation 2.7, MDP for roller operation on the calibration surface is approximately 0 kJ/s. MDP is a relative value referencing the material properties of the calibration surface, which is generally a stiff, fully compacted soil. Positive MDP values therefore indicate material that is less compact than the calibration surface, while negative MDP values would indicate material that is more compact (i.e., less roller drum sinkage).

2.2.4.2 GPS-Based Mapping and Documentation Software

Caterpillar's Compaction Viewer software was used during testing. A Navigator 10.4cTS operator interface is located within the operator's field of view and performs data acquisition functions as well as displaying real-time position and compaction values. The system uses RTK GPS with accuracy capabilities of ±10 mm (0.4 in) in the horizontal plane and ±20 mm (0.8 in) in the vertical plane. The roller width is divided into a series of 30-cm (12-in) divisions for mapping roller coverage. Postprocessing and visualization of data can be performed with Caterpillar's Compaction Viewer software on a PC. Caterpillar has developed a production version mapping and documentation system for use with commercially available machines. This system is compatible with the AccuGrade software produced by Caterpillar for earthwork applications (Figure 2.19).

2.2.5 Sakai

2.2.5.1 Measurement Value

Sakai CCC rollers employ a CCV index. The unitless CCV is an extension of the CMV. The Sakai measurement system involves one accelerometer to monitor vertical drum vibration. Analog bandpass filters are used to capture acceleration at the excitation frequency Ω_0 and at 0.5 Ω_0, 1.5 Ω_0, 2 Ω_0, 2.5 Ω_0, and 3 Ω_0 (see Figure 2.20). The amplitudes at each of these frequency components are used to determine the CCV, as shown in Equation 2.9. CCV is provided at a rate of 5 Hz.

$$CCV = \left[\frac{A_1 + A_3 + A_4 + A_5 + A_6}{A_1 + A_2} \right] \times 100 \qquad (2.9)$$

2.2.5.2 GPS-Based Mapping and Documentation Software

Sakai has implemented GPS-based mapping and documentation software for its Compaction Information System. The onboard PC and screen are illustrated in Figure 2.21. Office PC software is also provided.

2.3 Existing CCC Specifications

Specifications to use roller-integrated measurement systems for CCC have been introduced in Austria (in 1990, with revisions in 1993 and 1999), Germany (1994, with revision in 1997), and Sweden (1994, with revision in 2004). The ISSMGE recently developed recommended construction specifications based primarily on the Austrian specifications

Figure 2.19. CD700 Caterpillar documentation system illustrating completed passes (left) and CMV (right) (courtesy of Caterpillar).

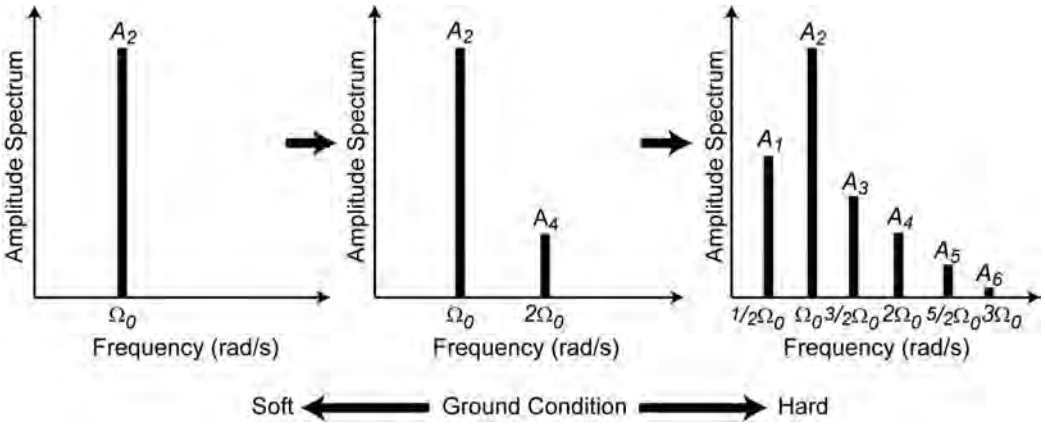

Figure 2.20. Drum acceleration frequency domain components used in Sakai CCV (adapted from Scherocman et al. 2007).

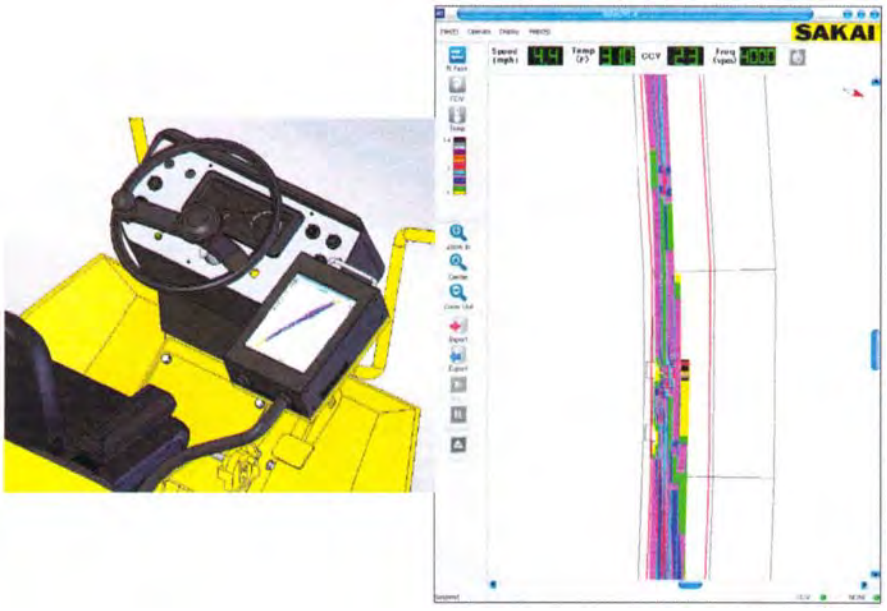

Figure 2.21. Example of Sakai display (courtesy of Sakai).

(Adam 2007). In the United States, Minnesota implemented pilot specifications for CCC in 2007–2008 and has developed a revised 2009 specification. The principal components of the various specifications and planned revisions are described below.

2.3.1 German CCC Specifications

German specifications for earthwork QC/QA using CCC were introduced in 1994 and updated in 1997. Further revisions are expected in 2009. Referred to as ZTVE-StB, the German CCC specifications apply to subgrade and embankment soils. The lack of CCC specifications for base and subbase layers is predicated on the belief that roller MVs measure much deeper than the 20- to 30-cm-thick base course layers used in Germany. There are two ways in which CCC can be specified in Germany. First, CCC can be implemented through initial calibration of roller MVs to PLT modulus or density and subsequent use of the correlation during QA. A second approach uses CCC to identify weak areas for spot testing via PLT, LWD, or density methods. The key elements of each approach are described here, as are the proposed 2009 revisions.

2.3.1.1 Calibration Approach (Method M2 in German Specifications)

This CCC approach involves two principal steps: (1) on-site initial calibration to develop the correlation(s) between the roller MV to be used and soil density or PLT modulus (E_{V2}); (2) identification of roller MV target value (MV-TV) consistent with required density or E_{V2}; and (3) acceptance testing by comparing roller MV data against the MV-TV. Calibration is performed on an area equal to three 20-m (66-ft)-long (minimum) test strips (see Figure 2.22). Roller MV data are collected during roller operation on a low degree of compaction test strip (e.g., after one compaction pass), a medium degree of compaction test strip (e.g., three to five compaction passes), and a high degree of compaction test strip (multiple passes until no further compaction observed). Three to five static PLTs or density tests are performed on each test strip. Regression analysis is performed on the roller MV versus spot-test data (see Figure 2.22). When using the PLT, the German procedure uses the unload-reload secant modulus (M_{E2} or E_{V2}). The correlation coefficient r must be ≥ 0.7 ($R^2 \geq 0.5$). Additional spot tests may be performed to achieve $R^2 \geq 0.5$. If $R^2 \geq 0.5$ cannot be achieved, CCC is not permitted via Method M2.

The regression equation and required minimum values for E_{V2} or density lead to determination of an MV-TV. In Germany, minimum E_{V2} values must be achieved for the top of subgrade. Specifically, E_{V2} must be 45 MPa for clay or silty soils and 80 to 100 for granular materials. Density requirements (typically 98% standard Proctor) exist for all layers below the top of subgrade. There are no moisture requirements.

During acceptance testing, 90% of all roller MVs in an evaluation area must exceed the MV-TV value. There are currently no additional criteria for acceptance using this method. The German specification does not permit variable frequency and amplitude control or jump-mode during calibration or acceptance testing. The project site must be homogeneous in soil type and in underlying stratigraphy; otherwise CCC-based QA is not recommended.

The German group overseeing the CCC specifications is planning some moderate updates (G. Bräu, personal communication, 2008). The LWD or dynamic PLT may be used in place of the static PLT. Target values of LWD modulus (E_{LWD}) will be published but were not available at press time. In addition, the issue of uniformity criteria was addressed. The German specifications will require that the 10% of MVs that fall below MV-TV be reasonably distributed around the evaluation area. Acceptance of this issue will be subjective and left to the on-site engineer. The German specifications will include

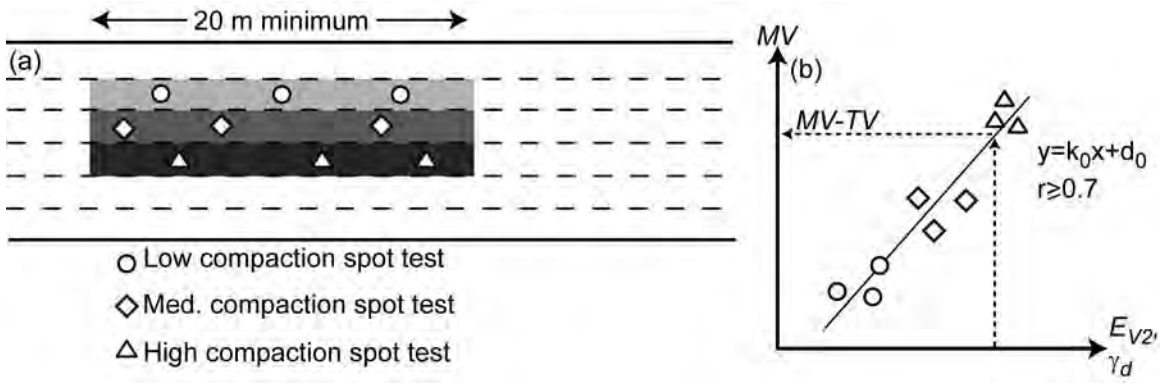

Figure 2.22. Illustration of calibration approach for German specifications.

language permitting the use of automatic feedback control intelligent compaction rollers during compaction but will prohibit their use during calibration and acceptance testing.

2.3.1.2 CCC to Identify Weak Areas for Spot Testing

In this approach, CCC is used to map the compacted area. The weakest spots are identified from the roller-generated maps for spot testing (density methods or PLT). A minimum number of spot tests are specified (e.g., four per 5,000 m^2). To meet acceptance, each density or E_{V2} value must be greater than or equal to the desired value. If acceptance is not achieved, the soil must be reworked until the criterion is met. Assuming roller operating parameters are held constant and the soil, moisture, and subsurface have not changed, then by inference all other areas of the map meet acceptance. There is no initial calibration required for this approach. This approach is the more common of the two approaches used in Germany (G. Bräu, personal communication, 2008).

2.3.2 Austrian/ISSMGE Specifications

Austria first introduced roller-integrated CCC specifications in 1990 with revisions in 1993 and 1999. Further revisions are not currently being considered. The ISSMGE recently developed recommended CCC specifications (ISSMGE 2005), largely based on Austrian standards (Adam 2007). The Austrian/ISSMGE specifications allow two different approaches for roller-integrated CCC. The first approach involves acceptance testing using a regression-based correlation developed during on-site calibration. An alternative approach, recommended for small sites or where calibration cannot be performed, involves compaction with roller-integrated measurement until the mean roller MV increases by no more than 5%. Acceptance is then based on static PLT or LWD (dynamic PLT) modulus at the weakest area. In the Austrian/ISSMGE specifications, roller MVs must be dynamic (i.e., based in part on measurement of drum acceleration). The specification is applicable to all subgrade, subbase, and base materials and recycled materials that can be compacted dynamically and statically. For soils compacted dynamically, measurement occurs during compaction. For soils compacted statically, dynamic measurement occurs after static compaction. If the fine-grained portion [< 0.06 mm (0.002 in)] exceeds 15%, moisture content must be given special attention; however, moisture content criteria are not specified.

2.3.2.1 Method 1: Acceptance Based on Calibration

The more recently developed Austrian/ISSMGE roller-integrated CCC method involves the development of a relationship between roller MV and the initial PLT modulus E_{V1} or E_{LWD}. Density spot testing is allowed as an alternative, although it is not recommended. Calibration is required over the entire width of the construction site and for a length of at least 100 m (328 ft) for each material (subgrade, subbase, and base). Roller-integrated measurement must be carried out with constant roller parameters (frequency, amplitude, and forward velocity) throughout calibration. Roller MV data are captured during each measurement run, and subsequent PLT or LWD testing is performed at values of low, medium, and high roller MV (see Figure 2.23). PLT is required at a minimum of nine locations. If LWD testing is used, the average of

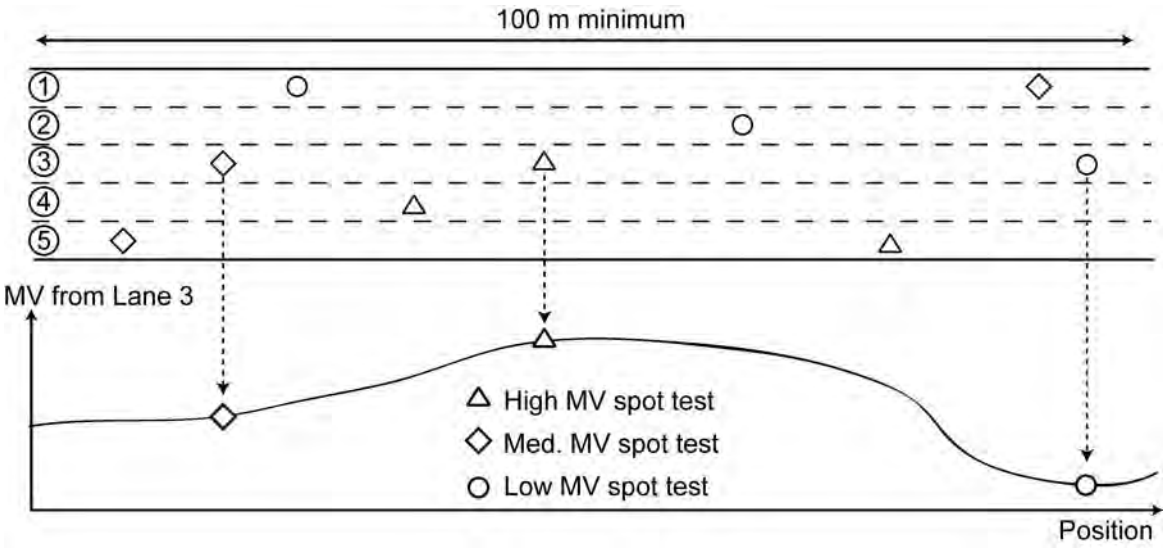

Figure 2.23. Illustration of calibration approach for Austrian/ISSMGE specifications.

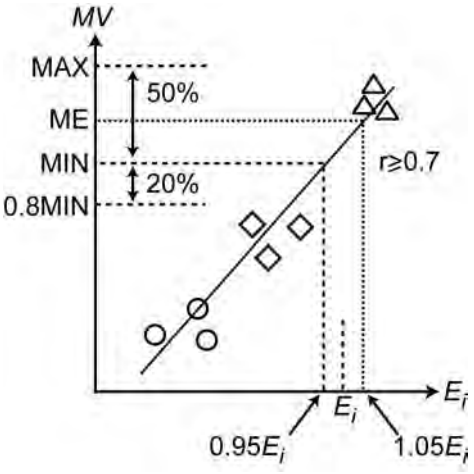

Figure 2.24. Roller MV vs. E_{V1}/E_{LWD} regression and key parameters in Austrian/ISSMGE specifications.

four E_{LWD} values at a minimum of nine locations is reported (hence 36 LWD tests are required). The engineer of record is given the authority to design the rolling and measurement pattern used during calibration.

Linear regression analysis is performed on the resulting roller MV versus E_{V1} or E_{LWD} values (see Figure 2.24). The regression coefficient R^2 must be ≥ 0.5; additional PLT or LWD tests may be performed to achieve $R^2 \geq 0.5$. The engineer of record may remove outliers if good cause exists. This approach may not be carried forward to production QA if $R^2 < 0.5$. Using the regression equation and a specified E_{V1} or E_{LWD} (see Table 2.3 for Austrian values) leads to determination of a minimum roller MV (MIN) and a mean roller MV (ME). As illustrated in Figure 2.24, the MIN corresponds to 0.95 E_{V1} or E_{LWD}, and the ME corresponds to 1.05 E_{V1} or E_{LWD}. The MAX value is defined to be 1.5 MIN. The Austrian/ISSMGE acceptance criteria are summarized as follows:

- The mean roller MV must be ≥ ME;
- 100% of roller MVs must be ≥ 0.8 MIN;
- 90% of roller MVs must be ≥ MIN.

In addition to these requirements, compaction must be continued until the mean roller MV is less than 5% greater than the mean value from the previous pass. The Austrian/ISSMGE specification also requires the following uniformity criteria:

- If 100% of roller MVs ≥ MIN, then the roller MV coefficient of variation (COV) for the entire area must be ≤ 20%.
- If 0.8 MIN ≤ minimum roller MV ≤ MIN, then 100% of roller MVs must be ≤ MAX = 1.5 MIN.

Table 2.3. E_{V1} and E_{LWD} values required (Austria).

Level	E_{V1} (MN/m²)
1 m below subgrade[a]	15 (cohesive); 20 (cohesionless)
Top of subgrade	25 (cohesive); 35 (cohesionless)
Top of subbase	60 (rounded); 72 (angular)
Top of base	75 (rounded); 90 (angular)
Level	**E_{LWD} (MN/m²)**
1 m below subgrade[a]	18 (cohesive); 24 (cohesionless)
Top of subgrade	30 (cohesive); 38 (cohesionless)
Top of subbase	58 (rounded); 68 (angular)
Top of base	70 (rounded); 82 (angular)

[a]If fill section is to be constructed.

The recommended control area over which acceptance should be performed has traditionally been 100 m (328 ft) long by the width of the roadway. However, recent experience with 200- to 500-m (656- to 1,640-ft)-long control areas has shown effective results (D. Adam, personal communication, 2008). These ISSMGE/Austrian correlations and acceptance criteria are valid for roller/soil contact and partial loss of contact roller operation. The Austrian/ISSMGE specifications permit measurement during double jump mode; however, a separate calibration is required for such operation.

2.3.2.2 Method 2: Acceptance Based on Percentage Change of MVs

For small construction sites and areas where calibration cannot be reasonably performed, the Austrian/ISSMGE recommends the following method. Compaction should be continued until the mean roller MV is less than 5% greater than the mean roller MV from the previous pass. Subsequently, PLT or LWD testing is conducted at the weakest area as determined by the roller MV output. The E_{V1} or E_{LWD} must be greater than or equal to the required value (e.g., Table 2.3 for Austria). A minimum of three PLT or nine LWD tests must be performed in the weakest area.

2.3.3 Swedish CCC Specifications

Specifications for the use of CCC on unbound materials in Sweden were first introduced in 1994; current use of roller-integrated CCC is governed by 2005 specifications (ATB Vag 2005). The QA of unbound material is mandated at two surface levels: (1) top of the base course and (2) a layer 300 to 750 mm (1 to 2.5 ft) below the top of the base layer. Typically, Swedish construction includes a 300- to 700-mm (1- to 2.3-ft)-thick base layer and a 300- to 500-mm (1- to 1.6-ft) subbase or frost protection layer. Therefore, QA is typically performed on the surface of the base and subbase layers. QA is not required for the subgrade due primarily to the consid-

erable thickness of base and subbase layers used. The maximum percentage of particles less than 0.06 mm (0.002 in) permitted in base and subbase layers is 7%; therefore, by default CCC is only performed on material with predominantly cohesionless soil.

Swedish specifications permit the use of roller-integrated CCC to identify weak spots for PLT. First, it is useful to explain the general QA specification. In Sweden, conventional QA of base and subbase layers is based solely on PLTs performed at a minimum of eight randomly selected locations within each 5,000 m^2 (1,993 yd^2) control area. Density and moisture QA are not prescribed. The number of tests can be reduced to five if no previous control area has failed or if the standard deviation σ is small. The unload-reload PLT deformation modulus E_{V2} and the ratio E_{V1}/E_{V2} are used. All measured E_{V2} values must exceed a layer-dependent minimum value for acceptance (see Table 2.4). The average E_{V2} should also meet the criteria summarized in Table 2.4. If criterion 2 is violated, an alternative can be used for the top 500 mm (1.6 ft) only.

When using roller-integrated CCC, the number of PLTs can be reduced to two. The PLTs are conducted at the two weakest areas as indicated by the roller MV data map. The number of PLTs can be reduced from two to one if no control area has failed the test or the previous control areas show small variations. The criteria for acceptance are summarized in Table 2.5. The E_{V2} value in these points must not be lower than the threshold value, which is different for different levels below the top of the base layer and for flexible and rigid pavements. For granular base materials an additional criterion based on the E_{V2}/E_{V1} ratio must also be fulfilled.

LWD testing cannot currently be used in place of static PLT for QA of base and subbase materials. Sweden does recommend QC/QA during subgrade compaction via either PLT or LWD testing. LWD testing can be used instead of PLT "if similar results can be shown." The Swedish specifications provide recommended E_{V2} and E_{LWD} for depths of 800 mm (2.6 ft) or greater (see Table 2.6). A note within the specifications states that the average of five LWD tests can be used over a 2,500-m^2 (997-yd^2) area.

Table 2.4. Unbound material acceptance criteria [per 5,000-m^2 (1,993-yd^2) control area].

		Asphalt Pavement			Concrete Pavement		
Depth Below Base Course Surface (mm)	*N*	(1) $E_{V2(min)}$ (MPa)	(2) $E_{V2(ave)}$ (MPa)	(3) E_{V2}/E_{V1} Alternative if (2) not met	(1) $E_{V2(min)}$ (MPa)	(2) $E_{V2(ave)}$ (MPa)	(3) E_{V2}/E_{V1} Alternative if (2) not met
0–250	8	125	$\geq 140 + 0.96\sigma$	≤ 2.8	105	$\geq 120 + 0.96\sigma$	≤ 2.8
0–250	5	125	$\geq 140 + 0.83\sigma$	$1 + 0.013\ E_{V2}$	105	$\geq 120 + 0.83\sigma$	$1 + 0.015\ E_{V2}$
251–500	8	32	$\geq 40 + 0.96\sigma$	≤ 3.5	45	$\geq 55 + 0.96\sigma$	≤ 3.5
251–500	5	32	$\geq 40 + 0.83\sigma$	$\leq 1 + 0.063\ E_{V2}$	45	$\geq 55 + 0.83\sigma$	$\leq + 0.046\ E_{V2}$
500–550	8	32	$\geq 40 + 0.96\sigma$	NA	45	$\geq 55 + 0.96\sigma$	NA
500–550	5	32	$\geq 40 + 0.83\sigma$	NA	45	$\geq 55 + 0.83\sigma$	NA
551–650	8	20	$\geq 30 + 0.96\sigma$	NA	30	$\geq 35 + 0.96\sigma$	NA
551–650	5	20	$\geq 30 + 0.83\sigma$	NA	30	$\geq 35 + 0.83\sigma$	NA
651–750	8	15	$\geq 20 + 0.96\sigma$	NA	20	$\geq 25 + 0.96\sigma$	NA
651–750	5	15	$\geq 20 + 0.83\sigma$	NA	20	$\geq 25 + 0.83\sigma$	NA

NA= not applicable

Table 2.5. Unbound material acceptance criteria when CCC used [per 5,000-m^2 (1,993-yd^2) control area].

		Asphalt Pavement		Concrete Pavement	
Depth Below Base Course Surface (mm)	*N*	(1) $E_{V2(min)}$ (MPa)	(2) E_{V2}/E_{V1} Alternative if (2) not met	(1) $E_{V2(min)}$ (MPa)	(2) E_{V2}/E_{V1} Alternative if (2) not met
0–250	1–2	125	$\leq 1 + 0.0136\ E_{V2}$	105	$\leq 1 + 0.0162\ E_{V2}$
251–500	1–2	32	$\leq 1 + 0.078\ E_{V2}$	45	$\leq 1 + 0.056\ E_{V2}$
500–550	1–2	32	NA	45	NA
551–650	1–2	20	NA	30	NA
651–750	1–2	15	NA	20	NA

Table 2.6. Recommended PLT and LWD QA values at depth.

Depth Below Base Course Surface (mm)	Construction with Only Base and Subbase Material Above Crushed Rock		Construction with Only Base and Subbase Material Above Sand Subgrade	
	E_{V2} (MPa)	E_{LWD} (MPa)	E_{V2} (MPa)	E_{LWD} (MPa)
800	12	10–15	16	12–18
900	9	8–12	11	10–14
1,000	6	5–8	8	7–11
1,100	4	4–5	5	5–8
1,200	3	3	4	3–5
1,300	2	2	3	3

2.3.4 Minnesota DOT Pilot Specifications

In 2007 the Minnesota Department of Transportation (Mn/DOT) developed pilot specifications for QC/QA of granular and nongranular embankment soil compaction using CCC and/or LWD. At the time of this writing, Mn/DOT was in the process of revising these specifications; the most recent version is available online at *http://www.dot.state.mn.us/materials/gbintellc.html*. The 2007 specification required QC by the contractor and QA by the engineer on designated proof layers to ensure compliance with control-strip-determined roller-integrated measurement target values and LWD target values. Proof layers are designated at the finished subgrade level (directly beneath the base) and at certain additional levels depending on the height of the constructed embankment. Additional proof layers are required for every 600 mm (2 ft) of placed granular soil thickness and every 300 mm (1 ft) of placed nongranular soil thickness. The engineer has the authority to modify proof layer designations.

The Mn/DOT specification requires construction of control strips to determine the intelligent compaction target value (IC-TV) for each type and/or source of soil. Note that Mn/DOT's use of the term "intelligent compaction" is equivalent to CCC as defined in this study in that automatic feedback control of roller operating parameters is not permitted during measurement. Additional control strips are required if variations in material properties that affect the IC-TV are observed by the engineer. Each control strip must be at least 100 m (328 ft) long and at least 10 m (33 ft) wide, or as determined by the engineer. Lift thickness must be equal to planned thickness during production. To determine the moisture sensitivity correction for the IC-TV, a control strip is constructed at or near each extreme of 65% and 95% of standard Proctor optimum moisture—the moisture content limits specified in Mn/DOT earthwork construction. The resulting data are utilized to produce a moisture correction trend line showing a linear relationship of the IC-TV with moisture content. The control strip construction procedure is as follows:

- The bottom of the excavation is mapped with the roller to create a base map. This map is reviewed by the engineer to ensure that the control strip subsurface is uniform and to identify areas that must be corrected prior to fill placement.
- The embankment soil is placed in lifts; each lift is compacted with repeated passes and with roller compaction measurement. The optimum value is reached when additional roller passes do not result in a significant increase in the roller MV as determined by the engineer.
- Moisture content testing is required at a minimum of 1 per 3,000 m^3 of earthwork; the moisture must be maintained within 65% to 95% of standard Proctor optimum.
- Lift placement and CCC is repeated for additional lifts until the level-of-proof layer has been reached.
- The control strip IC-TV is defined to be the optimum MV obtained from the roller measurements during construction of the control strip. The optimum value is reached when additional passes do not result in a significant increase in MV, as determined by the engineer of record. The IC-TV is defined such that 90% of the MVs are greater than 90% of the IC-TV.

The IC-TV values for control strips at moistures near 65% and 95% of optimum are used to create a moisture correction trend line. It should be noted that the Mn/DOT pilot specifications also require LWD testing (three per proof layer) and the establishment of LWD target value (LWD-TV) for each proof layer. The LWD-TV is corrected for moisture in a way similar to that for IC-TV.

During QA the engineer observes the final compaction recording pass of the roller on each proof layer. For acceptance at each proof layer during general production operations, all segments shall be compacted so that at least 90% of the MVs are at least 90% of the moisture-corrected IC-TV prior to placing the next lift. All of the MVs must be at least 80% of the moisture-corrected IC-TV. The contractor must recompact (and dry or add moisture as needed) until all areas meet these acceptance criteria.

If a significant portion of the grade is more than 20% in excess of the selected corrected IC-TV, the engineer shall reevaluate the selection of the applicable control-strip-corrected IC-TV. If an applicable corrected IC-TV is not available, the contractor shall construct an additional control strip to reflect the potential changes in compaction characteristics. Control section size criteria are currently under development.

The engineer will also perform an LWD test and a moisture content test at the minimum rate of one LWD test measurement per proof layer, per 300 m (1,000 ft) for the entire width of embankment being constructed during each operation. The engineer may perform additional LWD tests and moisture content tests in areas that visually appear to be noncompliant or as determined by the engineer. Each LWD test measurement taken shall be at least 90% but not more than 120% of the moisture-corrected LWD-TV obtained on the applicable control strip prior to placing the next lift. The contractor shall recompact (and dry or add moisture as needed) to all areas that do not meet these requirements.

CHAPTER 3

Fundamentals of Roller Measurement Values

This chapter provides a detailed evaluation of several aspects of roller measurement values (MVs), including the surface area reflected in individual MVs, spatial resolution in MV records, and uncertainty in roller MVs. Results from independent evaluations of MVs and the relationship between different MVs are presented. The influence of vibration amplitude and frequency, roller speed, and forward/reverse driving mode on roller MVs is examined. Finally, the influence of soil heterogeneity on roller MVs is examined.

3.1 Roller MV Reporting Characteristics

Roller MVs and their position (determined traditionally via wheel encoder and more recently via GPS) are provided as discrete spatial records. Figure 3.1 presents samples of single-lane MV data records from Dynapac (CMV_D), Case/Ammann (k_s), Sakai (CCV), and Bomag (E_{vib}) smooth drum vibratory rollers. Position data were collected using RTK differential GPS and converted to Cartesian x and y coordinates (x is the driving direction). Figure 3.1 illustrates the discrete nature of MV data as well as the difference in travel direction spatial resolution of each recording system.

Roller MVs are computed based on drum sensor data and provided to the onboard PC at a frequency f_{MV} (see Figure 3.2). The onboard PC also receives a stream of position data from the roller-mounted GPS receiver at a frequency f_{GPS}. These two data streams are often provided at different frequencies (i.e., $f_{MV} \neq f_{GPS}$) and must be merged by the manufacturer's software. The merged MV and position data are reported via PC graphical view or data export at the frequency f_{report}. The resulting spatial resolution of MVs (Δx in the direction of roller travel in Figure 3.2) is a function of f_{report} and roller speed v. Values for f_{MV}, f_{GPS}, f_{report}, and Δx for the rollers evaluated are provided in Table 3.1. The methodology for merging and reporting MVs with GPS-determined positions varies across manufacturers and will clearly evolve in the future. The reader is referred to Facas & Mooney (2010) for a thorough description of roller MV reporting.

Each reported MV is often a reflection of vibration data averaged over a time window t_{MV}. Values of t_{MV} vary across manufacturers and are somewhat user programmable (values observed during this study are summarized in Table 3.1). The corresponding spatial window over which an individual roller MV is representative (x_{MV} in Figure 3.2) is a function of t_{MV} and roller speed v ($x_{MV} = t_{MV} \times v$). Values of the spatial window x_{MV} observed using $v = 1$ m/s (3.3 ft/s) ranged from 0.06 to 1.0 m (0.2 to 3.3 ft) and varied across manufacturers (see Table 3.1). For current roller MVs, the averaging window y_{MV} (see Figure 3.2) is equal to the length of the drum [typically 2.1 m (6.9 ft)].

The spatial reporting resolution of roller MVs in the direction of roller travel ($\Delta x = f_{report} \times v$ in Figure 3.2) also varies across manufacturers. In this study, Δx varied from 0.2 to 1.0 m (0.66 to 3.3 ft) for $v = 1$ m/s (3.3 ft/s). The spatial reporting resolution Δy is a function of overlap between two adjacent roller passes. The recommended overlap is 0.1 m (0.3 ft); therefore, $\Delta y = 2$ m (6.6 ft), typically.

The combination of Δx and x_{MV} reflects the continuity and relative coverage of MV data provided by each roller (see Figure 3.3). Records for k_s provide complete coverage with no overlap ($\Delta x = x_{MV}$). CMV_D and CCV records provide complete coverage with considerable overlap ($\Delta x < x_{MV}$). E_{vib} records provide less than complete coverage ($\Delta x > x_{MV}$). It is worth noting that the parameters Δx and x_{MV} can be modified in the roller software. The $\Delta x = x_{MV}$ configuration is optimal since the resulting MVs are reasonably independent while providing complete coverage.

For the purpose of consistency in data reporting and statistical analysis and to ensure complete coverage via roller MV records, some standardization of key spatial reporting parameters is recommended. These key parameters include the spatial reporting resolutions (Δx, Δy) and the spatial averaging windows (x_{MV}, y_{MV}). For all current roller MVs, y_{MV} is

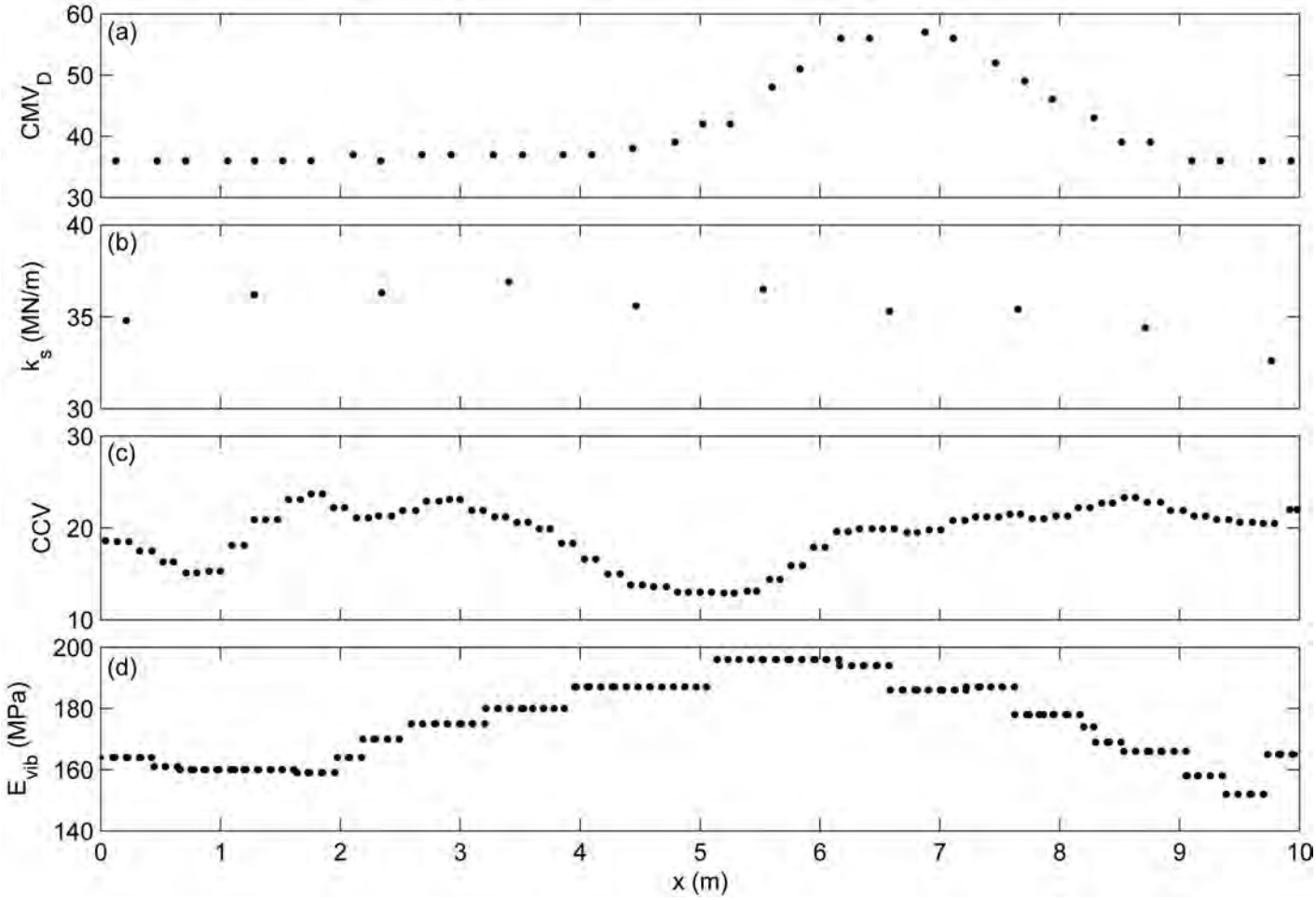

Figure 3.1. Sample roller MV data records for (a) Dynapac CMV_D, (b) Case/Ammann k_s, (c) Sakai CCV, and (d) Bomag E_{vib} over 10 m [32.8 ft; from various test beds (TBs)].

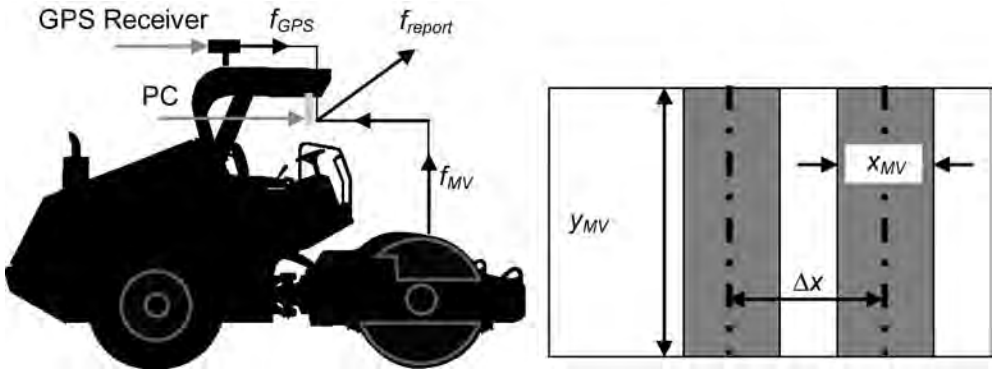

Figure 3.2. Schematic of roller variables.

Table 3.1. Summary of roller MV reporting characteristics.

Roller	MV	f_{mv} (Hz)	f_{GPS} (Hz)	f_{report} (Hz)	t_{MV} (s)	x_{MV}[a] (m) (ft)	Δx[a] (m) (ft)
Case/Ammann	k_s	~30[b]	1	1	1.0	1.0 (3.3)	1.0 (3.3)
Bomag	E_{vib}	3	10	10	0.1	0.06 (0.2)	0.33 (1.1)
Dynapac	CMV_D	1–5	10	1–4	1.0	1.0 (3.3)	0.2–1.0 (0.7–3.3)
Sakai	CCV	5	10	10	1.0	1.0 (3.3)	0.2 (0.7)

[a]Assuming roller speed = 1 m/s (3.3 ft/s).
[b]Based on operating frequency, here 30 Hz.

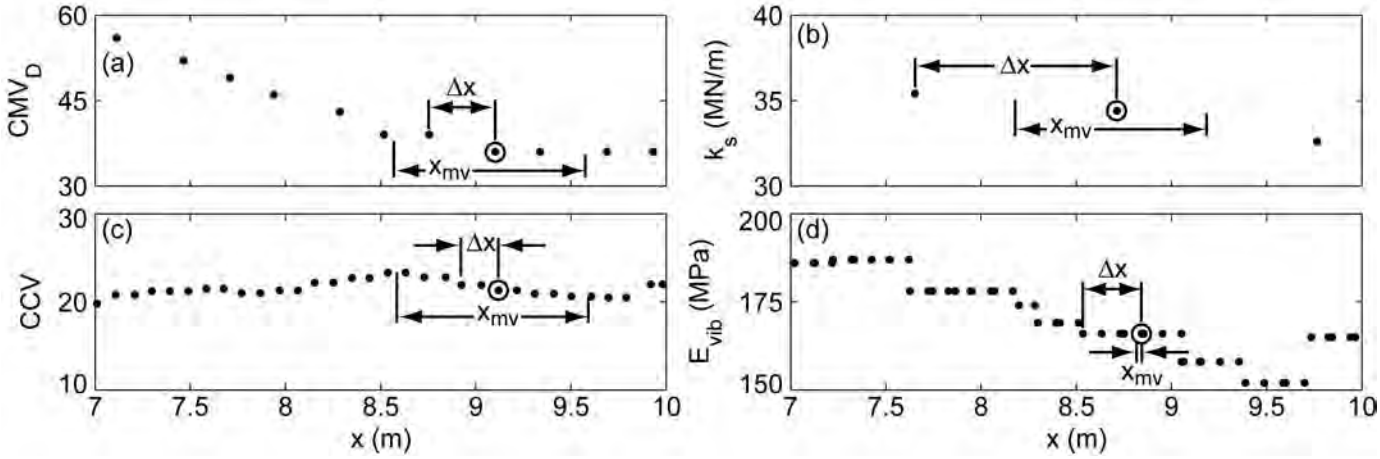

Figure 3.3. Continuity of roller MV data (from various TBs).

the drum length [2.1 m (6.9 ft) for the rollers used here], and Δy is a function of the overlap between adjacent roller passes. A minimum overlap of 0.1 m (0.3 ft) is recommended. Roller MVs will likely evolve to capture soil heterogeneity along the length of the drum (see Section 3.6) and estimate soil properties within the drum length (i.e., y_{MV} and Δy less than the drum length). Recommended values of y_{MV} and Δy should be modified accordingly.

Together with the desire to provide complete (full) coverage and independent MVs ($x_{MV} = \Delta x$), the recommended reporting parameters x_{MV} and Δx are influenced by position accuracy provided by GPS. Table 3.2 summarizes the horizontal accuracy (x_{error}) and vertical accuracy (z_{error}) of available GPS. RTK differential GPS will likely become standard practice for highway-scale projects and was used throughout this study. The recommended x_{MV} should be an order of magnitude greater than the error ($x_{MV} \geq 10\ x_{error}$). It follows that x_{MV} and Δx need not be less than 0.25 m (0.82 ft) when using RTK differential GPS with an error of 2.5 cm (0.08 ft).

3.2 Roller MV Position Reporting Error

Documenting the correct position of the drum and thus the location of underlying material reflected in each roller MV is important for implementation of QA specifications that require local comparison of roller MV with spot-test measurements or pass-to-pass comparisons of MV data (see Facas &

Table 3.2. Levels of GPS position accuracy.

GPS Type	Horizontal Accuracy,[a] cm (in)	Vertical Accuracy,[a] cm (in)
Real-time kinematic (RTK)	2.5 (0.98) + 2 ppm[b]	3.7 (1.46) + 2 ppm[b]
Satellite differential GPS (subscription)	10–78 (3.94–30.71)	10–78 (3.94–30.71)
Satellite differential GPS	95 (37.4)	95 (37.40)

[a] Two standard deviations; may vary across GPS units.
[b] ppm = parts per million, regarding distance from base station to receiver [e.g., for base station 1 km (0.62 mi) from receiver, 2 ppm = 0.1 cm (0.039 in); for base station 10 km (6.2 mi) from receiver, 2 ppm = 1 cm (0.39 in)].

Mooney 2010). The first of two sources of MV position error results from the physical offset of the GPS receiver from the drum center (see Figure 3.4). The software for most rollers accounts for this GPS offset, and in some cases the offset is zero (e.g., when the GPS receiver is mounted directly above the drum center). The correct reporting position should be verified on project sites by comparing roller GPS-provided position with independently measured drum position using similar accuracy GPS (e.g., RTK handheld unit). This is reflected in the recommended continuous compaction control (CCC) specifications (Section 7.5.3).

The second source of MV position error occurs while the roller is moving and stems from data averaging during the calculation of each roller MV (i.e., t_{MV} and x_{MV}; see Facas & Mooney 2010). Due to the way in which roller MVs and GPS position data are merged (Section 3.1), the resulting MVs are often associated with a position that reflects the end of the t_{MV} and x_{MV}. This leads to position reporting error. The position of each roller MV should be reported at the center of the averaging window. Any latency in the MV calculation prior to merging with GPS position would cause additional position error. This source of position error is roller speed and direction dependent.

Roller position error due to physical offset of the GPS receiver from the drum was checked for each roller on each field site and accounted for in the data analysis. To investigate the accuracy of MV position reporting during roller travel, wood beams were placed at known locations to create an artificial spike in roller MV data. Two tests beds were constructed similarly on a 60-m (200-ft)-long by one-lane-wide fully compacted soil. Two wood beams were placed across the lane approximately 10 m (33 ft) apart (see Figure 3.5) to introduce spikes in roller MV data at known locations (measured with GPS). The rollers were driven in the north direction with forward roller travel (north forward, NF) and then in the south direction with forward roller travel (south forward, SF). This was repeated three or four times with each roller.

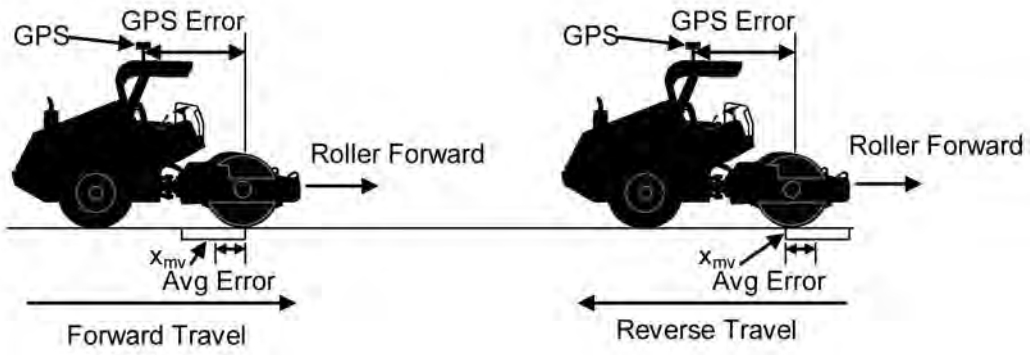

Figure 3.4. Schematic of roller, GPS receiver offset, and spatial window for determination of roller MVs.

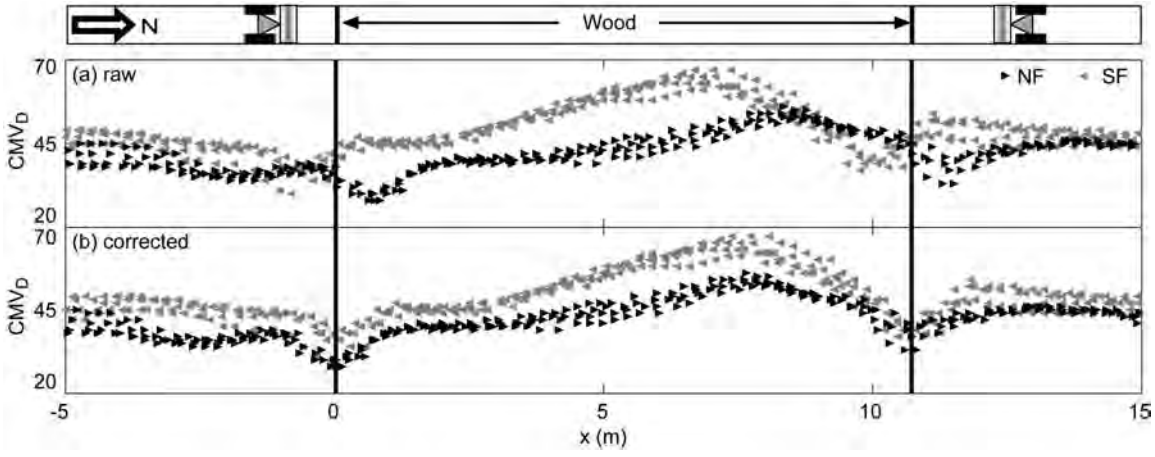

Figure 3.5. Position error observed in CMV_D data records (TB FL18): (a) observed MV records with no correction; (b) MV position corrected by -0.70 m (2.3 ft).

Table 3.3. Observed position reporting errors for roller MVs.

MV	Position Reporting Error (m)
CMV_D	+0.70
k_s	-0.40[a]
CCV	+0.55
E_{vib}	+0.80

[a] ± 0.5 m uncertainty.

Figure 3.5 illustrates the CMV_D response from all NF and SF passes. The solid black lines represent the location of the wood beams. Four passes in each direction demonstrate repeatable behavior within NF and SF passes. The difference in roller MVs between NF and SF passes is due to transverse heterogeneity and is discussed in Section 3.6. As shown in Figure 3.5a, the location of each dip in the recorded MV data is direction dependent and is different from the locations of the wood posts by +0.7 m (2.3 ft) in the direction of roller travel. By applying a position correction of –0.7 m (–2.3 ft) to the MV data with respect to the direction of roller travel, the resulting NF and SF records align (Figure 3.5b). The –0.7-m position correction is consistent with the spatial shift required to report CMV_D at the center of its averaging window x_{MV}. Recall that t_{MV} = 1 s for CMV_D. With the observed v = 1.2 m/s (3.9 ft/s) and a required averaging window correction of -0.5 s, the position correction due to averaging should be -0.60 m (-2.0 ft). The 0.10-m (0.33-ft) discrepancy may be attributed to GPS error and/or potential latency in the MV calculation. This method was applied to the other rollers (see Table 3.3 and Appendix B). In practice these offsets should be determined in the field and accounted for as appropriate.

3.3 Repeatability of Roller Measurement Values

Repeatability tests were performed to quantify the pass-to-pass uncertainty in roller MV records and to verify the proper working condition of the roller measurement systems. An example of smooth drum vibratory roller MV data from consecutive roller passes with similar operating parameters (direction, speed, amplitude, etc.) is presented in Figure 3.6 (other data are presented in Appendix B). The pairs of MV data from each pass are visually repeatable (e.g., the various peaks and valleys in MV are consistently captured in both passes). Mild increases or decreases in roller MVs are attributed to minor compaction or loosening and to minor deviations in driving path.

To quantify the repeatability, the percent difference in pass-to-pass roller MV ($\%\Delta MV_i$) at each spatial location was determined via Equation 3.1 and is plotted in Figure 3.6b. In Equation 3.1, MV_i represents the MV data for pass i, and $\%\Delta MV_i$ represents the percent difference between pass i and $i-1$. Each pass of MV data was placed on a similar x-direction grid using linear interpolation to enable the spatial quantification.

$$\%\Delta MV_i = \frac{MV_i - MV_{i-1}}{MV_{i-1}} \times 100 \tag{3.1}$$

The mean and standard deviations of the %ΔMV values ($\mu_{\%\Delta MV}$ and $\sigma_{\%\Delta MV}$) are shown as a solid line and dashed line, respectively. The $\mu_{\%\Delta MV}$ reflects the effect of minor compaction, loosening, and roller track deviation. Observed $\mu_{\%\Delta MV}$ ranged from 0.1% to 3.6% for the testing performed here. Minor changes in pass-to-pass MV are unavoidable in practice. The $\sigma_{\%\Delta MV}$ provides a quantifiable measure of repeatability and pass-to-pass uncertainty. This quantity may be used to

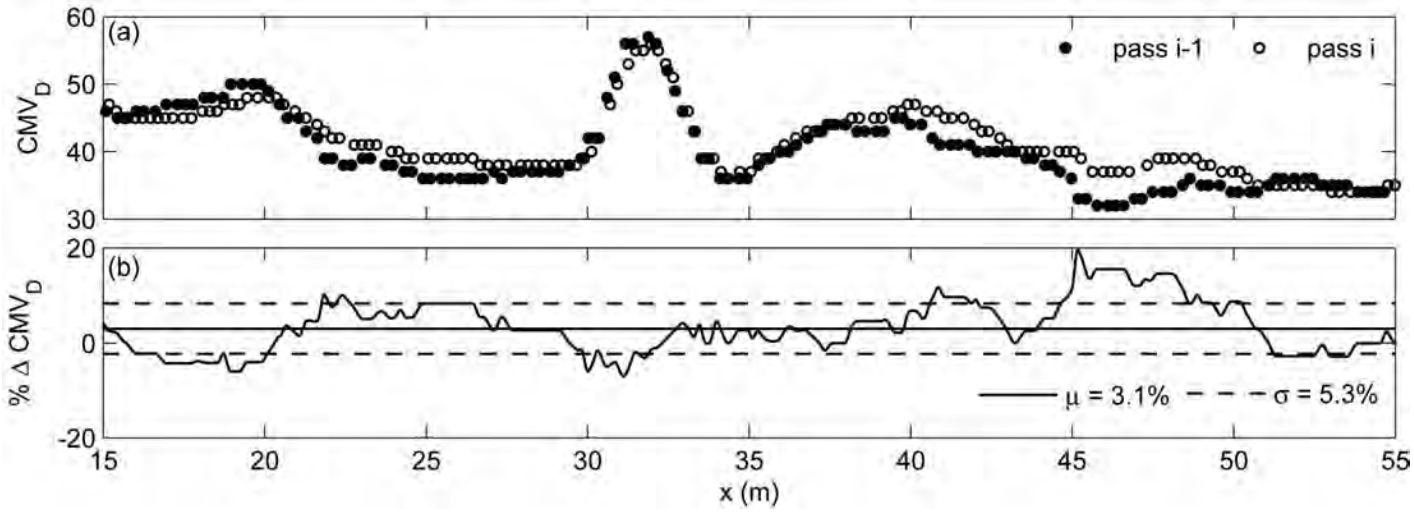

Figure 3.6. Percent difference in CMV_D (smooth drum) determined via repeatability testing (TB FL18).

verify the proper working condition of a roller measurement system and should be considered when interpreting pass-to-pass changes in MVs commonly used in CCC specifications (see Sections 7.5.3 and 7.7.2). Smooth drum vibratory roller MV records were generally found to be repeatable, and values of $\sigma_{\%\Delta MV}$ typically ranged from 5% to 7%. Data records for pad foot vibratory roller MVs collected during this study exhibited a high degree of scatter and general lack of repeatability. Values of $\sigma_{\%\Delta MV}$ for pad foot vibratory roller MVs were found to exceed 25%.

Repeatability testing plays an important role in verifying the proper working condition of a vibratory roller and/or roller measurement system. Figures 3.7 and 3.8 provide two examples where repeatability testing revealed a problem. In Figure 3.7, sporadic shifts in the roller MV data are visually evident and result in $\sigma_{\%\Delta MV}$ = 14%. In Figure 3.8, roller MV data from a vibratory pad foot roller revealed a lack of repeatability ($\sigma_{\%\Delta MV}$ = 27%). In both cases the roller MV system should not be used in roller-integrated CCC quality assurance (QA). To this end, repeatability testing is recommended and detailed in Section 7.5.3. A suggested criterion is $\sigma_{\%\Delta MV} \leq 10\%$, though the engineer of record may approve the roller measurement system based on a qualitative evaluation of the repeatability data.

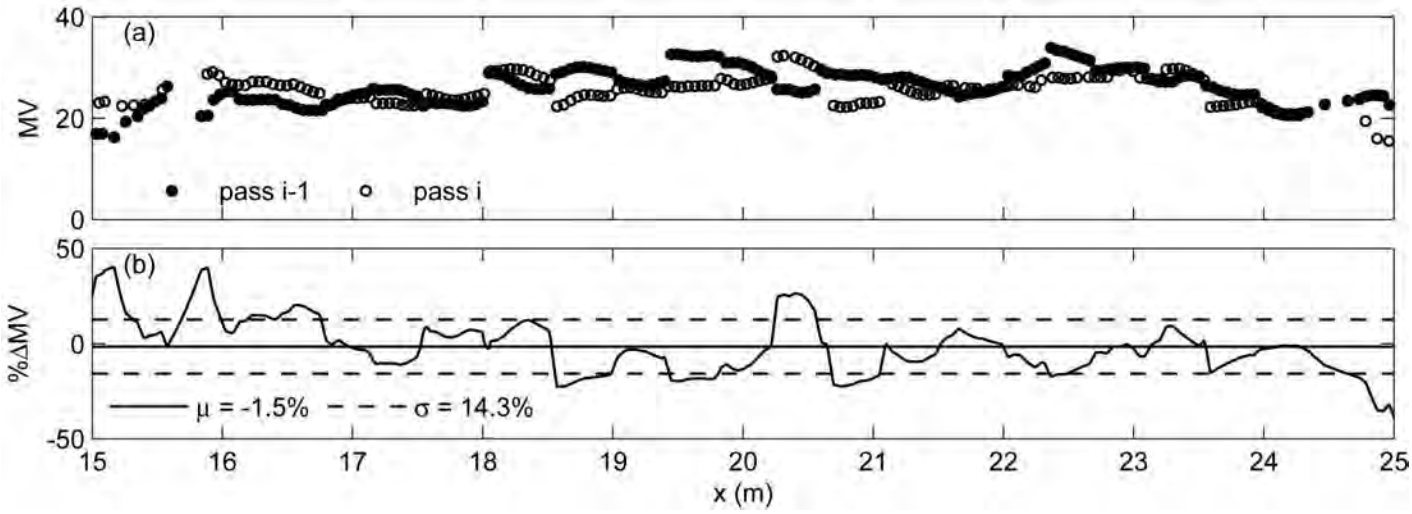

Figure 3.7. Percentage difference in MV (smooth drum) due to faulty roller measurement system.

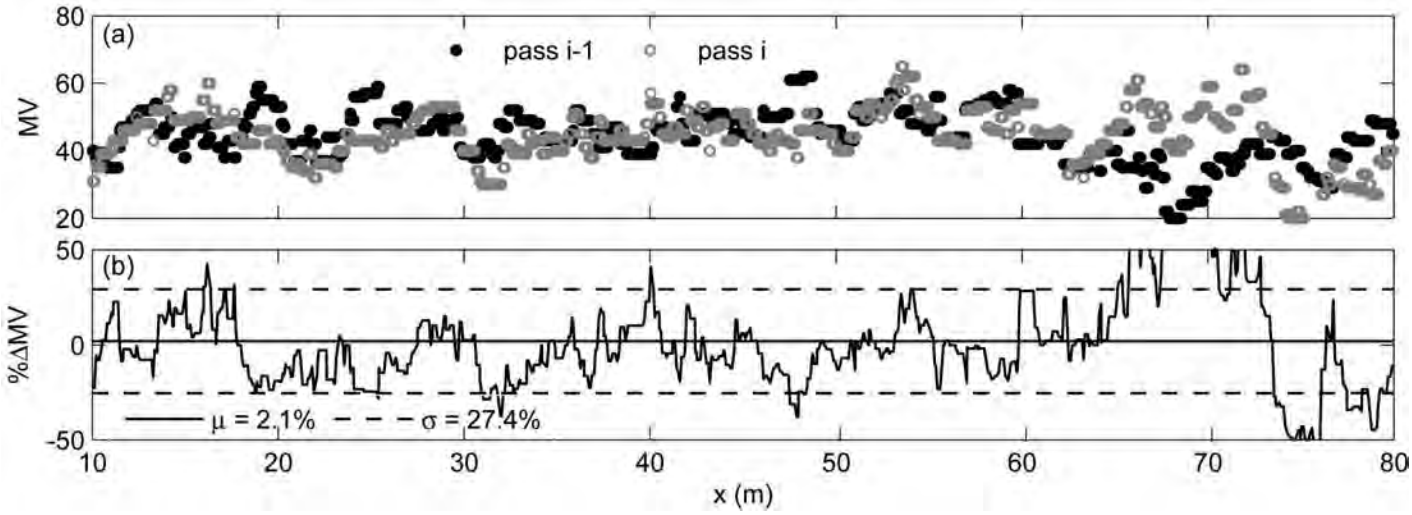

Figure 3.8. Percentage difference in MV (vibratory pad foot) determined via repeatability testing.

The repeatability tests described here provide useful insight into the limitations of roller MV data in QA specifications, particularly the spatial comparison of pass-to-pass roller MV. As described in Section 2.3.2, one Austrian and ISSMGE specification approach for roller-integrated CCC examines the pass-to-pass change in mean MV (averaged over the evaluation section). A natural extension of this approach afforded by GPS is to introduce a spatial percentage change criterion (i.e., the percentage change in local roller MV—single MV) must be less than a specified percent. Such a criterion would address localized weak zones that may be overlooked in the averaging approach. The results of repeatability testing illustrate that the uncertainty (one standard deviation) alone in point-based percentage difference is 5% to 7%. To this end, the criterion for pass-to-pass spatial percent difference could not reasonably be less than 10% to 15% (two standard deviations) if based on single-point measurements. It follows that spatial averaging (e.g., via kriging) might be used to reduce this uncertainty and allow a smaller percentage difference criterion (e.g., 5%).

3.4 Comparison of Roller Measurement Values

As described in Chapter 2, a number of roller measurement values are used in practice. Though different in methodology, each roller MV is based on the principle that measurable changes in roller vibration are due to changes in soil stiffness (and damping). This section examines roller MV trends via side-by-side comparison. The independent calculation of roller MVs using research team instrumentation also enables verification of roller MVs and how they work (i.e., dispelling the "black box" approach that tends to inhibit adoption by the engineering community).

3.4.1 Independent Evaluation of MVs

Sakai and Caterpillar smooth drum vibratory rollers were equipped with instrumentation to independently validate and assess roller MVs. Published algorithms to compute CMV, CCV, and k_s (summarized in Chapter 2) were used. E_{vib} was not calculated independently due to the significant differences in eccentric excitation technology and the differences that vectoring the excitation force would have on roller MVs. Independently determined MVs are denoted with the subscript CSM (Colorado School of Mines) to distinguish them from the roller manufacturer MVs.

The independently determined CCV_{CSM} is compared with Sakai CCV in Figure 3.9, and the independently determined CMV_{CSM} is compared with Caterpillar CMV_C in Figure 3.10. The data match closely; subtle differences may be due to differences in how the systems average data and small differences in sensor locations.

Dynapac CMV_D was compared with CMV_{CSM} (determined with Sakai vibration data) by consecutively driving the two rollers in the same lane (see Figure 3.11). While minor differences will result from different roller properties, discrepancies in the values here are attributed to deviations

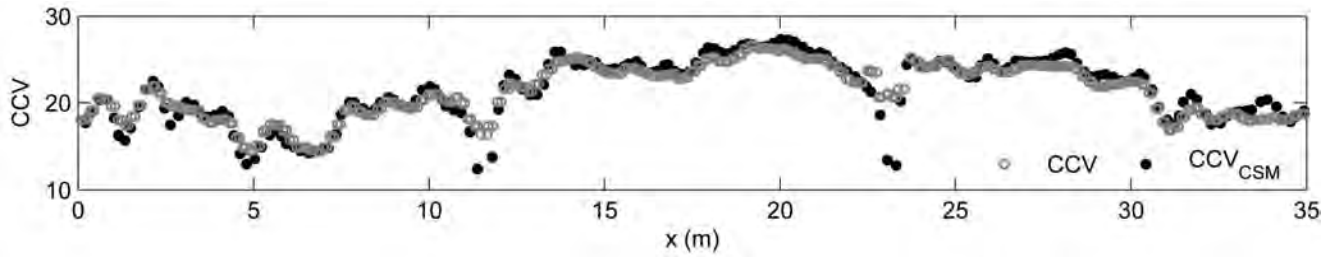

Figure 3.9. Comparison of Sakai CCV and CCV_{CSM} determined via independent instrumentation (TB FL12).

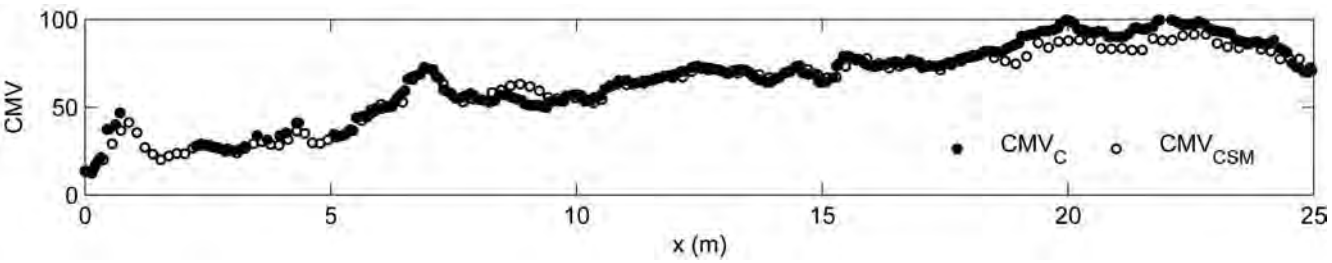

Figure 3.10. Comparison of Caterpillar CMV_C and CMV_{CSM} determined via independent instrumentation (TB MN 29).

in the tracks of the two rollers and differences in reporting methods.

The Case/Ammann k_s value was compared with the $k_{s\text{-}CSM}$ determined from the Sakai roller vibration data (see Figure 3.12a). k_s is calculated differently based on whether the drum is in contact or partial loss of contact operational mode (Anderegg & Kaufmann 2004). The two different algorithms were used for the independent assessment and are shown in Figure 3.12. The $k_{s\text{-}CSM}$ trends well with k_s but does not match. The Ammann k_s is scaled by a fixed factor and might be the reason for the discrepancy, though the occurrence of k_s = 0 suggests possible errors within the measurement system. The $k_{s\text{-}CSM}$ was transformed using a linear equation (see Figure 3.12b) to provide a good match with the manufacturer's k_s. Given this need to apply a scale factor, the black box surrounding k_s partially remains.

3.4.2 Relationship Between Roller Measurement Values

Figure 3.13 presents a comparison of E_{vib}, k_s, and CMV_C data collected from a test bed with considerable stiffness variability (TB MN42). The soft areas reflect clay subgrade, and the stiff areas reflect >1 m (3.3 ft) thickness of crushed rock. Roller MVs were normalized by their peak values for direct comparison. In general, the roller MVs matched each other over the range of underlying stiffness present. Figure 3.14 shows the relationship between CMV_D, CCV, and k_s collected during operation on granular soil (TB FL18). Each data set was normalized by its peak value. These MVs also trend similarly.

Figure 3.15 shows the relationship between $k_{s\text{-}CSM}$, CMV_{CSM}, and CCV_{CSM} computed with data from independent instrumentation on the Sakai roller. The $k_{s\text{-}CSM}$ values were com-

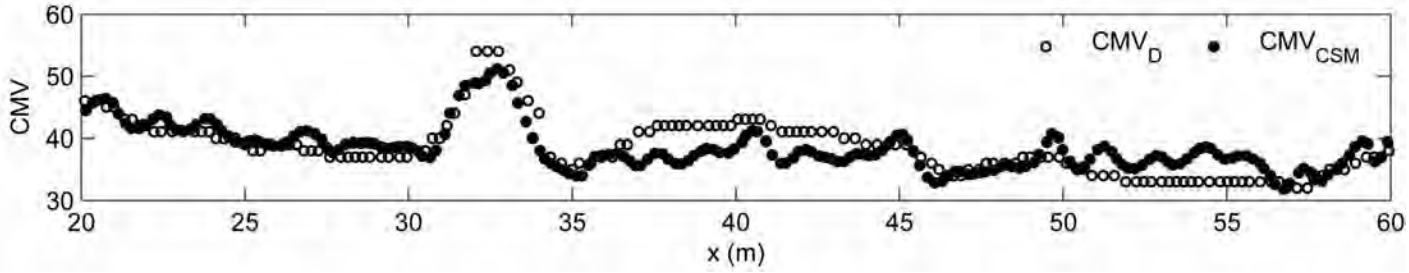

Figure 3.11. Comparison of Dynapac CMV_D and CMV_{CSM} determined via independent instrumentation on Sakai roller (TB FL18).

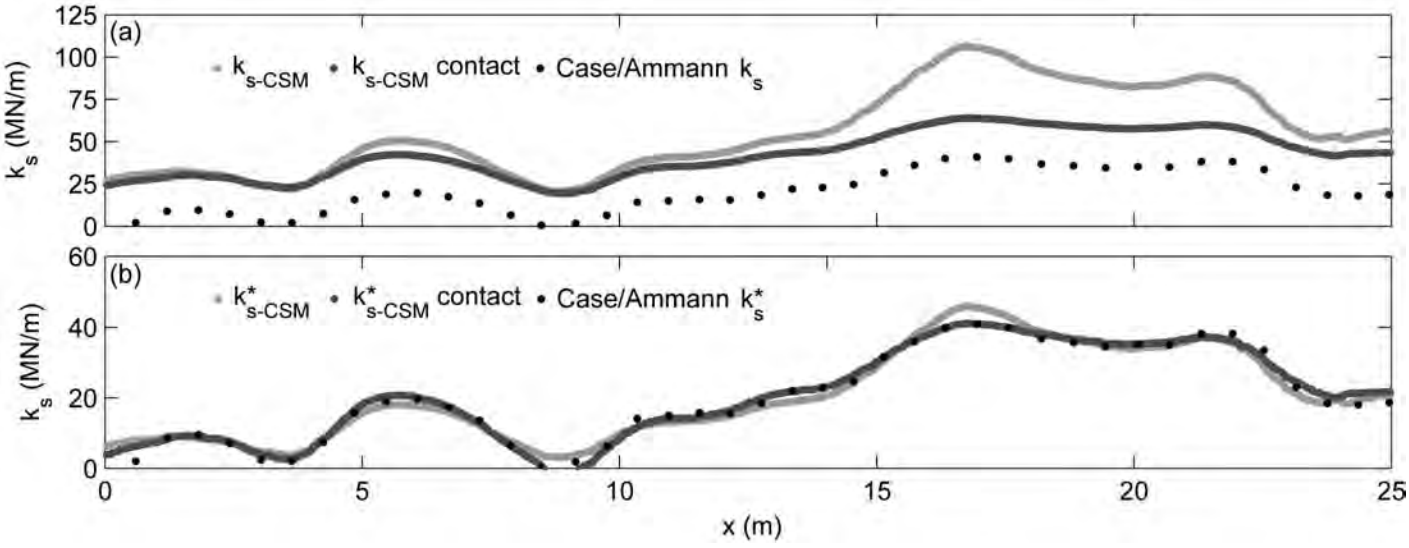

*Figure 3.12. Comparison of Case/Ammann k_s and $k_{s\text{-}CSM}$ determined via independent instrumentation: (a) raw data; (b) scaled data: $k^*_{s\text{-}CSM}$ contact = 0.94 * $k_{s\text{-}CSM}$ contact-19, $k^*_{s\text{-}CSM}$ = 0.5* $k_{s\text{-}CSM}$-7.2 (TB NC27).*

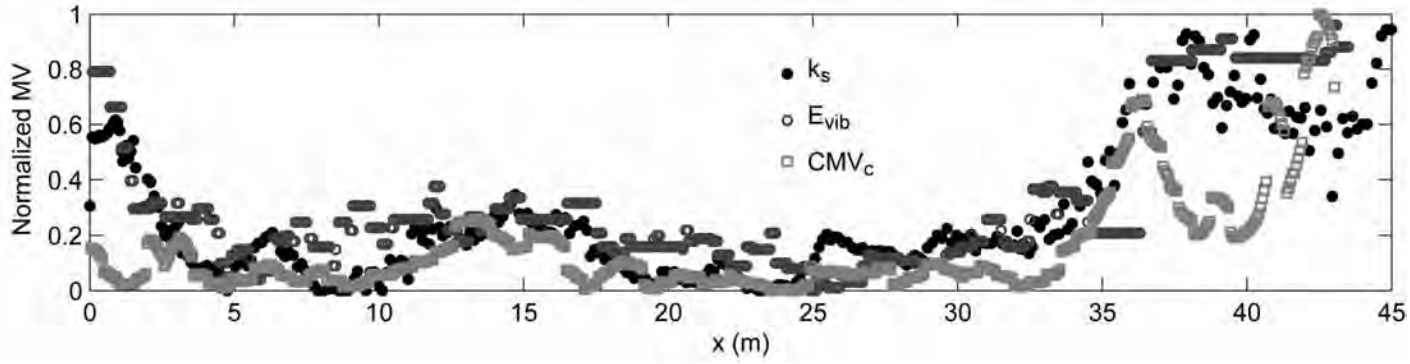

Figure 3.13. Observed relationship between Case/Ammann k_s, Bomag E_{vib}, and Caterpillar CMV_C (all smooth drum) on a mixed material test bed (TB MN42).

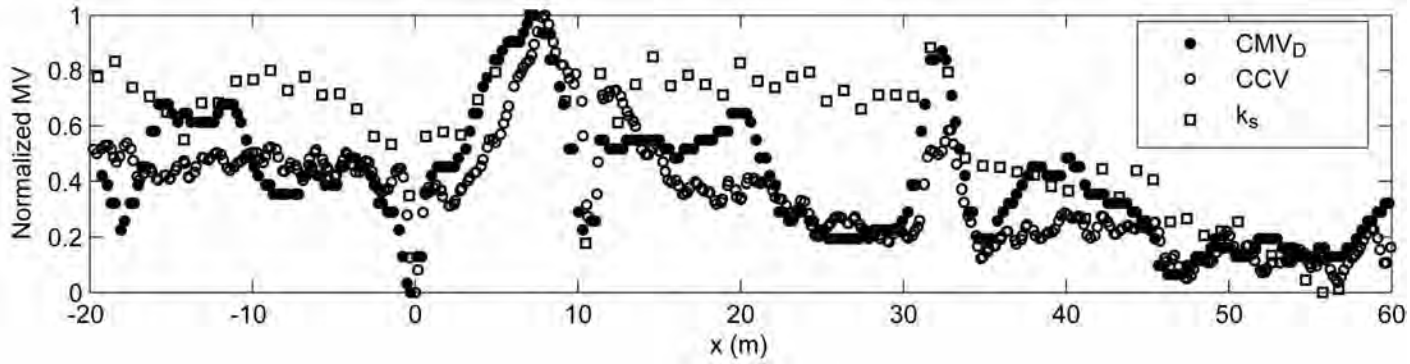

Figure 3.14. Comparison of Case/Ammann k_s, Dynapac CMV_D, and Sakai CCV data on granular soil (TB FL18).

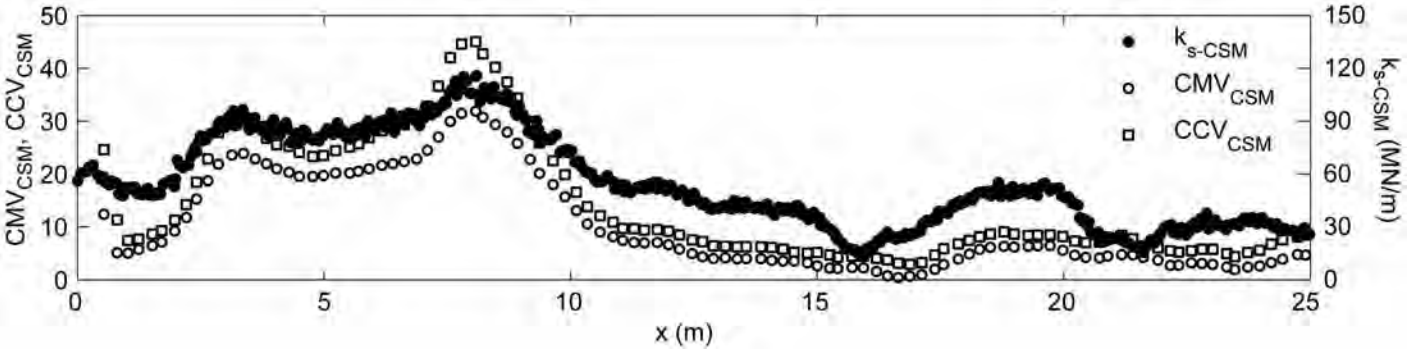

Figure 3.15. Relationship between independently determined $k_{s\text{-}CSM}$, CMV_{CSM}, and CCV_{CSM} (TB NC27).

puted at ~30 Hz, whereas the CMV_{CSM} and CCV_{CSM} were computed at 1 Hz; therefore, differences within a meter are not considered. The biggest difference in trends can be observed from $x = 18$ to 25 m. The CMV and CCV MVs trend well with each other and with k_s when the values are greater than approximately 8 to 10.

The correlations between various roller MVs are shown in Figure 3.16. The diagonals reveal the individual roller MV histograms. As anticipated, CMV_{CSM} and CCV_{CSM} exhibit the strongest correlation. Assuming that k_s is an effective measure of soil stiffness, the correlation plots reveal lack of sensitivity of both CCV_{CSM} and CMV_{CSM} for values less than approxi-

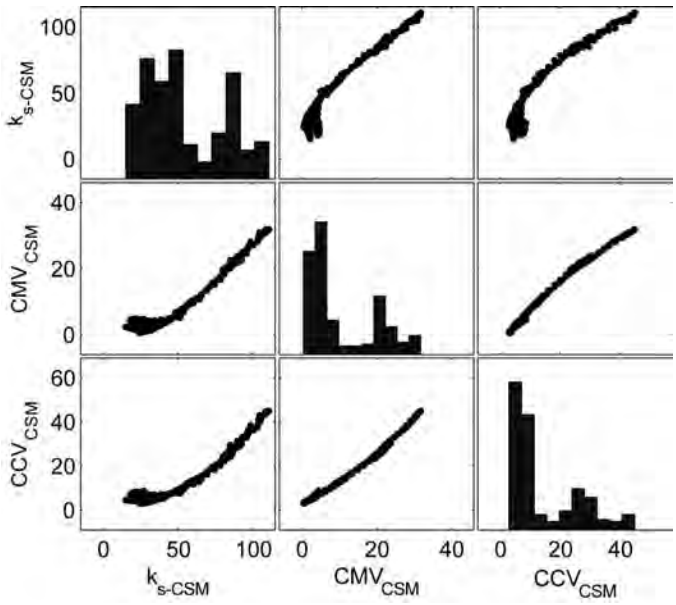

Figure 3.16. Observed correlations between $k_{s\text{-}CSM}$, CMV_{CSM}, and CCV_{CSM} (TB NC27).

mately 10, underscoring the findings in the literature (see Chapter 2). For values above 10, CMV_{CSM} and CCV_{CSM} are approximately linearly related to k_s and therefore provide effective measures of soil stiffness.

3.5 Measurement Value Dependence on Machine Parameters

Measurement systems are typically standardized; that is, the magnitude, rate, and procedure are established to be constant from test to test. With CCC and IC rollers, however, measurement occurs during roller operation, and roller operation parameters can vary considerably. The fact that roller MVs are influenced by roller operating parameters is reasonably well known (as was described in Chapter 2). What is not clear is whether the influence of operational parameters on roller MVs is predictable and therefore can be allowed during roller-integrated CCC specifications. This section characterizes the influence that eccentric force amplitude, vibration frequency, roller speed, and direction have on roller MVs.

3.5.1 Dependence of Roller Measurement Values on Eccentric Excitation Amplitude

The Ammann smooth drum IC roller was operated on the previously discussed TB MN42 to evaluate the influence of theoretical amplitude A (per Equation 2.2). Figure 3.17a presents roller MV records for low, medium, and high amplitudes. The nature of the roller k_s dependence on A varies along the 50 m (164 ft) test bed. The dependence of k_s on A was considerably more significant for $x = 20$ to 30 m than for $x = 37$ to 48 m [see percentage difference in mean roller MV

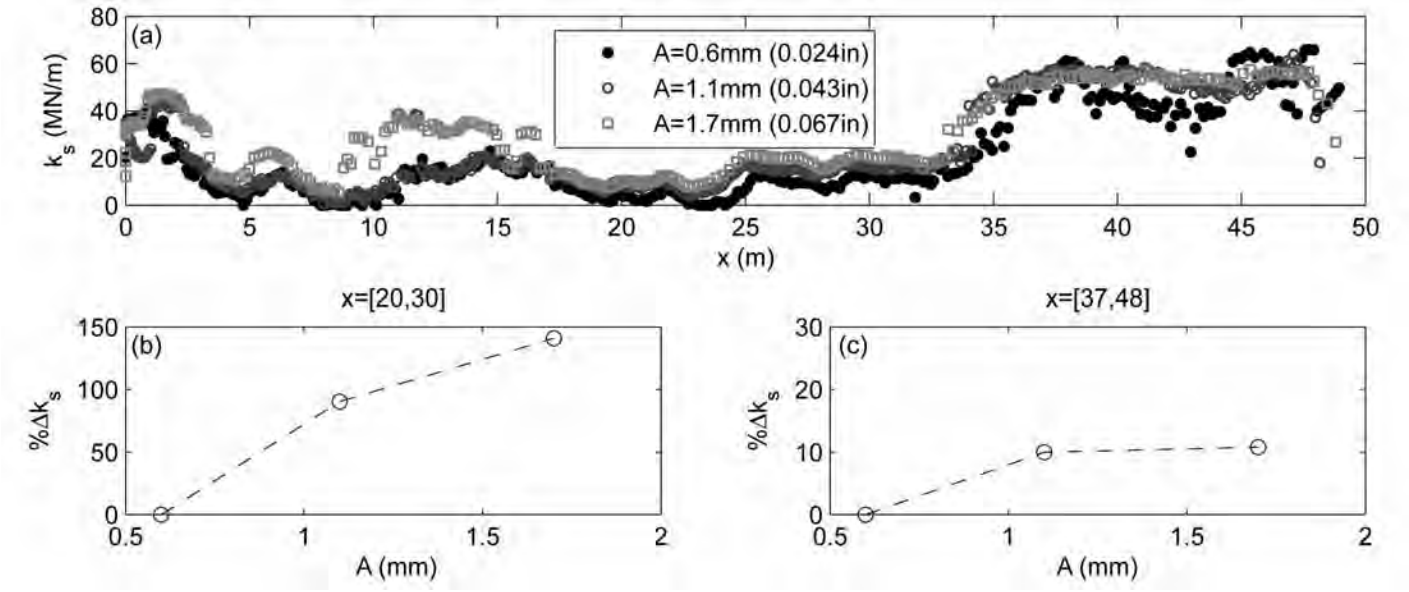

Figure 3.17. Influence of A on k_s (smooth drum) on granular and fine-grained material (TB MN42). Percentage difference in mean roller MV shown for two regions: x = 20 to 30 m (left); x = 37 to 48 m (right).

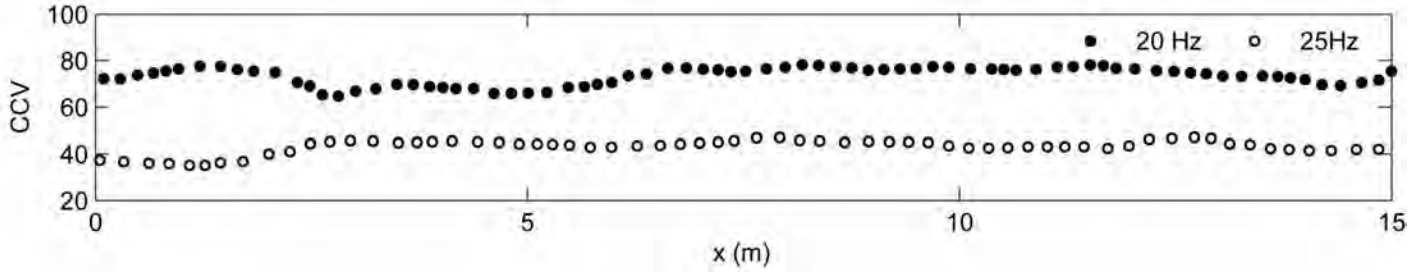

Figure 3.18. Influence of excitation frequency on Sakai CCV (TB FL6).

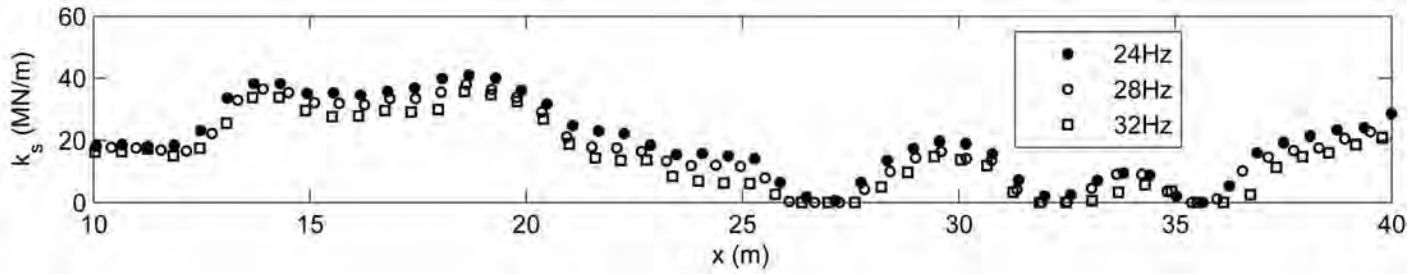

Figure 3.19. Influence of excitation frequency on Case/Ammann k_s (TB NC27).

(%ΔMV) in Figures 3.17b and c]. Similar results were found for the other rollers and soils (see Appendix B). The dependence of roller MV on A is not simply MV dependent but also (as discussed later in Chapter 4) depends on the soil and layering present.

The dependence of roller MVs on excitation frequency was examined with the Sakai and Ammann/Case rollers (see Figures 3.18 and 3.19). The strong frequency dependence of CCV is related to partial loss of contact, similar to that described above. At $f = 20$ Hz the Sakai roller is close to resonance and exhibits a considerably higher degree of loss of contact than at $f = 25$ Hz. The influence of frequency on k_s is more subtle yet still evident.

3.5.2 Influence of Roller Speed on Measurement Values

The influence of forward travel speed on roller MVs was investigated with numerous CCC and IC rollers. Shown below are the results of testing on fully compacted material using various rollers. In all cases, roller MV records from two forward travel speeds are compared. The E_{vib} data shown in Figure 3.20 exhibit a mean decrease of 6.3% from 0.8 m/s (2.6 ft/s) to 1.5 m/s (4.9 ft/s). However, some areas reveal similar E_{vib} for the two speeds; therefore, the results are inconclusive. Both Sakai CCV (see Figure 3.21) and Dynapac CMV_D (see Figure 3.22) exhibit a decrease in value with increasing speed. At higher speed the vibration energy is spread over more soil, and therefore the degree of partial loss of contact is reduced. These results agree with the literature presented in Section 2.1.2.

3.5.3 Influence of Forward and Reverse Driving Directions on Roller Measurement Values

Most production compaction efforts occur in a forward/reverse driving pattern. It follows that measurement would be convenient during both forward and reverse operation. The influence of driving mode was investigated on the Ammann, Bomag, Dynapac, and Sakai rollers. Typical results are presented in Figure 3.23. The figure indicates that Case/Ammann k_s decreases by approximately 10% when driving in the reverse direction. The significant discrepancy for $x = 15$ to 30 m may be due to misalignment of the roller in the presence of heterogeneous soil (see Section 3.6). Results from other roller investigations are provided in Appendix B. The data presented here and in Appendix B, though limited, suggest there are only subtle differences in forward versus reverse mode driving. Site-specific evaluation of the influence of driving mode on roller MV should be performed if roller MVs are to be considered in both directions.

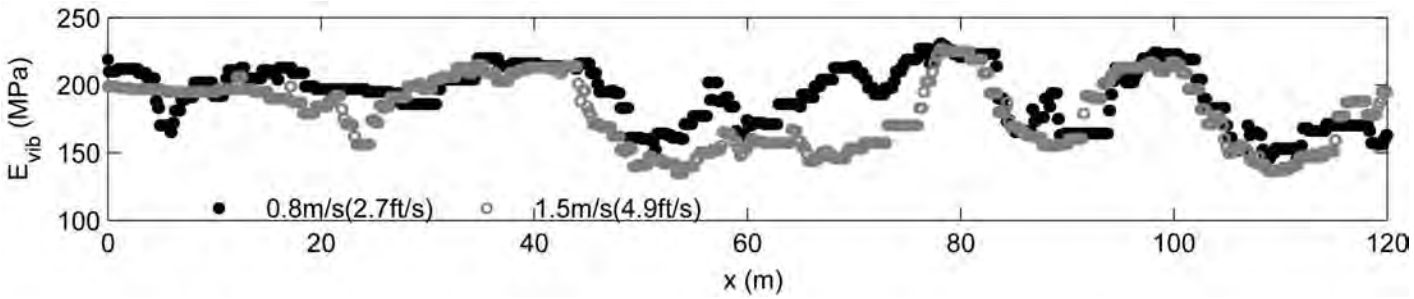

Figure 3.20. Influence of roller speed on Bomag E_{vib} (TB CO42).

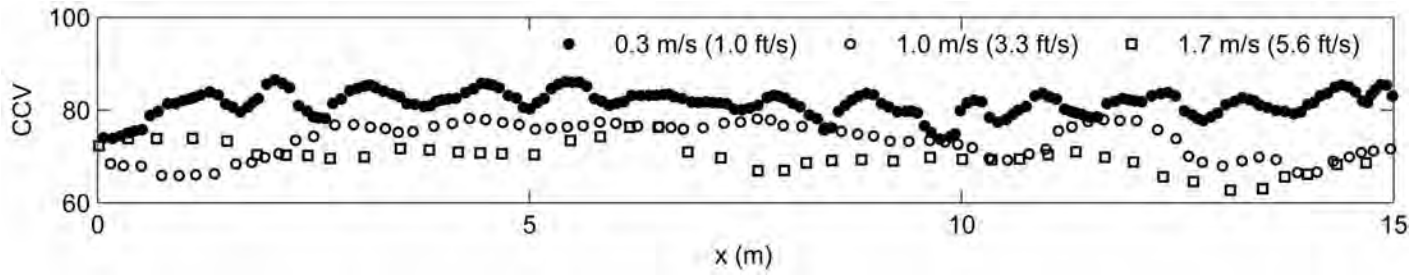

Figure 3.21. Influence of roller speed on Sakai CCV (f = 20 Hz) (TB F6).

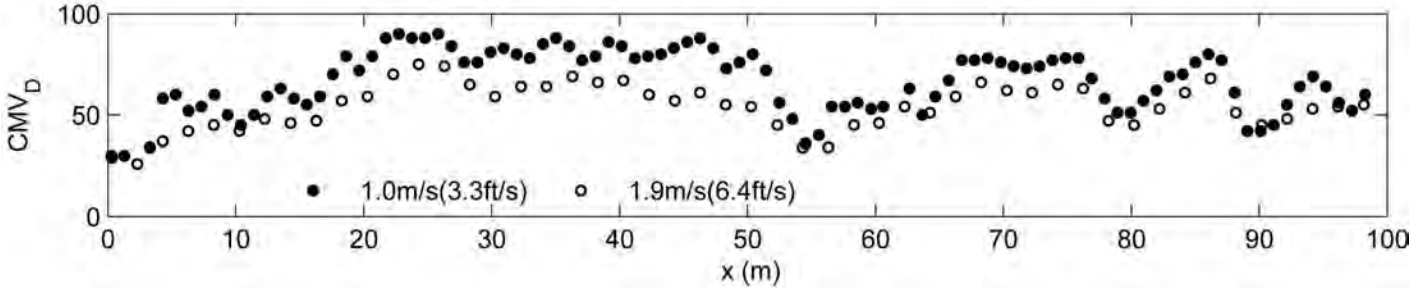

Figure 3.22. Influence of roller speed on Dynapac CMV_D (TB CO33).

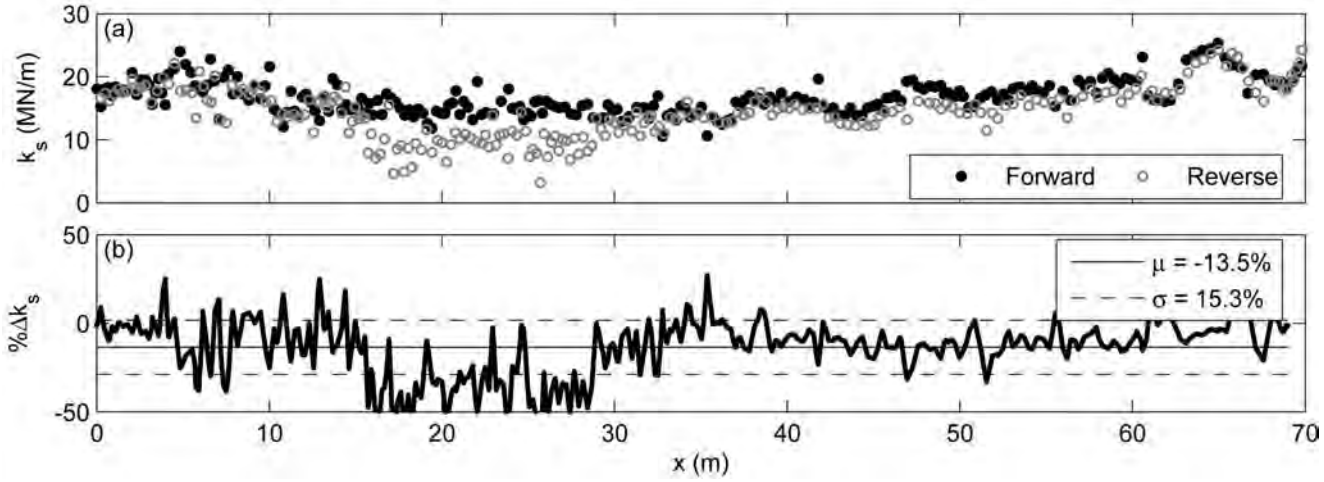

Figure 3.23. Influence of forward and reverse driving modes on k_s (smooth drum; TB MN17). Percentage difference (forward/reverse) is shown in plot b.

3.6 Influence of Transverse Soil Heterogeneity on Roller Measurement Values

Soil density, moisture, and stiffness vary locally. A review of the roller MV records presented in this chapter illustrates that soil properties vary, sometimes considerably, within a length scale of tenths of a meter (one-third of a foot). With a reporting resolution as low as 0.1 m (0.3 ft), roller MVs are capable of capturing the variability in the *x* direction. In the transverse direction, however, the 2.1-m (6.9-ft)-long rigid drum coupled with current instrumentation and MV algorithms are unable to reflect *y*-direction (transverse) heterogeneity. This section addresses the influence that transverse soil heterogeneity can have on roller MVs and, in turn, the limitation of roller MVs as a result of transverse heterogeneity.

A 100-m (330-ft)-long fully compacted lane [2.1 m (6.9 ft)] of clayey silt was traversed in the forward north and forward south travel directions. Figure 3.24 shows the resulting E_{vib} and CMV_D data records. The accelerometers on the Bomag roller from which the MV is derived are housed on the drum end, as depicted in Figure 3.24 (the driver's left). The accelerometer location for the Dynapac roller is opposite (the driver's right). This 100-m (330-ft)-long stretch of subgrade is clearly heterogeneous in the *x* direction. Figure 3.24 shows that the bidirectional roller MV records are different for almost 40% of the 100-m (330-ft) length.

The directional dependence of roller MVs was investigated by performing light weight deflectometer (LWD) tests across the drum lane at the locations in Figure 3.24 identified with arrows. The LWD results are presented in Figure 3.25, along with the roller MVs reported at the position of the accelerometer. At each location eight LWD tests were performed across the lane. The LWD results explain the directional dependence observed in the roller MVs. In Figure 3.25a, LWD data clearly show the lane is stiffer on the west side. This is corroborated by the higher roller MVs when the sensor is in the west (W) position. In Figure 3.25b the roller MVs are relatively equal in both directions, yet the LWD data are quite heterogeneous. The heterogeneity is symmetrical, however, and therefore leads to symmetry in the roller MV data.

The directional dependence of roller MVs in the presence of local heterogeneity has implications for the use of roller-integrated CCC and the implementation of specifications. To best relate roller MVs to spot-test measurements, multiple spot tests should be performed across the drum lane. The implication of directional dependence suggests that if pass-to-pass analysis is to be performed, consecutive passes must follow similar paths.

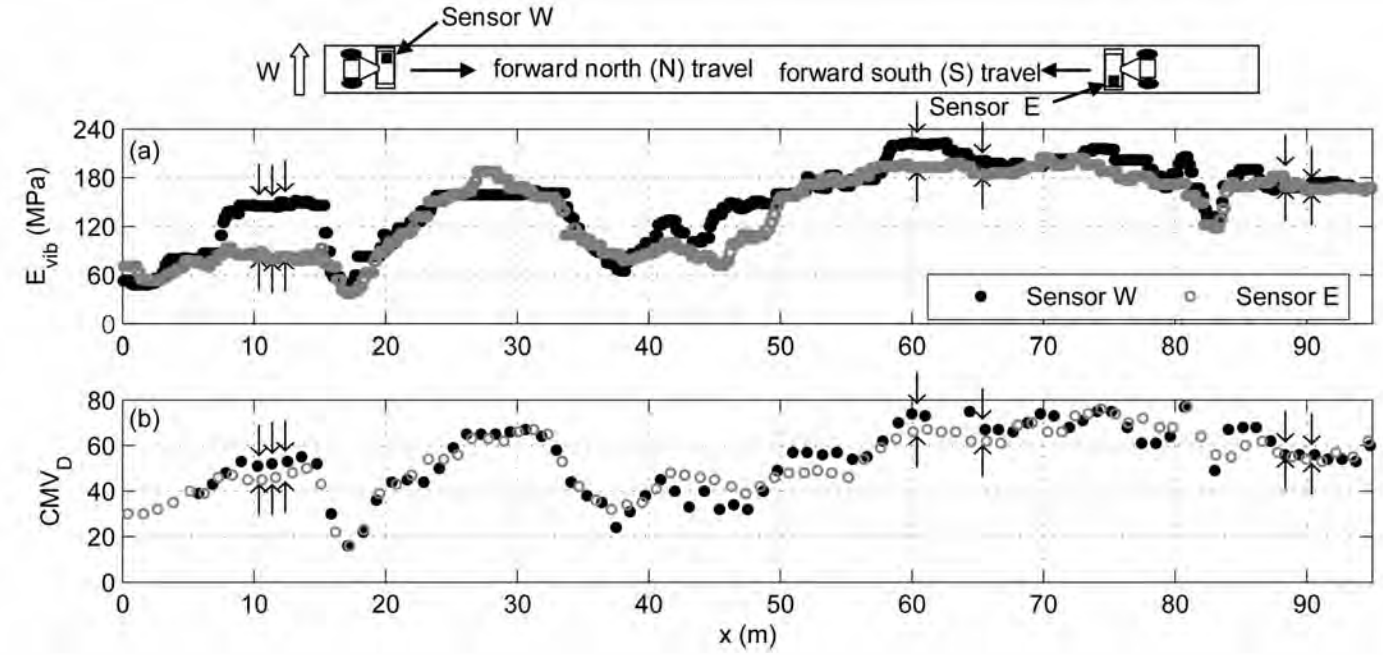

Figure 3.24. Observed differences in directional roller MV (TB MD20) due to soil heterogeneity: (a) Bomag roller E_{vib}, (b) Dynapac roller CMV_D.

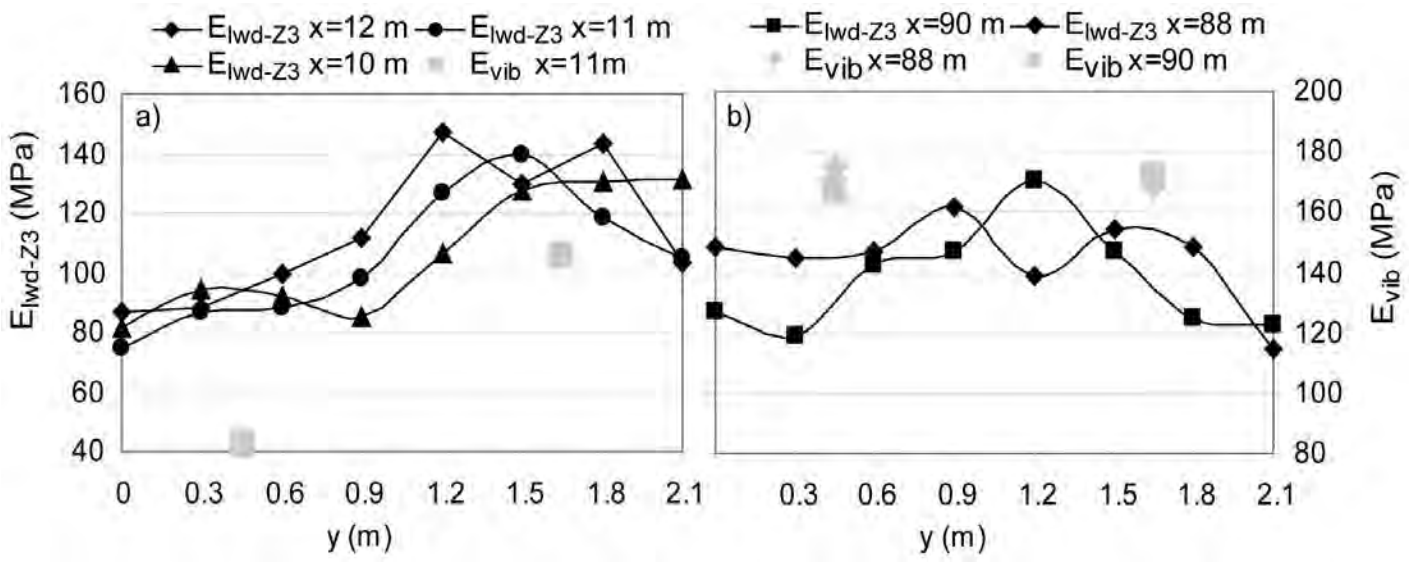

Figure 3.25. Comparison of transverse E_{LWD} profiles with bidirectional roller MVs (TB MD20); roller MVs are depicted at the sensor offset locations.

3.7 Conclusions and Recommendations

The following conclusions can be drawn from the results presented in this chapter:

- Each vibration-based roller MV investigated—Ammann and Case/Ammann k_s, Bomag E_{vib}, Dynapac CMV_D, and Sakai CCV—is a reflection of soil stiffness over a spatial distance that varies across MVs [0.06 to 1.0 m (0.2 to 3.3 ft) observed]. The reporting resolution of roller MVs in the direction of roller travel varied from 0.2 to 1.0 m (0.66 to 3.3 ft). To ensure full coverage with roller-integrated CCC, the spatial distance over which a single roller MV is reported should equal the reporting resolution. The reporting spatial resolution should be no less than 10 times the GPS accuracy; for example, if RTK differential GPS is used (recommended), the spatial resolution should be no less than 0.25 m [0.82 ft; with GPS accuracy = 2.5 cm (0.082 ft)].
- The GPS-based position reporting of roller MVs exhibited errors of 0.4 to 1.5 m (1.3 to 4.9 ft) for the rollers and measurement systems investigated. A position reporting verification procedure was developed and is recommended for roller-integrated CCC specifications (see Chapter 7).
- Repeatability testing of properly working CCC/intelligent compaction rollers and roller measurement systems revealed an uncertainty of ±10% (one standard deviation); that is, a repeated pass over the same area will yield individual roller MVs within ±10%. A repeatability testing procedure was successful in identifying when a roller or roller measurement system was faulty. Repeatability testing of pad foot measurement systems revealed single MV uncertainties in excess of ±25%. The repeatability testing procedure outlined in this chapter is recommended for CCC specifications and is described further in Chapter 7.
- Roller MVs are influenced by the magnitude of eccentric force (or theoretical drum vibration amplitude A). From low to high A vibration on the same material, roller MVs were found to vary by as much as 100%. The amplitude dependence of roller MVs was not determinate and not predictable. Roller MVs were found to increase, decrease, or remain the same with increasing A depending on the soil and layering conditions. The nature of A dependence of roller MVs is discussed from a perspective of soil mechanics in Chapter 4. Owing to the unpredictability in A dependence, a fixed amplitude is recommended for roller-integrated CCC.
- CCV and CMV_D were found to decrease considerably with increased roller speed. The influence of roller speed on E_{vib} was inconclusive within the uncertainty of the measurement approach and the limited data collected. These findings suggest that roller speed should be fixed when using at least CCV and CMV_D during QA.
- Roller MVs were found to be mildly dependent on forward versus reverse driving modes. Roller MVs differed by 2% to 13% in forward versus reverse driving mode. Given that typical compaction work involves forward/reverse driving

sequences, there is considerable benefit to using roller MVs in both forward and reverse modes. Forward and reverse mode measurement should be considered; however, site-specific calibration is required to characterize and verify the relationship between forward-measuring and reverse-measuring roller MVs.

- The vibration-based roller MVs investigated—Ammann and Case/Ammann k_s, Bomag E_{vib}, Dynapac CMV_D, and Sakai CCV—correlate well with each other over a range of soft to stiff soil conditions. CCV and CMV were found to be insensitive to soil stiffness below values of approximately 8 to 10, as is consistent with the literature.
- Many of the roller MVs employed by manufacturers were validated using independent instrumentation and implementation of published roller MV algorithms. This dispels the "black box" mentality that would inhibit implementation within the engineering community.
- Local soil heterogeneity transverse to the direction of roller travel has a significant influence on roller MVs. Owing to the nature of drum instrumentation, roller MVs are directionally dependent on heterogeneous soil. Roller MVs collected by traversing in opposite directions were found to vary by 100% due to transverse soil stiffness variability. This was confirmed by LWD testing across the drum lanes. As a result, spot testing should be conducted across the drum lane when correlating to roller MVs, and great care should be used when performing spatial statistical analysis of pass-to-pass data maps in the presence of heterogeneity.

CHAPTER 4

Relationship Between Roller-Based Stiffness and In Situ Response

This chapter explores the relationship between roller-measured stiffness and in situ stress-strain-modulus behavior. Numerous vertically homogeneous embankments and layered subgrade/subbase/base TBs were instrumented with stress and strain sensors at multiple levels to capture in situ behavior during static and vibratory roller passes. Three smooth drum vibratory rollers were operated over the TBs: Ammann AC110, Bomag BW213, and Sakai SV510 with independent instrumentation (see Table 4.1). The three distinct force delivery approaches employed by the three rollers were summarized in Chapter 2. This chapter describes how current stiffness-based vibratory roller measurement values (MVs; i.e., E_{vib}, k_s) are related to in situ soil response in vertically homogeneous and layered structures. From a mechanics perspective, this chapter explains the vibration amplitude dependence of roller MVs and measurement depth of the instrumented roller. This chapter also discusses the sensitivity of roller-measured stiffness to thin lifts (e.g., base over subbase/subgrade). A detailed, more technical presentation of this investigation and the results is provided in Rinehart & Mooney (2009a, 2009b), Rinehart et al. (2008, 2009), and Mooney & Rinehart (2009).

4.1 Roller-Induced Stress Paths and Levels

In current pavement design procedures, laboratory-determined resilient modulus (M_r) serves as one key performance indicator for unbound materials. In addition, mechanistic-empirical (M-E) pavement design promotes the use of layered analysis and nonlinear modulus functions. To enable performance-based QA, the relationship between roller-measured soil stiffness and soil modulus must be better understood, including the relationship between the stress state/stress path induced by vibratory roller loading and the stress state/stress path used in laboratory M_r testing (AASHTO T307).

A considerable amount of testing has been performed to characterize the stress-dependent nature of M_r. The consensus model describing M_r of granular soils that reflects the confining and deviator stress dependence of soil (Uzan 1985, Witczak & Uzan 1988) is given by:

$$M_r = k_1 p_a \left(\frac{\theta}{p_a}\right)^{k_2} \left(\frac{q}{p_a}\right)^{k_3} \tag{4.1}$$

Table 4.1. Summary of roller parameters.

Roller Characteristic	Ammann AC110	Bomag BW213	Sakai SV510
Drum width, m (ft)	2.20 (7.22)	2.13 (7.00)	2.13 (7.00)
Drum radius, m (ft)	0.75 (2.46)	0.75 (2.46)	0.75 (2.46)
Static mass, kg (lb)	11,500 (25,350)	14,900 (32,850)	12,500 (27,600)
Static linear load, kN/m (kip/ft)	31.5 (2.2)	42.4 (2.9)	32.2 (2.2)
Operating frequency (Hz)	20–34	28	37, 28[c]
Vertical eccentric force F_{ev}, kN (kip)	0–277 (0–62)[a]	0–365 (0–82)[b]	186, 245 (42, 55)[c]

[a] One hundred preprogrammed amplitude settings.
[b] Six preprogrammed amplitude settings.
[c] Low- and high-amplitude settings.

$$\theta = 3p = \left(\sigma_z + \sigma_x + \sigma_y\right) \tag{4.2}$$

$$q = \frac{1}{\sqrt{2}}\sqrt{\begin{matrix}\left(\sigma_z - \sigma_x\right)^2 + \left(\sigma_x - \sigma_y\right)^2 + \left(\sigma_y - \sigma_z\right)^2 \\ + 6\tau_{zx}^2 + 6\tau_{xy}^2 + 6\tau_{yz}^2\end{matrix}} \tag{4.3}$$

where p is the mean normal stress, q is the deviator stress, the bulk stress $\theta = 3p$, p_a is atmospheric pressure, and k_i are best-fit parameters determined by evaluation of laboratory data. Santha (1994) determined model parameters k_i for a wide range of granular and cohesive soils. Average ± standard deviation values of k_1, k_2, and k_3 were found to be 420 ± 173, 0.34 ± 0.09, and -0.37 ± 0.10, respectively, for granular materials. For cohesive soil, average ± standard deviation values were reported to be 645 ± 252, 0, and -0.26 ± 0.13 for k_1, k_2, and k_3, respectively. The deviator stress q is equivalent to the von Mises stress commonly used in solid mechanics and can be related to the octahedral shear stress τ_{oct} via $q = 3\tau_{oct}/\sqrt{2}$. For assessment of laboratory M_r data, Equation 4.3 reduces to the commonly observed form $q = (\sigma_z - \sigma_x)$.

Commercially available earth pressure cells (EPCs) and linear voltage displacement transducers (LVDTs; see Figure 4.1) were used to measure total normal stresses σ_x, σ_y, and σ_z and normal strains ε_x, ε_y, and ε_z induced by static and vibratory roller compactors. The sign convention used throughout includes z positive downward from the soil surface, x positive in the direction of roller travel, and y positive to the roller operator's right. Total stresses were measured and assumed equal to effective stress. This is similar to the methodology employed in lab testing of M_r, where total stresses are also measured and used to determine M_r. While suction-induced pore pressures likely exist, their influence is considered minimal compared to the high roller-induced normal stresses. A complete discussion of in situ measurement of stress and strain, including sensor dimensions, sensor calibration, field installation techniques, and measurement uncertainty is provided in Rinehart & Mooney (2009a).

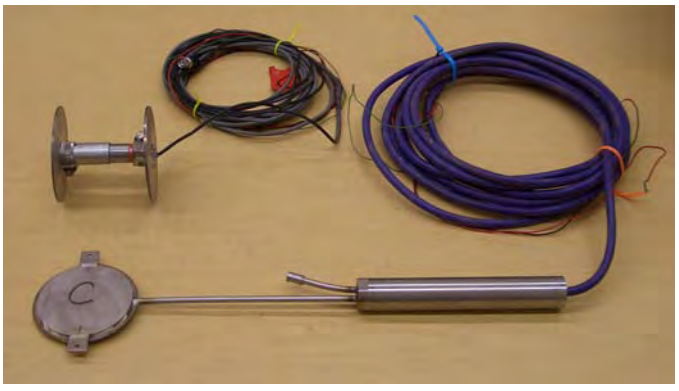

Figure 4.1. LVDT strain sensor (top) and EPC (bottom).

To complement the measured in situ stresses from discrete depths during vibratory roller passes, the complete state of stress was investigated with a boundary element method (BEM) approach (see Rinehart et al. 2008, 2009). The boundary element formulation used is appropriate for two-dimensional plane-strain conditions and can accommodate general anisotropy (Ting 1996). Experimental results show that plane strain conditions exist beneath the center of the 2.1-m (6.9-ft)-long drum but not at the edges (Rinehart et al. 2008). The two-dimensional approach offered by the boundary element tool used here is a good first step in characterizing the stresses induced by the vibrating drum.

Results from low-vibration amplitude roller passes over two different soils are discussed: clayey sand subgrade [A-6(1)] and granular subbase (A-1-b). To compare stress paths in the field and laboratory (i.e., during M_r testing per AASHTO T-307), profiles of mean normal stress p and deviator stress q were calculated according to Equations 4.2 and 4.3. Figure 4.2 presents p-q stress paths from four depths during low-excitation force (F_{ev}, see Section 2.1.1) vibratory roller loading on a clayey sand subgrade and granular subbase. The paths shown represent the least squares best fit to the in-ground sensor measurements determined by BEM analysis (see Rinehart et al. 2009 for more detail). The paths are not strictly linear, but it is a reasonable assumption. For the medium stiff subgrade of TB MN29, the maximum value of roller-induced q is much greater than that used in M_r testing. Figure 4.2 also shows that for base materials the slope of the p-q loading line m in M_r testing is very similar to that induced by the roller, 3.0 and 3.1, respectively. For subgrade materials, m varies between 1.8 and 2.2, lower than the value of 3.0 used in M_r testing.

In general, inspection of the p and q profiles with depth (see Rinehart et al. 2009) reveals that for $z < 0.5$ m (1.6 ft), levels of q observed in the subgrade material are greater than the highest value of q used in AASHTO T307 lab M_r testing by a factor of 1 to 3. For $z > 0.5$ m (1.6 ft), values of q observed in the field are similar to those used in lab testing. Levels of p in the subgrade material are greater than the highest lab value by a factor of 1 to 5 for $z < 0.25$ m (0.8 ft). Levels of p in the field are similar to lab levels at depths between $z = 0.25$ (0.8 ft) and 0.5 m (1.6 ft); for $z > 0.5$ m (1.6 ft), lab levels of p are greater than those used in the field. For the subbase material [i.e., $z = 0.25$ m (0.8 ft) in Figure 4.2b], the levels of roller-induced q are greater than the highest value of q used in the lab by a factor of 1 to 2.5. Levels of p in the lab are greater than those observed in the field by a factor of 1 to 5.

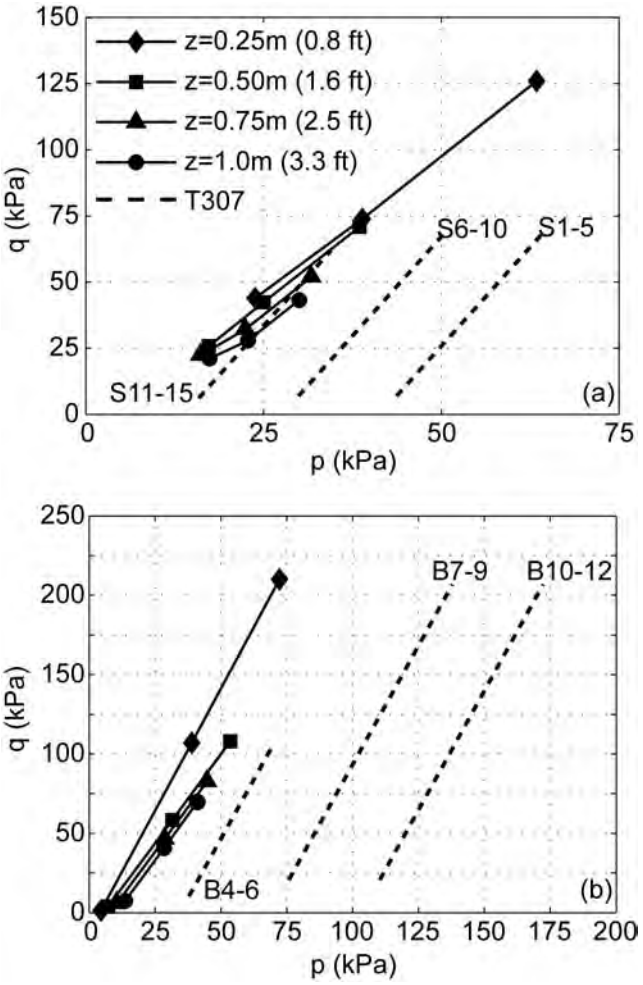

Figure 4.2. Stress paths due to vibratory roller loading and laboratory M_r testing per AASHTO T307: (a) subgrade soil, A-6(1) [f = 30 Hz, F_{ev} = 87 kN (19.6 kip), v = 0.5 m/s (1.6 ft/s)] and (b) subbase material, A-1-b [f = 28 Hz, F_{ev} = 88 kN (19.8 kip), v = 1.0 m/s (3.3 ft/s)]; selected AASHTO T307 subgrade (S) and base (B) loading sequences shown for reference (adapted from Rinehart et al. 2009).

4.2 Measurement Depth in Vertically Homogeneous Embankments

Roller MVs from typical highway construction earthwork rollers (11 to 15 tons) measure to depths significantly greater than a typical 15- to 30-cm (6- to 12-in)-thick lift and to depths greater than the 20- to 50-cm (8- to 20-in) depths of traditional spot tests [e.g., nuclear gauge, static PLT, and LWD; Mooney & Miller 2008]. Pavement earthwork involves various combinations and thicknesses of embankment subgrade, subbase, and base course materials; therefore, roller-measured stiffness of homogeneous and layered structures will be significantly influenced by measurement depth. This section presents an investigation of roller measurement depth and how it is influenced by F_{ev}.

4.2.1 Measurement Depth from Layer Buildup Experiments

One approach to experimentally assess measurement depth is to monitor roller-measured stiffness as successive layers of a stiff material are placed and compacted above a softer subsurface. Roller-measured stiffness provides a composite measure of the soil from the surface to the measurement depth and therefore should increase with increasing thickness of the overlying stiff material. Beyond a critical stiff soil thickness H_c, the roller-measured stiffness should remain constant, indicating it is no longer sensing the underlying soft material. Figures 4.3a and b show how this layer buildup approach was used to investigate measurement depth. The study is described in detail in Rinehart & Mooney (2009b).

These data suggest that the measurement depth (i.e., H_c) reflected by the roller-measured stiffness is approximately 1.0 to 1.2 m (3.3 to 3.9 ft) for this 11,500-kg (25,350-lb) Ammann roller when operated on this crushed stone (A-1-a) material. Within the 0.1- to 0.2-m (0.3- to 0.6-ft) uncertainty associated with this approach (i.e., one-half layer thickness), H_c does not depend strongly on F_{ev}. This finding contradicts previous literature that indicates measurement depth varies considerably with vibration amplitude (Anderegg & Kaufmann 2004, Kopf & Erdmann 2005); for example, H_c should have varied by 1.0 m (3.3 ft) over the range of F_{ev} tested here per the relationship suggested by Anderegg and Kaufmann. In Section 4.2.2 below, it is shown that H_c does vary slightly with F_{ev}. It is also worth noting that the roller-measured stiffness does not begin to increase until the third lift of crushed stone [$H >$ 0.5 m (1.6 ft)], suggesting that roller-based stiffness measures are insensitive to "thin" layers of stiff soil over softer material, which are common in pavement earthwork construction (e.g., base over subgrade). This critical point is discussed in more detail in Section 4.4.

Figures 4.4a and b show how the layer buildup approach was employed during a second experimental investigation of measurement depth. Seven layers of the crushed rock base material [totaling 1.72 m (5.64 ft) thick] were placed and compacted within a trench cut into a sandy silt embankment (TB MD4). Several 15-ton Bomag roller-measured E_{vib} records measured during the buildup of base course layers over subgrade are presented in Figure 4.4c. The embankment subgrade in TB MD4 had two distinct stiffness zones, as evidenced by the $H = 0$ m MV record. Figure 4.4d shows that the roller-measured stiffness values increase substantially with H and plateau at approximately $H = 1.2$ to 1.4 m (3.9 to 4.6 ft)

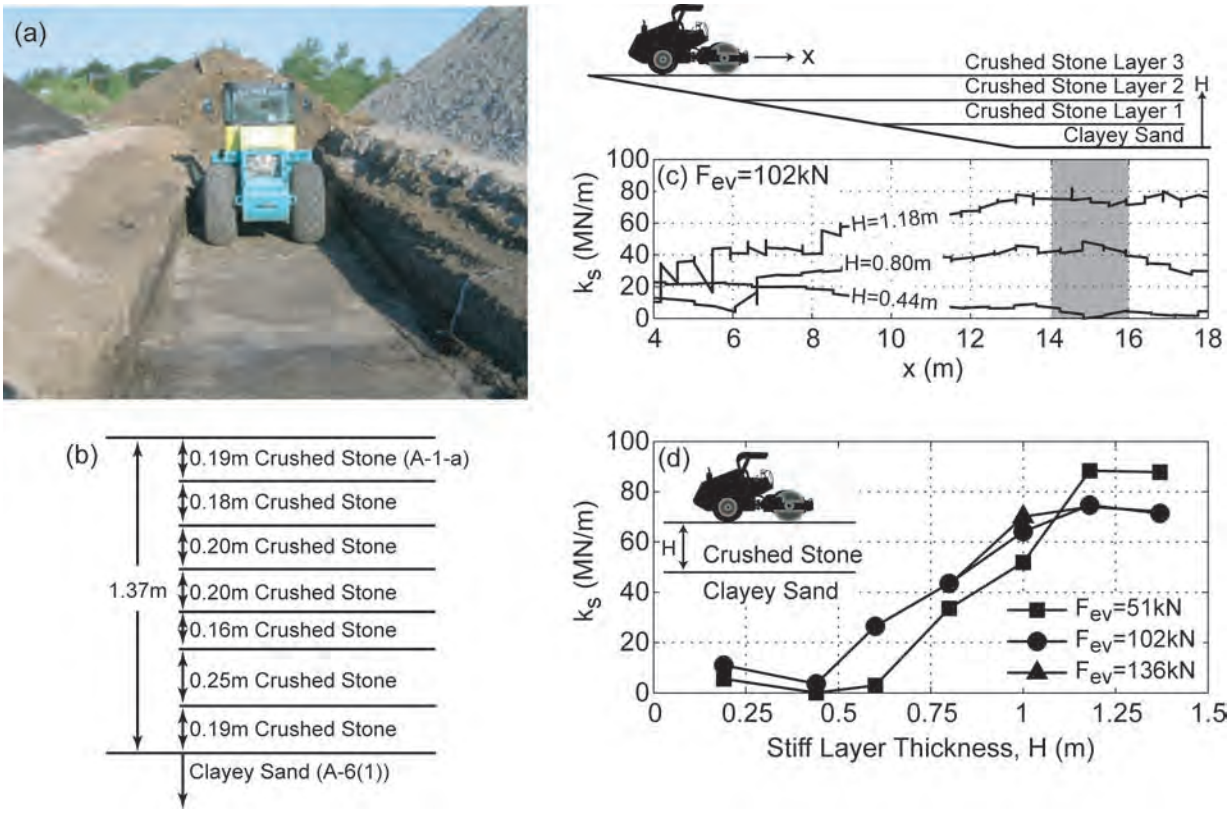

Figure 4.3. (a) photo and (b) schematic of stiff-layer buildup portion of TB MN29, (c) roller-measured stiffness records at three values of stone thickness H, and (d) variation of roller-measured stiffness with H for three levels of F_{ev} (adapted from Rinehart & Mooney 2009b).

for the stiffer section and at approximately $H = 1.1$ to 1.3 m (3.6 to 4.3 ft) for the softer section.

These data suggest that the measurement depth (i.e., H_c) reflected by the roller-measured stiffness is approximately 1.1 to 1.4 m (3.6 to 4.6 ft) for this 14,900-kg (32,850-lb) Bomag roller when operating on this crushed rock (A-1-b) material. Similar to results from MN29, within the 0.1- to 0.2-m (0.3- to 0.6-ft) uncertainty of this technique, H_c does not vary strongly over these low, medium, and high F_{ev} values.

The base-to-subgrade stiffness ratio does not appreciably affect H_c. An inspection of Figure 4.4d data shows that H_c was the same for both the soft and stiff subgrade sections [within the 0.1- to 0.2-m (0.3- to 0.6-ft) uncertainty]. For $H > H_c$, the roller-measured stiffness is not influenced by the underlying subgrade material.

For base course thickness more typical of practice (i.e., $H < H_c$), Figures 4.4d and e illustrate that roller-measured stiffness is clearly a composite measure of the underlying subgrade and overlying base material. The relative contribution of each material to roller MV is a function of layer thickness, base/subgrade modulus ratio, F_{ev}, and other roller/soil interaction factors (contact area, dynamics). A comparison of Figures 4.4d and e illustrates that the base-to-subgrade stiffness ratio influences the roller-measured stiffness for $H < H_c$. This is described further in Section 4.4.

4.2.2 Measurement Depth from Profiles of Vertical Stress and Strain

Profiles of vertical stress and strain measured during roller passes on TB MN29 clayey sand and during the buildup of MD4 crushed rock over silt were examined to determine a mechanistic rationale for H_c. Magnitudes of $\sigma_{z,peak}$ and $\varepsilon_{z,peak}$ at the experimentally determined H_c [1.2 m (3.9 ft)] were identified from the TB MD4 theoretical profiles. Total and cyclic $\sigma_{z,peak}$ and $\varepsilon_{z,peak}$ at $z = 1.2$ m (3.9 ft) were found to be 8% to 12% of their maximum values (termed $\sigma_{z,max}$ and $\varepsilon_{z,max}$) at or near $z = 0$ (see Table 4.2). The observed ratios of $\sigma_{z,peak}$ and $\varepsilon_{z,peak}$ to their maximum values increased slightly with F_{ev}. Specifically, cyclic $\varepsilon_{z,peak}$ values increased from 9% of maximum at low F_{ev} to 11% of maximum at high F_{ev}. These results suggest that H_c does increase slightly with F_{ev}. Further, these

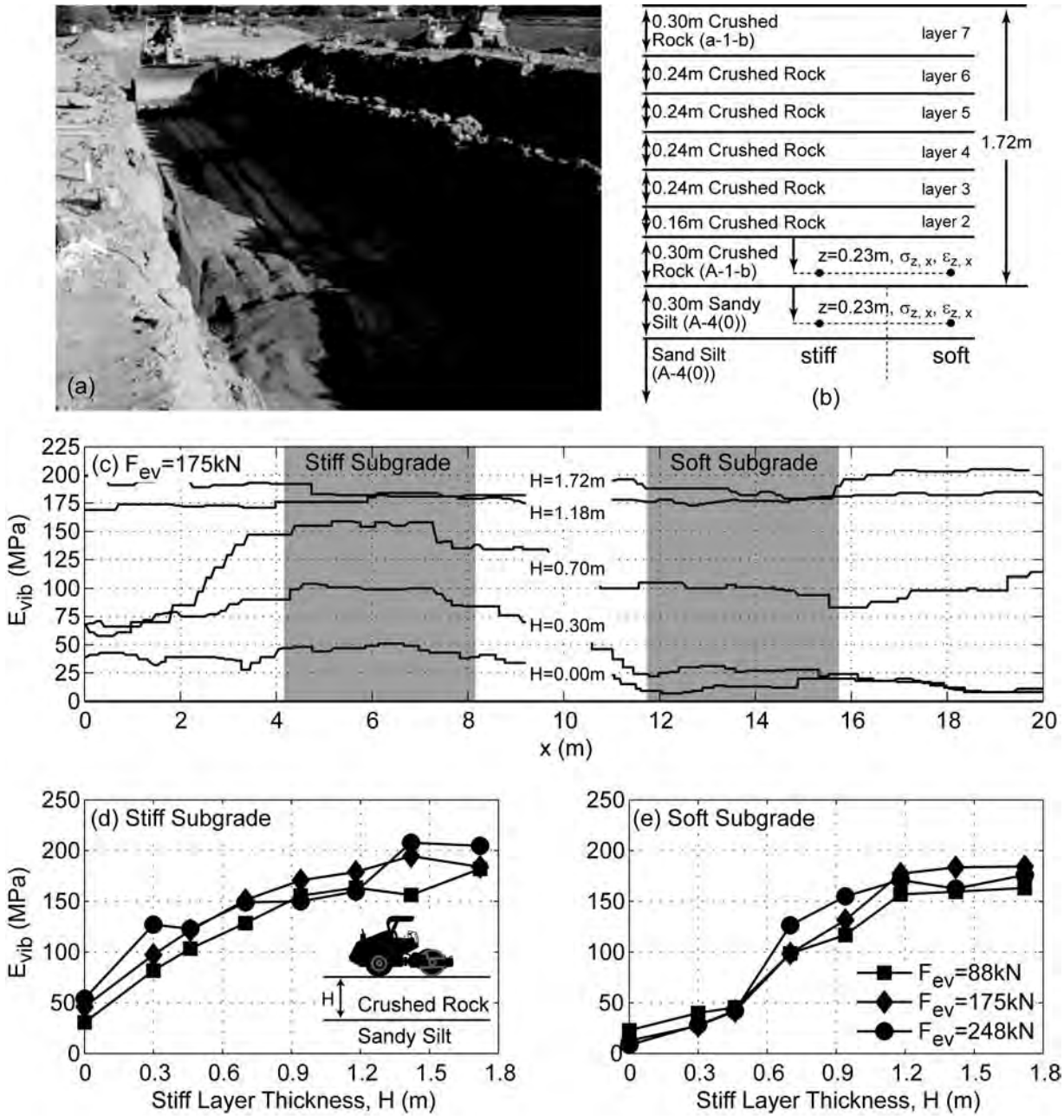

Figure 4.4. (a) photo and (b) schematic of stiff-layer buildup portion of TB MD4, (c) roller-measured stiffness records at three values of H, and (d–e) variation of roller-measured stiffness with H for three levels of F_{ev} (adapted from Rinehart & Mooney 2009b).

results show that measurement depth is a function of stress and strain decay and that H_c is reached when stress or strain has decayed to about 10% of its peak value (i.e., at or near the surface). The relationship between H_c and cyclic ε_z reduction to approximately 10% of maximum is consistent with classical settlement analysis used in foundation engineering.

Given that roller MVs are based on cyclic deformation, the following analysis focuses on the decay of cyclic strain. The 10% cyclic $\varepsilon_{z,peak}$ criterion for estimating H_c was applied to the profiles of cyclic $\varepsilon_{z,peak}$ from the TB MN29 clayey sand. Figure 4.5a presents the variation of estimated H_c as a function of actual vertical drum displacement z_d from several IC roller passes. These values of z_d reflect the range of low to high F_{ev}. Figure 4.5a shows that measurement depth increases from 0.8 m (2.6 ft) at low F_{ev} and z_d to 1.2 m (3.9 ft) at high F_{ev} and z_d. Here, a 0.1 mm (0.004 in) increase in z_d corresponds to a 3-cm (1.2-in) increase in measurement depth. This is considerably less than the 0.1 mm (0.004 in) = 10 cm (3.9 in)

Table 4.2. σ_z and ε_z decay at the experimentally determined measurement depth.

F_{ev} (kN)	$\left(\frac{\sigma_z\|_{z=1.2m}}{\sigma_{z,max}}\right)$ (%)	$\left(\frac{\sigma_z\|_{z=1.2m}}{\sigma_{z,max}}\right)_{Cyclic}$ (%)	$\left(\frac{\varepsilon_z\|_{z=1.2m}}{\varepsilon_{z,max}}\right)$ (%)	$\left(\frac{\varepsilon_z\|_{z=1.2m}}{\varepsilon_{z,max}}\right)_{Cyclic}$ (%)
88	8.3	6.5	11.7	9.2
175	9.7	7.8	12.0	10.4
248	10.5	8.7	9.4	11.0
Mean	9.5	7.7	11.0	10.2

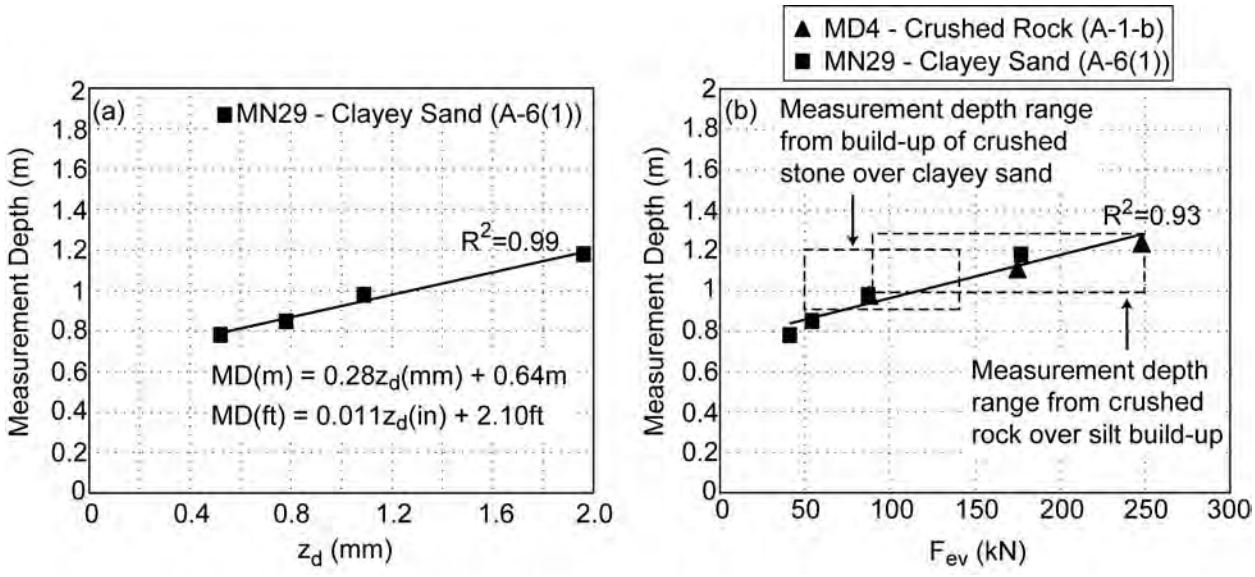

Figure 4.5. Variation of measurement depth with (a) actual vertical drum displacement z_d from TB MN29 and (b) F_{ev} from both TB MN29 and TB MD4 (adapted from Rinehart & Mooney, 2009b).

rule of thumb reported in the literature (e.g., Anderegg and Kaufmann 2004).

Using the 10% cyclic $\varepsilon_{z,peak}$ criteria, measurement depth was estimated from data collected during IC roller passes on the MN29 clayey sand and on the MD4 crushed rock over silt (see Figure 4.5b). Two different IC rollers were used. Measurement depth is plotted versus F_{ev} because actual drum deflection values (z_d) were not reported by both rollers. There is very good agreement across the two materials and rollers using the cyclic strain criteria. Additionally, the range of H_c observed experimentally in the layer build-up experiments agree reasonably well and within the 0.1-0.2 m (0.3-0.6 ft) uncertainty of that technique. Regarding the measurement volume of roller MVs (i.e., 3D), Rinehart and Mooney (2009b) shows that peak stress and strain propagate roughly twice as far in the vertical direction than in the horizontal direction. The results presented here along with those in the literature show that a given roller-measured stiffness value is representative of soil approximately 0.25-0.3 m (0.8-1.0 ft) in front of and behind the center of the drum and to a depth of 0.8-1.2 m (3.0-3.9 ft). This area of influence is important to consider when performing correlations of roller-measured stiffness to spot-test measurements that reflect a much smaller volume.

4.3 Relating Roller-Based Stiffness to In Situ Response

An important objective of this study was to understand the nature of roller-measured stiffness through its relationship to in situ soil modulus. This relationship holds the key to the development of performance-based specifications and the prediction of pavement performance using roller-measured soil properties. A more detailed presentation of these results is available in Mooney and Rinehart (2009).

As illustrated in Figure 4.6g-i, roller-based stiffness is derived from cyclic drum deformation z_d and is indirectly influ-

enced by the soil response in the *x* and *y* directions. Similarly, a vertical dynamic deformation modulus *M* can be extracted from the cyclic in situ σ_z-ε_z response to vibratory loading. As illustrated in Figure 4.6a-d, the cyclic soil response is calculated by subtracting the portion due to the static roller weight. Figures 4.6e and f show individual cyclic σ_z-ε_z paths and illustrate the measures of *M* evaluated in this study as determined from the σ_z-ε_z response during vibratory roller passes over clayey sand subgrade and granular base material, respectively. M_L is the tangent modulus of the loading portion of the σ_z-ε_z response, and M_S is the secant modulus from zero σ_z-ε_z through the point of maximum ε_z. The extracted *M* values are not constitutive (e.g., Young's modulus); rather, *M* is akin to a partially constrained dynamic modulus that is influenced by the σ_y-ε_y and σ_x-ε_x fields. In Figures 4.6h-i, k_1 is equivalent to the stiffness term used by Bomag to determine E_{vib} (see Section 2.2.2) and is comparable to M_L. The stiffness term k_2 in Figures 4.6h-i is equivalent to Ammann k_s (see Section 2.2.1) and is comparable to M_S (Mooney and Rinehart 2009).

4.3.1 Embankment Situations

Roller-measured stiffness was related to in situ moduli *M* from multiple depths within a 1-m (3.3-ft)-deep vertically homogeneous subgrade soil (TB MN29). Instrumentation was installed at four depths during construction of a clayey sand embankment test bed (see Figure 4.7a). Four lifts of the clayey sand subgrade soil (A-6(1)) were placed and compacted with the IC roller with instrumentation in place, resulting in a 1.0-m (3.3-ft)-thick layer of subgrade soil above the underlying crushed stone. This 1.0 m (3.3 ft) of subgrade soil extends beyond the measurement depth of the IC roller at low-medium amplitude levels (see Section 4.2). Therefore, roller MVs reflect the clayey sand only, and this test bed represents a vertically homogeneous embankment situation.

Roller MVs and in situ stress-strain data were collected simultaneously during Ammann IC roller passes using various excitation frequency and amplitude combinations. Figures 4.7b and c present M_L and M_S values determined at three depths during vibratory passes. The *M* versus vertical excitation force amplitude F_{ev} (see Equation 2.1) data were characterized statistically with power relationships ($M_L = b(F_{ev})^c$) at each depth. Figure 4.7d shows that roller-measured k_s decreases as F_{ev} increases. Figures 4.7e and f illustrate the relationship of in-situ M_L and M_S (from three depths) to the roller-measured k_s. The data were collected over the range of F_{ev} shown using three excitation frequencies and four eccentric mass moments.

As shown in Figures 4.7b and c, M_L and M_S generally increased with depth and decreased with increasing F_{ev}. The sensitivity of M_S values to depth and to F_{ev} was similar to that shown by M_L. *M* varied by a factor of two for these low to high amplitude F_{ev} values typically employed in the field. *M* values also varied by a factor of two over the depths measured (0.14-0.65m [0.46-2.1 ft]). The variability of *M* with depth coupled with the varying stiffness along the length of the drum illustrate that roller-measured stiffness—even at low F_{ev}—provides a composite reflection of a field of spatially varying modulus, i.e., there is not just one value of soil modulus reflected in a roller MV. For performance-related specifications, this nonlinear variation in modulus should be taken into consideration together with the differences between roller-induced and traffic-induced stress conditions and their effect on modulus.

The observed M_L and M_S behavior as a function of F_{ev} are a field manifestation of the stress dependence of soil modulus that has been well established in the laboratory (e.g., Ishihara 1996, Andrei et al. 2004). Generally, modulus increases with increasing confining stress and decreases with increasing shear (deviatoric) stress. For fine-grained cohesionless and cohesive soils, the decrease in modulus with increasing shear stress typically outweighs the increase in modulus due to increasing effective confining stress (Andrei et al. 2004). Roller vibration induces both confining and shear stresses. During vibratory loading here, the substantial levels of σ_z and σ_y coupled with very low values of σ_x at $x = 0$ (see Rinehart and Mooney 2009a) lead to the significant levels of deviatoric stress that results in the decrease in *M* with increasing F_{ev}. The decrease in roller-measured stiffness with increasing F_{ev} has been documented previously for embankment granular material and attributed to stress-induced softening (e.g., Mooney & Rinehart 2007); these results now confirm this hypothesis.

Figures 4.7e and f show that roller-measured stiffness is positively correlated with M_L and M_S implying that changes in roller-measured stiffness are representative of the response of the soil. The strength of the *M* versus roller-measured stiffness relationship (evidenced by R^2) and the sensitivity of *M* to roller-measured stiffness (evidenced by slope of the best fit line) were found to be greater at $z = 0.36$ (1.2 ft) and 0.65 m (2.1 ft) than at $z = 0.14$ m (0.46 ft), implying that the roller MV is less reflective of soil very near the surface.

The results illustrate one mechanism by which roller-measured stiffness varies with F_{ev} during operation on vertically homogeneous embankment soil, a situation commonly encountered in earthwork. Generalizing to all vertically homogeneous embankments, the relationship between roller-measured stiffness and F_{ev} (or amplitude *A*) will be dictated by the stress-dependent modulus relationship of the involved soil. Because the modulus relationship varies across soils, the relationship between roller-measured

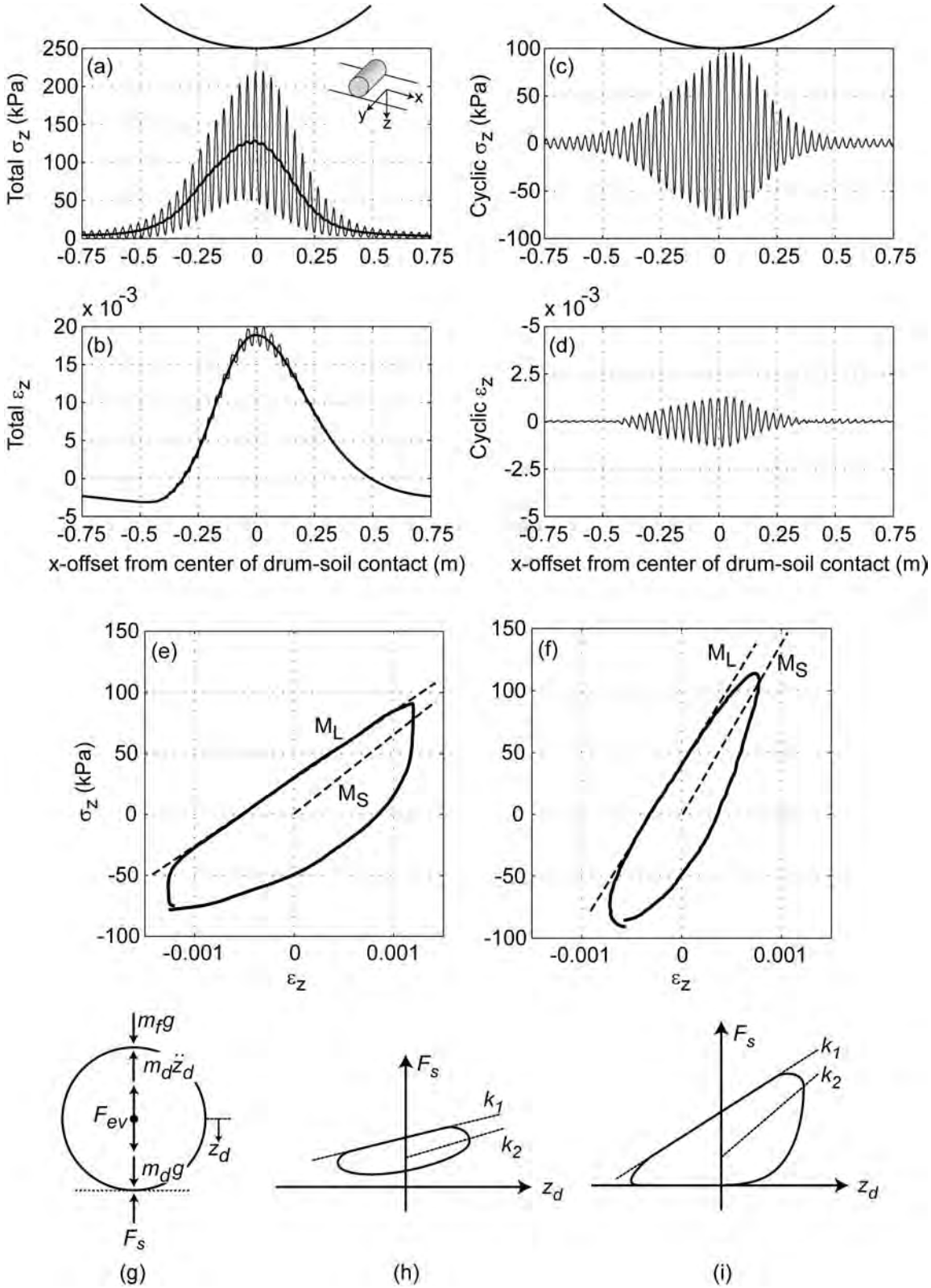

Figure 4.6. Total roller-induced (a) σ_z, (b) ε_z, cyclic roller-induced (c) σ_z, (d) ε_z, individual σ_z-ε_z paths showing extraction of the vertical deformation moduli M_L and M_S for (e) subgrade soil, (f) base material, (g) free body diagram of roller drum, and F_s-z_d paths showing extraction of roller-measured stiffness for (h) contact operation and (i) partial loss of contact operation (adapted from Mooney & Rinehart, 2009 and Rinehart & Mooney, 2009b).

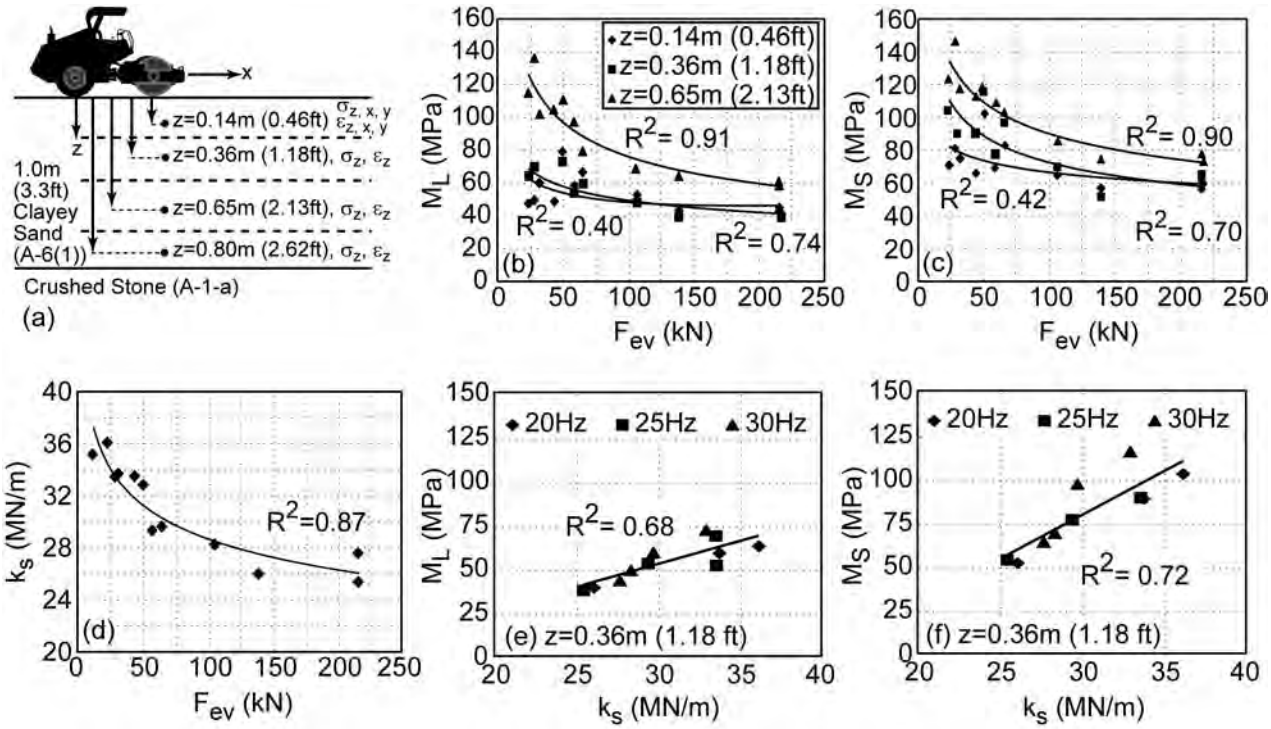

Figure 4.7. (a) MN29 embankment test bed schematic, (b-c) variation of in situ vertical deformation modulus with F_{ev}, (d) variation of roller-measured stiffness with F_{ev} and (e-f) correlation between roller-measured stiffness and in situ vertical deformation modulus (adapted from Mooney & Rinehart, 2009).

stiffness and F_{ev} will not be unique and may change as the soil is compacted.

The considerable variation of stress with depth combined with the stress dependent soil modulus indicates that the modulus field may vary significantly with depth. To investigate this, Equation 4.1 was used to calculate soil modulus based on the stress profiles calculated with the BEM model and typical k_i values for cohesive and granular soils (e.g., from Santha, 1994). Average k_i values are taken to be 420, 0.25 and -0.30 for k_1, k_2, and k_3, respectively. Applying Equation 4.1 with average k_i values to data from TB MN29 shows a relatively constant modulus profile, with only 10% variation from $z = 0.25$ to $z = 1.0$ m (0.8-3.3 ft) (see Figure 4.8a). However, results presented earlier from analysis of M_L and M_S from in-ground instrumentation revealed that the modulus in TB MN29 was a factor of two greater at $z = 0.65$ m (2.13 ft) than at $z = 0.14$ m (0.46 ft). Using k_i values more typical of a cohesive soil (e.g., 420, 0 and -0.6 for k_1, k_2, and k_3, respectively) results in a modulus profile more representative of the observed behavior (see Figure 4.8d) with modulus ranging from 37 MPa at $z = 0.25$ m to 71 MPa at $z = 1.0$ m (0.8-3.3 ft). Figure 4.8 illustrates that the modulus profile with depth can vary considerably and is strongly dependent on modulus function parameters (Rinehart et al. 2009).

4.3.2 Layered Earthwork

Another common earthwork situation is the layered system involving a base course overlying a subbase or subgrade, or a subbase course overlying a subgrade. In these situations, roller MVs provide a composite measure of the involved layers. In layered systems, the dependence of roller MV on F_{ev} does not always parallel in situ modulus behavior as was the case in the homogeneous embankment discussed earlier. The structure of the layered system plays a significant role in the nature of the roller MV. As illustrated in Figure 4.9a, TB MD4 was constructed by compacting several lifts of crushed rock subbase material (A-1-b) over a sandy silt subgrade A-4(0). In-ground instrumentation was installed in the subgrade and the first lift of subbase material to measure σ_z and ε_z. Roller MV data (E_{vib}) were collected during operation on the subgrade and on the first three lifts of subbase material.

Figures 4.9(b-d) illustrate the relationships observed between in situ M and F_{ev} and between roller-measured stiffness and F_{ev} observed during testing on MD4. Within the data from each lift, roller-measured stiffness values increased with F_{ev} (Figure 4.9d), however, M_L and M_S in the crushed rock both decrease with increasing F_{ev} (Figures 4.9b and c). Focusing on M_L behavior because it more closely parallels the definition

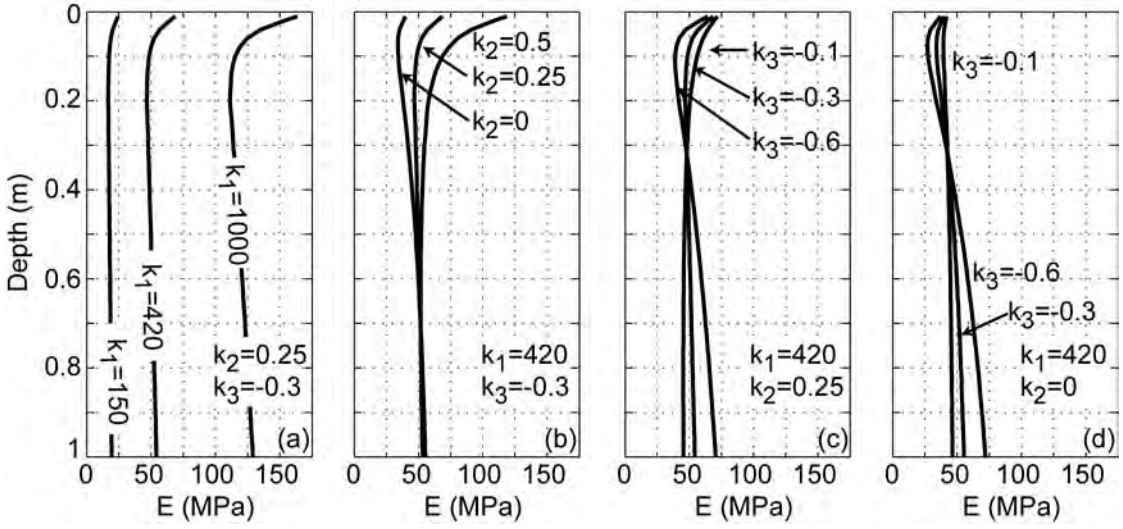

Figure 4.8. Modulus variation with depth in clayey sand subgrade (TB MN29) (adapted from Rinehart et al. 2009).

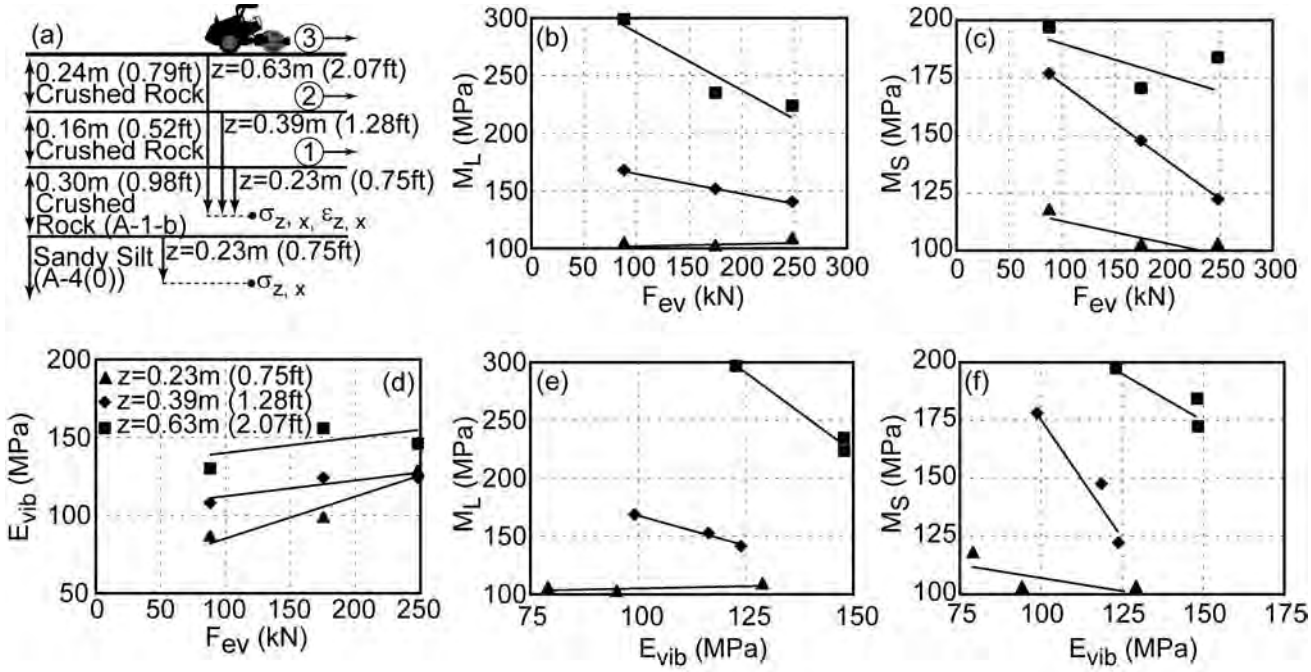

Figure 4.9. (a) TB MD4 layered test bed schematic, (b-c) variation of M with F_{ev}, (d) variation of roller-measured stiffness with F_{ev}, and (e-f) correlation between roller-measured stiffness and M (adapted from Mooney & Rinehart 2009).

of the roller-based stiffness measurement E_{vib}, the decrease in M_L with increasing F_{ev} at $z = 0.39$ and 0.63 m (1.3, 2.1 ft) is consistent with shear stress-dependent modulus behavior. Similar to clayey sand behavior (TB MN29 presented earlier), the M_L versus F_{ev} sensitivity increased with depth, and was reasonably insensitive at $z = 0.23$ m (0.75 ft).

The layered structure is the primary cause for the increase in roller-measured stiffness with increasing F_{ev} despite the decrease in base course M_L. As described in significant detail elsewhere (Mooney & Rinehart 2009), the stiffer base material takes on a greater portion of the load with increasing F_{ev}. Vibratory roller interaction with layered earthwork is in-

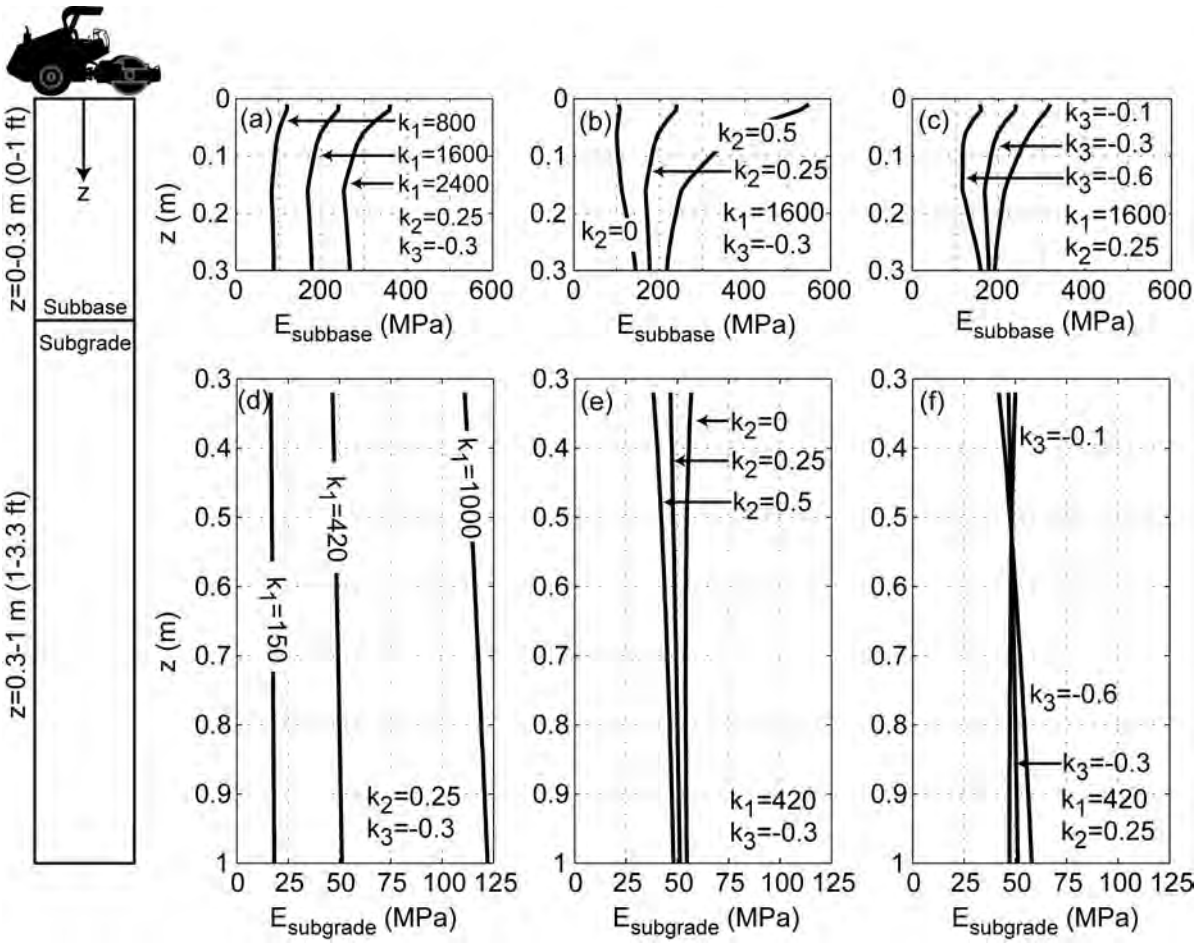

Figure 4.10. Modulus variation with depth in TB MD4 (adapted from Rinehart et al. 2009).

fluenced by a number of factors including stress-dependent modulus of each material, drum/soil contact width, the stiffness ratios of the involved layers, and roller/soil dynamics. The topic is not fully understood and is an area of ongoing research.

Modulus profiles determined from the p and q distributions in TB MD4 are presented in Figure 4.10. The value of k_1 for the subbase material (z = 0-0.3 m [0-1 ft]) was increased beyond the range presented by Santha (1994) to account for the high stiffness of this material. Analysis of TB MD4 data shows that the modulus profile with average k_i values is nearly constant with depth within the base layer. However, the k_i parameters have a significant influence on the variation of modulus with depth. Depending on k_i parameters selected, the modulus can vary more than 100% within only a 0.3-m (1.0-ft)-thick base layer (Rinehart et al. 2009).

In layered base over subbase or subgrade structures, roller MVs are a composite measure of the two materials. The modulus in the underlying subgrade material is considerably lower than the base course modulus (Figure 4.10), and modulus in base and subgrade materials can both vary significantly with depth given the roller-induced stress states shown here. Therefore, knowledge of the roller-induced stresses and material specific k_i parameters combined with the appropriate numerical analysis tools to predict performance is important if roller MVs are to be used in pavement performance prediction.

4.4 Sensitivity of Roller-Based Stiffness to Thin Lifts

Using typical highway construction rollers (11-15 ton) with low to high amplitude vibration, the measurement depth for vertically homogeneous embankment conditions was found to be 0.8-1.2 m (2.6-3.9 ft). The total thickness of most base-subbase-subgrade structures is on this order, and therefore, roller MVs will reflect a composite action of these layers. As described in Sections 4.2 and 4.3, roller MVs on layered struc-

tures are a function of layer thickness, the relative stiffness of the layers, vibration amplitude or F_{ev}, and other drum/soil interaction factors. This section addresses the instrumented roller's ability to sense stiff layers atop a softer subsurface, i.e., to what degree are roller MVs representative of a relatively thin layer or lift of base or subbase material atop subgrade? To address this question, several layered test beds were constructed. The stiff layer buildup experiments described earlier represent layered test beds, particularly when the first few layers of stiff material are being compacted (before the test beds approach the embankment condition). In addition, TB FL1-6 and TB NC6-10 involved placement and compaction of thin lifts of aggregate base course material atop subgrade.

Figure 4.4 presented roller MV data records versus H for the crushed rock subbase (A-1-b) over soft and stiff sections of sandy silt subgrade (A-4(0)) (TBMD4). For $H < H_c$, the roller MV is a composite measure of both the underlying subgrade and overlying stiff subbase layer. The contribution of the subbase increases with H. The roller-measured stiffness is more sensitive to the crushed rock base atop the stiffer subgrade than atop the softer subgrade. For the stiff subgrade (base/subgrade stiffness ratio ≈ 4), E_{vib} increased by 110% to 170% from the subgrade to the first layer of subbase. By contrast, E_{vib} increases 65% to 90% from the subgrade to the first layer of subbase on the soft subgrade portion of the test bed (base/subgrade stiffness ratio ≈ 10). This trend continues with the second lift of subbase material. Similar results are found by examining Figure 4.3d where the stiffness ratio of crushed stone (A-1-a) to clayey sand (A-6(1)) subgrade is also 10. This indicates that the roller MV is more sensitive to thin lifts when the subgrade is stiff.

Figure 4.4 also showed that an increase in amplitude (F_{ev}) results in increased sensitivity to the stiff, overlying layer. This is in part attributable to an increased portion of stress being taken by the stiff material (Mooney & Rinehart 2009). However, as described earlier, roller-measured stiffness is amplitude dependent, and it is unclear how the interplay of these two factors affects the results presented in Figure 4.4.

TBs FL1-6 were created to further explore the influence of layer stiffness ratio on roller-measured stiffness. As shown in Figure 4.11a, four 15-cm (6-in)-thick lifts of aggregate base material (A-1-b) were placed and compacted atop 30-cm (12-in)-thick granular subgrade (A-3) and ash-stabilized granular subgrade material (A-3). The ash-stabilized subgrade was prepared by in-place mixing 8 cm (3 in) of bed ash with 22 cm (9 in) of the native granular subgrade material. Figures 4.11b and c present roller-measured stiffness data and LWD modulus results collected during compaction of the stabilized subgrade and base material layers. Roller-measured stiffness $k_{s\text{-}CSM}$ (computed from independent instrumentation installed by the research team on the Sakai CCC roller) was reported every 4 cm (1.6 in), and the data presented are the average of the MV over 1.0 m (3.3 ft) distance (the trends presented are representative of the test strip as a whole). The Prima LWD with a 300-mm (12-in), diameter plate was used ($E_{LWD\text{-}P3}$). The average of five locations across the width of the drum is reported.

Figure 4.11a shows the roller-measured stiffness on the 30-cm (12-in)-thick stabilized subgrade increases from less than 40 MPa after pass 2 to more than 60 MPa after pass 11. LWD test results show a similar trend during compaction of the stabilized subgrade with $E_{LWD\text{-}P3}$ increasing from less than 50 MPa after the second pass to more than 70 MPa after the 12th (and final) pass. However, roller-measured stiffness data collected during compaction of the first lift of aggregate base material (Base L1 in Figure 4.11a), remain at approximately

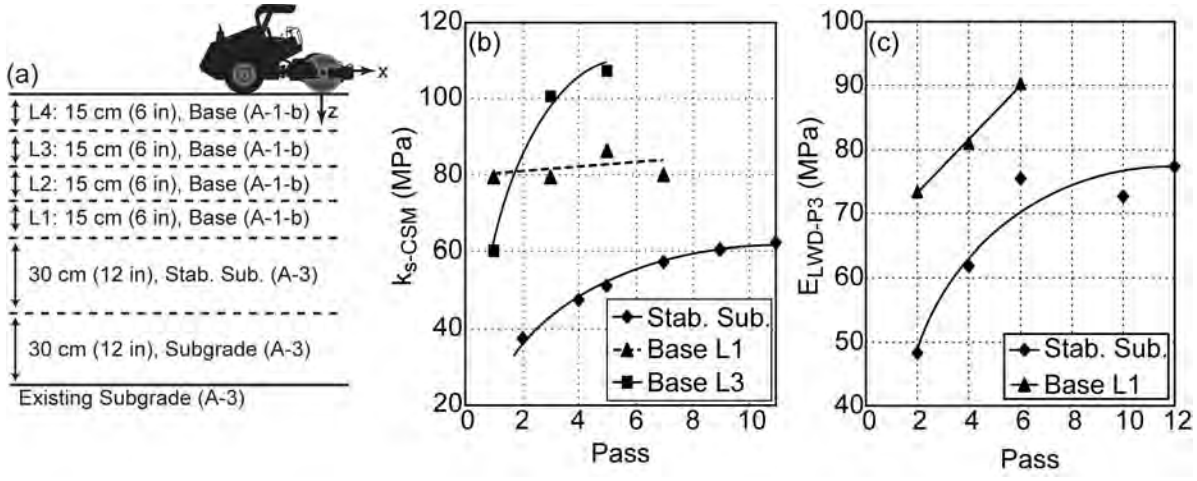

Figure 4.11. Roller MV and LWD test results during compaction of TB FL1-6.

80 MPa throughout compaction, while $E_{LWD\text{-}P3}$ increases from about 75 MPa after the second pass to 90 MPa after the sixth (and final) pass for the first lift of base material. Testing with the nuclear gauge revealed that unit weight increased from 16.83 kN/m³ (107.1 pcf) after pass 2 to 17.44 kN/m³ (111.0 pcf) after pass 6. The spot-test results indicate that compaction took place and the base material stiffened with consecutive roller passes. Therefore, the roller-measured stiffness was insensitive to the compaction-induced stiffness increase in this 15-cm (6-in) lift. Similar results were observed for the second 15-cm (6-in)-thick base lift. Note that the base: stabilized subgrade modulus ratio (based on roller-measured stiffness and LWD testing) was about 2:1.

Figure 4.11b also shows that the roller-measured stiffness increased from 60 MPa to 110 MPa during compaction of the third 15-cm (6-in)-thick lift of base material (base L3). Here, the roller-measured stiffness was sensitive to compaction of a 15-cm (6-in)-thick layer atop existing (stiff) base material. These results show that the stiffness contrast between layers is critical. The sensitivity of roller MVs to compaction of thin lifts of subbase or base material improves as the stiffness contrast between the two layers decreases. This is consistent with previous findings (e.g., Mooney et al. 2005).

The influence of base course thickness on roller-measured stiffness was further examined on TB NC6-10. TB NC6-10 involved compacting 15- and 30-cm (6-, 12-in) lifts of aggregate base material atop a silty sand subgrade (see Figure 4.12a). After compaction of the first 15-cm (6-in)-thick lift it was scarified (loosened) before an additional 15 cm (6 in) was placed. This 30 cm (12 in) of loose material formed the second lift of base material. This sequence was repeated for the third and fourth lifts. Figure 4.12b shows roller-measured stiffness data collected during compaction of the four distinct lifts of base material. The roller MV (E_{vib}) was found to be fairly insensitive to compaction of the 15-cm (6-in)-thick lift directly atop the subgrade (Base L1). The roller MV sensitivity increases for the 30-cm (12- in)-thick lift placed directly atop the subgrade (Base L2). Roller MV sensitivity decreases for the 15 cm Base L3 and then increases significantly for the 30 cm Base L4. Results from LWD testing (not shown here) confirm that compaction took place for all lifts. Note that the base:stabilized subgrade modulus ratio (based on roller-measured stiffness and LWD testing) was about 4:1. These results corroborate those presented in Figure 4.11 and illustrate that the sensitivity of roller-based stiffness to compaction of base course material over subgrade improves with increased lift thickness and as the modulus ratio decreases. For the two base over subgrade situations examined here, roller MVs were not sensitive to compaction of 15 cm (6 in) of base material placed directly atop subgrade material.

Generalizing these findings to all layered situations is challenging due to the interplay of several factors including lift/layer thickness, stiffness contrast between the layers, stress dependency of the materials involved and the amplitude of vibration. The results presented above indicate that CCC-based QA of thin base layers directly atop softer subgrade might be unreliable as roller-measured stiffness can be insensitive to these layers. With more knowledge of the roller-induced stress-strain field in layered situations and the ability to perform dynamic analysis of the roller-induced stress-strain field, it should be possible to more accurately predict each layer's contribution to the composite stiffness.

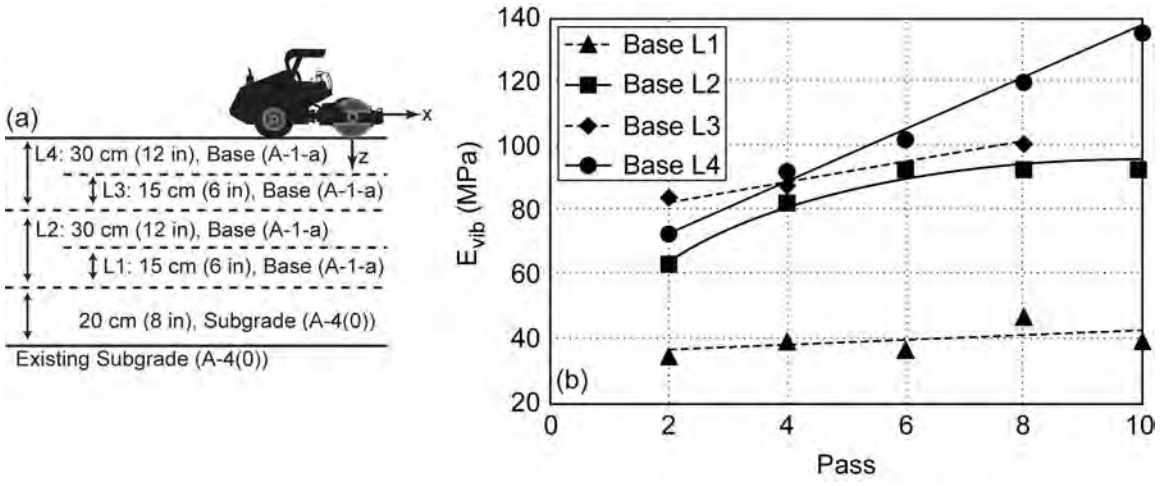

Figure 4.12. Roller-measured stiffness data collected during compaction of TB NC7-10.

4.5 Conclusions

The following conclusions can be drawn from the results presented in this chapter.

- Vibratory and static rolling induces a complex three-dimensional stress-strain-modulus state in the soil. For vertically homogeneous embankment conditions and the 11-15 ton smooth drum vibratory rollers used in this study (and commonly used in practice), the volume of soil reflected in a roller MV is cylindrically shaped extending to 0.8-1.2 m (2.6-3.9 ft) deep and 0.2-0.3 m (0.7-1.0 ft) in front of and behind the drum. Therefore, for typical base, subbase, and subgrade structures, roller MVs are a composite reflection of these layers. The contribution of each layer to the roller MV is influenced by layer thickness, relative stiffness of the layers, vibration amplitude, the stress-dependent modulus function for each soil, and drum/soil interaction issues (contact area, dynamics). Sublift material properties contribute significantly to roller MVs.
- For embankment situations, the measurement depth of roller MVs is controlled by relative decay of roller-induced cyclic stress and strain and is reached when values have decayed to about 10% of their peak. The measurement depth was mildly influenced by vibration amplitude, i.e., a 0.1 mm (0.004 in) increase in A yielded a 3-cm (1.2-in) increase in measurement depth.
- Roller MVs were found to be insensitive to the compaction of thin lifts (e.g., 15 cm [6 in]) of stiff base material placed directly over a soft subsurface. Roller MVs were more sensitive to compaction of 30-cm (12-in) lifts of the same stiff material over soft subgrade. Further, roller MVs were sensitive to compaction of 15-cm (6-in) lifts of base material placed atop similar (stiff) base material. The sensitivity of roller MVs to compaction of thin lifts improves as the modulus ratio of the overlying stiff to underlying soft layer decreases and as layer thickness increases. These results imply that CCC-based QA of thin base layers atop softer subgrade may be unreliable.
- In situ stress-strain-modulus measurements at depths to 1 m (3.3 ft) beneath the roller indicate highly nonlinear modulus behavior within the bulb of soil reflected in roller MVs. In base, subbase, and subgrade structures, modulus varies widely from layer to layer and within layers. Modulus values increased by a factor of two with depth in vertically homogeneous embankment test beds. In situ modulus is strongly influenced by the vibratory loading. A change in vibration amplitude from low to high created a two-fold change in modulus.
- The amplitude (A) dependence of roller MVs—particularly stiffness measures such as E_{vib} and k_s—is a result of stress-dependent soil modulus, layer interaction, and drum/soil contact mechanics. For vertically homogeneous embankment conditions, the nature of the MV-A dependence, that is, positive, negative, or neutral, depends on the modulus function parameters of the soil. Coarse granular soils (i.e., gravels) that are governed by mean effective stress-induced hardening may generally exhibit a positive roller MV-A dependence (i.e., increase in A yields an increase in roller MV). Conversely, finer grained granular soils (i.e., sands) and cohesive soils governed by shear stress-induced softening may generally exhibit a negative roller MV-A dependence. (i.e., increase in A yields a decrease in roller MV).
- The roller MV-A dependence of layered structures is more complex and is influenced by stress-dependent soil modulus (modulus function parameters), layer thickness, relative stiffness of layers, and drum/soil interaction issues. Both positive and negative roller MV-A dependence is possible, even within the same material. The roller MV-A relationship is site dependent and cannot be predicted a priori.
- Levels of vibratory roller-induced deviator stress were found to be considerably greater than those used in M_r testing, while levels of confining stress are considerably less. Even during low excitation force associated with finishing passes and proof rolling of compacted soil, estimated deviator stresses q from z = 0-0.5 m (0-1.6 ft) in the clayey sand were up to three times greater than the maximum q values used for laboratory M_r testing of subgrade soils. Similarly, estimated q values in the crushed rock base course were up to 2.5 times greater than the maximum q used for laboratory M_r testing of base materials. For $z > 0.5$ m, field and maximum laboratory q values were reasonably similar. Conversely, values of p observed in the field were approximately 0.3-0.5 of those used during laboratory M_r testing (below z = 0.25 m).
- The extraction of mechanistic material parameters using roller-based measurements for performance-based specifications consistent with M-E–based design (e.g., AASHTO 2007 Pavement Design Guide) is possible. However, the extraction of appropriate parameters must account for the three-dimensional nature of the roller/soil interaction, the influence of layers, the nonlinear modulus of each involved material, and the dynamics of the drum/soil interaction.

CHAPTER 5

Analysis of Intelligent Soil Compaction

Intelligent systems sense their environment and adapt to improve performance. In the context of current roller technology, IC involves sensing via vibration-based measurement and adapting via feedback control of roller parameters. Automatic feedback control (AFC) of the applied excitation force has been enabled by the recent introduction of variable excitation force amplitude and, in some cases, variable excitation forcing frequency. Here, the roller adapts per the roller MV. Based on the unpredictable dependence of roller MV on excitation amplitude and frequency (characterized in Chapters 2, 3, and 4), specifications for QA using current CCC technology should require roller operation with constant operational parameters (amplitude, frequency, speed, direction). Therefore, CCC-based QA should not be performed during AFC operation (in its current form). AFC may be used during the compaction process (i.e., during non-QA roller passes). To this end, this chapter explores current AFC used by IC rollers and characterizes the benefits of using AFC for soil compaction.

At the time of this study, three manufacturers offered commercially available AFC of excitation force: Bomag, Case/Ammann, and Dynapac. At a minimum level, each manufacturer controls the vertical excitation force amplitude to prevent unstable jump mode vibration of the roller (see Section 2.1.2). When the measurement system senses jump mode, the vertical excitation amplitude is decreased until the measurement system indicates stable vibration. This level of AFC is aimed at protecting the roller from accelerated wear and the operator from chaotic response of the roller. The philosophy behind additional AFC varies across manufacturers. Dynapac does not perform additional AFC. Its philosophy regarding optimal compaction is to maximize excitation force during compaction (I. Nordfelt of Dynapac, 2009, personal communication). At the end of compaction, Dynapac recommends low-amplitude excitation as a finishing pass; however, this is not automatically performed. As described in Section 2.2.2, Bomag controls vertical excitation amplitude based on the relationship of the current E_{vib} to a limit E_{vib}. The limit E_{vib} is entered into the onboard computer by the operator prior to compaction. The vertical excitation is maximized within one of five levels chosen by the operator and decreased if E_{vib} exceeds the limit. As described in Section 2.2.1, Ammann and Case/Ammann control the excitation amplitude and frequency to maintain one of three levels of force transmitted to the soil. The operational approach and responsiveness of the Ammann/Case and Bomag AFC systems is presented in Section 5.1.

AFC-based IC aims to provide improved compaction efficiency (e.g., fewer passes) as well as more uniform compaction (e.g., Adam & Kopf 2004). Due to the amplitude and frequency dependence of roller MVs, it is difficult to assess the benefits of AFC using roller MVs. The benefits of AFC-based IC must, therefore, be determined via independent assessment of compaction (i.e., density testing). Section 5.2 presents an investigation of compaction efficiency and uniformity from IC based on spot-test measurements.

5.1 Operational Evaluation Of AFC-Based IC

5.1.1 Bomag Variocontrol

Bomag AFC (termed Variocontrol) was used over an area of compacted material where a wide range of soil stiffness was present (TB MN42). The data in Figure 5.1 illustrate the operational principle of Bomag AFC. The roller was set to operate at maximum theoretical amplitude, A_{max} = 1.5 mm (0.059 in), and a preset limit of E_{vib} = 45 MPa. Recall that A is a surrogate for vertical excitation force (Equation 2.2). The operator must choose one of five maximum eccentric force levels [A_{max} = 0.6, 1.1, 1.5, 2.1, 2.5 mm (0.024, 0.043, 0.059, 0.083, 0.098 in)] and must prescribe a limit E_{vib}. Here, the choices of A_{max} = 1.5 mm

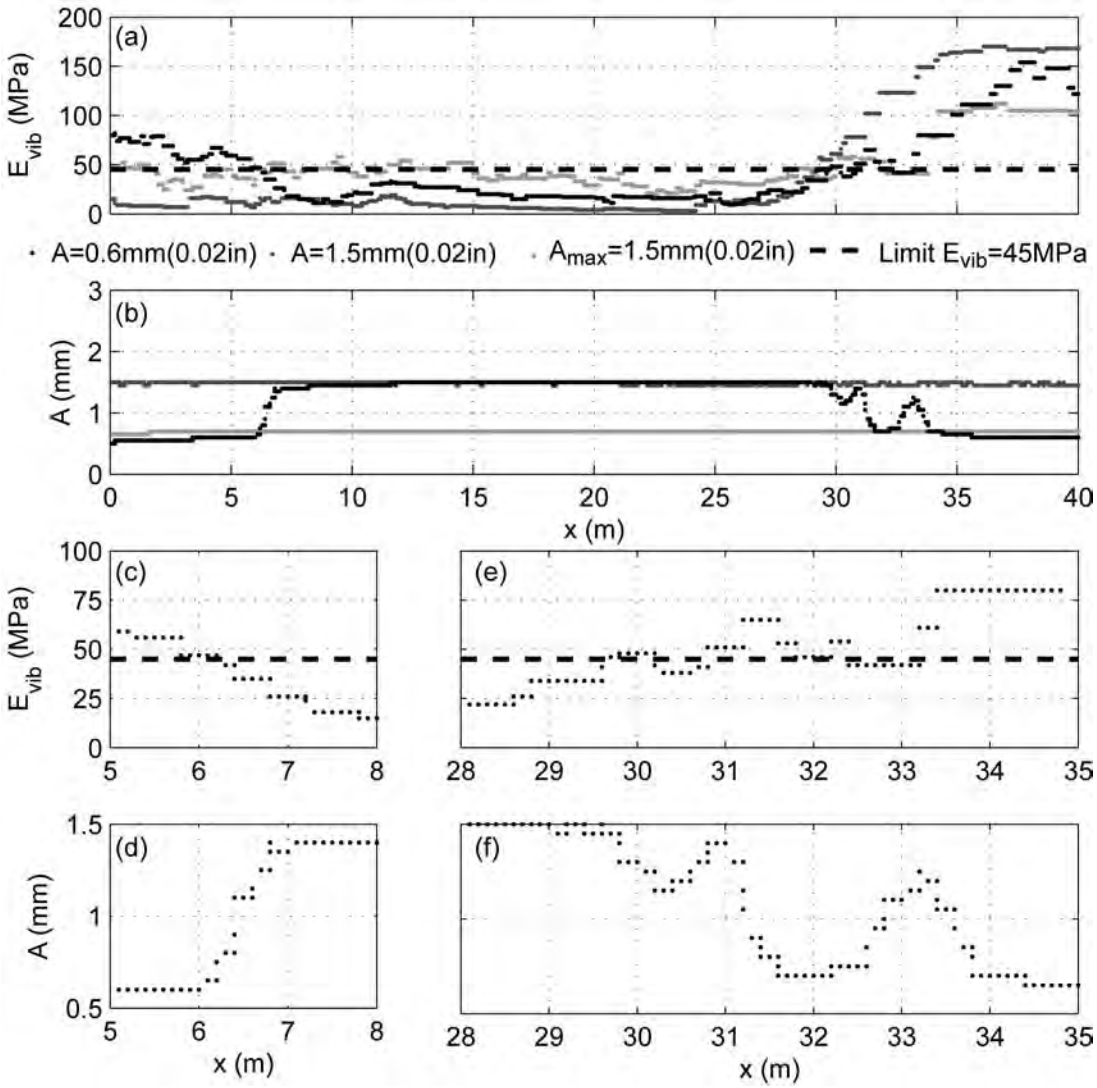

Figure 5.1. Bomag Variocontrol with f = 28 Hz, limit E_{vib} = 45 MPa, and A_{max} = 1.5 mm (0.059 in; TB MN42).

(0.059 in) and limit E_{vib} = 45 MPa imply medium compactive effort and medium soil stiffness. As shown in Figures 5.1a and b, if E_{vib} > limit E_{vib}, A is reduced to 0.6 mm (0.024 in). When E_{vib} < limit E_{vib}, A is increased to A_{max}.

The E_{vib} record during AFC suggests that a very soft zone exists from x = 7 to 30 m. The implication within the Variocontrol system is that the soil in this area requires further compaction, and A_{max} is therefore prescribed. In actuality the material may be a different soil, it may be too moist, or the sublift soil may be soft, and additional passes would not improve conditions. For x < 7 m and x > 30 m, the implication is that the soil has reached near-final compaction and the lowest-possible A should be prescribed to prevent overcompaction or loosening. Here, A = 0.6 mm (0.024 in) is prescribed because it is the lowest A for which E_{vib} can be reliably measured.

The dependence of E_{vib} (and all roller MVs) on A can result in a misleading record of soil stiffness while operating in AFC mode. This is evidenced by the comparison of E_{vib} records collected during AFC and constant A roller passes in Figure 5.1a. Constant A = 0.6 mm (0.024 in) and A = 1.5 mm (0.059 in) roller passes were performed prior to the AFC pass. Comparison of E_{vib} records during constant A operation revealed quite a different stiffness profile. The nature and degree of roller MV dependence on A (termed MV-A dependence) are a complex function of material modulus functions and layered structure (see Chapter 4). A roller MV may increase with increasing A (termed positive MV-A dependence), as shown for

$x > 30$ m in Figure 5.1a. Conversely, a roller MV may decrease with increasing A (termed negative MV-A dependence), as shown for $7 < x < 30$ m. The result of MV-A dependence can be a different and more variable roller MV record while operating in AFC mode than in constant A mode.

In Figure 5.1a, constant A operation and measurement reveal a much more uniform subsurface stiffness than that measured during AFC. Due to the E_{vib}-A dependence, measurement during AFC reveals an artificial and misleading level of variability in soil stiffness. The influence of E_{vib}-A dependence can be observed from $x = 6$ to 7 m, as highlighted in Figures 5.1c and d. Here, E_{vib} decreases below the limit E_{vib}, triggering an increase in A from 0.6 to 1.5 mm (0.024 to 0.059 in). The $A = 0.6$ mm (0.024 in) pass suggests a subtle decrease in soil stiffness; however, due to the strong negative MV-A dependence, E_{vib} decreases from 40 to 15 MPa. While a legitimate decrease in soil stiffness had to be present to trigger the increase in A, the soft area suggested by the E_{vib} record is primarily a result of strong MV-A dependence.

The MV-A dependence described above can also trigger AFC changes in A. Figure 5.2 shows Bomag AFC operation with a limit $E_{vib} = 100$ MPa and $A_{max} = 2.5$ mm (0.098 in). At $x = 31$ m, E_{vib} eclipses 100 MPa. The resulting decrease in A coupled with the strong positive E_{vib}-A dependence causes E_{vib} to dip below 100 MPa and trigger an increase in A. This increase in A and the positive E_{vib}-A dependence again causes E_{vib} to eclipse 100 MPa. The sequential decrease, increase, and decrease in A is driven by E_{vib}-A dependence and not by a legitimate soft area.

A second aspect of interest is the responsiveness of AFC (i.e., how quickly the roller adapts to threshold changes in soil stiffness). A closer look at two zones highlighted in Figures 5.1c, d, and f illustrates the responsiveness. The limit E_{vib} was crossed six times during the AFC pass. The AFC reacted (i.e., A began to change) within 0.2 to 0.3 m (0.7 to 1 ft) of the position where the limit E_{vib} was crossed. The response distance, defined as the distance required for the roller to completely modify A, was found to be approximately 1 m (3.3 ft). These reaction and response distances speak to the ability of AFC to address very localized areas of poor compaction. The reaction and response distances are a function of roller speed; here, the roller was traveling at a typical operating speed of 1 m/s (1 ft/s).

Bomag AFC was used on a second area where variable stiffness was present (TB MN43). Constant A passes reveal a strong positive E_{vib}-A dependence. In one area ($x = 55$ to 70 m), the surface gravel was underlain by old asphalt pavement, as reflected by the very high E_{vib} values in Figure 5.3a. During a constant $A = 2.5$ mm (0.098 in) pass, the Bomag roller exhibited jump mode vibration from $x = 59$ to 67 m as a result of the high underlying stiffness (Figure 5.3). During an $A = 0.6$ mm (0.024 in) pass, the roller did not experience jumping. During AFC operation with a limit $E_{vib} = 100$ MPa, A was reduced for much of the stiff zone (see Figure 5.4), preventing the roller from entering jump mode. Similar to the behavior observed in Figure 5.2, Bomag AFC is artificially engaged by the positive E_{vib}-A dependence. At numerous locations depicted in Figure 5.3c, E_{vib} eclipses 100 MPa and triggers a decrease in A. What follows are several cycles of E_{vib} increase and

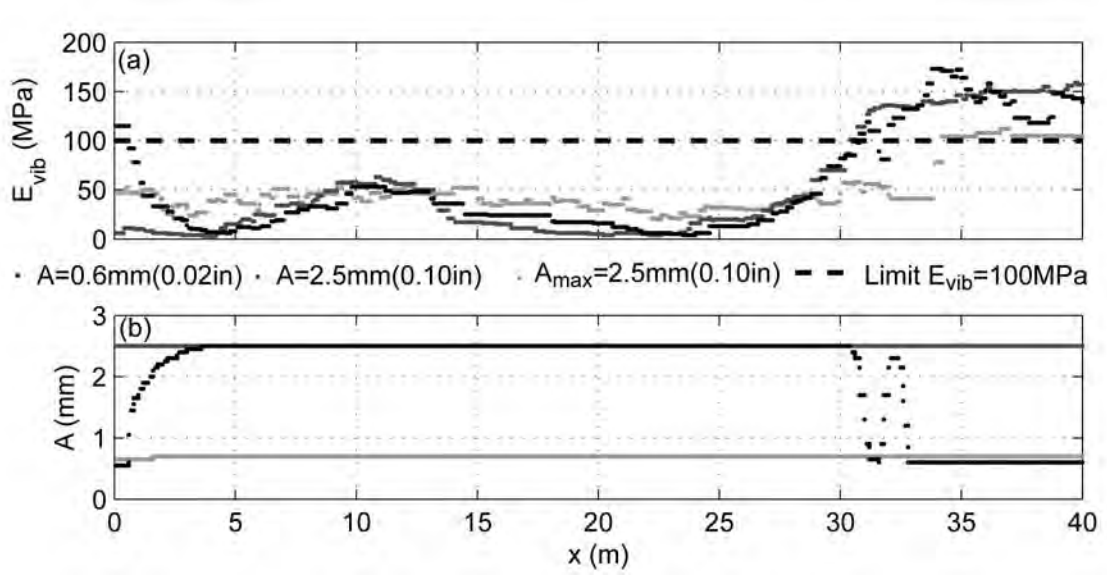

Figure 5.2. Bomag Variocontrol with f = 28 Hz, limit E_{vib} = 100 MPa, and A_{max} = 2.5 mm (0.098 in; TB MN42).

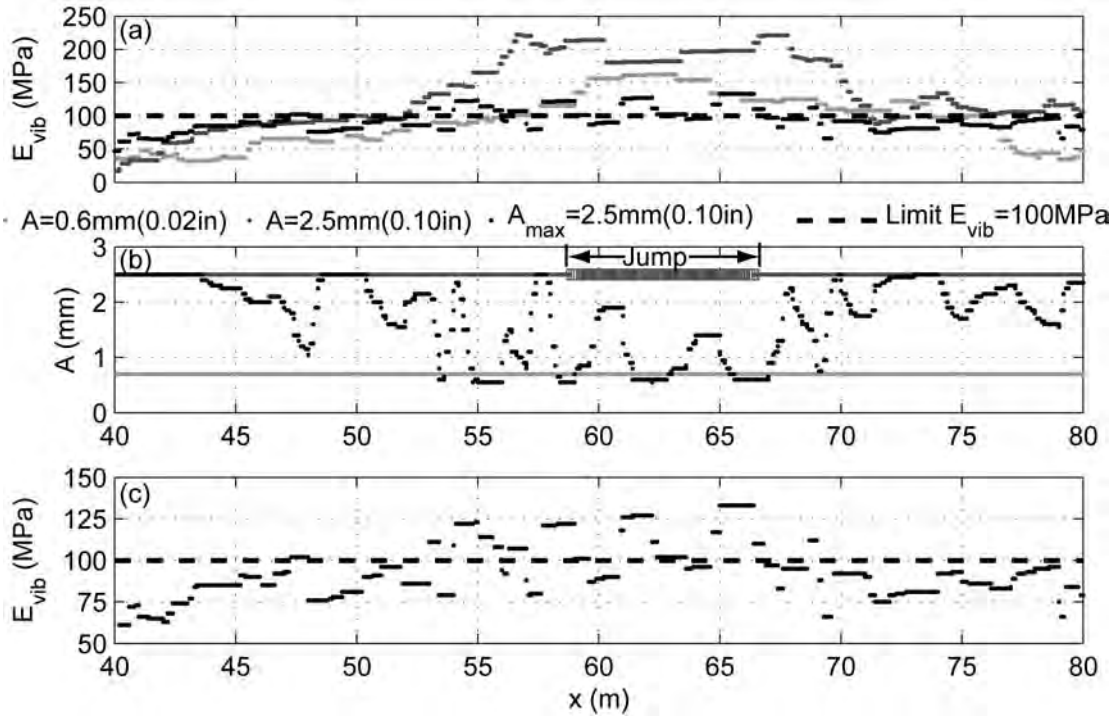

Figure 5.3. Bomag operation with and without feedback control, with A_{max} = 2.5 mm (0.098 in) and E_{vib} limit = 100 MPa (TB MN43).

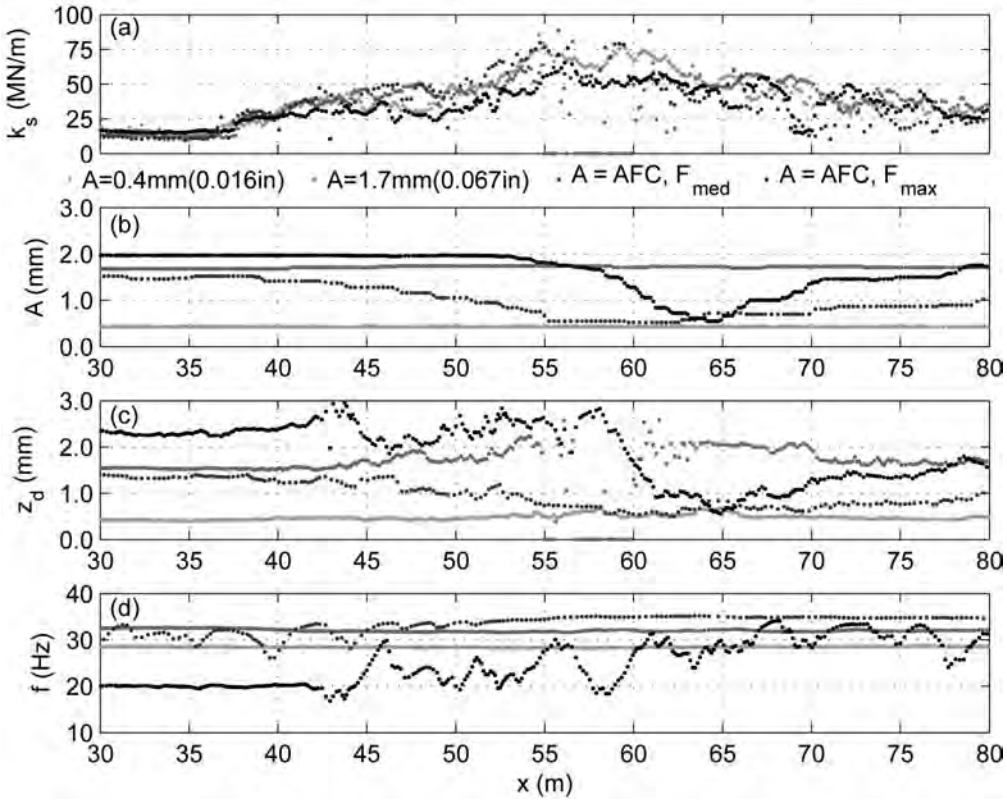

Figure 5.4. Comparison of Ammann constant-amplitude mode with AFC mode (TB MN43); A = theoretical amplitude and z_d is measured amplitude.

decrease due to the AFC of A and the positive E_{vib}-A dependence. The resulting variable E_{vib} record is artificial.

5.1.2 Ammann ACE

As described in Section 2.2.1, the Ammann AFC system (termed Ammann Compaction Expert, ACE) maintains one of three contact force settings $F_{s(max)}$. The $F_{s(max)}$ is controlled by varying the eccentric mass positions (and thus A) and the frequency. Frequency is controlled to maintain the phase angle between vertical drum displacement and eccentric force between 140° and 160°. The level of A is then varied to maintain low [14 kN (3.1 kip)], medium [20 kN (4.5 kip)], or high (unlimited) $F_{s(max)}$ (Anderegg & Kaufmann 2004).

The Case/Ammann roller was used in constant A and AFC mode on a variable stiffness test bed (TB MN43). Two constant A passes were performed [A = 0.4 mm (0.016 in) and 1.7 mm (0.067 in)], and two AFC mode passes were performed [$F_{s(max)}$ = 20 kN (4.5 kip) and $F_{s(max)}$ = unlimited]. Figure 5.4 presents the measured soil stiffness k_s, theoretical amplitude A, actual amplitude z_a, and vibration frequency f. The $F_{s(max)}$ and phase angle data are not stored by the roller measurement system. Values of k_s varied from 15 to 80 kN/m and represented a range of soft to stiff conditions. During constant A operation, z_d remained reasonably consistent with A in soft areas. In stiffer areas, z_d can be significantly greater than A (e.g., x = 45 to 70 m). The Ammann roller exhibited jump behavior from x = 55 to 60 m during constant A = 1.7 mm operation, wherein the measurement of k_s and z_d is unreliable (values go to zero).

To maintain constant $F_{s(max)}$ while soil stiffness increases during AFC passes, the controller decreases A and increases excitation frequency. This occurs during both AFC passes. From x = 55 to 63 m, the soil stiffness remained fairly constant and yields a constant $F_{s(max)}$. In this case the controller does nothing since the $F_{s(max)}$ is at the desired value. From x = 63 to 80 m, the stiffness decreases. To maintain $F_{s(max)}$, the controller increases A. Vibration amplitude and frequency seemed to have an influence on k_s values. The k_s data from each pass trend similarly; however, the k_s at discrete locations could be highly variable between passes. For instance, at x = 47 m, k_s ranges between 25 and 50 MN/m.

5.2 Influence of AFC on Compaction

Test beds in Colorado and Maryland were selected to investigate the influence of AFC on compaction efficiency and uniformity according to measurement values (MVs) and spot-test measurements. Operating the rollers in AFC and constant-amplitude modes for alternate roller passes provided the opportunity to further evaluate AFC response distance and the effectiveness of AFC in preventing roller jumping. The test beds were selected primarily because they represented different underlying layer conditions: relatively uniform versus highly variable.

5.2.1 Uniform Underlying Layer Conditions—Bomag

Two granular base layers (TBs CO16 and CO17) were prepared side by side and compacted in AFC and constant-amplitude modes, respectively, to provide similar conditions for comparing compaction efficiency and resulting uniformity for different machine operations. E_{vib} measurements were recorded for the same test bed in constant-amplitude mode and in AFC mode with two different limit E_{vib} values. During test strip construction, spot-test measurements were obtained at several intermediate compaction passes. The test bed conditions and material types are presented in Figure 5.5. The moisture content of the compaction layer material was relatively uniform between 4.0% and 5.6%. The underlying compacted subbase layers (TBs CO11 and CO12) were relatively uniform and similar in terms of coefficient of variation (COV) according to spot-test measurements (see Table 5.1).

TB CO16 was compacted in AFC mode for passes 1 through 12 and in manual mode for passes 13 and 14. AFC with limit E_{vib} = 100 MPa was used for passes 1 through 8 with A_{max} = 2.50 mm (0.098 in). For passes 9 through 12, limit E_{vib} = 120 MPa with A_{max} = 1.90 mm (0.075 in) [v = 4 km/h (3.6 ft/s) constant throughout]. Spot-test measurements (γ_d, $E_{LWD\text{-}Z2}$, and California Bearing Ratio [CBR]) were obtained after 4, 8, 12, and 14 passes. Figure 5.6 shows roller MVs (solid lines) in comparison with spot-test measurements. For reference, final pass spot-test and roller measurements for the underlying subbase layer (TB CO11) are also presented. Figure 5.7 shows the roller MVs in comparison with amplitude measurements during compaction in AFC mode for passes 4, 8, and 12 and in manual mode for pass 14.

TB CO17 was compacted in manual mode with A = 0.70 mm (0.028 in) for passes 1 through 8, A = 1.90 mm (0.075 in) for passes 9 and 10, and A = 0.70 mm (0.028 in) for passes 11 and 12 [v = 4 km/h (3.6 ft/s) constant throughout]. Spot-test measurements (γ_d, $E_{LWD\text{-}Z2}$, and CBR) were obtained after 4, 8, 10, and 12 roller passes. Roller MVs in comparison with spot-test measurements are presented in Figure 5.8. For reference, final pass measurements for the underlying subbase layer (TB CO12) are provided in Figure 5.8.

Roller MV and spot-test measurement compaction curves for TBs CO16 and CO17 are provided in Figure 5.9. The average amplitude during AFC mode compaction for TB CO16 decreased from pass 1 to pass 8, consistent with increasing average E_{vib} values. The COV of roller MV and spot-test measurements after pass 8 for the two test beds are summarized

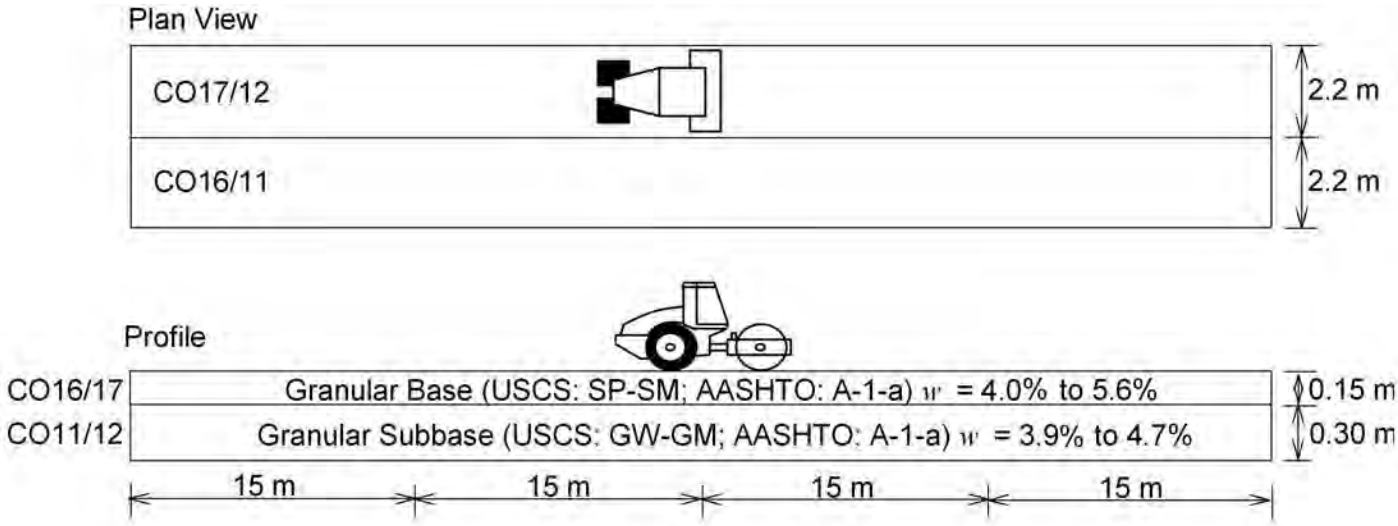

Figure 5.5. Plan and profile views of granular base (TB CO16/17), subbase (TB CO11/12), and subgrade layer (TB CO1/2) construction.

Table 5.1. Comparison of COV of roller MVs and spot-test measurements.

	COV (%)					
	CO16		CO11[a]	CO17		CO12
Parameter	Pass 8 (AFC)	Pass 14 (Manual)	Pass 12 (Manual)	Pass 8 (Manual)	Pass 12 (Manual)	Pass 12 (Manual)
E_{vib}	12	21	12	21	21	18
$E_{LWD\text{-}Z2}$	12	10	14	10	10	15
γ_d	1	—	2	1	2	2
CBR	22	—	21	29	25	21

[a] Underlying subbase layer.

in Table 5.1 for purposes of comparing the final compaction pass uniformity. Compaction curves from spot-test measurement average values from the two test beds show similar trends with no noticeable difference. The COV of spot-test measurements is similar after pass 8 for the two test beds. The COV of roller MVs for TB CO17 (21%) is higher than the COV of MVs for TB CO16 (12%). Given the significant fluctuations in *A* (see Figure 5.8) and the roller MV-*A* dependence described in Figures 5.1 and 5.2 and visible in Figure 5.9, lower COV of roller MVs does not necessarily reflect increased uniformity. Final-pass roller MVs from constant-amplitude operation (pass 12 or pass 14) for the two test beds produced similar COV (21%). During constant-amplitude operation, the COV of roller MVs provides a good measure of uniformity. The synopsis of results from this test bed study is that AFC operations did not produce improved compaction or uniformity compared to constant-amplitude mode compaction for these test bed conditions [i.e., 0.15 m (0.5 ft) thick layer of base atop uniform subbase].

5.2.2 Nonuniform Underlying Layer Conditions—Bomag and Dynapac

Results from granular base layer (TBs MD11, 13, 14) placed over compacted granular base layer (TBs MD6, 8, 9), and underlain by subgrade (TBs MD2, 4, 5) are presented in this section. The influence of heterogeneous underlying layer conditions on MVs obtained in AFC mode is evaluated here in comparison with MVs obtained in constant-amplitude mode for two different roller MVs (CMV_D and E_{vib}). These results are particularly interesting in that they demonstrate the influence of underlying layer conditions on AFC operations and resulting MVs. For CMV_D measurements, AFC compaction was performed using a preselected A_{max} setting. For Dynapac IC, the vibration amplitude in AFC mode is controlled to prevent jump mode only. The degree of jump is measured by the bouncing value (BV). Reportedly, the vibration amplitude was reduced when BV approached 14. CMV_D was arbitrarily reported in the output as 250 for BV > 25.

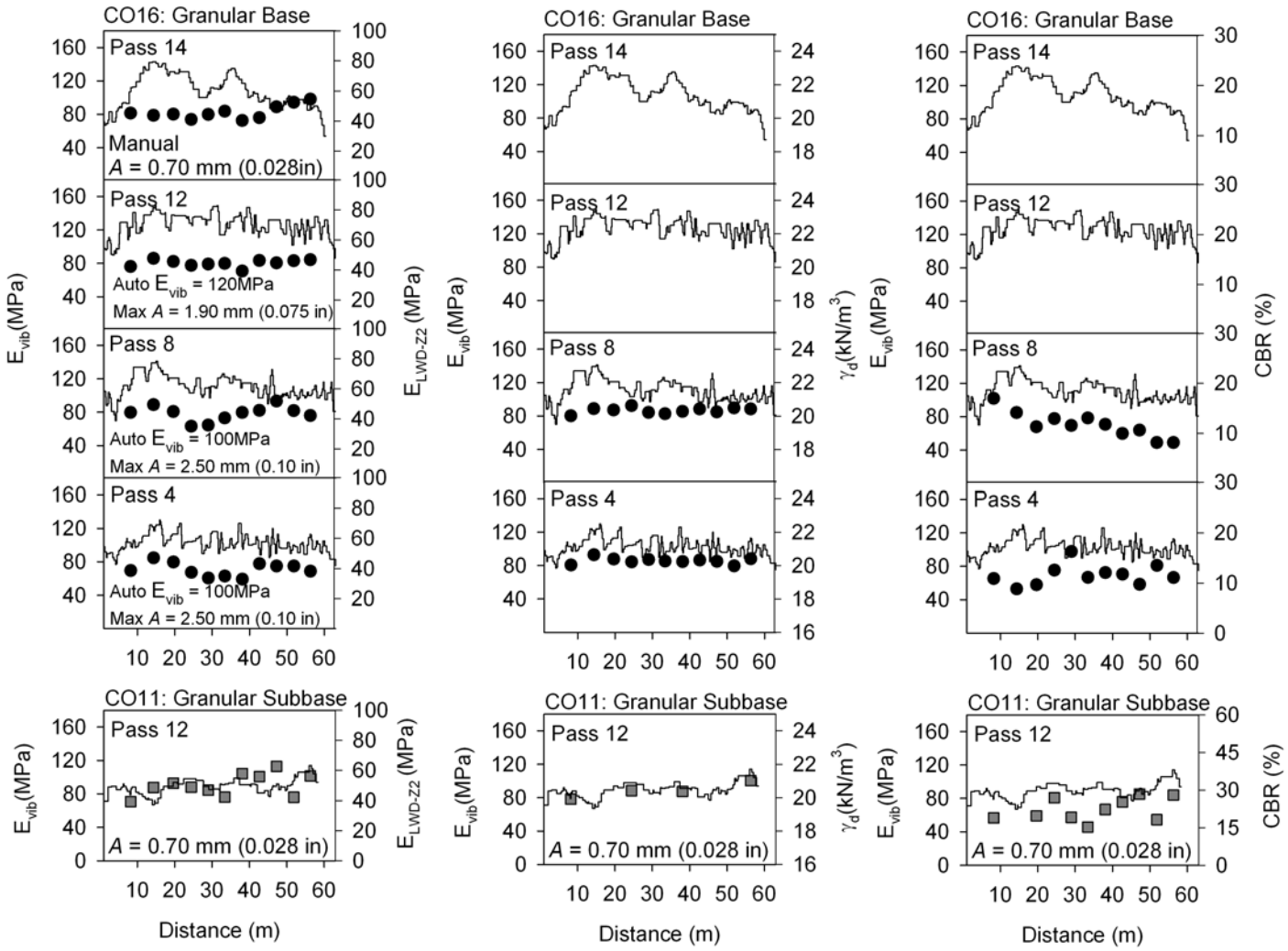

Figure 5.6. Comparison of roller MVs with spot-test measurements from TB CO16 granular base layer (MVs obtained in AFC and constant-amplitude modes) and underlying TB CO11 granular subbase layer (MVs obtained in constant-amplitude mode).

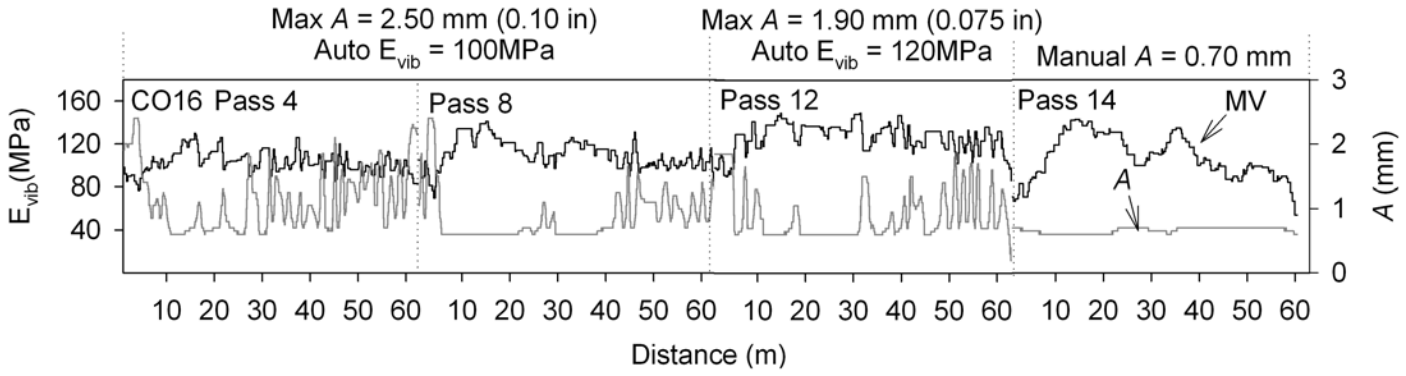

Figure 5.7. Roller MV and A measurements on TB CO16 granular base layer.

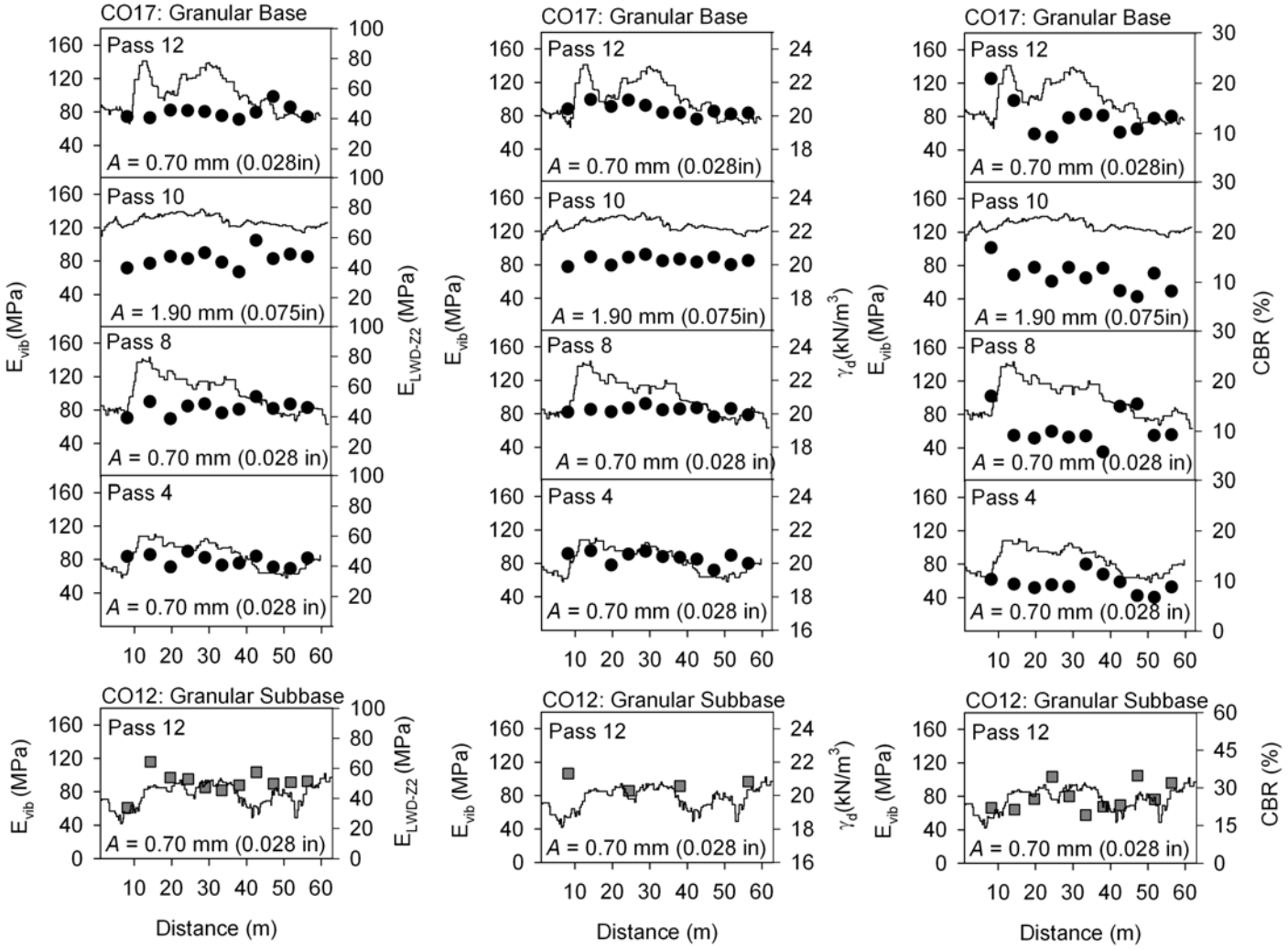

Figure 5.8. Comparison of roller MV with spot-test measurements from TB CO17 base layer (AASHTO: A-1-a) underlain by CO12 subbase layer (AASHTO: A-1-a) (MVs obtained in constant-amplitude mode).

The geometry of the soil layers and associated soil classifications are presented in Figure 5.10. The granular base layers were placed at relatively consistent moisture content (w = 3.5% to 5.0%). The subgrade TB MD2 was relatively soft and homogeneous, and TBs MD4 and 5 were relatively stiff and heterogeneous. TBs MD4 and 5 consisted of an isolated zone of fractured rock mixed with the subgrade soil. For TB MD2 the average $E_{LWD\text{-}Z2}$ = 5.9 MPa, with COV = 10%; for TB MD4 the average $E_{LWD\text{-}Z2}$ = 19.8 MPa, with COV = 45%; and for TB MD5 the average $E_{LWD\text{-}Z2}$ = 30 MPa, with COV = 48%.

After compaction passes, the test beds were mapped with the rollers using constant-amplitude and AFC settings. E_{vib} measurements were obtained in constant-amplitude mode with nominal A = 0.70 mm (0.028 in) and A = 1.90 mm (0.075 in), and in AFC mode with limit E_{vib} = 40 MPa and 80 MPa [f = 30 Hz and v = 4 km/h (3.6 ft/s) were constant] with A_{max} = 2.50 mm (0.098 in). CMV_D measurements were obtained in constant-amplitude mode with nominal A = 0.80 mm (0.031 in) and A = 2.40 mm (0.094 in) and in AFC mode with maximum A = 2.50 mm (0.098 in) [f = 28 Hz and v = 4 km/h (3.6 ft/s) were constant].

Figure 5.11 presents E_{vib} values obtained in constant-amplitude and AFC modes for TBs MD11, 13, and 14. E_{FWD} measurements are shown in comparison with E_{vib} values during constant A = 0.70 mm (0.028 in) operation. Amplitude measurements (shown as gray lines) are also presented in comparison with E_{vib} measurements (shown as black lines) obtained in AFC mode. Similarly, Figure 5.12 presents CMV_D

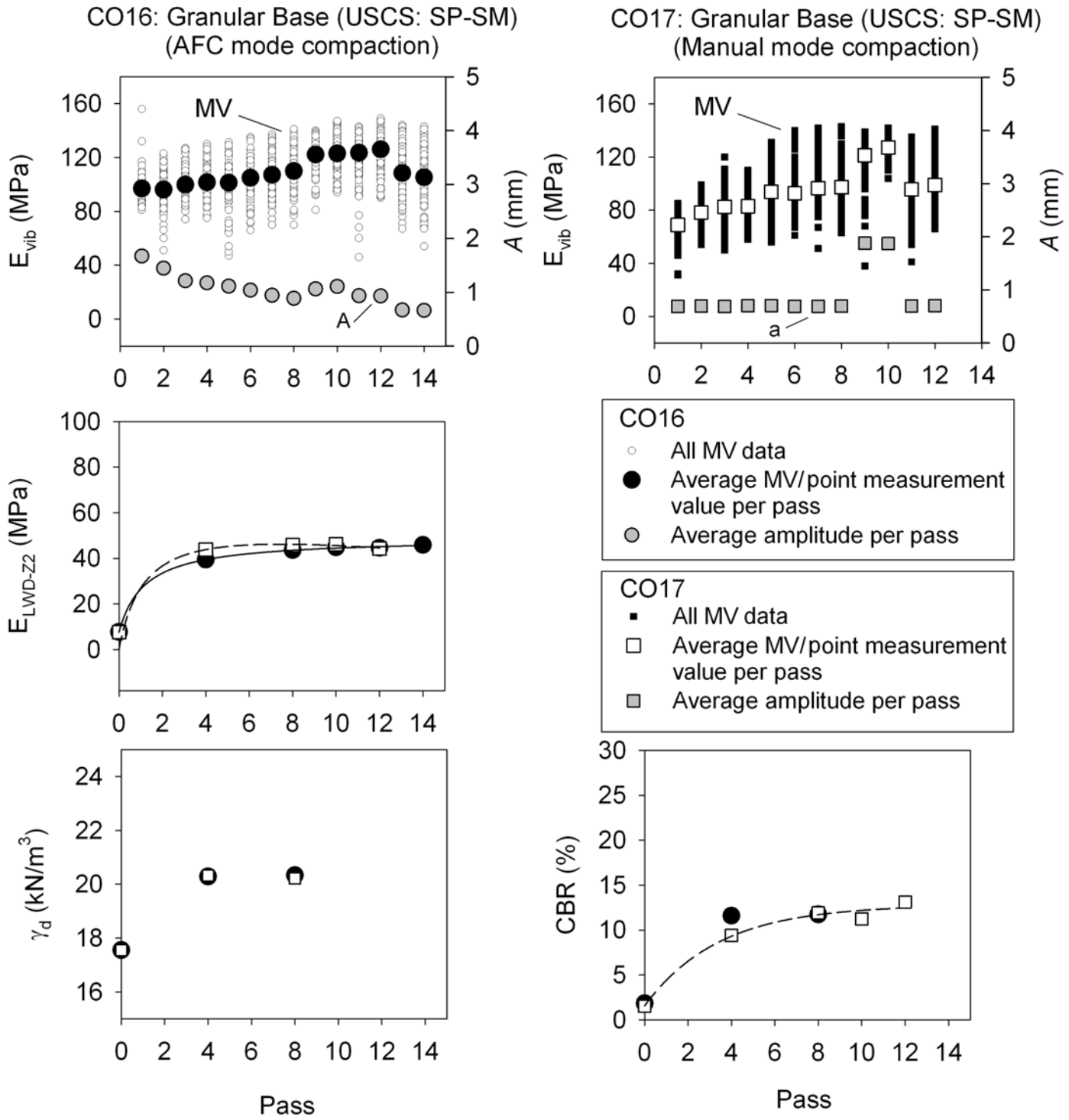

Figure 5.9. Comparison of roller MV and spot-test measurement compaction curves from TB CO16 (operated in constant-amplitude mode) and TB CO17 (operated in AFC mode).

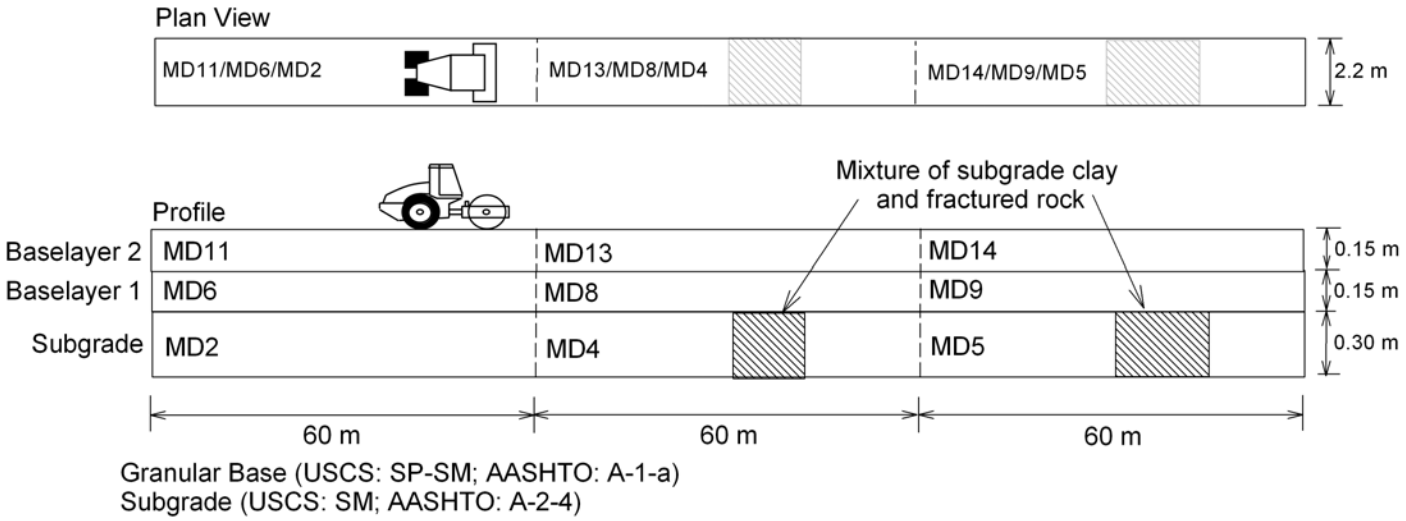

Figure 5.10. Plan and profile views of granular base (TBs MD6, 8, 9, 11, 13, 14) and subgrade layer (TBs MD2, 4, 5) construction (layer thicknesses are nominal).

measurements obtained in constant-amplitude and AFC modes for TBs MD11, 13, and 14, along with E_{FWD} measurements in comparison with CMV_D measurements with constant A = 0.80 mm (0.031 in) operation. The underlying layer roller MVs are also shown in Figures 5.11 and 5.12 for reference. Both roller MVs and E_{FWD} measurements showed similar variation along the test beds, with relatively soft and homogeneous conditions on TB MD11 and relatively stiff and heterogeneous conditions on TBs MD13 and 14.

E_{vib} measurements in constant-amplitude mode with A = 1.90 mm (0.075 in) showed roller jumping (jump values > 0) on TBs MD13 and 14, generally at locations with $E_{FWD\text{-}D3}$ > 120 MPa and E_{vib} > 100 MPa. During AFC mode compaction with maximum E_{vib} = 80 MPa, no roller jumping was observed across the test beds and the amplitude was effectively reduced to A = 0.6 mm (0.024 in) at locations where E_{vib} was > 80 MPa. For AFC operation with maximum E_{vib} = 120 MPa, the amplitude was reduced to A = 0.6 mm (0.024 in) where $E_{vib} \geq$ 120 MPa, but roller jumping was not prevented. Response distance for this test bed study was about 0.5 to 1 m (1.6 to 3.3 ft).

CMV_D measurements in constant-amplitude mode with A = 2.40 mm (0.094 in) showed roller jumping at several locations across TBs MD13 and 14 with E_{FWD} > 120 MPa. In AFC mode the roller generally maintained A > 2.00 mm (0.079 in) for the three test beds. No jumping was observed on TB MD13. Jumping was noticed on TB MD14 from about 0 to 15 m, where the amplitude increased despite the increase in BVs. Response distance for this test bed study was about 0.5 to 1.0 m (1.6 to 3.3 ft).

5.3 Conclusions

The following conclusions can be drawn from the results presented in this chapter:

- The dependence of roller MVs on A can provide a misleading record of soil stiffness when operating in AFC mode. Both positive and negative MV-A dependence were observed during testing and resulted in an artificial and misleading level of variability/uniformity in soil stiffness. For this reason, AFC that involves changing A is not recommended during measurement passes in QA (see Chapter 7).
- The roller MV-A dependence can trigger AFC changes in A. This is problematic when roller MVs hover around a target or limit MV.
- The response distance of AFC-based IC evaluated here was found to be approximately 1 m when operating at typical roller speeds, indicating that rollers in AFC mode can respond to relatively localized changes in soil conditions. AFC-based IC rollers would struggle to react to very localized areas of soft soil (e.g., above a buried pipe or narrow backfilled trench).
- An investigation of the influence of AFC-based IC on compaction efficiency and uniformity revealed no measurable benefits of AFC mode over constant-amplitude mode. Spot-test measurements obtained from side-by-side test beds (e.g., one compacted using AFC and one compacted with constant low-amplitude vibration) did not show any significant differences in soil compaction or uniformity of soil properties. Final-pass constant-amplitude roller MVs recorded on both test beds revealed no difference in uniformity.

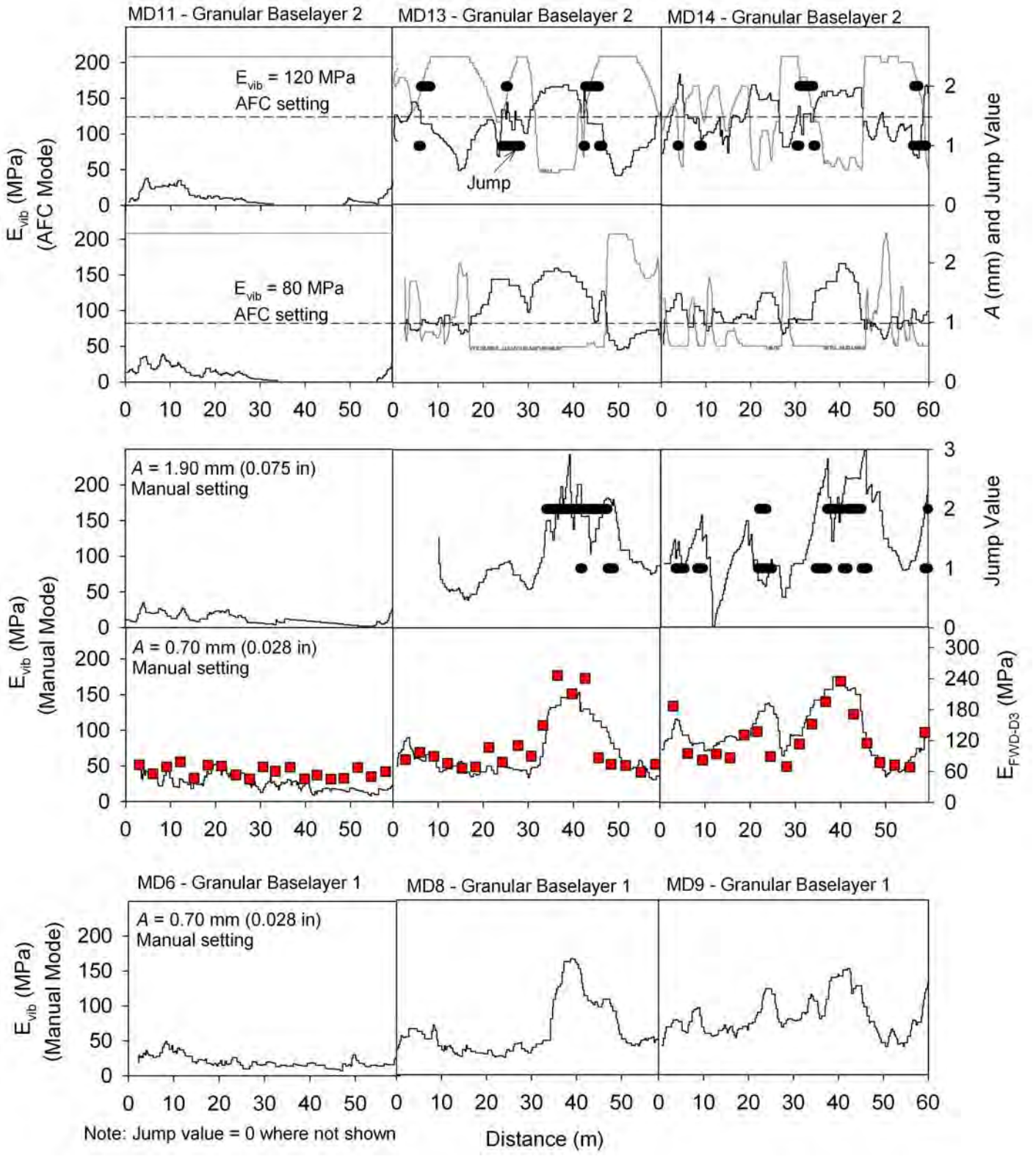

Figure 5.11. Roller MV, amplitude, and jump measurements from AFC and manual high- and low-amplitude settings with comparison to E_{FWD} measurements and underlying layer roller MVs.

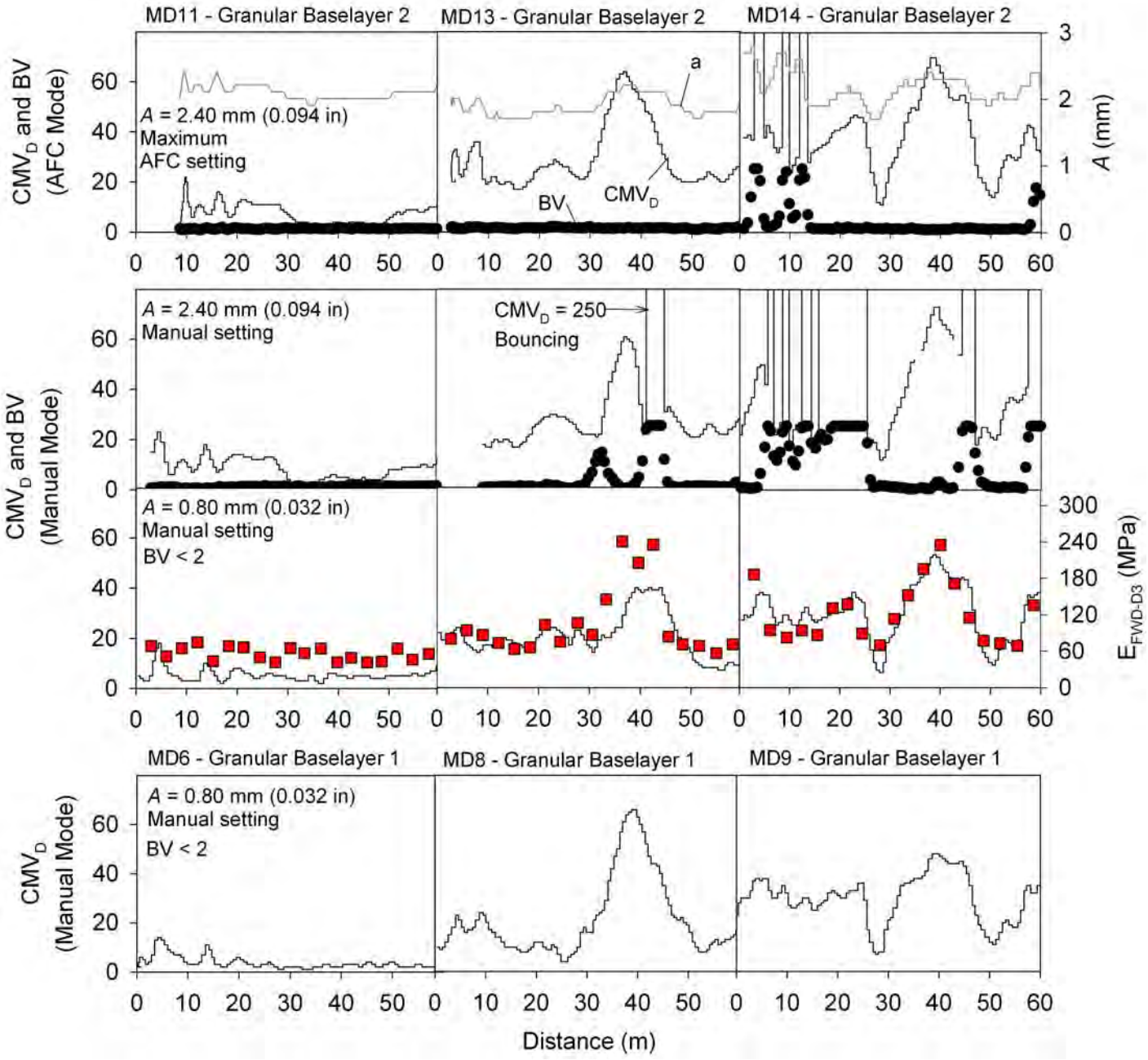

Figure 5.12. Roller MV, amplitude, and BV measurements from AFC and manual high- and low-amplitude settings with comparison to E_{FWD} measurements and underlying layer roller MVs.

CHAPTER 6

Relationships Between Roller Measurement Values and Point Measurements

Implementation of roller-integrated compaction monitoring technologies into earthwork specifications requires an understanding of relationships between roller MVs and soil compaction measurements. Previous studies (e.g., Floss et al. 1983; Samaras et al. 1991; Brandl & Adam 1997; White & Thompson 2008; Thompson & White 2008; White et al. 2008a, 2008b, 2008c) have documented relationships between roller MVs and a variety of in situ soil properties but are generally limited to one roller measurement type and limited soil and field conditions.

This chapter presents results from a comprehensive evaluation of five roller-integrated compaction measurement systems, each with a unique MV (i.e., MDP, CMV_D, E_{vib}, k_s, CCV) and 17 different soil types. The relationships presented here are divided into three material groups: nongranular subgrade, granular subgrade, and granular subbase/base materials. MVs were obtained from CCC and IC rollers set up with smooth and pad foot drums on 60 controlled TBs. The beds varied in material types, moisture content, and underlying layer support conditions. Roller MVs were obtained for different amplitude, frequency, and roller travel speed settings. The objectives of the evaluation were to (1) investigate simple linear relationships between roller MVs and various in situ point (spot-test) measurements, (2) identify key factors that influence these relationships, and (3) evaluate multiple regression relationships that consider variations in soil conditions and machine operation settings. A variety of conventional and mechanistic related in situ spot-test measurements (i.e., γ_d, CBR, E_{LWD}, E_{FWD}, E_{V1}, E_{V2}, CIV, k_{SSG}) and laboratory M_r test measurements were used in correlation analysis to MVs.

In brief, results indicate that simple linear correlations between roller MVs and in situ point measurements are possible for a compaction layer underlain by relatively homogeneous and stiff/stable supporting layer. Heterogeneous conditions in the underlying layers, however, can adversely affect the relationships. A multiple regression analysis approach is described in this chapter that includes parameter values to represent underlying layer conditions when statistically significant, to improve the correlations. E_{LWD}, E_{V1}, E_{V2}, and E_{FWD} measurements generally capture the variation in roller MVs better than γ_d measurements. DCP tests are effective in detecting deeper "weak" areas [at depths greater than 300 mm (1 ft)] that are commonly identified by roller MVs and not by compaction layer point measurements. High variability in soil properties across the drum width and soil moisture content contribute to scatter in relationships. Averaging measurements across the drum width and incorporating moisture content into multiple regression analysis, when statistically significant, can help mitigate the scatter to some extent. Relatively constant machine operation settings are critical for calibration strips (i.e., constant amplitude, frequency, and travel speed), and correlations are generally better for low-amplitude settings [e.g., 0.7 to 1.1 mm (0.028 to 0.043 in)]. A field testing protocol to obtain reliable correlations during implementation/roller calibration testing and establishing target values from simple and multiple regression relationships are described in Chapters 7 and 8.

An approach to relate M_r to roller MVs using laboratory-determined w-γ_d-M_r relationships is described in this chapter. Despite the challenges involved in relating field to laboratory measurements, encouraging relationships are observed between roller MVs and M_r. Similar to relationships between MVs and compaction layer point measurements, correlations are possible for materials with relatively stiff/homogeneous subsurface conditions. Again, heterogeneous underlying support conditions adversely affect correlations. These correlations can be improved by including parameter values that represent the underling layer conditions through multiple regression analysis. An approach to develop target values from the MV-M_r relationship with respect to a targeted in situ moisture content range is presented in Chapter 8.

6.1 Materials and Testing

6.1.1 Materials

A total of 17 different soils were evaluated as part of 60 TBs for the correlation study. The soils were divided into nongranular subgrade (13 TBs), granular subgrade (9 TBs), and granular subbase/base (38 TBs) materials, depending on their soil classification and location within the pavement foundation layers for each project (Table 6.1). Regression relationships presented later in this report are separated according to these general material groupings. Detailed TB information, including soil classification, preparation and construction, roller operations, and roller data maps are provided in Appendix C.

6.1.2 Test Bed Construction and Testing

Roller MVs and in situ point measurements (w-γ_d, DCP-CBR, E_{LWD}, E_{FWD}, E_{V1}, E_{V2}, $CIV_{20\text{-kg}}$, k_{SSG}) were obtained from controlled TBs with varying plan dimensions [2.5 m × 30.0 m to 10 m × 65 m (8.2 ft × 98.4 ft to 33 ft × 213 ft)] to (1) evaluate empirical relationships between roller MVs and in situ point measurements and (2) investigate the effects of moisture content, amplitude, and underlying layer support conditions on compaction layer roller MVs. In situ point measurements were obtained at several locations at select roller passes to obtain measurements over a wide range of compaction conditions. Point measurements were obtained at one or three test locations over the drum width. When three tests were performed, the point measurements were averaged over the drum width for comparison to the roller MV, which is representative of an integrated response over the drum width. Laboratory M_r tests were performed on "undisturbed" Shelby tube samples collected from a compacted subgrade test bed (CO3), and the measurements were directly correlated to the roller MVs. M_r tests were also performed on samples reconstituted in the laboratory to obtain w-γ_d-M_r relationships for correlation to w-γ_d-MV relationships.

Nuclear moisture-density gauges (ASTM D6938) and drive cylinders (ASTM D2937) were used to determine in situ w-γ_d. DCP tests (ASTM D6951) were performed to determine CBR profiles using CBR = 292/(DCPI)$^{1.12}$ (ASTM D6951) relationship (measured as mm/blow). Zorn, Keros, and Dynatest LWD devices set up with 200- or 300-mm (8- or 12-in) plate diameters were used to determine E_{LWD} (Zorn 2003, Dynatest 2004). A Dynatest falling weight deflectometer (FWD) device with 300-mm (12-in)-diameter plate was used to determine E_{FWD} (Maryland TB locations only). FWD loads were obtained that targeted three contact stresses: 400 kPa, 500 kPa, and 650 kPa. E_{V1} and E_{V2} were determined using a 300-mm (12-in)-diameter plate at 100- to 200-kPa contact stress levels for nongranular and granular subgrade soils, and 200- to 400-kPa contact stress levels for granular base/subbase soils. Poisson's ratio $\nu = 0.4$ was assumed for all soils, and shape factors $f = \pi/2$ for nongranular subgrade soils and $f = 8/3$ for granular subgrade/subbase/base soils were assumed in E_{LWD}, E_{FWD}, E_{V1}, and E_{V2} calculations. More details on testing methods are presented in Appendix A.

Table 6.1. Summary of test beds and material types used in correlation study.

TB Number	USCS (AASHTO)[a] Classification	Material Group	Roller Drum Configuration
MN4–MN13 CO1–CO3	CL (A-6(5)) SC-SM (A-4(3)), CL (A-6(7))	Nongranular subgrade	Pad foot and smooth drum
MD2–MD5 FL23 FL24 FL25 NC1–NC2	SM (A-2-4) SP-SM (A-3) SM (A-3) SM (A-2-4), SP-SM (A-3) SM (A-2-4)	Granular subgrade	Pad foot and smooth drum
MN17–MN39 CO6–CO15 CO16–20 MD6–MD14 FL19–FL20 NC4	SP-SM (A-1-b) GW-GM (A-1-a) SP-SM (A-1-a) SP-SM (A-1-a) SM (A-1-b) SP-SM (A-1-a)	Granular subbase/base	Smooth drum

[a]United Soil Classification System (American Association of State Highway and Transportation Officials).

6.2 Simple Linear Regression Relationships

Simple linear regression analysis involves developing a relationship between independent and dependent variables using an intercept and slope coefficient. This analysis has the advantage of being simple enough to perform on a hand calculator. For each linear univariate regression model, the coefficient of determination R^2 provides a measure of how well the regression model describes the data. The linear correlation coefficient r used in the European specification options (see Chapter 2) is equivalent to $\sqrt{R^2}$. For reference, correlations considered acceptable per the European specification options meet the requirement of $R^2 \geq 0.5$.

Although simple linear regression analysis is relatively straightforward, there are many factors that can affect the quality of the correlation between MVs and the various point measurement values. A list of these factors is provided to aid the reader in interpretation of the results. Multiple regression analysis was identified as one approach to overcome some of the factors that affect the simple linear regression relationships and is discussed later in this chapter.

6.2.1 Analysis Approach

Simple linear regression relationships were developed by considering in situ point measurements as "true" independent variables and roller MVs as dependent variables using the model shown in Equation 6.1, where b_0 = intercept, b_1 = slope, and α = point measurement value. Statistical significance of the independent variable was assessed based on p- and t-values. The selected criteria for identifying the significance of a parameter included p-value <0.05 = significant, <0.10 = possibly significant, >0.10 = not significant, and t-value <-2 or >+2 = significant.

$$\text{Roller MV} = b_0 + b_1\ \alpha \tag{6.1}$$

6.2.2 Factors Affecting Quality of Regression Relationships

As with any regression analysis, it is important to identify factors that affect the quality of the regressions. Factors affecting regression relationships are broadly identified in Table 6.2 for the purpose of linking some of these factors to various TB conditions. This list was derived from linking TB conditions with correlation analysis but also from experiences gained from field tests as part of this study. Four examples described in the next section illustrate some of the TB conditions that led to development of Table 6.2. Heterogeneity in support conditions of layers underlying the compaction layer is one of the major factors that affect correlations between MVs and point measurements. This is largely due to differences in measurement depths between the roller and the point measurements (see Figure 6.1). As discussed in Chapter 4, roller MVs from 11- to 15-ton vibratory rollers can be representative of conditions to depths of 1.0 to 1.2 m (3.3 to 3.9 ft). Use of underlying layer MVs and use of point measurements with comparable measurement influence depths are ways to overcome this obstacle. This approach is discussed in detail in the multiple regression analysis section.

Table 6.2. Summary of factors affecting correlations between MVs and in situ point measurements.

No.	Factors Affecting Correlations
1	Heterogeneity in underlying-layer support conditions
2	High moisture content variation
3	Narrow range of measurements
4	Machine operation setting variation (e.g., amplitude, frequency, speed) and roller "jumping"
5	Nonuniform drum/soil contact conditions
6	Uncertainty in spatial pairing of point measurements and roller MVs (see Chapter 3)
7	Limited number of measurements
8	Not enough information to interpret the results
9	Intrinsic measurement errors associated with roller MVs and in situ point-test measurements (see Chapter 3)

6.2.3 Examples of Simple Linear Regression Analysis

Below are discussions from select TB studies to highlight different aspects of simple linear regression analysis. Detailed information for all TB regression analyses is provided in Appendix C. The examples present correlations of roller MVs to different in situ point measurements with homogeneous to heterogeneous support conditions and variable conditions across the drum and at different amplitude settings. These conditions represent some of the key aspects of regression analysis for all TBs summarized in Appendix C.

6.2.3.1 Example 1: TB MN7(2)

TB MN7(2) was constructed by scarifying an existing nongranular subgrade layer (classified as CL according to the USCS classification) to a depth of about 350 mm (14 in) using a soil reclaimer and by moisture conditioning to w = 13.0% to 14.5%. Plan dimensions of this TB were about 2.5 m × 120 m (8.2 ft × 394.0 ft). Twelve compaction passes were performed with a Caterpillar CS-563E vibratory pad foot roller with constant operation settings using nominal A = 0.80 mm (0.031 in), f = 33 Hz, and v = 4 km/h (2.5 mph). In

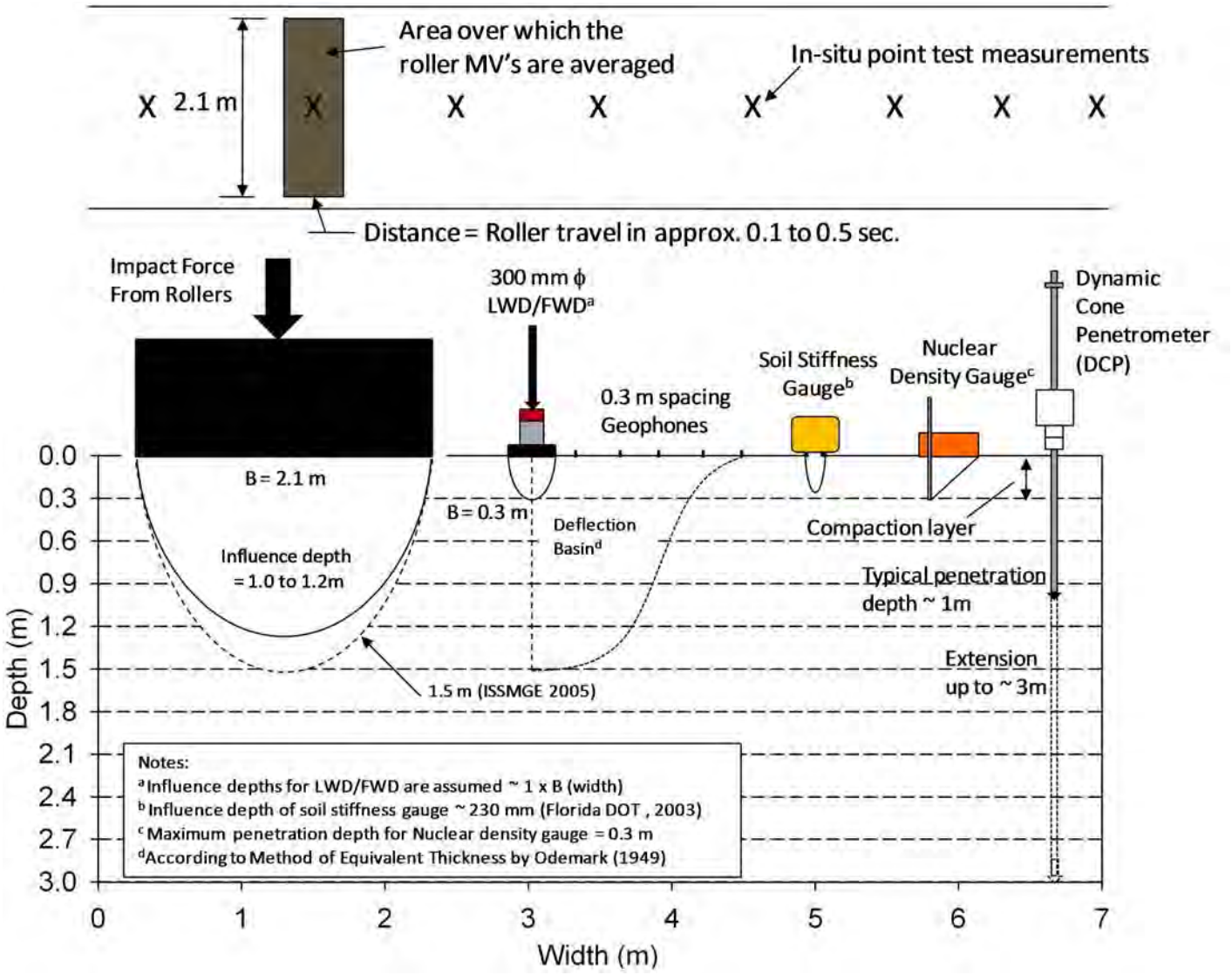

Figure 6.1. Illustration of differences in measurement depths for different measurements.

situ point measurements (γ_d, CBR, and $E_{LWD\text{-}Z2}$) were obtained at roller passes 0, 1, 2, 4, and 8 at five test locations along the centerline of the roller path. DCP tests indicated that the layer below the compaction layer [from 350 to 700 mm below the surface (14.0 to 27.6 in)] was relatively homogeneous with CBR = 14 to 18.

Figure 6.2 shows roller machine drive power (MDP) MVs as solid lines for roller passes 1, 2, 4, and 8 in comparison with in situ point measurements on the compaction layer. Compaction growth curves for average roller MV and in situ point measurements with a hyperbolic fit are presented in Figure 6.3. The curves indicate that on average the roller MVs and in situ point measurements generally increased up to eight roller passes (note that a decrease in MDP indicates increasing compaction). Linear regression relationships were developed based on spatially nearest point data (i.e., no averaging performed) as shown in Figure 6.3, producing correlations with $R^2 = 0.50$ to 0.89. This example illustrates that with relatively homogeneous compaction layer and underlying layer support conditions, good correlations ($R^2 \geq 0.5$) are possible between MDP and in situ point measurements.

6.2.3.2 Example 2: TB FL19B

TB FL19B was constructed by placing a nominal 150-mm (5.9-in)-thick loose layer of granular base material (SM according to the USCS classification) over relatively stiff stabilized subgrade ($E_{LWD\text{-}Z2} = 132$ to 145 MPa). In situ moisture content of the base material was relatively consistent ($w =$ 8.8% to 9.2%). Thirteen compaction passes were performed

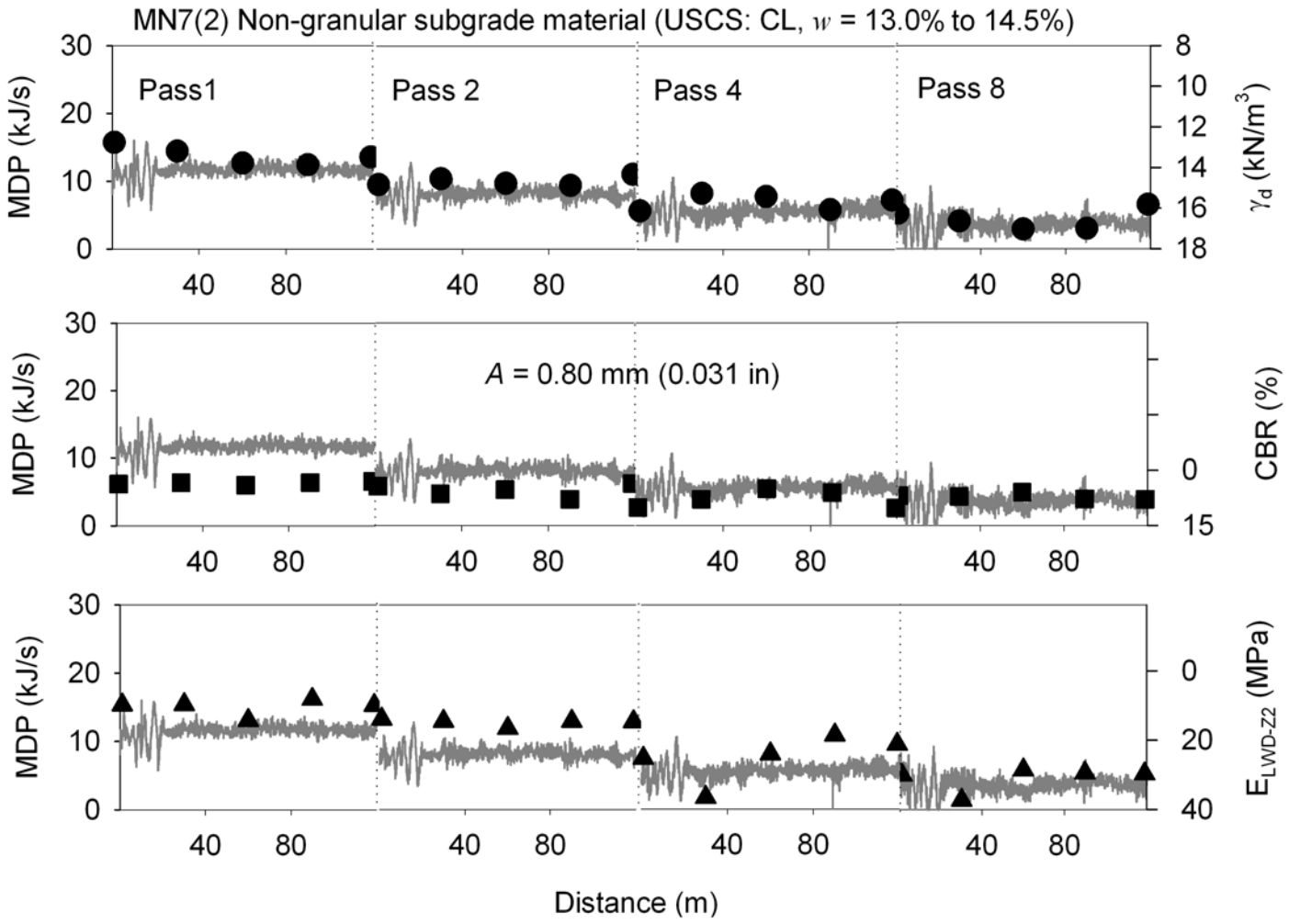

Figure 6.2. Example 1: Comparison between roller MV and in situ point measurements.

with a Dynapac CA362 vibratory smooth drum roller at constant operation settings, with nominal A = 0.90 mm (0.035 in), f = 30 Hz, and v = 4.0 to 4.5 km/h (2.5 to 2.8 mph). In situ point measurements (γ_d and $E_{LWD\text{-}Z3}$) were obtained at five locations along the test bed after roller passes 1, 2, 3, 4, 8, and 12. Tests were conducted at three positions across the width of the drum lane at each point measurement location.

Compaction growth curves for average roller MVs (CMV_D) and in situ point measurements with hyperbolic curves are presented in Figure 6.4. In situ point measurement data are presented separately for measurements along the center of the drum and measurements along the rear-wheel path. Different compaction trends were observed between center and wheel path measurements. On average, measurements along the center were about 1.1 to 1.6 times greater than measurements along the rear-wheel path (this observation should not be considered typical because at other sites similar measurements showed higher measurements in the wheel path as opposed to the center of the drum).

Linear regression relationships that were developed based on spatially nearest point data also are presented in Figure 6.4. Results are presented separately for the average of three measurements across the drum width and for one measurement at the drum center. Relationships for the average of three measurements showed significant improvement in correlations over one measurement at the center for γ_d and E_{LWD} from $R^2 < 0.5$ to $R^2 > 0.8$, while correlation to CBR was relatively high for both cases. Note that this example includes 5 of 30 data points with $CMV_D < 10$. Chapters 2 and 3 showed that CMV < 10 is insensitive to soil stiffness due to the nature of the measurement. The inclusion of $CMV_D < 10$ generally artificially increases R^2 and its use is not recommended.

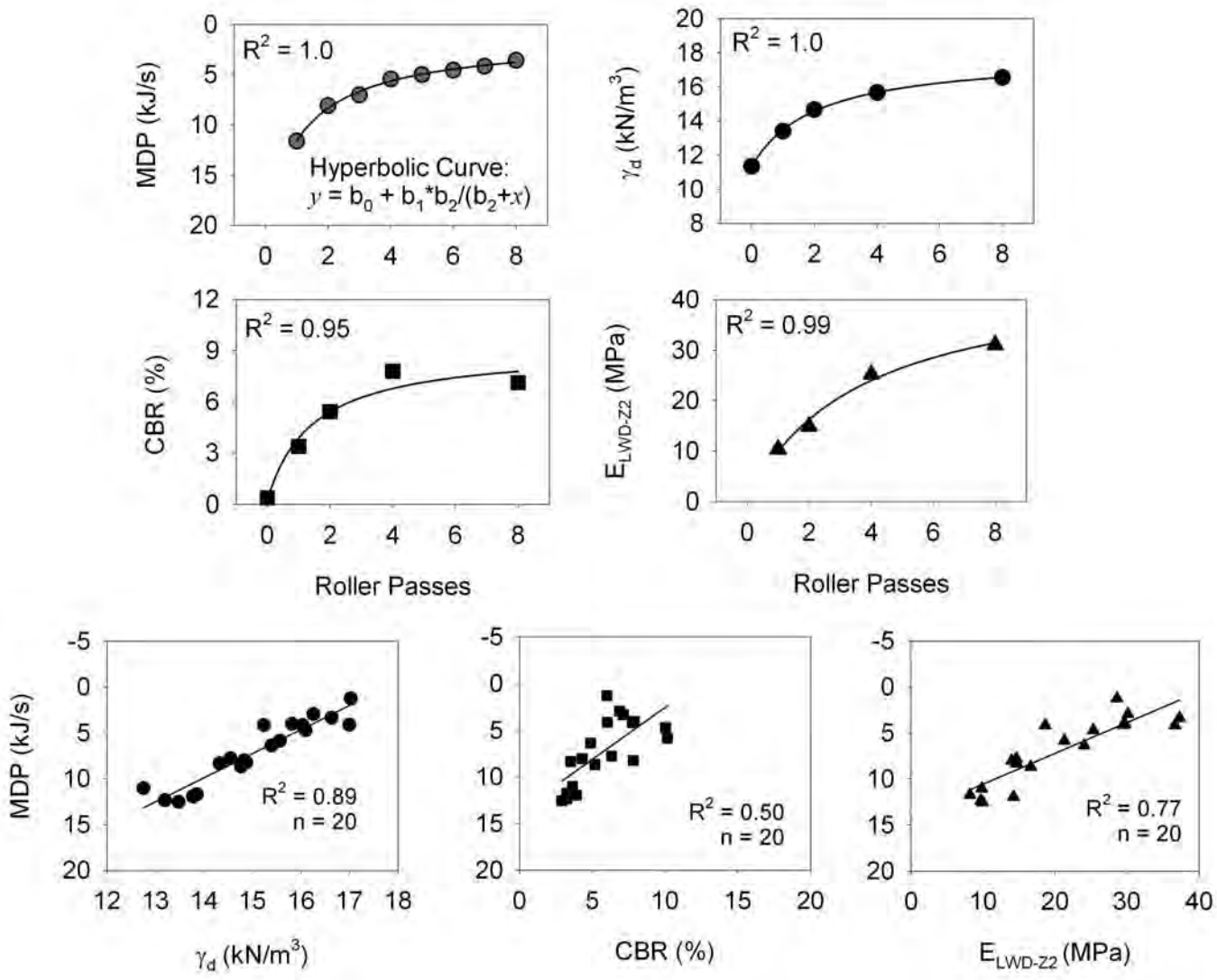

Figure 6.3. Example 1: Average compaction curves of roller MV and in situ point measurements (top) and simple linear regression relationships between spatially nearest roller MV and in situ point measurements (bottom).

6.2.3.3 Example 3: TB NC4B

TB NC4B consisted of granular base material (SP-SM according to the USCS classification system) that was scarified in place using a motor grader to a depth of about 100 mm (4 in). In situ moisture content of the material was relatively constant (w = 3% to 4%). Compaction was performed using a Case SV212 vibratory smooth drum roller with 16 roller passes at constant settings with nominal A = 0.80 mm (0.031 in), f = 30 Hz, and v = 4.0 km/h (2.5 mph). In situ point measurements (γ_d, $E_{LWD\text{-}Z2}$, and $E_{LWD\text{-}D2}$) were obtained after 1, 2, 4, 8, and 16 roller passes at seven test locations, and DCP tests were performed after 16 roller passes. DCP tests were performed to a depth of about 400 to 850 mm (15.7 to 33.5 in). Three point measurements were performed across the drum lane at each location.

Figure 6.5 shows roller MVs (k_s) as solid lines for 1, 2, 4, 8, and 16 roller passes in comparison with in situ point measurements. The in situ point measurements did not track well with variations in MVs. Compaction growth curves for average roller MV and point measurements with a hyperbolic curve fit are presented in Figure 6.6. On average, roller MVs and point measurements showed limited increase in compaction from pass 1 to pass 4 [k_s from 15.5 to 18.0 MN/m, $E_{LWD\text{-}Z2}$ from 40 to 52 MPa, $E_{LWD\text{-}D2}$ from 65 to 72 MPa, and γ_d from 19.3 to 20.5 kN/m^3 (123.1 to 130.7 lb/ft^3)]. Average γ_d increased to 20.9 kN/m^3 (133.3 lb/ft^3) after pass 16. The MV compaction curve showed evidence of what can be

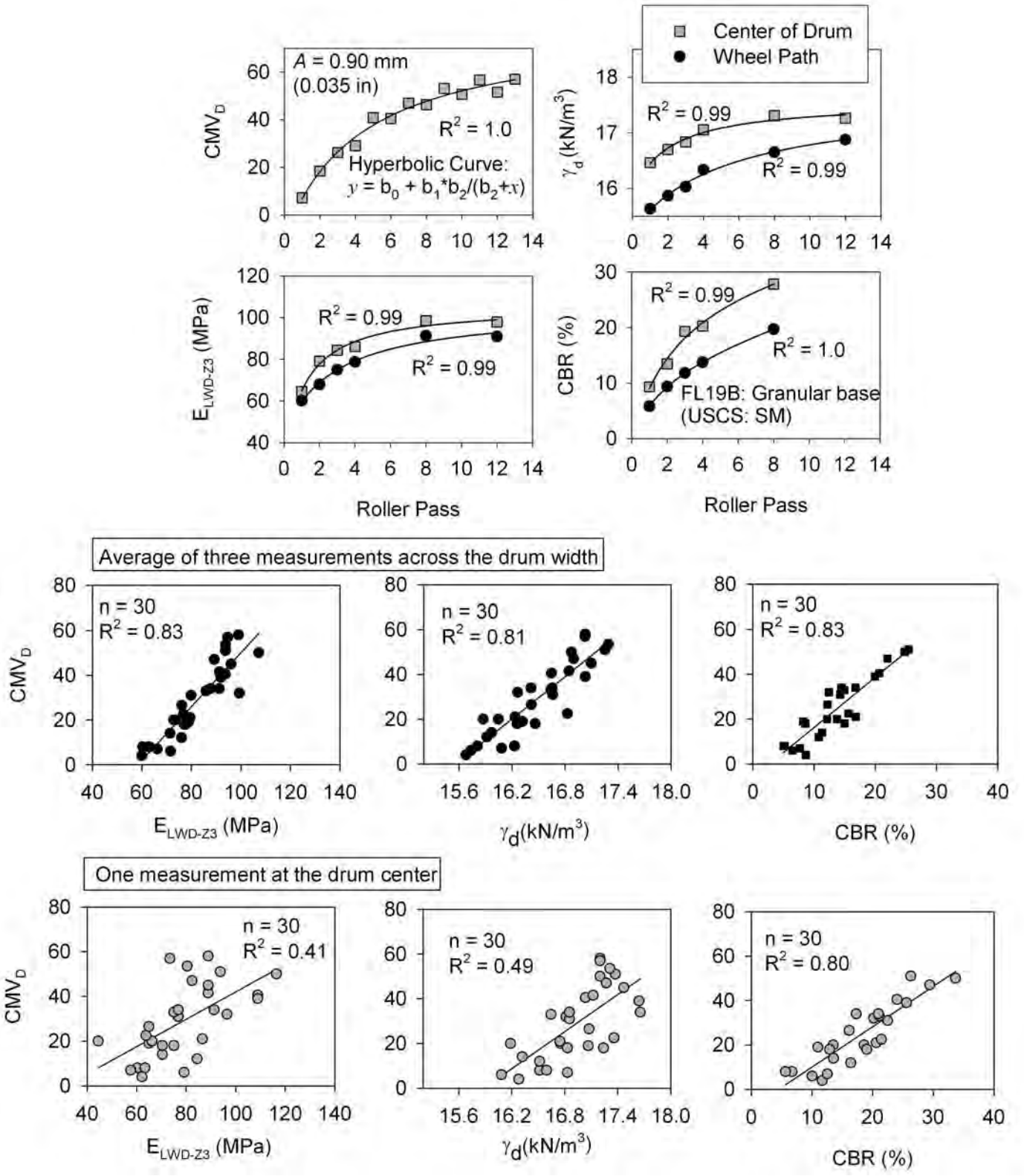

Figure 6.4. Example 2: Roller MV and in situ point measurement compaction curves (top) and simple linear regression relationships between MVs and in situ point measurements (bottom).

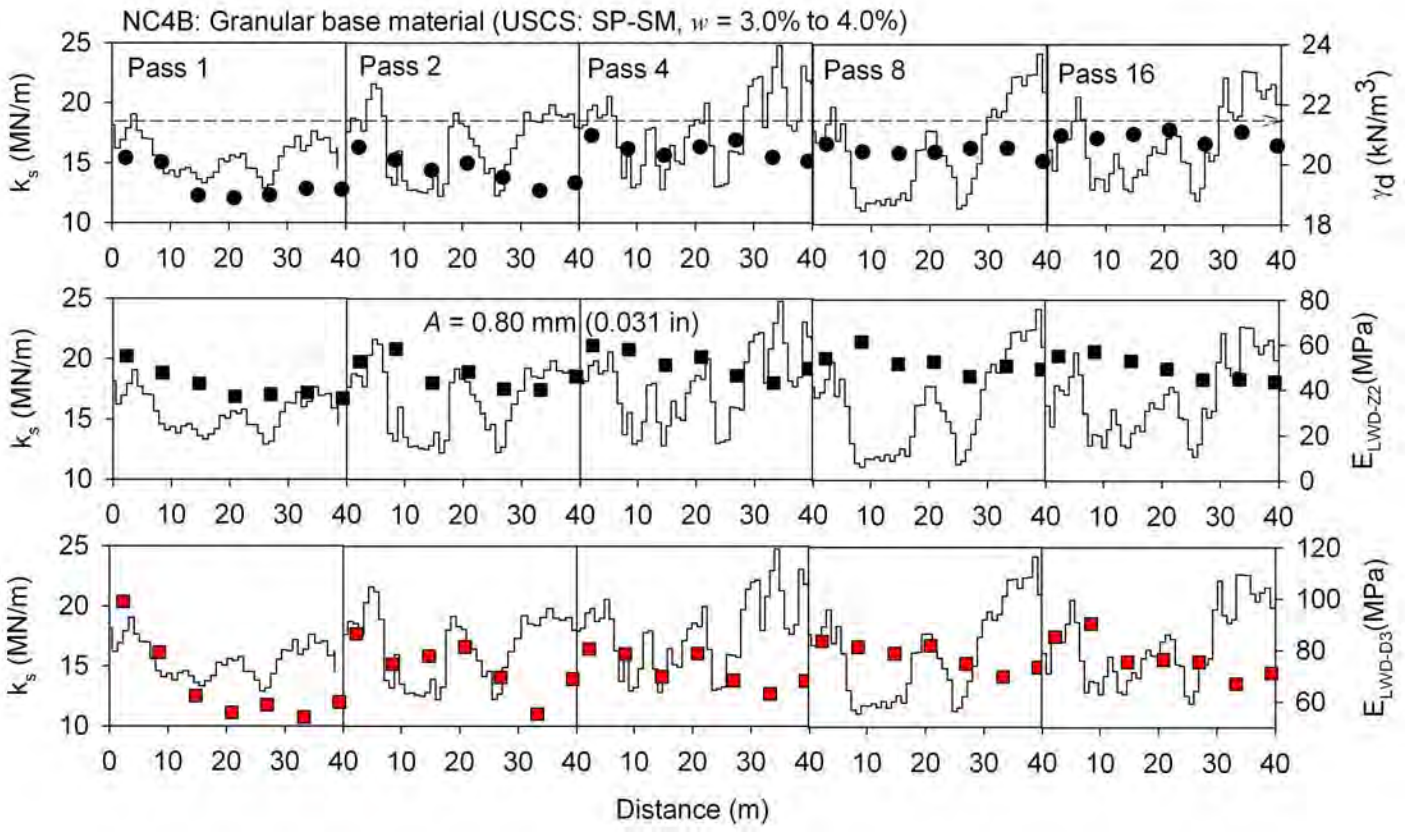

Figure 6.5. Example 3: Comparison MV and in situ point measurements.

interpreted as decompaction and recompaction for passes 7 and higher. This is common for granular materials (e.g., White & Thompson 2008) and can often be overcome by alternating static and vibratory passes (see, e.g., Brandl & Adam 2000). Linear regression relationships between roller MVs and point measurements based on spatially nearest point data produced poor correlations (Figure 6.6).

To further investigate the relationship between roller MVs and point measurement data, DCP tests are presented in Figure 6.7 along with pass 16 roller MVs. The CBR profiles showed a nonuniform subsurface layer below about 300.0 mm (11.8 in) from the surface. Average CBR calculated from depths of 300 to 600 mm (11.8 to 23.6 in) are plotted in comparison with roller MVs in Figure 6.8. CBR values from depths of 300 to 600 mm (11.8 to 23.6 in) tracked well with variations in roller MVs along the test bed. Regression relationships between spatially nearest point roller MVs and CBR values produced a good correlation with $R^2 = 0.62$.

The results presented here indicate that roller MVs can be insensitive to thin compaction layers and can be strongly influenced by underlying layers. This example also illustrates that in situ point measurements (e.g., γ_d, E_{LWD}) may not correlate well with roller MVs when nonuniform subsurface conditions are evident at depths greater than the influence depth of the point measurements. In situ testing devices that provide information deeper than the compaction layer (e.g., DCP, FWD) can help interpret the vibratory roller MVs that are influenced by material to the measurement depth of 1 to 1.2 m (3.3 to 3.9 ft) as described in Chapter 4.

6.2.3.4 Example 4: TBs MD6–MD9

TBs MD6–MD9 consisted of a nominal 150.0-mm (5.9-in)-thick layer of granular base material (SP-SM according to the USCS classification). The TBs were mapped using Dynapac CA362 and Bomag BW213-DH vibratory smooth drum rollers at a constant high-amplitude setting to assess the influence of drum "jumping" on correlations. CMV_D measurements were obtained at constant settings with nominal A = 2.40 mm (0.094 in), f = 30 Hz, and v = 4.0 km/h (2.5 mph). E_{vib} measurements were obtained at constant settings with nominal A = 1.90 mm (0.075 in), f = 28 Hz, and v = 4.0 km/h (2.5 mph). Roller "jumping" was measured as bouncing value (BV) for CMV_D and jump for E_{vib}. Following mapping passes, E_{V1} measurements were obtained at 40 test locations across the test beds.

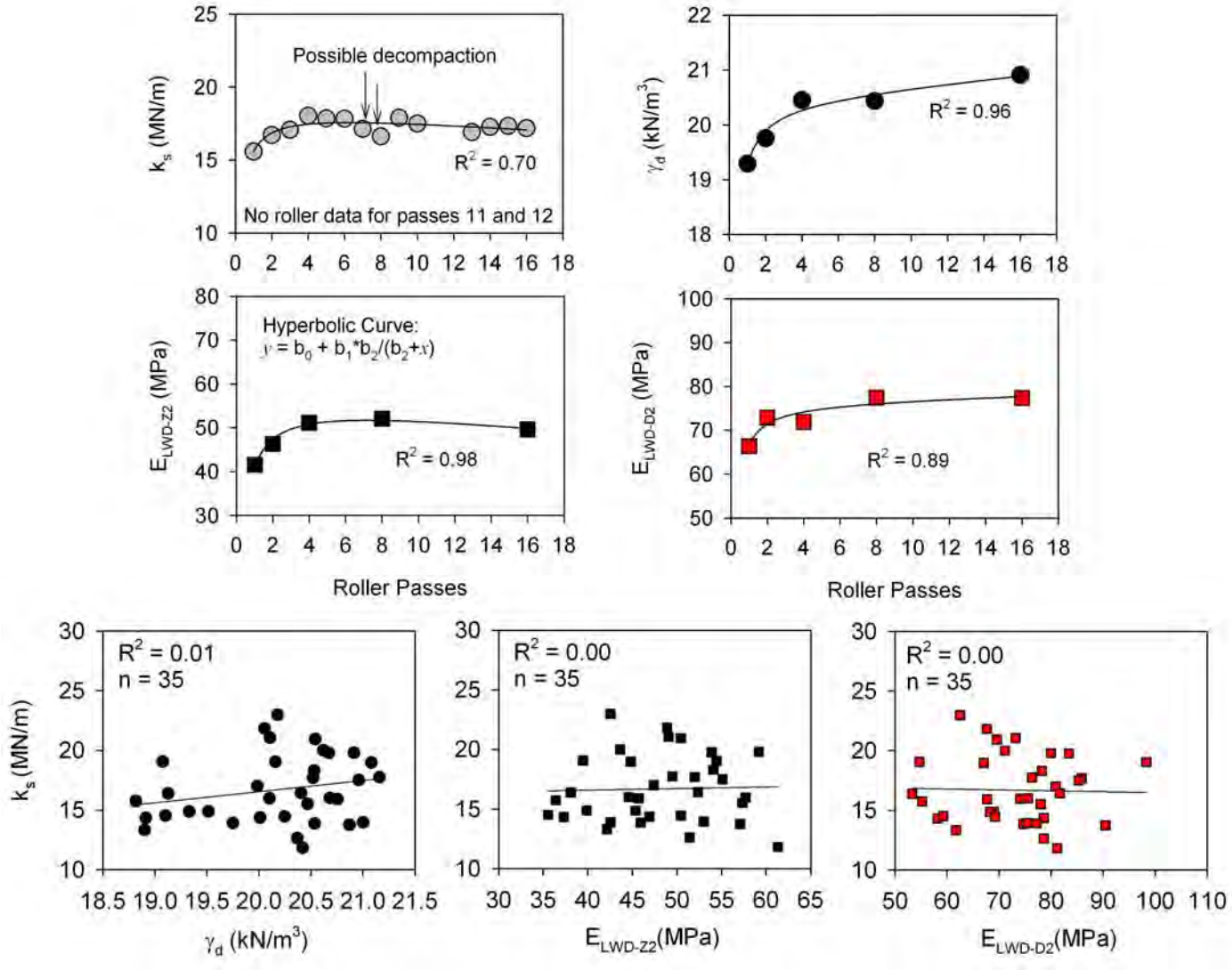

Figure 6.6. Example 3: Compaction curves of average roller MV and in situ point measurements and simple linear regression relationships.

Relationships between roller MVs and corresponding "jumping" values are presented in Figure 6.9. Based on theoretical simulations, Adam & Kopf (2004) and Anderegg (1998) found that accelerometer-based CMV, E_{vib}, and k_s MVs are affected by roller "jumping." It was shown that with increasing ground stiffness the roller drum transitions to a jump mode, where the "jumping" values increase and the roller MVs decrease. With further increase in ground stiffness, the roller MVs decrease to a minimum value and then increase again (see Chapter 2). The relationships presented in Figure 6.9 for roller MVs and "jumping" values show a similar feature.

Linear regression relationships developed between roller MVs and E_{V1} measurements are also presented in Figure 6.9. Roller MVs at three test locations were identified as being out of trend for CMV_D where BV > 10. Similarly, roller MVs at two test locations were found to be out of trend for E_{vib} where jump = 2. Regression relationships improved after removing the out-of-trend points due to drum jumping (R^2 = 0.29 to 0.72 for CMV_D and 0.47 to 0.71 for E_{vib}). This example includes 10 of 38 data points with CMV_D < 10 that artificially increases R^2.

This example illustrates that it is important to remove roller MVs during drum "jumping" from the analysis. This is an issue, in particular, for stiff ground conditions when the machine is operated in the high-amplitude setting. Operating in the low-amplitude settings [e.g., A < 1.10 mm (0.043 in)] effectively eliminates jump mode. Further, AFC rollers automatically reduce vibration amplitude when jump mode is detected (although as discussed in Chapter 5, using AFC during quality control/quality assurance is not recommended).

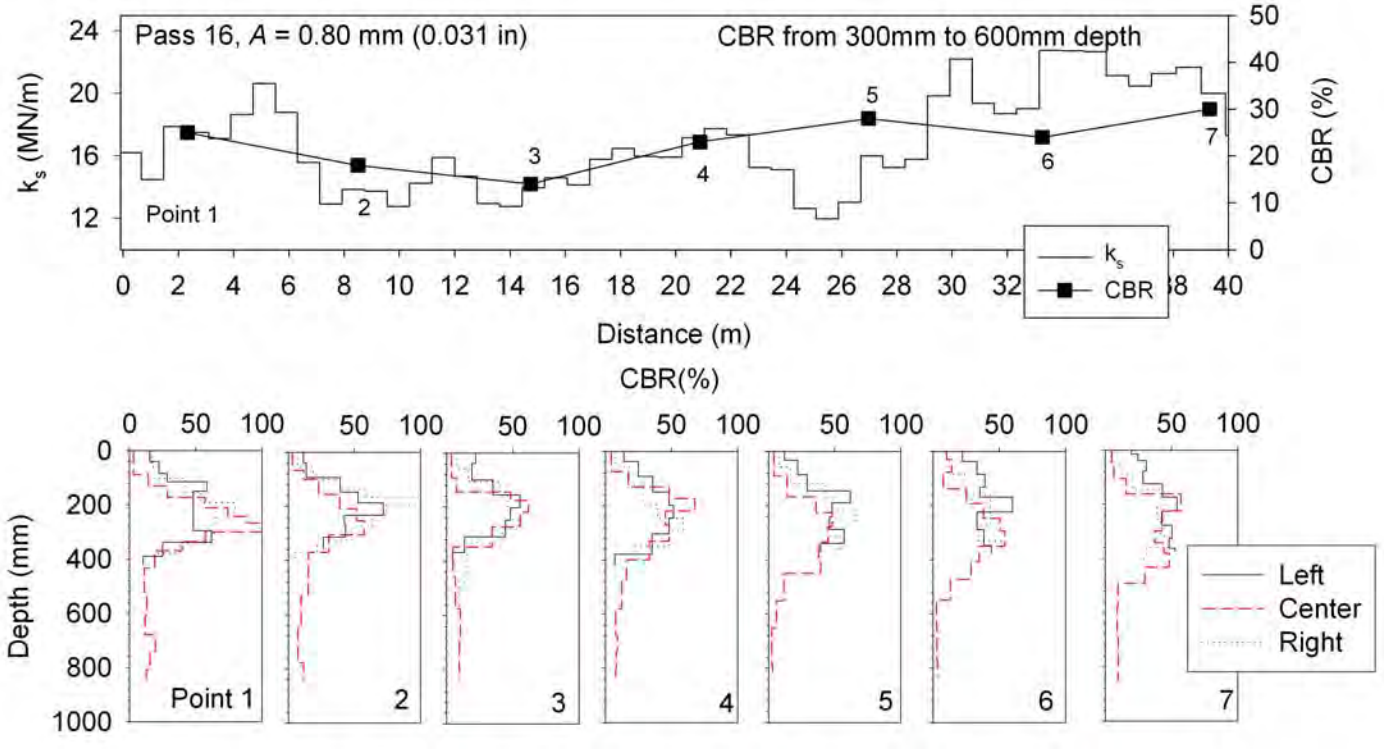

Figure 6.7. Example 3: Comparison of pass 16 roller MVs with CBR profiles.

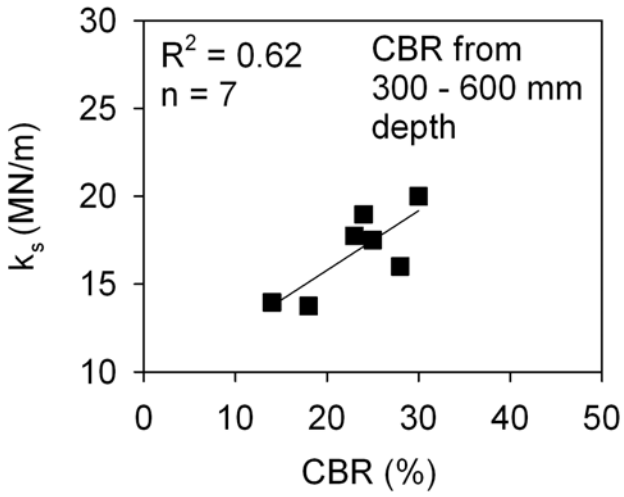

Figure 6.8. Example 3: Simple linear regression relationship between roller MV and CBR from depths of 300 to 600 mm (11.8 to 23.6 in).

6.2.4 Summary of Simple Linear Regression Analysis

Simple linear regression relationships between the various in situ point measurements and roller MVs for the referenced test beds with nongranular subgrade, granular subgrade, and granular subbase/base materials are summarized in Appendix C. The regression relationships are identified with possible factor(s) (see Table 6.2) influencing the relationships (see notes on R^2 values in Appendix C). For some cases with poor correlations, sufficient information was not available to identify a factor. A summary of observed range of R^2 values for dry unit weight, modulus (i.e., E_{LWD}, E_{FWD}, E_{V1}, E_{V2}), and CBR measurements for different conditions is provided in Table 6.3. The R^2 values resulted in a wide range that is attributed to various factors that affect the regression relationships (as identified in Table 6.2). The influence of some of these factors (i.e., soil moisture content, compaction layer lift thickness, underlying layer properties) and machine operation settings (A, f, v) were statistically analyzed using multiple regression analysis, as discussed in the following section.

MVs are generally better correlated to compaction layer modulus measurements compared to dry unit weight and CBR measurements, especially where the underlying layer is

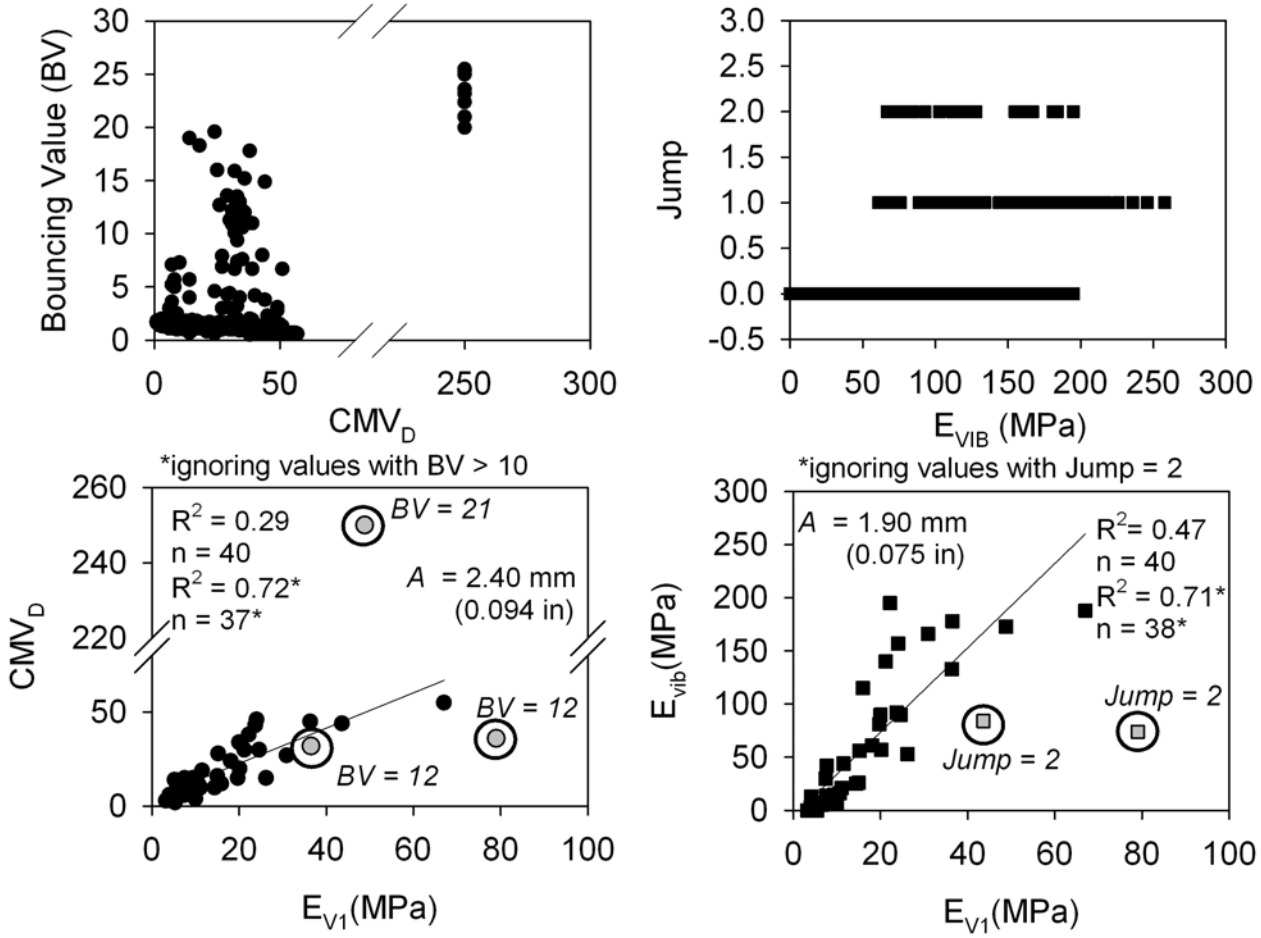

Figure 6.9. Example 4: Influence of roller "jumping" on regression relationships, TBs MD6–MD9 (granular base material, USCS: SP-SM).

Table 6.3. Observed range of R^2 values from simple linear regression analysis with roller MVs.

Material	Modulus[a]	CBR	γ_d
Nongranular subgrade	0.1–0.7	0.1–0.7	0.0–0.6
Granular subgrade	0.3–0.7	0.0–0.4	0.1–0.5
Granular subbase/base	0.2–0.8	0.0–0.6	0.0–0.5

[a] Includes modulus obtained from LWD, FWD, and static PLT.

heterogeneous. For TBs with relatively homogeneous material and subsurface conditions, MVs generally correlate well with dry unit weight, CBR, and modulus measurements.

6.3 Multiple Linear Regression Analysis

Use of multiple regression analysis to statistically assess the influence of variability in underlying layer soil conditions and variability in machine operation conditions is presented in this section. Multiple regression analysis is performed by incorporating variables of interest as independent variables into a general multiple linear regression model, as shown in Equation 6.2. The statistical significance of each variable is assessed based on *p*- and *t*-values. The selected criteria for identifying the significance of a parameter included *p*-value <0.05 = significant, <0.10 = possibly significant, >0.10 = not significant, and *t*-value <-2 or >+2 = significant. The *p*-value indicates the significance of a parameter, and the *t*-ratio value indicates the relative importance (i.e., the higher the absolute value, the greater the significance).

$$\text{Roller MV} = b_0 + b_1 \times \alpha + b_2 \times w + b_3 \times A + b_4 \times \beta + b_5 \times \gamma + b_6 \times w^2 + b_7 \times f + b_8 \times v \quad (6.2)$$

where b_0 = intercept; b_1, b_2, b_3, b_4, b_5, b_6, b_7, and b_8 = regression coefficients; A = amplitude (mm); α = point measurement value (γ_d, E_{LWD}, etc.); β = underlying layer roller MV or point measurement; γ = lift thickness (mm); f = vibration frequency (Hz); and v = velocity (km/h).

For multiple regression analysis, the reported R^2 values have been adjusted for the number of regression parameters, as shown in Eq. 6.3, where n = the number of data points and p = the number of regression parameters. The adjusted coefficient of determination R^2_{adj} from multiple regression analysis may be compared with R^2 from simple linear regression analysis to assess which regression model best captures variation in the data.

$$R^2_{adj} = 1 - (1 - R^2)\frac{n-1}{n-p} \quad (6.3)$$

Complications with *collinearity* should be avoided when performing multiple regression analysis. Collinearity refers to inclusion of two or more strongly related independent variables into a model to predict a dependent variable, which may result in misleading R^2_{adj} values (Ott & Longnecker 2001). This is possible in the above-described model if, for example, underlying layer MV and point measurement values are included together. Collinearity in a model can be detected using variance inflation factors (VIF). VIF of the ith independent variable is defined as $1/(1 - R_i^2)$, where R_i^2 is the coefficient of determination for the regression of the ith independent variable on all other independent variables. Although there are no formal criteria on the acceptable magnitude of VIF, a common rule of thumb is that if VIF of the ith independent variable is $<1/(1 - R^2)$, where R^2 is the coefficient of determination of the univariate model, then it can be concluded that the variable is not contributing to collinearity (Freund et al. 2003).

Example results of representative test beds where vibration amplitude, soil moisture content, and underlying layer conditions affected the regression relationships are discussed below. The influence of moisture content and underlying layer properties was assessed in the analysis of all test beds for which measurements were available. Variability in soil moisture content and underlying layer conditions was intentionally introduced in the Colorado and Maryland test beds under controlled field conditions to study their influence on the relationships. Data obtained at different amplitude settings were combined to assess the influence of amplitude. This process was exercised for all test beds/layers, and summary relationships are presented separately for nongranular subgrade, granular subgrade, and granular subbase/base materials in Appendix C. At the end of this section, results from multiple sites and test beds are combined in an attempt to capture a wide range of variations to obtain relationships between different roller MVs and modulus measurements (i.e., E_{LWD}, E_{V1}, E_{V2}).

6.3.1 Influence of Vibration Amplitude and Frequency

Two examples are presented in the following discussion: Example 1 describes data with influence of vibration amplitude; Example 2 describes data with influence of vibration amplitude and frequency on roller MVs.

6.3.1.1 Example 1: TBs MD6–MD9

Relationships between E_{vib} and E_{V1} measurements obtained from TBs MD6–MD9 with granular base materials are presented in Figure 6.10. E_{vib} measurements were obtained at A = 1.9 and 0.7 mm (0.075 and 0.028 in) and constant f = 28 Hz and v = 4.0 km/h (2.5 mph) nominal settings. As described in Figure 6.9, the out-of-trend values due to roller "jumping" were not included in the analysis.

For the multiple regression model to predict E_{vib}, the intercept was not significant and the R^2_{adj} = 0.66 (Table 6.4) was lower compared to simple linear regression relationships (R^2 = 0.71 and 0.82). This is important to note because, although a parameter may be statistically significant in a multiple regression model, it may not always contribute to an improved model fit. In this case it is appropriate to interpret the relationships between E_{vib} and in situ point measurements separately for different amplitude settings, instead of combining the results.

6.3.1.2 Example 2: TBs MN19, MN20, MN26, FL20A, FL20B, FL23A, FL23B, and FL25

Relationships between roller MVs (k_s) and $E_{LWD\text{-}Z2}$ measurements obtained from TBs MN19, MN20, and MN26 and between roller MVs (k_s) and $E_{LWD\text{-}Z3}$ measurements from TBs FL20A, FL20B, FL23A, FL23B, and FL25 are presented in Figure 6.11. MN19, MN20, and MN26 consisted of granular base materials. FL20A and FL20B consisted of granular subbase, and FL23A, FL23B, and FL25 consisted of granular subgrade materials. The A and f settings in the beds varied from 0.3 to 1.7 mm (0.012 to 0.067 in) and 25 to 33 Hz, respectively. Settings in each bed are summarized in Figure 6.11.

Simple linear regression relationships while treating data from each test bed separately are presented in the legends for Figure 6.11. For MN test beds, R^2 varied from 0.0 to 0.6, and for FL test beds, R^2 varied from 0.4 to 0.6. As shown in Figure

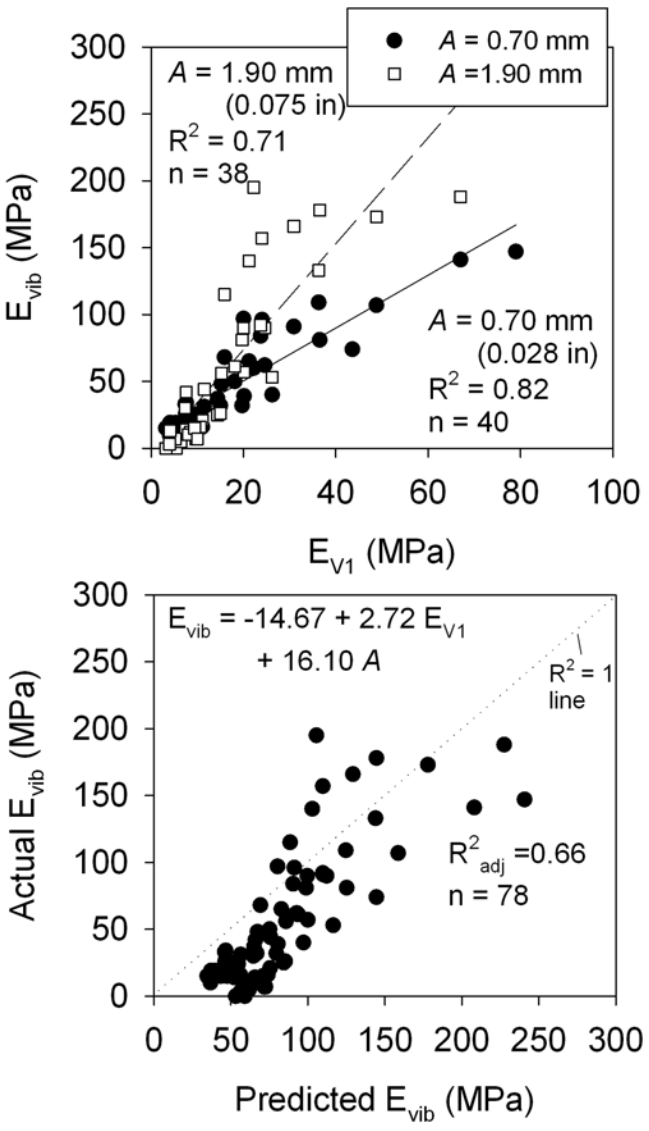

Figure 6.10. Influence of amplitude on E_{vib} —TBs MD6–MD9 granular base material (USCS: SP-SM).

6.11, the relationships showed different trends, primarily due to differences in the A and f settings between the test beds. Multiple regression analysis was performed by combining data from different MN and FL test beds by incorporating the $E_{LWD\text{-}Z2}$, $E_{LWD\text{-}Z3}$, A, and f values as independent variables. The analysis results (see Table 6.5) indicate that both A and f are statistically significant parameters for both MN and FL test beds with R^2_{adj} = 0.80 and 0.79, respectively, for the models. The resulting predicted MVs using the multiple regression equation are shown versus the actual MVs in Figure 6.11. The regression coefficient for frequency (b_7) is negative for MN test beds and positive for FL test beds. A negative coefficient suggests that increasing f causes a decrease in roller MV and vice versa for a positive coefficient. In contrast, the coefficient for amplitude (b_3) is positive for MN test beds and negative for FL test beds. This indicates that the frequency and amplitude dependency on roller MVs change with soil types and field conditions (see also Chapter 4).

This example illustrates that an amplitude- and frequency-dependent regression model would be suitable for interpretation of results for these site conditions and roller MVs. It is an interesting and encouraging finding that shows potential for analyzing measurements obtained in AFC mode and warrants more research.

6.3.2 Influence of Moisture Content

Results obtained from TB MN11 are discussed to demonstrate the influence of moisture content on correlations between in situ point measurements and the MDP roller MV. The influence of moisture content on roller MVs for cohesive soils has been further documented by Thompson & White (2008). The test bed was constructed by placing a 375.0-mm (14.8-in)-thick loose lift of nongranular subgrade layer (CL according to the USCS soil classification system). Maximum dry unit weight and optimum moisture content as determined by the standard Proctor method were 16.95

Table 6.4. Results of multiple regression analysis for influence of amplitude—MD6–MD9.

Model	Term	Estimate	Std Error	*t*-Ratio	Prob > *t* (*p*-value)	R^2_{adj}	VIF
$E_{vib} = b_0 + b_1 E_{V1} + b_3 A$	b_0	-14.67	9.28	-1.58	0.1183	0.66	—
	b_1	2.72	0.23	12.02	< 0.001		1.00
	b_3	16.10	5.77	2.79	0.0066		1.00

Note: Check for no collinearity: VIF < $[1/(1 - R^2)]$.

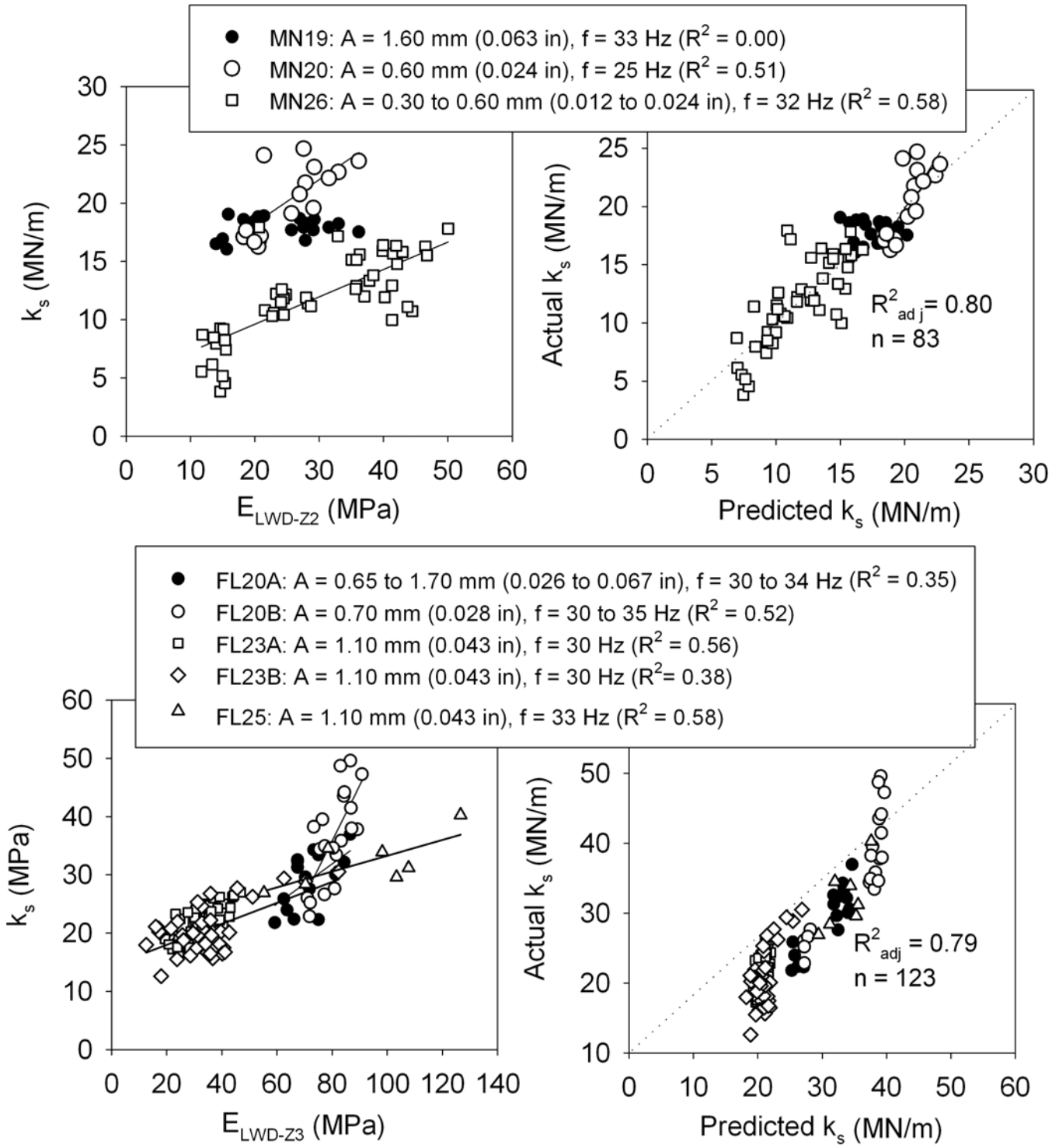

Figure 6.11. Influence of amplitude and frequency on roller MVs.

Table 6.5. Results of multiple regression analysis for influence of amplitude and frequency—MN19, MN20, MN26 and FL20A, FL20B, FL23A, FL23B, FL25.

TB	Model	Term	Estimate	Std Error	*t*–Ratio	Prob > t (*p*-value)	R^2_{adj}	VIF
MN19, 20, 26	$k_s = b_0 + b_1 E_{LWD\text{-}Z2} + b_3 A + b_7 f$	b_0	39.87	2.55	15.64	<0.0001	0.80	—
		b_1	0.23	0.02	9.33	<0.0001		1.07
		b_3	6.85	0.51	13.36	<0.0001		1.11
		b_7	-1.18	0.08	-13.94	<0.0001		1.08
FL20A/B23A/B, 25	$k_s = b_0 + b_1 E_{LWD\text{-}Z3} + b_3 A + b_7 f$	b_0	-40.86	6.91	-5.91	<0.0001	0.79	—
		b_1	0.12	0.02	5.81	<0.0001		2.53
		b_3	-2.90	1.26	-2.30	0.0232		1.07
		b_7	2.03	0.25	8.12	<0.0001		2.48

Note: Check for no collinearity: VIF should be $<[1/(1-R^2)]$.

kN/m^3 (105.20 lb/ft^3) and 16.4%, respectively. The test bed had plan dimensions of about 2.4 m × 90.0 m (7.9 ft × 295.3 ft) and was divided into three 30.0-m (98.4-ft)-long sections with target moisture contents of approximately -3%, 0%, and +3% of standard Proctor w_{opt}. The subgrade layer was moisture conditioned using a water truck and mixed using a reclaimer.

Vibratory compaction was performed with eight passes of a Caterpillar CS-563E vibratory pad foot roller at nominal constant settings of A = 0.80 mm (0.031 in), f = 33 Hz, and v = 4.0 km/h (2.5 mph). In situ point measurements (w, γ_d, $E_{LWD\text{-}K2}$, CBR) were obtained at 15 test locations (five locations in each moisture section) along the test bed. Tests were conducted after 1, 2, 4, and 8 roller passes. Figure 6.12 shows MDP as solid lines in comparison with in situ point measurements. Simple linear regression relationships between roller MDP and in situ point measurements were developed based on spatially nearest data, as presented in Figure 6.13. Regression relationships produced R^2 = 0.72, 0.50, and 0.57 for γ_d, CBR, and $E_{LWD\text{-}K2}$ measurements, respectively.

Multiple regression analysis was performed by adding moisture content as an independent variable in predicting roller MDP. Results from the analysis are summarized in Table 6.6. Moisture was statistically significant in predicting MDP from γ_d and $E_{LWD\text{-}K2}$ measurements and was not significant for CBR measurements. The regression coefficient (b_2) for both measurements is positive, which indicates that increasing moisture content resulted in an increase in MDP (i.e., lower stiffness). Using the multiple regression models, relationships between predicted and actual roller MDP are presented in Figure 6.13. Correlations improved with R^2_{adj} = 0.78 and 0.67 for predicting MDP from γ_d and $E_{LWD\text{-}K2}$, respectively, by including moisture content as an independent variable.

Generally, moisture content was not found to be statistically significant in the regression analysis for most of the test bed studies. Factors contributing to this observation are (1) moisture content did not vary enough over the length of the test beds; (2) in situ point measurements typically only measure moisture content to about 80 mm (3 in) below the surface, whereas the measurement influence depth of the roller is much larger; and (3) when correlating with elastic modulus-based in situ point measurements using multiple regression analysis, moisture content is collinear (i.e., highly correlated to in situ measurement).

6.3.3 Results of Multiple Regression Analysis

The examples described above demonstrate the approach of applying multiple regression analysis to relate MVs with in situ point measurements. This same approach was exercised for results from all test beds listed in Table 6.1 to evaluate the influence of moisture content, underlying layer stiffness, lift thickness, amplitude, and frequency. If a variable was not statistically significant or assessed as collinear (based on VIF), it was removed from the model. Multiple regression relationships for all test beds are summarized in Appendix C. A summary of the typical range of R^2_{adj} values for modulus, CBR, and dry unit weight measurements for the three referenced material groups from multiple regression analysis is provided in Table 6.7.

Where heterogeneous conditions were evident below the compaction layer, the underlying layer properties (MVs and point measurements) were often statistically significant in the multiple regression model. Regression relationships improved by incorporating the underlying layer properties. For some cases, when underlying layer properties are included in a multiple regression model, the compaction layer point measurements were found statistically not significant in the analysis. This is possible when MVs are more influenced by the underlying layer properties than the compaction layer properties. Moisture content was significant for two non-granular subgrade layer test beds and one granular base layer test bed. Lift thickness and w^2 terms were not statistically significant. Amplitude variation was statistically significant for

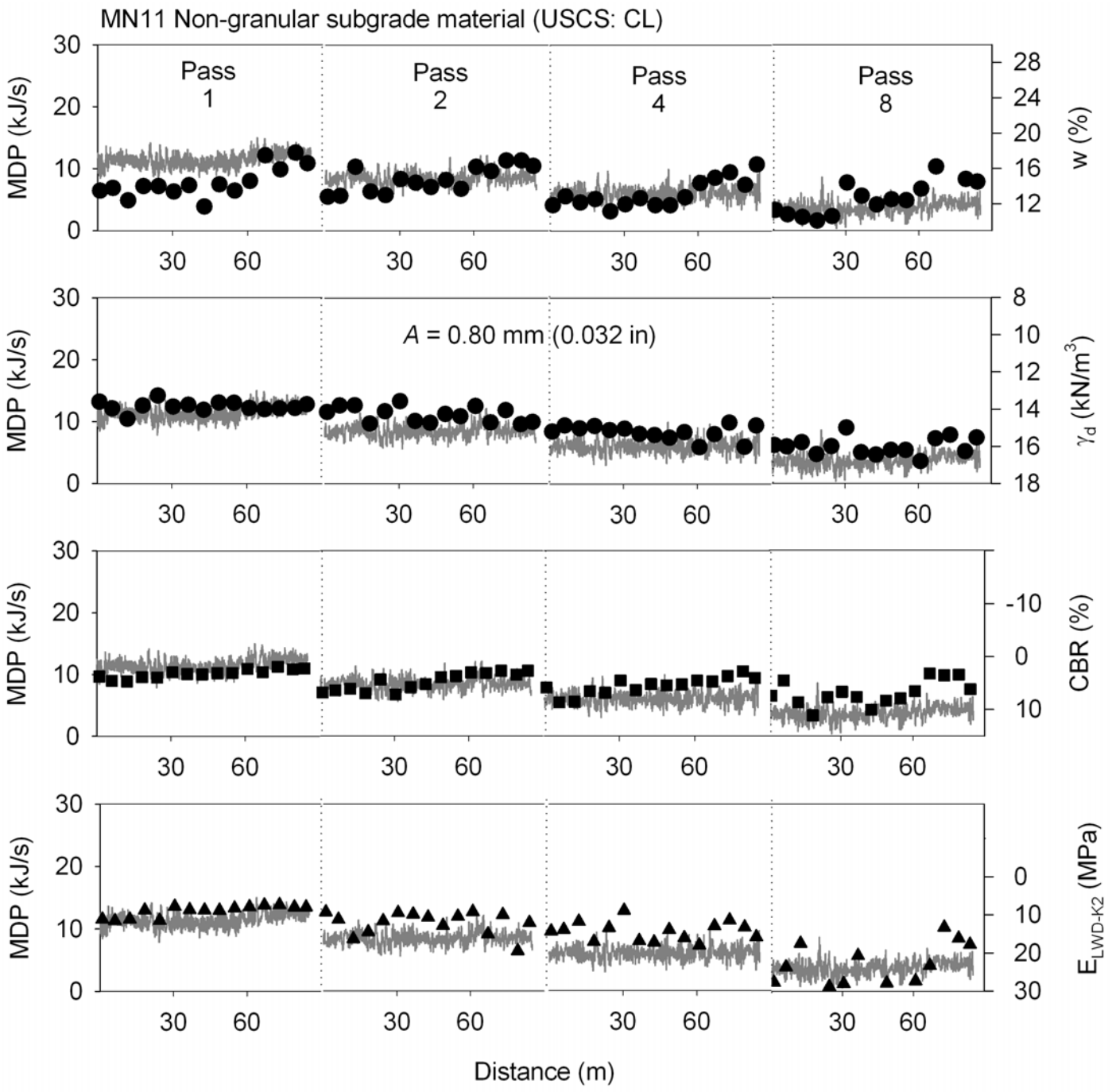

Figure 6.12. Roller MVs in comparison with in situ point measurements (TB MN11).

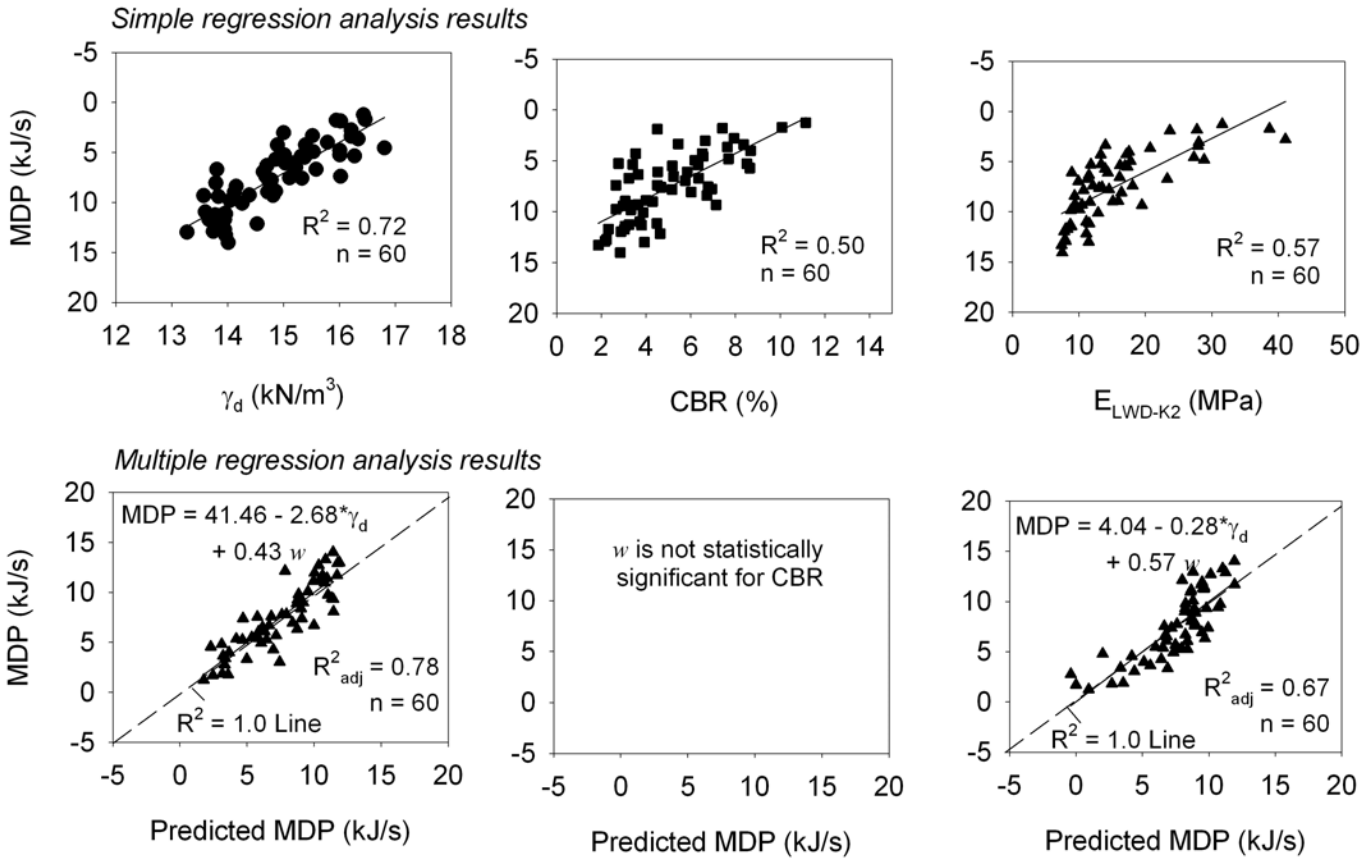

Figure 6.13. Simple regression relationships between roller MVs and in situ point measurements (top) and multiple regression relationships, including moisture content for predicting roller MVs (bottom).

Table 6.6. Results of multiple regression analysis for influence of moisture content—TB MN11.

Model	Term	Estimate	Std Error	*t*-Ratio	Prob > t	R^2_{adj}	VIF
$MDP = b_0 + b_1\gamma_d + b_2 w$	b_0	41.46	4.98	8.33	< 0.0001	0.78	—
	b_1	-2.68	0.26	-10.22	< 0.0001		1.26
	b_2	0.43	0.13	3.27	0.0019		1.26
$MDP = -b_0 + b_1 CBR + b_2 w$	b_0	9.03	3.67	2.46	0.0168		
	b_1	-0.99	0.19	-5.38	< 0.0001	—[a]	—[a]
	b_2	0.26	0.22	1.23	0.2238		
$MDP = -b_0 + b_1 E_{LWD-K2} + b_2 w$	b_0	4.04	2.36	1.71	0.0928		—
	b_1	-0.28	0.036	-7.70	< 0.0001	0.67	1.19
	b_2	0.57	0.15	3.79	0.0004		1.19

[a] Not statistically significant according to $p < 0.10$ and $t < -2$ or $> +2$.
Note: Check for no collinearity: VIF should be $< [1/(1 - R^2)]$.

all cases where minimum amplitude variation of ±0.30 mm (±0.012 in) was present in the data.

Results from multiple sites and test beds (MD6, 7, 8, 9, 11, 12, 13, and 14; CO6, 7, 8, 11, 12, 13, 16, 17, and 18) were combined to capture a wide range of variations to obtain relationships between E_{vib} and modulus measurements (i.e., E_{LWD}, E_{V1}, E_{V2}). Only test beds with underlying layer measurements were considered in this analysis. The influence of w, underlying layer properties (roller MV or point measurement), A, f, and v was assessed.

Table 6.7. Typical range of R^2_{adj} values for multiple linear regression analysis.

Material	γ_d	Modulus[a]	CBR
Nongranular subgrade	0.6–0.8	0.2–0.6	0.3–0.7
Granular subgrade	—	0.5–0.7	—
Granular subbase/base	0.4–0.8	0.6–0.9	0.4–0.8

[a]Includes modulus obtained from LWD, FWD, and static PLT.

Example results of multiple regression analysis combining Maryland and Colorado test beds for the E_{vib} MV are presented in Figure 6.14. Table 6.8 provides a summary of the complete analysis results. Results indicate that E_{LWD}, E_{V1}, E_{V2}, and E_{FWD} measurements correlate well with E_{vib}. Amplitude was statistically significant for all cases, and underlying layer properties were significant for most cases. In some cases the underlying layer properties were collinear with compaction layer measurements and therefore were removed from the model. For all the test beds considered, the frequency variation was within ±2 Hz and the speed variation was 3.0 to 5.0 km/h (1.9 to 3.1 mph). For this variation, both *f* and *v* were not statistically significant.

6.4 Relationships Between Roller MV and Resilient Modulus

Developing relationships between field and laboratory mechanistic parameters was an objective of this project and provided interesting results from an empirical perspective. A number of field studies over the past three decades have documented the challenges involved in developing these relationships (e.g., Anderson & Woods 1975, Rodhe & Scullion 1990, Daleiden et al. 1994, Nazarian et al. 1998). According to Anderson and Woods, primary factors that affect these relationships include (1) sampling disturbance, (2) differences in the stress states between the laboratory specimen and in-place pavement material, (3) nonrepresentative materials, and (4) inherent errors in the field and laboratory test procedures.

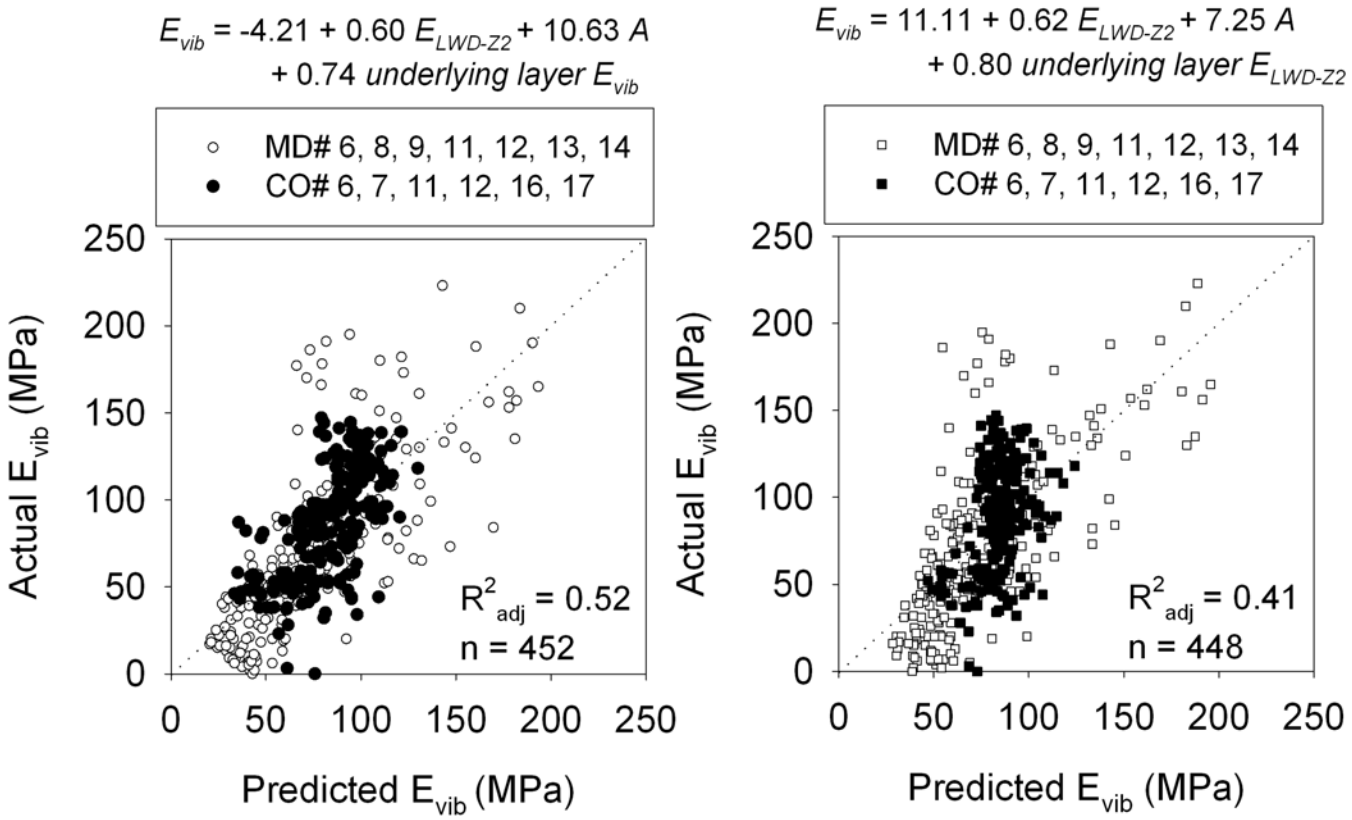

Figure 6.14. Results of multiple regression analyses from MD and CO test beds from compaction layer E_{LWD-Z2} and vibration amplitude measurements and underlying layer E_{LWD-Z2} and roller MVs.

Table 6.8. Results of multiple regression analyses combining multiple project sites and test beds.

TB	Model	Term	Estimate	Std Error	t-Ratio	Prob > t (p=value)	R^2_{adj}	VIF[a]
MD6, 8, 9, 11, 12, 13, 14; CO6, 7, 11, 12, 16, 17	$E_{vib} = b_0 + b_1 E_{LWD\text{-}Z2} + b_3 A + b_4 E_{vib}^{\chi}$ $n = 452$	b_0	-4.21	4.66	-0.90	0.3663	0.52	—
		b_1	0.60	0.07	8.2	< 0.0001		1.26
		b_3	10.63	2.31	4.59	< 0.0001		1.03
		b_4	0.74	0.05	14.73	< 0.0001		1.28
MD6, 8, 9, 11, 12, 13, 14; CO6, 7, 11, 12, 16, 17	$E_{vib} = b_0 + b_1 E_{LWD\text{-}Z2} + b_3 A + b_4 E_{LWD\text{-}Z2}^{\chi}$ $n = 448$	b_0	11.11	4.92	2.26	0.0243	0.41	—
		b_1	0.62	0.09	6.96	< 0.0001		1.16
		b_3	7.25	2.56	2.84	0.0048		1.06
		b_4	0.80	0.09	9.33	< 0.0001		1.10
MD8	$E_{vib} = b_0 + b_1 E_{LWD\text{-}Z3} + b_3 A + b_4 E_{vib}^{\chi}$ $n = 18$	b_0	-48.21	21.56	-2.24	0.0422	0.73	—
		b_1	0.94	0.22	4.22	0.0009		1.20
		b_3	26.29	8.56	3.07	0.0083		1.00
		b_4	1.32	0.54	2.43	0.0291		1.20
MD6, 8, 9, 11, 12, 13, 14	$E_{vib} = b_0 + b_1 E_{V1} + b_3 A$ $n = 222$ E_{V1}^{χ} *not significant and collinear with* E_{vib}^{χ}	b_0	-2.66	5.00	-0.53	0.59	0.61	—
		b_1	2.22	0.12	18.38	< 0.0001		1.00
		b_3	13.20	3.14	4.20	< 0.0001		1.00
MD6, 8, 9, 11, 12, 13, 14	$E_{vib} = b_0 + b_1 E_{V2} + b_3 A + b_4 E_{vib}^{\chi}$ $n = 111$ E_{V2}^{χ} *not significant*	b_0	-17.06	7.98	-2.14	0.0348	0.69	—
		b_1	0.43	0.06	6.93	< 0.0001		1.70
		b_3	13.07	4.59	2.84	0.0053		1.00
		b_4	0.65	0.10	6.22	< 0.0001		1.70

[a] Check for no collinearity: VIF should be < $[1/(1 - R^2)]$.
χ = underlying layer measurement.

An attempt was made as part of this study to relate roller MVs to laboratory-determined M_r. Laboratory M_r tests were conducted on "undisturbed" Shelby tube (ST) samples and reconstituted specimens. One confining and deviator stress combination was selected to correlate M_r with roller MVs. For undisturbed ST samples, M_r values at the selected stress condition were directly correlated with roller MVs at the sample location using simple linear regression analysis. For reconstituted laboratory samples, w-γ_d-M_r relationships were developed through multiple regression analysis, and the relationships were used to predict field M_r values from in situ w-γ_d point measurements. The predicted M_r values were then empirically correlated to MVs. Further, the influence of vibration amplitude and underlying layer support conditions on compaction layer MVs were statistically assessed through multiple regression analysis. Laboratory and in situ test results and analysis from TB MN10 are presented below, followed by a summary of results for other test beds.

6.4.1 TB MN10 Nongranular Subgrade

6.4.1.1 Site and Material Conditions

This test bed was constructed by placing a nominal 425.0-mm (16.7-in)-thick layer of nongranular subgrade material (CL according to the USCS soil classification system). DCP tests indicated that the layer below the compaction layer was relatively homogenous with CBR = 14 to 18. Maximum dry unit weight and optimum moisture content as determined by the standard Proctor method were 16.95 kN/m^3 (108.10 lb/ft^3) and 16.4%, respectively. The test bed had plan dimensions of about 2.4 m × 86.0 m. The material was moisture conditioned by dividing the test bed into three sections to approximately -3%, 0%, and +3% of standard Proctor w_{opt} and mixed using a reclaimer. Compaction passes were performed using a Bomag BW213-DH pad foot roller.

6.4.1.2 Laboratory Testing

To develop w-γ_d-M_r relationships for the subgrade material, laboratory M_r tests were performed on reconstituted laboratory-compacted specimens. Tests were conducted in general accordance with AASHTO T-307 standard procedure for Type 2 subgrade materials on 10 samples prepared at a selected range of w and γ_d values. Samples were compacted using the static compaction method. Test procedure and details regarding the resilient modulus test device are described in Appendix A. Average M_r was calculated for each confining and deviator stress condition based on data from the last five cycles of a loading sequence. The test results were analyzed to fit the "universal" model proposed by Witczak and Uzan (1988) shown in Equation 6.4.

$$M_r = k_1 P_a \left(\frac{\theta}{P_a}\right)^{k_2} \left(\frac{\sigma_d}{P_a}\right)^{k_3} \quad (6.4)$$

where M_r = resilient modulus; k_1, k_2, and k_3 = regression coefficients, typically with $k_1 > 0$, $k_2 \geq 0$, and $k_3 \leq 0$; θ = sum of principal stresses ($\sigma_1 + \sigma_2 + \sigma_3$); P_a = atmospheric pressure, same units as M_r and θ; and σ_d = deviator stress, same units as M_r and θ.

Results showing the effect of confining and deviator stresses on resilient modulus for four samples prepared at different w and γ_d are presented in Figure 6.15. Results show two commonly observed effects on fine-grained cohesive soils: (1) increasing w decreases M_r and (2) increasing deviator stress decreases M_r. Some differences with respect to these typical behaviors were observed in the results. For samples prepared dry of optimum (w_{opt} –7.5%), confining stress affects the M_r values more than deviator stress. Increasing confining stress tends to increase M_r (up to about 1.5 times), whereas increasing deviator stress did not show a significant change in M_r. On the other hand, as the moisture content increases (w_{opt} + 2%), the confining stress only slightly affected M_r while increasing deviator stress caused a decrease in M_r (up to about two times).

A summary of model coefficients (for Equation 6.4) for the different samples is provided in Table 6.9. The S5 and M5 samples with $w > 20\%$ experienced plastic strain ε_p greater than 5% after the fifth sequence (note that S group represent samples compacted to target standard Proctor, and M group represent samples compacted to target modified Proctor w-γ_d values), and therefore the model coefficients were not calculated (AASHTO T-307 requires the test be terminated when a sample reaches $\varepsilon_p > 5\%$). The k_3 values shown in Table 6.9 on samples compacted to standard Proctor densities (S series) show that k_3 decreased from about -0.24 to -0.60 with increasing w from w_{opt} –7.5% to w_{opt} + 6.5%. The smaller the k_3 value, the greater the influence of deviator stress, which

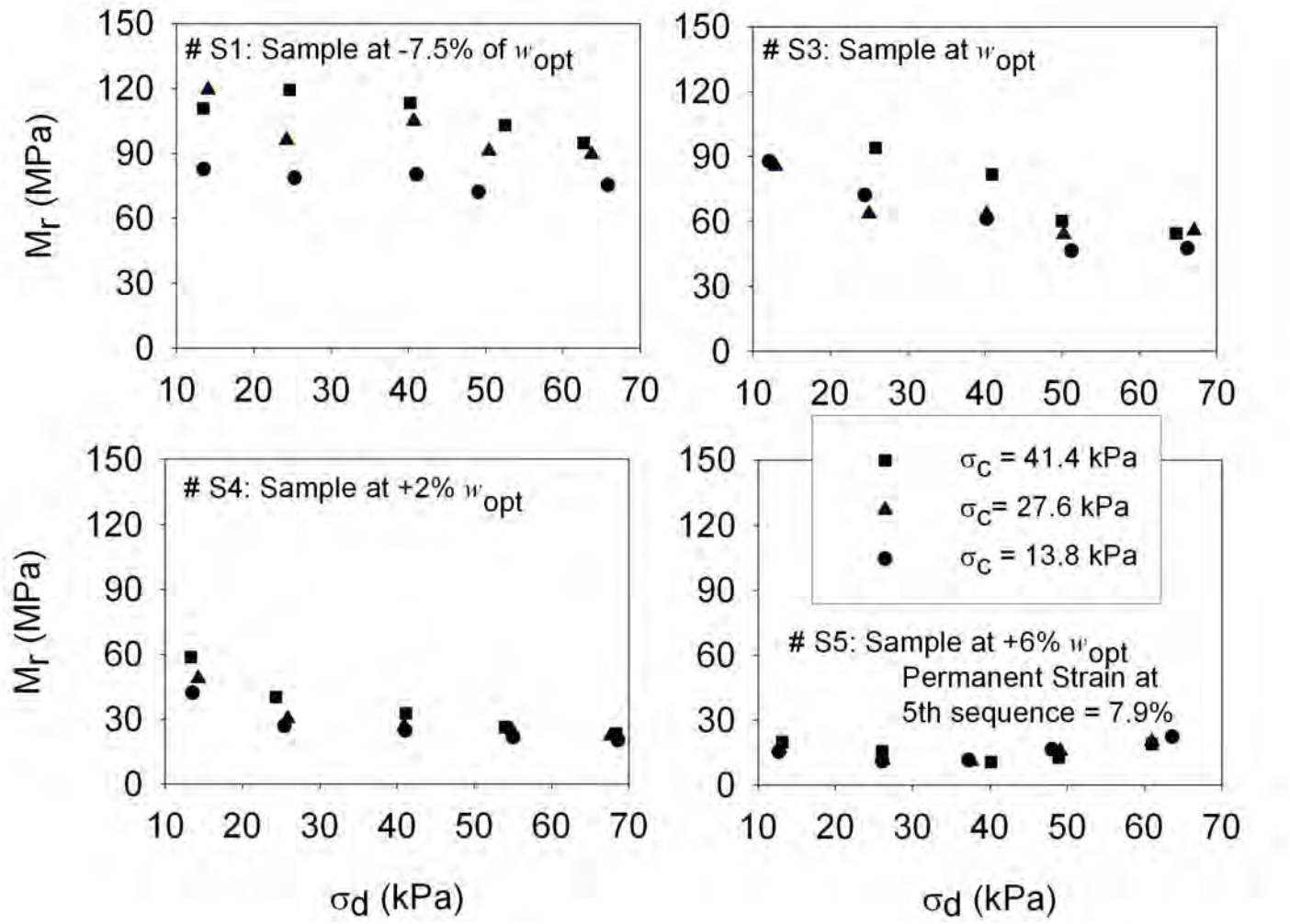

Figure 6.15. Effect of σ_c and σ_d on compacted TB MN10 subgrade material at different target w-γ_d.

Table 6.9. Summary of M_r model coefficients.

Sample ID	Dry Unit Weight (kN/m³)	Moisture Content (%)	Model Coefficients[a]		
			k_1	k_2	k_3
S1	16.1	8.9	675.4	0.45	-0.24
S2	16.8	11.9	706.7	0.00	-0.14
S3	17.4	16.2	431.5	0.17	-0.34
S4	16.8	18.5	149.6	0.35	-0.60
S5	15.7	22	—[b]	—[b]	—[b]
M1	16.9	8.8	969.6	0.13	-0.11
M2	19.3	11.1	1,755.9	0.17	0.08
M3	18.3	13.6	952.6	-0.01	-0.04
M4	16.7	18	159.8	0.43	-0.50
M5	15.7	20.8	—[b]	—[b]	—[b]

[a]Witczak & Uzan (1988) model.
[b]Samples with permanent strain >5%.

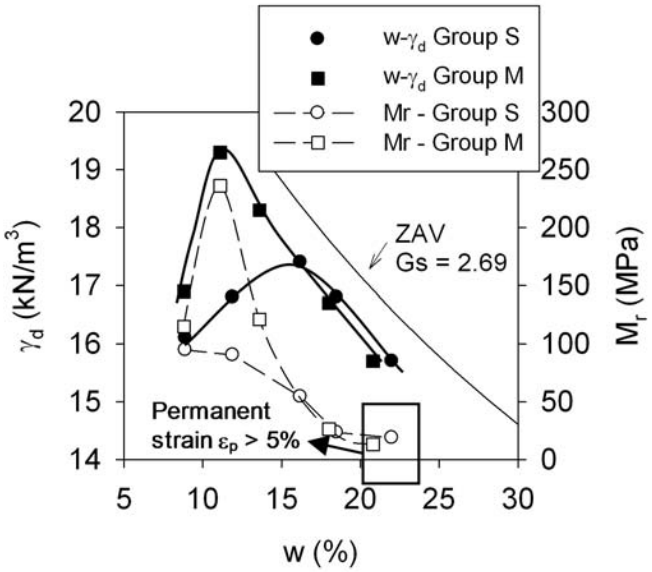

Figure 6.16. Relationship between w-γ_d and M_r at σ_d = 68.9 kPa and σ_c = 41.4 kPa.

illustrates that the influence of deviator stress increases with increasing w for these samples. k_3 values generally increased with increasing density. The samples compacted to target standard Proctor densities exhibited consistently lower k_3 values compared to samples compacted to target modified Proctor densities. One sample (M3) yielded $k_3 > 0$, which suggests an increase in M_r with increasing deviator stress. This behavior is common for granular materials but is not typical for fine-grained soils (Andrei et al. 2004).

Near surface ($z < 0.5$ m) in situ deviator stresses under 11- to 15-ton vibratory roller compactors are considerably higher than the axial stresses applied in the laboratory M_r test, whereas confining stresses are less (see Rinehart et al. 2009 and Chapter 4). To compare laboratory M_r values with roller MVs, the maximum applied cyclic deviator stress and the confining stress condition of 68.9 kPa (10 psi) and 41.4 kPa (6 psi) from the M_r test (following AASHTO T-307) were selected. Figure 6.16 shows the effect of w and γ_d on M_r for the subgrade material. Samples that produced $\varepsilon_p > 5\%$ before reaching the selected stress condition [σ_d = 68.9 kPa (10 psi) and σ_c = 41.4 kPa (6 psi)] are highlighted in Figure 6.16.

Multiple regression analysis was performed to predict M_r (at the selected stress condition) as a function of w and γ_d. The two samples with $\varepsilon_p > 5\%$ were not included in the regression analysis. The resulting multiple regression model from the analysis is presented in Equation 6.5, where b_0 = -593.33, b_1 = -10.86, and b_2 = 48.23 (for σ_d = 68.9 kPa and σ_c = 41.4 kPa), and shows strong correlations with $R^2_{adj} = 0.96$. The regression coefficients for w (b_1) and γ_d (b_2) were negative and positive, respectively, indicating that increasing moisture decreases M_r and increasing density increases M_r.

$$M_r\,(\text{MPa}) = b_0 + b_1 w + b_2\,\gamma_d \qquad (6.5)$$

6.4.1.3 In Situ Testing and Relationship Between Roller MV and M_r

After the material was carefully moisture conditioned, the test bed was compacted using the Bomag vibratory pad foot roller with eight roller passes at constant operation settings with nominal A = 0.70 mm (0.028 in), f = 30 Hz, and v = 4.0 km/h (2.5 mph). In situ w-γ_d point measurements were obtained on the compaction layer at 15 test locations (five locations in each moisture section) along the test bed. Point measurements were obtained after 1, 2, 4, and 8 roller passes.

Figure 6.17 shows w-γ_d point measurements in comparison with MVs (E_{vib}) shown as solid lines. Note the conclusion in Chapter 3 that vibration-based MVs for pad foot rollers are not repeatable and should therefore not be used in practice without consideration of statistical averaging. Their use here is for illustration only. Results show that E_{vib} measurements were spatially variable but generally increased from pass 1 to pass 2 and that in situ point measurement values increased with increasing passes. The multiple regression relationship developed for laboratory samples (Equation 6.5) was used to predict M_r values for the in situ w-γ_d point measurements. Since Equation 6.5 is valid only for the range of w-γ_d of the laboratory samples, the in situ point measurements only close to the laboratory sample values were selected for M_r prediction. Comparison of the predicted M_r and E_{vib} for the selected data is presented in Figure 6.18, which showed an acceptable correlation with $R^2 = 0.52$.

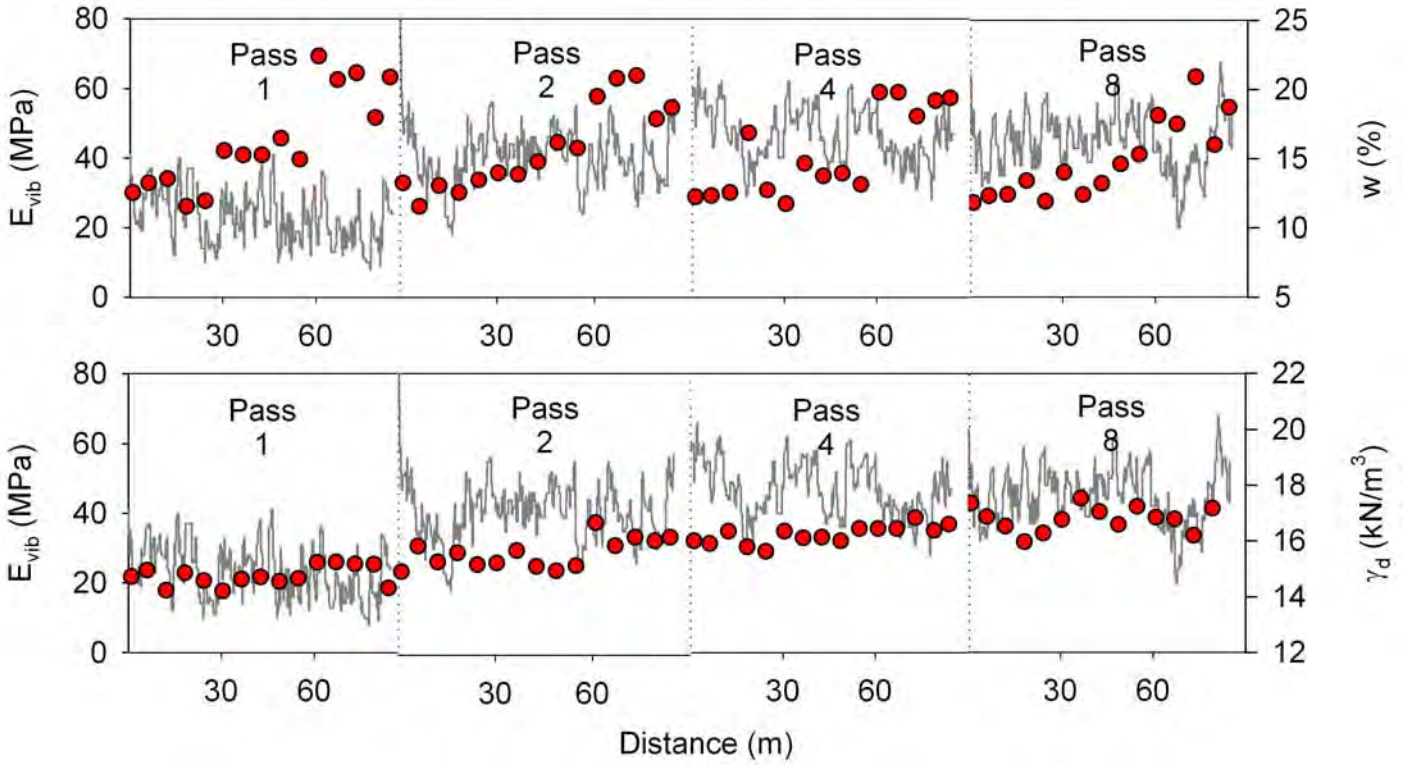

Figure 6.17. Comparison of E_{vib} and in situ compaction measurements.

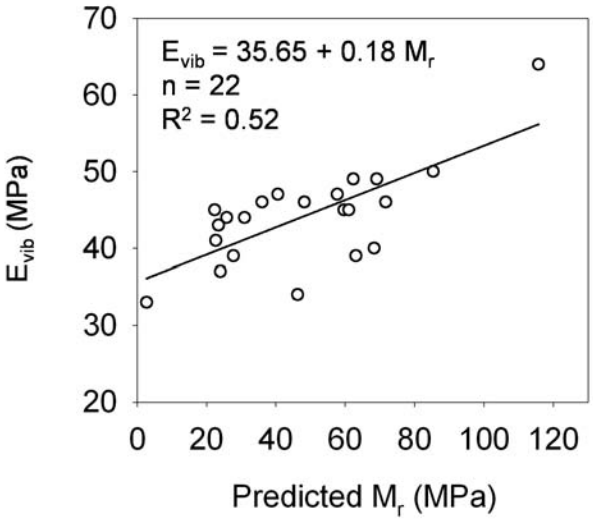

Figure 6.18. Simple linear regression relationship between roller MV and predicted M_r.

6.4.2 Summary of Relationships Between Roller MVs and M_r

6.4.2.1 Simple Linear Regression Relationships Between Roller MVs and M_r

A summary of laboratory determined w-γ_d-M_r multiple regression relationships for reconstituted and laboratory compacted nongranular subgrade, granular subgrade, and granular base materials is presented in Table 6.10. Shelby tube samples were obtained from a compacted nongranular subgrade layer for one test bed (CO3). w-γ_d-M_r relationships were developed only on materials with $n \geq 8$ (following a general rule of thumb of a minimum four measurements per each variable). With the exception of FL23, all other materials showed good correlations with R^2_{adj} = 0.6 to 1.0. M_r test results along with the universal model coefficients k_1, k_2, and k_3 (see Equation 6.4) are presented in Appendix A.

Simple linear regression relationships between predicted M_r values at the selected stress condition for reconstituted samples (using the approach described in the example above) and roller MVs are presented in Table 6.11. The relationships produced R^2 values of 0.0 to 0.6, with the majority at $R^2 <$ 0.5. Similar to the effect of underlying layer heterogeneity observed on simple linear regression relationships between

Table 6.10. Moisture–dry unit weight–M_r relationships.

Material	TB	USCS (AASHTO)	n	b_0	b_1	b_2	R^2_{adj}
Model: M_r [a] $= b_0 + b_1 w + b_2 \gamma_d$							
Nongranular subgrade	MN10, 11	CL (A-6(5))	8	-593.33	-10.86	48.23	0.95
	CO3[b]	CL (A-6(7))	6	*limited number of samples*			
Granular subgrade	MD2, 3, 4, 5	SM (A-2-4)	9	124.10	-7.56	0.03	0.83
	FL23	SP-SM (A-3)	13		NS		–
	NC2	SM (A-2-4)	16	-28.48	-1.17	4.12	0.94
Granular base	CO17, 18	SP-SM (A-1-a)	9	-248.29	-5.14	20.95	0.62
	MD2, 3, 4, 5	SM (A-2-4)	9	124.10	-7.56	0.03	0.83
	MD6, 7, 8, 9, 11, 12, 13, 14	SP-SM (A-1-a)	10	-426.37	-30.09	32.19	0.57
	FL19	SM (A-1-b)	5	*limited number of samples*			
	NC4	SP-SM (A-1-a)	14	-512.01	-7.05	32.85	0.59

[a] For σ_d = 68.9 kPa and σ_c = 41.4 kPa.
[b] Shelby tube samples.

γ_d point measurements and roller MVs, the relationships presented here to M_r are also affected. This is expected as the predicted M_r values are based on the measured w-γ_d point measurements. Multiple regression analysis was performed to further characterize the influence of underlying layers and amplitude in the following section. Further, relationships in Table 6.11 are presented separately for different nominal amplitude settings.

6.4.2.2 Influence of Amplitude and Underlying Layer Support Conditions

Multiple regression analysis was performed to assess the influence of amplitude and underlying layer support conditions on compaction layer MVs, using the multiple linear regression model shown in Equation 6.2. Results from the analysis are summarized in Table 6.12, which shows that including underlying layer MVs in the regression model produced improved correlations (e.g., R^2_{adj} values for CO17 and CO18 from < 0.2 to > 0.5). For some cases, when underlying layer properties are included in the multiple regression model, the compaction layer point measurements were not statistically significant in the analysis (e.g., TBs MD6, 7, 8, 9). A similar finding was noted above in multiple regression analysis with in situ point measurements and is possible when MVs are more influenced by the underlying layer properties than the compaction layer properties.

6.4.2.3 Discussion

Despite the challenges involved in relating field to laboratory measurements, encouraging results were observed for some test beds. Results indicated that good correlations (with R^2 or $R^2_{adj} > 0.5$) are possible for test beds with relatively stiff/homogeneous conditions below the compaction layer (e.g., MN10/11). Underlying layer variability contributed to poor correlations. Improved correlations are observed by factoring in the underling layer properties (using roller MVs on the underlying layer) through multiple regression analysis for some test beds. This observation is in line with findings for correlations between MVs and other in situ point measurements described earlier.

6.5 Summary and Conclusions

Results obtained from evaluation of five roller-integrated compaction measurements (i.e., MDP, CMV_D, E_{vib}, k_s, CCV) and 17 different soils were presented in this chapter. Relationships between roller MVs and a variety of in situ point measurements and laboratory-determined M_r measurements via simple and multiple linear regression analysis were described. Results from a few select test beds were presented to highlight different aspects of the analysis and challenges involved in interpretation of the results.

Results indicated that roller MV correlations are possible to in situ point measurements of dry unit weight, modulus via various devices, and CBR with simple linear regression analysis on test beds with homogeneous and relatively stiff underlying layer support conditions and MVs obtained under constant operation settings. Several factors can affect the quality of the regression relationship, including heterogeneous conditions in the underlying layers. Variability across the drum width also affected the correlations. Averaging point measurements across the drum width improved the correlations.

Table 6.11. Simple linear regression relationships between roller MVs and M_r.

Material	TB	MV	*A* (mm)	n	b_0	b_1	R^2
Model: $MV = b_0 + b_1 M_r$							
Nongranular subgrade	MN10[a]	E_{vib}	0.70	22	35.65	0.18	0.52
	MN11[a]	MDP	0.80	22	6.47	-0.05	0.58
	CO3[b]	CMV_D	0.80	6	3.73	0.07	0.43[c]
Granular subgrade	MD2,3, 4, 5[a]	CMV_D	0.50	28	NS		—[c]
Granular base	CO17[a]	E_{vib}	0.70	33	-67.33	1.05	0.16[d]
			1.90	11	56.5	0.47	0.17[d]
	CO18[a]	CMV_D	0.90	33	-21.04	0.32	0.34
			2.10	11	-16.90	0.37	0.46[d]
	MD6, 7, 8, 9[a]	CCV	0.92	81	NS		—[d]
			2.19	18	NS		—[d]
		CMV_D	0.90	80	NS		—[d]
			2.10	37	NS		—[d]
		E_{vib}	0.70	70	NS		—[d]
			1.90	14	NS		—[d]
	MD11, 12, 13, 14[a]	CCV	0.92	20	NS		—[d]
			2.19	32	NS		—[d]
		CMV_D	0.90	42	-21.33	0.26	0.19[d]
			2.10	26	-27.13	0.34	0.16[d]
		E_{vib}	0.70	40	-52.14	0.72	0.29[d]
			1.90	42	-133.05	1.37	0.22[d]
	NC4[a]	E_{vib}	0.70–1.10	35	-41.63	0.72	0.41[d]
	NC4[a]	k_s	0.80	35	NS		—[d]

[a] M_r predicted from laboratory w-γ_d-M_r relationship; see Table 6.10.
[b] M_r of ST samples (σ_d = 68.9 kPa; σ_c = 41.4 kPa).
[c] Narrow range of measurements and heterogeneous underlying layer.
[d] Heterogeneous underlying layer.

Table 6.12. Multiple linear regression relationships between roller MV and laboratory M_r—granular base materials.

TB	Model	*n*	b_0	b_1	b_3	b_4	R^2_{adj}
CO17	$E_{vib} = b_0 + b_1 M_r^{\ a} + b_3 A + b_4 E_{vib}^{\ \chi}$	44	-98.78	0.85	30.15	0.54	0.52
CO18	$CMV_D = b_0 + b_1 M_r^{\ a} + b_3 A + b_4 CMV^{\chi}$	44	-24.63	0.23	0.50	8.17	0.75
[c]MD6, 7, 8, 9	$CCV = b_0 + b_3 A + b_4 CCV^{\chi}$	168	-11.04	—[b]	12.58	0.92	0.41
	$CMV = b_0 + b_3 A + b_4 CMV^{\chi}$	274	-10.63	—[b]	5.77	4.95	0.59
	$E_{vib} = b_0 + b_3 A + b_4 E_{vib}^{\ \chi}$	216	4.58	—[b]	37.03	0.75	0.34
[c]MD11, 12, 13, 14	$CCV = b_0 + b_3 A + b_4 CCV^{\chi}$	75	29.27	—[b]	13.42	3.20	0.49
	$CMV = b_0 + b_1 M_r^{\ a} + b_3 A + b_4 CMV^{\chi}$	68	-13.94	0.11	4.05	0.73	0.79
	$E_{vib} = b_0 + b_1 M_r^{\ a} + b_3 A + b_4 E_{vib}^{\ \chi}$	76	-49.51	0.37	3.22	1.07	0.75

[a] M_r predicted from laboratory w-γ_d- M_r relationship, see Table 6.11.
[b] M_r not statistically significant based on $p < 0.10$ and $t < -2$ or $>+2$.
[c] Ignored data with BV > 10 for CMV_D and jump = 2 for E_{vib}.
χ = underlying layer measurement.

For a few cases, including soil moisture content in multiple regression analysis improved the regression relationships. Variations in machine vibration amplitude and frequency were also found to influence the regression relationships. Results from some test beds indicated that, although amplitude was statistically significant in multiple regression analysis, the quality of regression relationships was not (as identified as reduction in R^2_{adj} values). This emphasizes the importance of constant machine operation settings during correlation and calibration studies. A multiple regression model with amplitude and frequency as dependent variables was successful for a few test beds. This suggests the potential for analyzing IC measurements (obtained in AFC mode), although this topic warrants further research. Multiple regression analysis on in situ modulus data and roller MVs obtained from multiple sites and test beds produced good correlations when amplitude and underlying layer measurements are incorporated in the analysis.

An approach to empirically relate laboratory-determined M_r for a select stress condition and roller MVs was presented. The M_r values were predicted for in situ w-γ_d point measurements using a w-γ_d-M_r relationship developed from laboratory testing. Similar to other in situ point measurements, the relationships were possible for compaction layer material underlain by homogeneous and relatively stiff support conditions. Heterogeneous supporting layer conditions affected these relationships, and the relationships improved by including parameter values that represent the underlying layer conditions through multiple regression analysis.

CHAPTER 7

Quality Assurance of Pavement Earthwork Using Roller-Integrated Continuous Compaction Control (Recommended Specification Options)

This chapter presents recommended specification options for QA of subgrade, subbase, and aggregate base course compaction using roller-integrated CCC. Six viable QA options are proposed to accommodate the diverse site conditions and agency needs observed across the United States. Many of the recommended options were inspired by current European specifications (summarized in Chapter 2). Additional recommended options stem from the research findings presented in this report. The proposed specifications are technically end product based with required methodological aspects. Traditional method-based approaches (e.g., recording the number of roller passes) do not utilize the roller measurement values (MVs) per se and are therefore not addressed by this specification. None of the recommended options constitute performance-based specifications. Further research is required to implement, for example, the findings from Chapter 4 into viable performance-based specifications that can be efficiently implemented in practice. Each option can be adopted as the sole method for QA. Alternatively, two or more options can be combined to increase reliability. Uniformity criteria are discussed in Section 7.9 and can be added to any option.

The remainder of Chapter 7 is presented in the form of a specification and can be treated as a stand-alone document. The proposed specification provides a discussion on appropriate applications for the recommended options; defines important CCC-related terms; provides recommendations for roller measurement system requirements, including procedures to assess the validity of roller MVs; and concisely presents several important issues related to roller-integrated measurement. Chapter 8 presents several case studies illustrating how the various options are implemented and highlights the level and extent of analysis required.

CONTENTS

7.1 Scope

This specification covers the QA of subgrade, subbase, and aggregate base course compaction using roller-integrated CCC. The six recommended QA specification options are summarized in Table 7.1 and Figure 7.1. Options are numbered 1, 2a, 2b, 3a, 3b, and 3c and are distinguished by three principal categories. In Option 1, CCC is used to assist in QA and acceptance is based on spot-test measurements. Option 2a and 2b acceptance is based on roller MVs, though initial calibration of roller MV to spot-test measurements is not required. Option 3a, 3b, and 3c acceptance is based on roller MVs and requires initial calibration to determine an MV-TV. Each option can be adopted as the sole method for QA; alternatively, two or more options can be combined to increase reliability. Uniformity criteria discussed in Section 7.9 can be added to any option. Method-based approaches (e.g., using GPS positioning and documentation to record the number of passes) do not utilize roller-based MVs and are therefore not addressed by this specification. However, the implementation of such an approach is straightforward.

7.2 Definitions

Automatic Feedback Control: automatic adjustment of roller *Operating Parameters* such as vibration frequency and amplitude based on real-time feedback from measurement system.

Calibration Area: an area representative of an *Evaluation Section* but typically smaller and used to establish an MV-TV.

Compaction Pass: a static or vibratory roller pass performed during earthwork compaction, not necessarily employing an *Instrumented Roller*.

Continuous Compaction Control (CCC): continuous monitoring and documentation of earthwork compaction using an *Instrumented Roller*.

Evaluation Section: an area of earthwork with consistent properties where acceptance is evaluated.

Instrumented Roller: a roller compactor outfitted with drum vibration instrumentation or other means to compute a *Roller Measurement Value*, onboard computer, and position monitoring equipment.

Table 7.1. Summary of specification options.

Roller-Integrated CCC QA Option	Target Measurement Value (MV-TV)	Acceptance Criteria
Option1: Spot testing of roller-informed weakest area(s)	Not required	Spot-test measurements in roller-identified weakest area(s) satisfy contract spot-test measurement requirements (QA-TV)
Option 2a: Monitoring percentage change in mean MV	Not required	Achieving ≤ 5% change in mean MV between consecutive roller passes
Option 2b: Monitoring spatial percentage change (%Δ) in MVs	Not required	Achieving the %Δ-TV between consecutive passes over a defined percentage of an evaluation section
Option 3a: Empirically relating MVs to spot-test measurements	Based on correlation of MV to spot test measurement: MV-TV = MV corresponding to contract QA-TV[a]	Achieving MV-TV over a set percentage of an evaluation section
Option 3b: Compaction curve based on MVs	MV-TV = mean MV when the increase in pass-to-pass mean MV in a calibration area ≤ 5%	
Option 3c: Empirically relating MVs to lab-determined properties (e.g., M_r)	Based on correlation of MV to lab soil property: MV-TV = MV corresponding to contract QA-TV[b]	

[a] Assumption is that QA-TV is spot-test-based measurement of density, modulus, etc.
[b] For example, a QA-TV based on M_r.

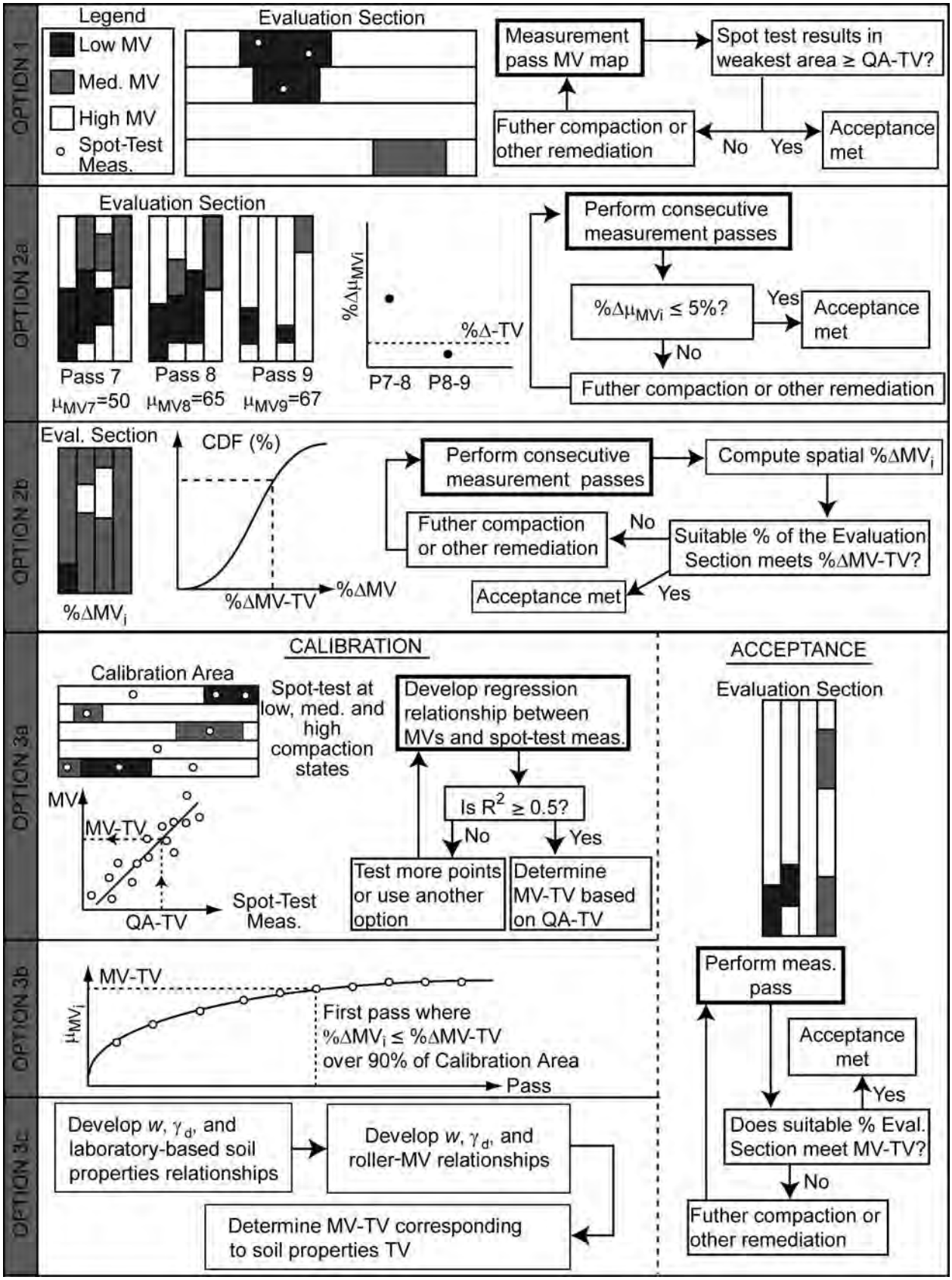

Figure 7.1. Summary of CCC specification options.

Intelligent Compaction: the combined use of an *Instrumented Roller* and *Automatic Feedback Control* in an attempt to improve earthwork compaction.

Layer: a component of the pavement earthwork with distinct soil properties (e.g., subgrade, subbase, or base course).

Lift: a unit of material within a *Layer* that is deposited at one time for compaction. A *Layer* may be comprised of a single lift or multiple lifts.

Measurement Depth: the soil depth to which *Roller Measurement Values* or *Spot-Test Measurements* are representative.

Measurement Pass: a pass performed by an *Instrumented Roller* during which all required information, including *Roller Measurement Values* and machine position, are recorded. Roller *Operating Parameters* must be held constant, and thus no *Automatic Feedback Control* is permitted during a *Measurement Pass.*

MV Reporting Rate: the time-dependent rate at which new *Roller Measurement Values* are reported.

MV-TV: a target *Roller Measurement Value* (e.g., the measurement value corresponding to a *QA-TV*).

Operating Parameters: roller machine parameters used during operation, including forward speed, driving direction, vibration frequency, and eccentric force amplitude.

Pass Sequence: a record of the roller pass history (pass number, *Operating Parameters*) over a specified area.

Quality Assurance (QA): evaluation methods and procedures administered by the owner or owner's representative to ensure that the constructed earthwork meets contract obligations.

QA-TV: the spot-test measurement–based QA target value specified in the project contract.

Quality Control (QC): testing performed by the contractor or contractor's representative to ensure that the constructed earthwork meets contract obligations.

Roller Measurement Value (MV): the roller-based parameter used for assessment of soil stiffness during compaction and based on roller vibration measurements.

Rolling Pattern: the path traversed by the roller during a *Measurement Pass.*

Spot-Test Measurement: a field test used during earthwork QC and QA that provides a measurement at a discrete location; common examples include the nuclear gauge for density and moisture and the lightweight deflectometer.

7.3 Notation

The following symbols are used throughout this specification:

A	theoretical vertical drum vibration amplitude
f	excitation frequency of eccentric mass within drum
M_r	resilient modulus (e.g., per AASHTO T-307)
MV_i	spatial *Roller MV* data from pass *i*. This is an array of data.
μ_{MV_i}	mean of spatial *Roller MV* data from pass *i*
σ_{MV_i}	standard deviation of spatial *Roller MV* data from pass *i*
$\%\Delta$	percent difference
$\%\Delta\mu_{MV_i}$	percent difference of the mean of spatial *Roller MV* data from pass $i-1$ to pass *i* (for Option 2a)
$\%\Delta MV_i$	spatial percent difference in *Roller MV* data from pass $i-1$ to pass *i*. This is an array of values.
$\mu_{\%\Delta MV_i}$	mean of spatial percent difference in *Roller MV* data from pass $i-1$ to pass *i*
$\sigma_{\%\Delta MV_i}$	standard deviation of spatial percent difference in *Roller MV* data from pass $i-1$ to pass *i*
v	forward travel velocity of roller
w_{opt}	optimum moisture content (e.g., from standard or modified Proctor density testing)

7.4 Important Considerations

7.4.1 Applicable Soil Types

This specification is applicable to cohesive and cohesionless soils and aggregate base materials. Research has shown that current *Roller MVs* are less reliable on cohesive soils and that particular attention must be given to soil moisture content.

7.4.2 Personnel Requirements

The implementation of roller-integrated CCC for earthwork QA requires knowledgeable field personnel. A certification process is highly recommended. QA personnel must be familiar with the aspects of CCC and IC described in the previous chapters of this report and with the CCC and IC equipment on the job site. QA personnel must be able to verify the proper working condition of an *Instrumented Roller*, identify appropriate *Evaluation Sections* and *Calibration Areas*, and conduct calibration if Option 3 is pursued. QA personnel must understand how to direct *Measurement Passes* and evaluate *Measurement Pass* data in a timely and reliable manner. To this end, QA personnel must direct the roller operator regarding required *Operational Parameters* and *Measurement Pass* procedures.

7.4.3 Roller MV Dependence on Operating Parameters

Current *Roller MVs* depend on machine *Operating Parameters* such as theoretical vertical drum vibration amplitude *A*, excitation frequency *f*, forward velocity *v*, and travel

orientation (e.g., forward, reverse). The nature of the *Roller MV* dependency on each *Operating Parameter* is soil, stratigraphy, and roller dependent and can vary considerably. As a result, machine *Operating Parameters*, including *A*, *f*, and *v*, must remain constant during a *Measurement Pass*. To this end, *Automatic Feedback Control* should not be used during a *Measurement Pass*. Variations in roller *Operating Parameters* should remain within the following tolerances: ±2 Hz for *f*, ±0.2 mm (0.0008 in) for *A*, and ±0.5 km/h (0.3 mph) for *v*. Manufacturer-recommended amplitudes should be used if provided. Otherwise, theoretical amplitudes *A* between 0.7 and 1.1 mm are recommended for *Measurement Passes*. Typical vibration frequencies range from 28 to 32 Hz. Typical roller speeds range from 3.0 to 5.5 km/h (1.9 to 3.4 mph). Once decided on, these *Operating Parameters* should remain constant for all *Measurement Passes* within an *Evaluation Section*. *Roller MVs* collected during startup, stopping, and turning typically violate these tolerances and should not be used for QA.

7.4.4 Roller MV Dependence on Driving Direction

Current roller-integrated vibration-based measurement systems include sensors on one side of the drum, resulting in MVs that are more representative of soil on the instrumented side of the drum. Accordingly, MVs can exhibit a strong dependence on driving direction in areas where material properties are heterogeneous. In extreme cases, MVs can vary by as much as 100% when the roller is driven over the same track in opposite directions. Therefore, care must be taken to ensure that the same *Rolling Pattern* is used for all *Measurement Passes* as well as any *Compaction Passes* used for QA.

7.4.5 Measurement Depth

Current roller-integrated vibration-based measurement systems for 11- to 15-ton vibratory roller compactors provide a composite measure of soil stiffness to depths of 0.8 to 1.2 m (2.6 to 3.9 ft) and three to four times deeper than typical 0.2 to 0.3 m (8 to 12 in) *Lifts* of subgrade, subbase, or base material. An increase in theoretical amplitude slightly increases the *Measurement Depth*. Typical spot-test measurements such as the nuclear density gauge and light weight deflectometer (LWD) typically reflect the properties of the 0.2- to 0.3-m (8- to 12-in)-placed *Lift* of soil, whereas *Roller MVs* reflect the properties of multiple *Lifts*. Consequently, sublift soil properties are reflected in *Roller MVs* much more significantly than in spot-test measurements. Therefore, CCC options that rely on obtaining correlations between *Roller MVs* and spot-test results are increasingly difficult to implement if the sublift conditions are variable. Further, as the sublift properties change, so too will the *Roller MV* and spot-test measurement correlations, even if the *Lift* material is the same.

7.4.6 Evaluation Section

Acceptance testing for all specification options is performed on *Evaluation Section*s. An *Evaluation Section* is an area of production earthwork that exhibits homogeneity, or consistently distributed heterogeneity, both in the longitudinal and transverse directions, as evidenced by the *Roller MV* map. An *Evaluation Section* is commonly the full width of the earthwork section by a length that varies depending on the pace of construction, longitudinal heterogeneity, and other factors (e.g., schedule). Typical lengths can vary from 100 to 500 m (330 to 1,640 ft). A number of factors can contribute to heterogeneity and thus the sizing of *Evaluation Section*s. A change in borrow material or a transition from a cut to a fill section may induce a distinct change in *Roller MV*, particularly in the longitudinal direction. In the transverse direction, edge material or shoulders can sometimes exhibit markedly different stiffness behavior. Figure 7.2 provides examples of appropriate and inappropriate *Evaluation Sections*.

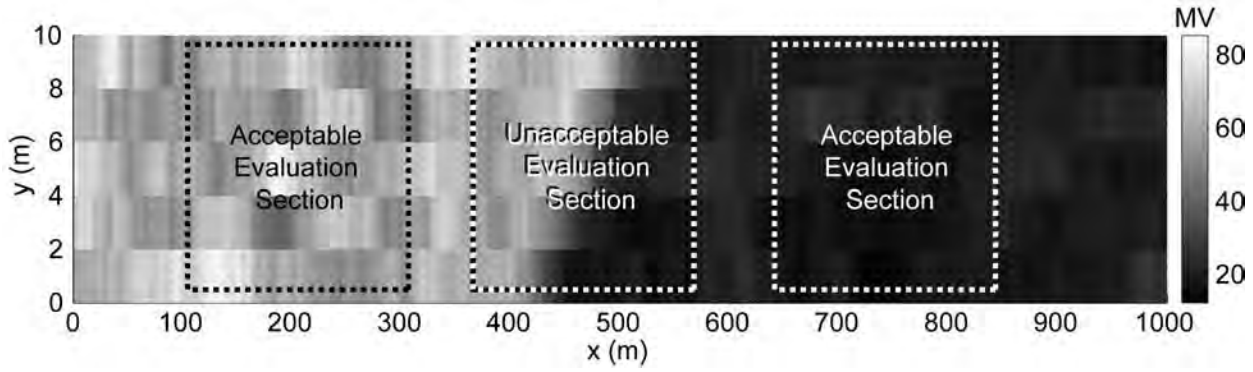

Figure 7.2. Acceptable and unacceptable evaluation sections based on roller MV data map.

7.4.7 Calibration Area

Option 3 requires the establishment of an MV-TV prior to acceptance testing in an *Evaluation Section*. If possible, a portion of the *Evaluation Section* should be used as the *Calibration Area*. A *Calibration Area* can range in size from a single roller width by 30 m (100 ft) long to the full width of the pavement earthwork section [10 to 30 m (33 to 100 ft)] by 100 m (330 ft) long. The underlying or sublift conditions of the *Calibration Area* must be representative of the *Evaluation Section* for which the MV-TV will be used. For this reason, larger *Calibration Areas* are preferred [e.g., full width of *Evaluation Section* by 100 m (330 ft) long]. Smaller *Calibration Areas* may be suitable for homogeneous site conditions. A *Roller MV* map of the sublift material or of the first roller pass of the *Evaluation Section* is helpful in selecting a *Calibration Area*. As a general guideline, the *Calibration Area* should capture 50% to 75% of the variation observed in the *Evaluation Section*. The *Calibration Area* material *Lift* should be constructed in the same manner as the *Evaluation Section*. Material type, material placement procedures, moisture conditioning, and *Lift* thickness all influence *Roller MVs* and should be consistent between the *Calibration Area* and the *Evaluation Section*.

It is important to consider the effects of edge lanes and other special features (e.g., shallow pipe crossings) that may exist in varying concentrations within the *Calibration Area* and the *Evaluation Section*. *Roller MVs* are influenced by the presence or absence of lateral confinement (e.g., an edge lane often only has lateral confinement on one side). Data from edge lanes or from other areas with special features should be used judiciously when developing correlations. If these features are predominant in some *Evaluation Sections*, QA personnel should consider developing separate correlations for these sections or using another option.

Recalibration is required if *Evaluation Section* conditions are sufficiently different from the *Calibration Area*. The appropriateness of a correlation should be periodically verified by comparing roller MV and spot-test measurements from the *Evaluation Section* to the correlation developed in the *Calibration Area*.

7.5 Instrumented Roller Requirements

An *Instrumented Roller* must meet minimum requirements regarding *Roller MV* reliability, documentation, and *Roller MV* and position reporting. In addition, QA personnel should verify that the selected roller is capable of producing the required level(s) of compaction in a reasonable amount of time.

7.5.1 Roller MV and Position Reporting

Roller MVs should be reported with a constant spatial resolution within the acceptable range of 0.2 to 1.0 m (8 to 40 in). All reported *Roller MVs* should be unique measurements (i.e., repeat *Roller MVs* should not be reported). To ensure full coverage of earth material properties, each *Roller MV* should reflect a spatial average over a distance not less than the *Roller MV* reporting resolution. Each reported *Roller MV* should be accompanied by a three-dimensional position (e.g., northing, easting, elevation, determined via roller-mounted GPS). RTK differential GPS is highly recommended. Each reported position should reflect the geometric center of the earthwork over which the corresponding *Roller MV* was determined.

7.5.2 Documentation

The *Instrumented Roller* must clearly document the following parameters:

- *Roller MV*
- Three-dimensional position (including time stamp and GPS quality)
- Vibration amplitude (theoretical A or actual z_d)
- Vibration frequency, f
- Travel speed, v
- Forward/reverse driving direction
- Automatic feedback control on/off
- Indication of jumping
- Vibration on/off
- *Pass Sequence*

These recorded data must be easily accessible via the *Instrumented Roller's* onboard computer, and units should be clearly documented (standard SI or English units are acceptable). In addition, these data should be easily exportable for postprocessing and record keeping. Simple text files are preferred, and files in a proprietary format (e.g., only compatible with the roller manufacturer's software) are not acceptable.

Basic statistics about the *Roller MV* data and the *Operating Parameters* should be readily available. Statistics of interest for the *Roller MV* data include the minimum, maximum, mean, standard deviation, and histogram. Statistics of interest for the *Operating Parameters* include the minimum, maximum, mean and standard deviation of the amplitude, frequency, and speed. This information allows QA personnel to efficiently determine if a data map meets the requirements of a *Measurement Pass*.

7.5.3 Verification of Roller MV Repeatability and GPS Position Reporting

Roller MVs must be repeatable (i.e., repeated *Measurement Pass*es over the same, fully compacted material must exhibit similar magnitudes and trends). It is also important to verify the accuracy of roller-mounted GPS position and that a position offset between the receiver and the center of the drum (i.e., where MVs are computed) and/or errors due to data averaging are properly considered. Accurate position reporting is particularly important for specification options that involve *Roller MV* correlation to spot-test measurements or spatial comparison of *Roller MVs* from consecutive passes.

7.5.3.1 Procedure to Verify Roller MV Repeatability

1. Perform two *Measurement Pass*es on a fully compacted test strip at least 100 m (330 ft) long. *Measurement Pass*es should be performed in the same direction, with static passes performed in the reverse direction between *Measurement Pass*es.
2. From the two *Measurement Pass*es, compute the spatial percent difference array $\%\Delta MV_i$ per Equation 7.1:

$$\%\Delta MV_i = \frac{MV_i - MV_{i-1}}{MV_{i-1}} \times 100 \quad (7.1)$$

where MV_i and MV_{i-1} represent the MV data array from pass i and pass $i-1$, respectively. If necessary, linear interpolation may be used to transform the data onto a grid for precise spatial comparison. If the mean of the $\%\Delta MV$ array ($\mu_{\%\Delta MV_i}$) is greater than 5%, the test strip may not have been fully compacted and the procedure should be repeated.

3. Compute the standard deviation of the $\%\Delta MV_i$ array ($\sigma_{\%\Delta MV_i}$). The $\sigma_{\%\Delta MV_i}$ quantifies the *Roller MV* repeatability. The recommended acceptable maximum $\sigma_{\%\Delta MV_i}$ is 10%, although visual inspection and engineering judgment should be employed when investigating repeatability and when deciding what level of repeatability is required and acceptable on a given project. Figure 7.3 illustrates acceptable and unacceptable levels of $\sigma_{\%\Delta MV_i}$ as well as an invalid test (due to increase in compaction of the test strip).

7.5.3.2 Procedure to Verify Roller Position Reporting

The accuracy of *Roller MV* position reporting should be verified when the *Instrumented Roller* is stationary as well as moving. When the roller is stationary, the roller-mounted GPS position can be compared with the position from a handheld RTK GPS unit (i.e., rover) placed at the drum cen-

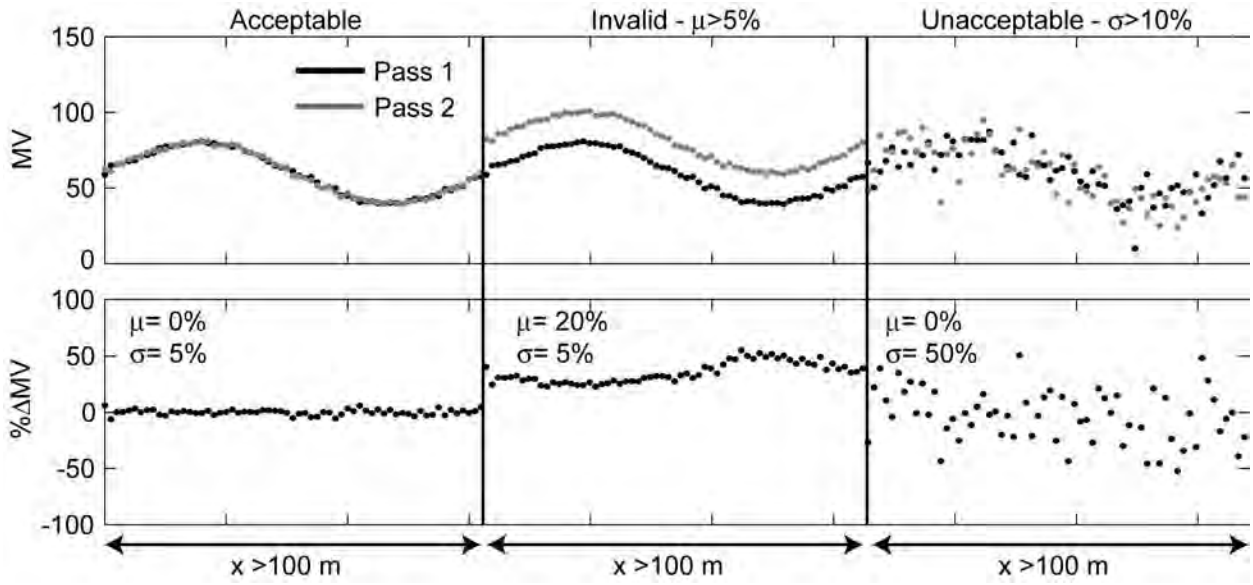

Figure 7.3. Roller MV repeatability testing: (left) acceptable repeatability, (middle) invalid test, and (right) unacceptable repeatability.

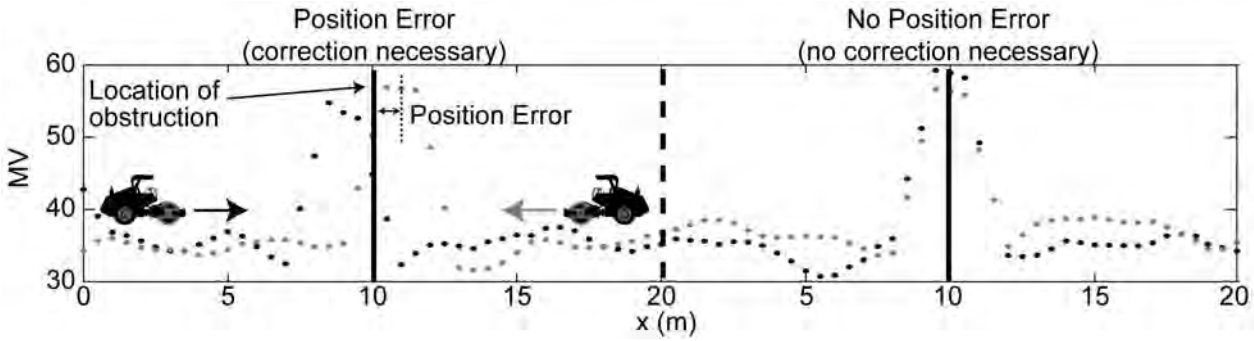

Figure 7.4. MV data records with position error (requiring correction) and without position error.

ter. This can also be accomplished by establishing a marker of known position on the ground and approaching the marker with the roller from different directions. In addition, the following procedure is recommended to ensure *Roller MV* position reporting accuracy while the roller is moving (see Figure 7.4). This procedure may be combined with the evaluation of *Roller MV* repeatability (see Section 7.5.3.1).

1. Create two obstructions in the earthwork spaced at least 10 m apart that will induce noticeable spikes in the *Roller MV* data record. Example obstructions include a wooden beam and narrow trenches perpendicular to the direction of roller travel. Note that the obstructions should span the drum width.
2. Perform two *Measurement Pass*es over the obstructions, one in each direction.
3. Superimpose the *Measurement Pass* records to observe if the spikes in the *Roller MV* data occur simultaneously. Any difference in location of a spike in the *Roller MV* data records is a reflection of position error. If this position error is greater than one-half of the *Roller MV* reporting resolution (see Section 7.5.1) or the accuracy of the GPS, this position error must be corrected.

7.6 QA Option 1: Spot Testing of Roller-Informed Weakest Area(s)

QA Option 1 utilizes roller-integrated CCC to identify the weakest area(s) of the *Evaluation Section*. The weakest area is defined by the lowest *Roller MVs* recorded during a *Measurement Pass*. More than one weakest area may be selected. Acceptance is based on spot-test measurements from the weakest area(s) (see Figure 7.5). If spot-test measurements from the weakest area(s) meet specified criteria, the *Evaluation Section* meets acceptance. The frequency of spot testing in the weakest area(s) and acceptance criteria for spot-test measurements should be based on existing spot-test-based QA practice. The selection of *Evaluation Sections* must be performed in accordance with Section 7.4.6.

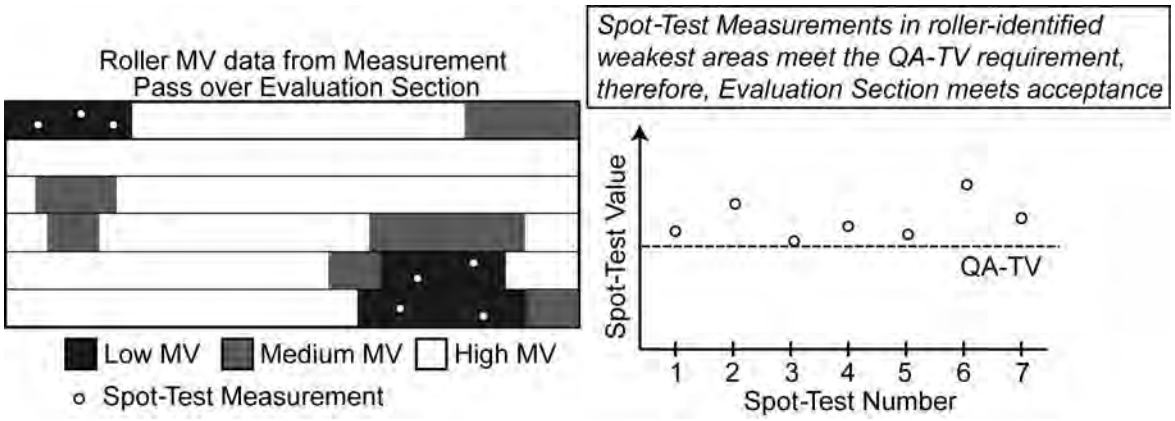

Figure 7.5. Acceptance testing via Option 1.

An important premise of Option 1 is that there is a positive correlation between *Roller MV* and soil compaction (i.e., the lowest *Roller MVs* correspond to lowest compaction). This positive correlation may not exist if the *Evaluation Section* exhibits localized soil variability (e.g., pockets of high clay content in an otherwise granular material) or significant variability in the sublift material. In cases where the lift and/or sublift material exhibits variability, the correlation between *Roller MVs* and spot-test measurements should be verified. This can be accomplished by comparing spot-test measurements with low, medium, and high *Roller MVs* across the *Evaluation Section*. In addition, low *Roller MVs* can result from fluctuations in machine operating parameters and surface unevenness. For this reason the weakest area(s) selected for testing should not be based on *Roller MVs* from areas less than 3 m (10 ft) long in the driving direction. Option 1 requires minimal changes to existing spot-test-based QA specifications and should be relatively easy to implement. To improve reliability, Option 1 may be implemented in combination with another recommended option.

7.7 QA Option 2: Limiting Percentage Change in Roller MV

QA Option 2 utilizes the pass-to-pass percentage change in *Roller MVs* to determine acceptance of an *Evaluation Section*. Acceptance is based on achieving a threshold or target $\%\Delta MV_i$ (i.e., $\%\Delta$-*TV*) between two consecutive *Measurement Passes* over the same *Evaluation Section*. There are two ways in which Option 2 can be implemented. Acceptance may be based on the pass-to-pass percentage change in mean MV ($\%\Delta\mu_{MV_i}$) of the *Evaluation Section*. Alternatively, acceptance may be based on a spatial analysis of the $\%\Delta MV_i$ data array. The dependence of *Roller MVs* on driving direction and the influence of soil heterogeneity within the drum length require that *Measurement Passes* must be performed with an identical pass-to-pass *Rolling Pattern*, particularly for Option 2b. The selection of *Evaluation Sections* must be performed in accordance with Section 7.4.6.

7.7.1 Option 2a: Monitoring Percentage Change in Mean MV

QA Option 2a involves computing $\%\Delta\mu_{MV_i}$ from two consecutive *Measurement Passes* over the *Evaluation Section* according to Equation 7.2:

$$\%\Delta\mu_{MV_i} = \left(\frac{\mu_{MV_i} - \mu_{MV_i-1}}{\mu_{MV_i-1}} \right) \times 100 \tag{7.2}$$

The recommended target value for $\%\Delta\mu_{MV_i}$ (i.e., $\%\Delta$-*TV*) is 5%. If $\%\Delta\mu_{MV_i}$ between consecutive passes is less than the $\%\Delta$-*TV*, acceptance is met (see Figure 7.6).

7.7.2 Option 2b: Monitoring Spatial Percentage Change in Roller MVs

QA Option 2b involves evaluating the spatial percent change in $\%\Delta MV_i$ from two consecutive *Measurement Passes* over the *Evaluation Section* according to Equation 7.3:

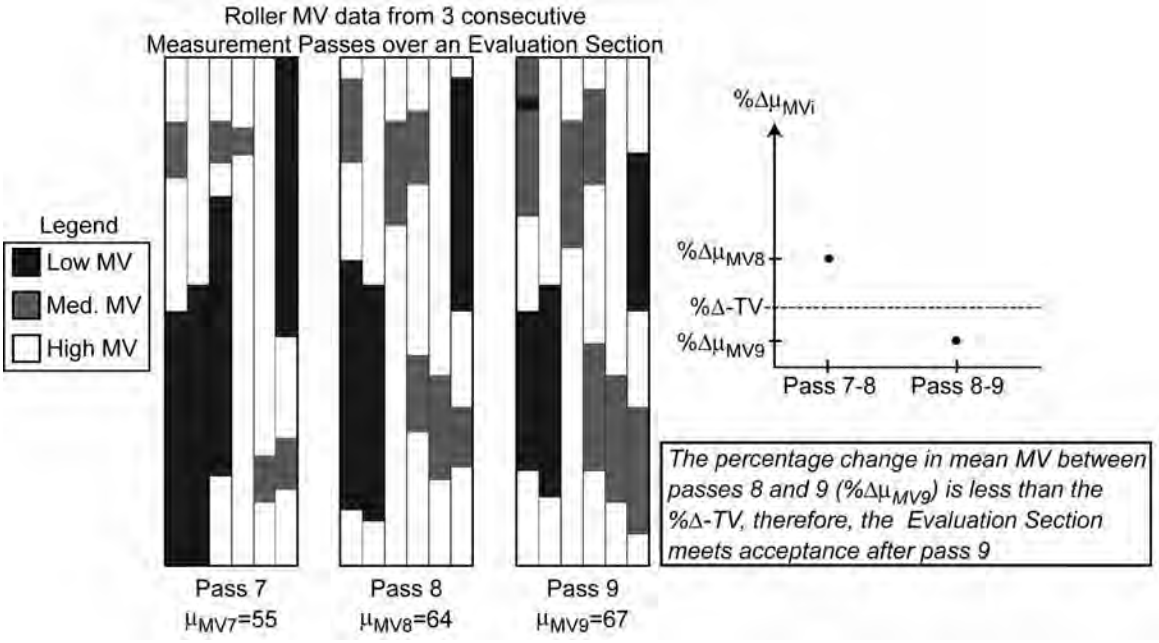

Figure 7.6. Acceptance testing via Option 2a.

$$\%\Delta MV_i = \frac{MV_i - MV_{i-1}}{MV_{i-1}} \times 100 \quad (7.3)$$

This spatial analysis involves transforming the *Roller MV* data onto a fixed grid for direct comparison. The percentage change in *Roller MV* is then computed for each grid location. The recommended %Δ-TV for Option 2b is two times the uncertainty $\sigma_{\%\Delta MV}$ determined from repeatability testing (as described in 7.1.5.1). Acceptance is based on achieving the %Δ-*TV* over a specified proportion or percent area threshold of the *Evaluation Section*, as shown in Figure 7.7. The recommended range for a specified proportion/percent area threshold is 80% to 95% (e.g., acceptance is met when the *Roller MV* increases by ≤%Δ-TV for 90% or more of the Earthwork Section). The process of transforming spatial *Roller MV* data onto a fixed grid is not trivial and has not been proven fully reliable. The simplest methods (e.g., nearest neighbor gridding, linear interpolation) may be more favorable than the more complex methods (e.g., nonlinear interpolation, kriging) until the geostatistical nature of *Roller MV* data is better understood.

QA Option 2 requires moderate changes to existing construction practice in that two *Measurement Pass*es must be performed with similar *Rolling Patterns*. If implemented correctly, Option 2 ensures that compaction has been achieved to the capability of the CCC roller and the selected *Operating Parameters* but does not necessarily ensure that adequate compaction has been achieved. The ability of the roller to produce adequate compaction should be verified before earthwork compaction begins. To improve the reliability of compaction QA, Option 2 may be used in combination with another QA option.

7.8 QA Option 3: Comparison of Roller MV Data to Target MV

Options 3a, 3b, and 3c each require that a specified percentage of *Roller MVs* in an *Evaluation Section* exceed a *Roller MV* target value (MV-TV). The MV-TV must be determined during field calibration prior to acceptance testing. In the future, MV-TVs may stem from a database of project information, documented case histories, and literature; however, extreme care should be exercised given the wide range of variables that influence *Roller MVs*. The approach to establish an MV-TV differs for each option and is described in the following sections. Acceptance for each option is similar and is based on

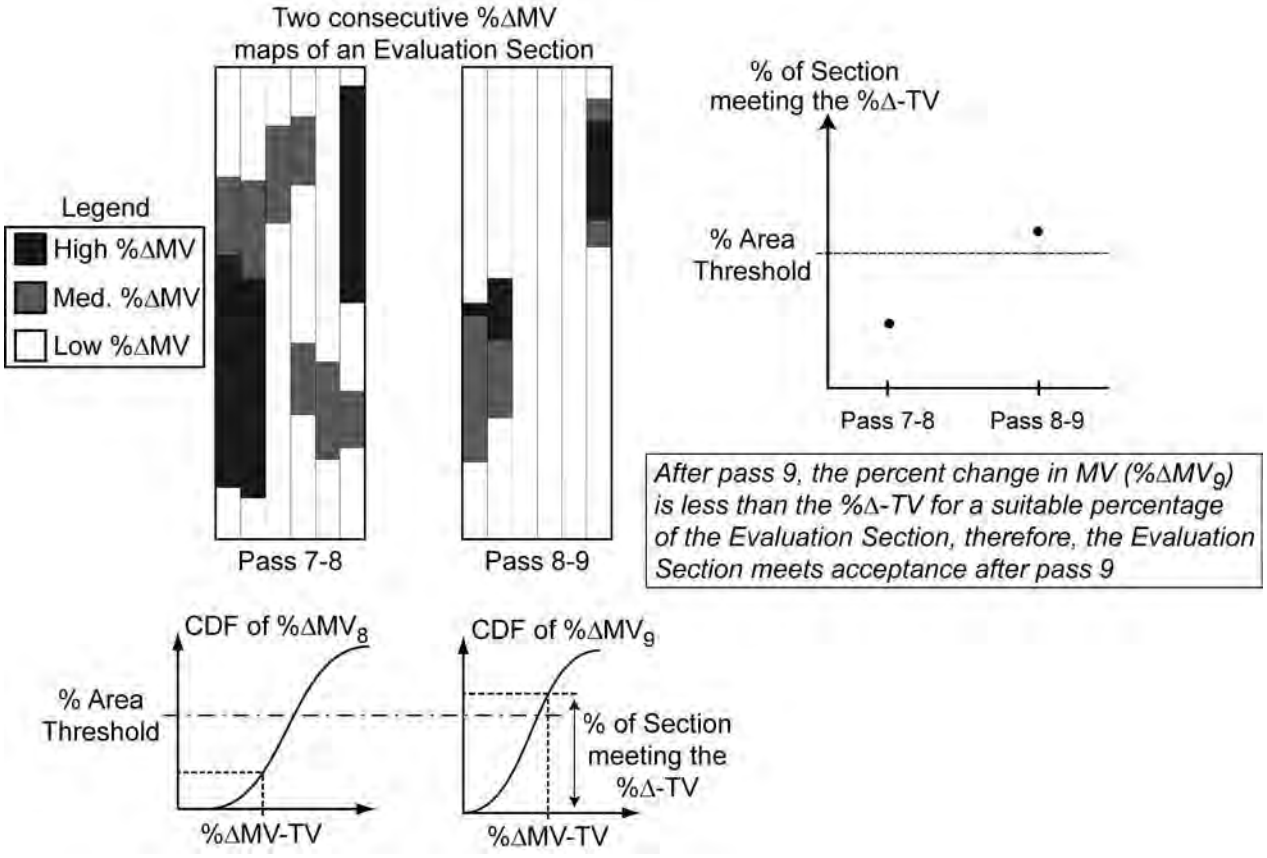

Figure 7.7. Acceptance testing via Option 2b.

achieving the MV-TV over a specified proportion or percent area threshold of the *Evaluation Section*. The range of recommended proportions is 80% to 95% and should be defined prior to testing. Figure 7.8 illustrates the acceptance process. The selection of *Evaluation Sections* must be performed in accordance with Section 7.4.6.

7.8.1 MV-TV Determination for QA Option 3a: Relating Roller MV to Spot-Test Measurements

In Option 3a, *Roller MVs* are related to *Spot-Test Measurements* using statistical regression analysis. The methodology is illustrated in Figure 7.9. A *Calibration Area* should be selected per Section 7.4.7. The *Calibration Area* is sequentially compacted to low, intermediate, and full (complete) compaction states. The full compaction state should meet or exceed the required QA-TV. At each compaction state a *Measurement Pass* is performed, followed immediately by spot testing at several locations in the *Calibration Area*. A minimum of five locations is recommended for spot testing at each compaction level. The *Measurement Pass* data can be used to identify locations for spot testing. To improve reliability, locations where *Roller MVs* are locally constant are recommended and locations where *Roller MVs* are highly variable should be avoided (see Figure 7.9). The collection of locations should represent the range of variability observed in the *Measurement Pass* data. At each selected location, three to five spot-test measurements should be collected across the roller drum lane and averaged to generate one regression point. The *Roller MVs* at each location may be averaged over a 1-m distance in the direction of roller travel to generate one regression point.

Regression analysis is performed with the *Roller MV* as the dependent variable and *Spot-Test Measurement* as the independent variable. In general, the coefficient of determination R^2 is used to judge correlations, with acceptable correlations being defined by $R^2 \geq 0.5$ (e.g., the correlation depicted in Figure 7.9 is acceptable). This level of acceptability for R^2 is commonly used when correlating soil properties measured from different devices because loading conditions, seating issues, and representative volumes vary. In Ping et al. (2002), $R^2 = 0.3$ was found acceptable when correlating modulus back calculated from a FWD with lab data. In Vennapusa & White (2009), $R^2 = 0.5$ to 0.9 was found acceptable when correlating data collected from different LWDs and $R^2 = 0.40$ to 0.66 was found acceptable for correlations between LWD and static PLT moduli.

When correlating *Roller MVs* to stiffness-based spot tests (e.g., PLT, LWD), single-variable regression is usually sufficient. When correlating *Roller MVs* to density, single-variable regression may not be successful. Multivariate regression may be required if the material behavior is moisture dependent.

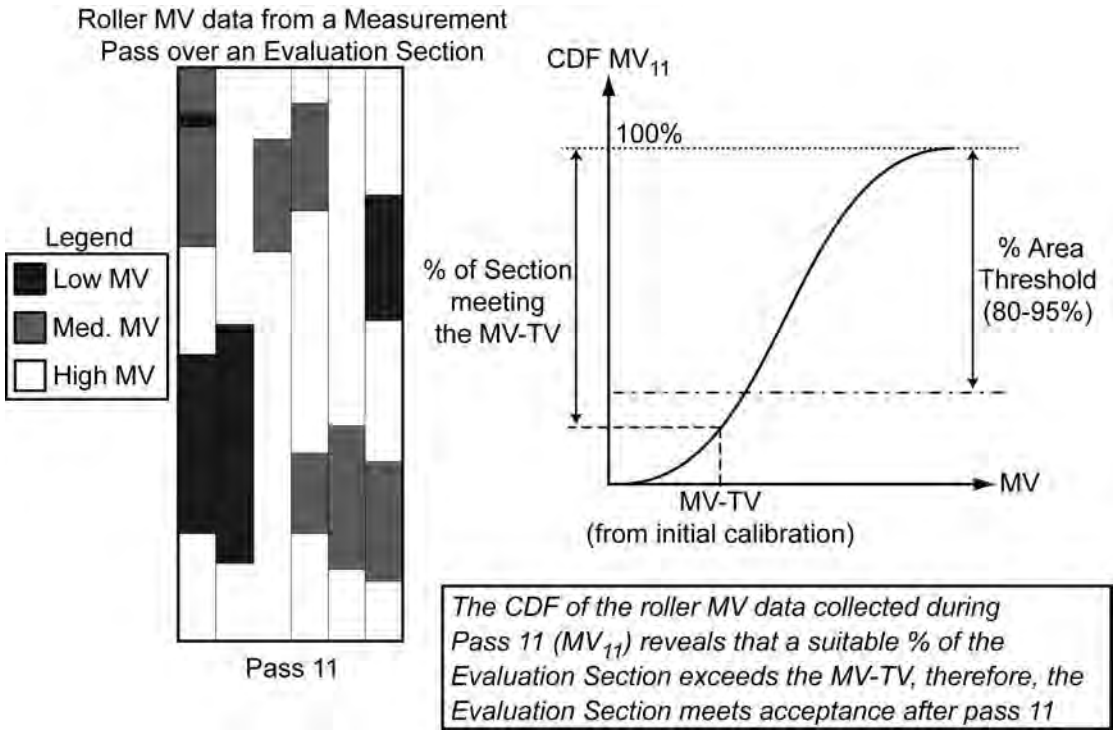

Figure 7.8. Acceptance testing via Option 3.

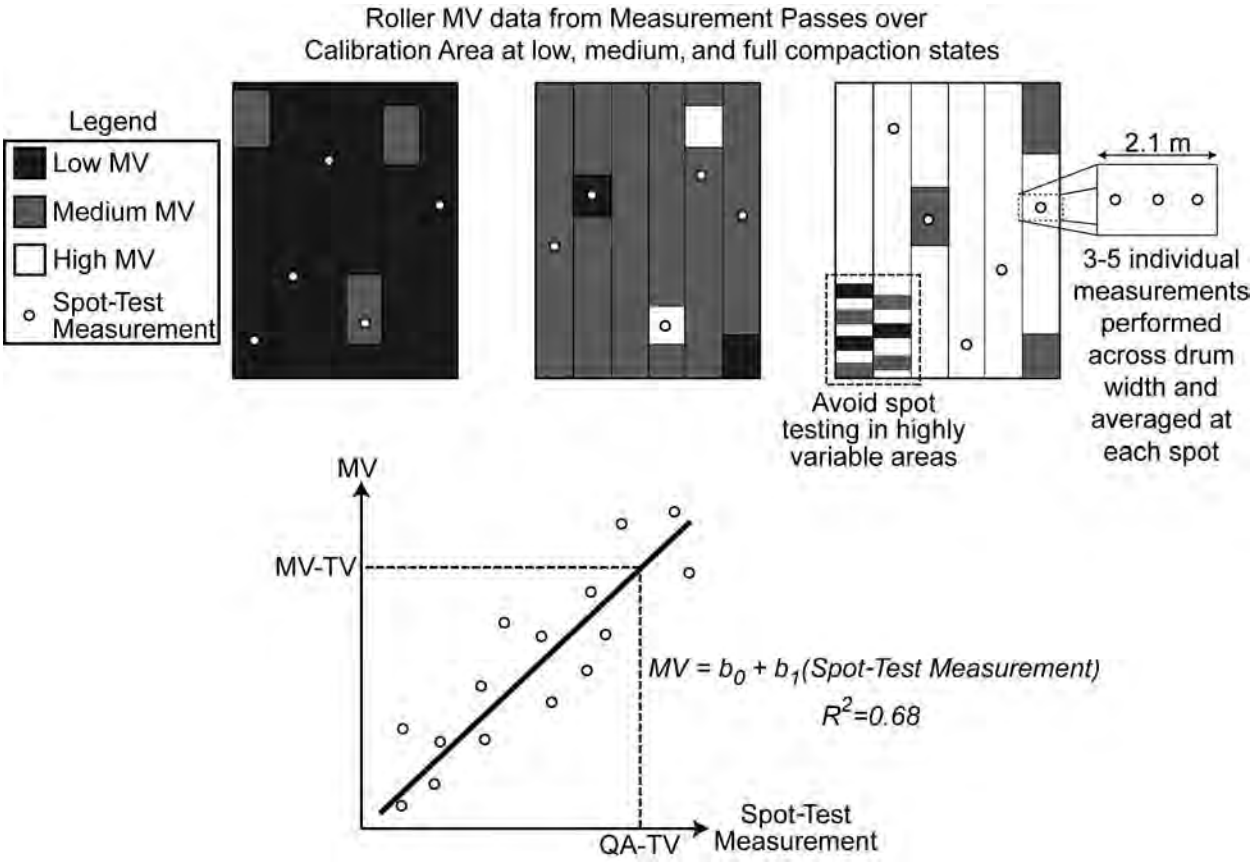

Figure 7.9. Determination of MV-TV via Option 3a.

It may also be desirable to perform multivariate regression analysis that takes sublift conditions into consideration to account for the significant difference in measurement depth of *Roller MVs* and *Spot-Test Measurements*. Prior experience and a sound fundamental understanding of both *Roller MVs* and *Spot-Test Measurements* will increase the probability of achieving acceptable correlations.

If a suitable correlation is determined ($R^2 \geq 0.5$), an MV-TV is selected from the regression equation based on the existing *Spot-Test Measurement*–based target value (QA-TV; e.g., 95% maximum dry density; see Figure 7.9). The QA-TV used to determine the MV-TV may be increased to increase confidence. Prediction limits can be employed when performing correlations to select the MV-TV. An MV-TV can be established using the upper prediction limit, as shown in Figure 7.10. The greater the prediction interval specified, the higher the MV-TV.

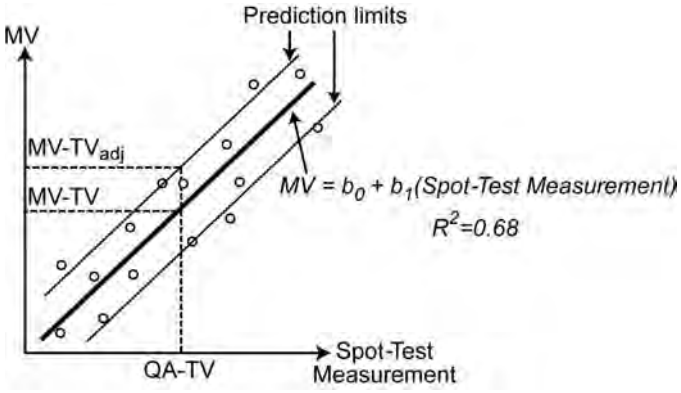

Figure 7.10. Illustration of use of prediction limits when selecting an MV-TV.

7.8.2 Determination of MV-TV for QA Option 3b: Compaction Curve

In Option 3b the change in *Roller MV* is monitored to determine when compaction is complete. During compaction of the *Calibration Area* (selected per Section 7.4.7), the *Roller MV* and pass number are continuously recorded. The MV-TV is established as the μ_{MV_i} when the $\%\Delta MV_i \leq 5\%$ for 90% of the *Calibration Area*, as shown in Figure 7.11. The calibration procedure for Option 3b is similar in principle to acceptance testing of Option 2b.

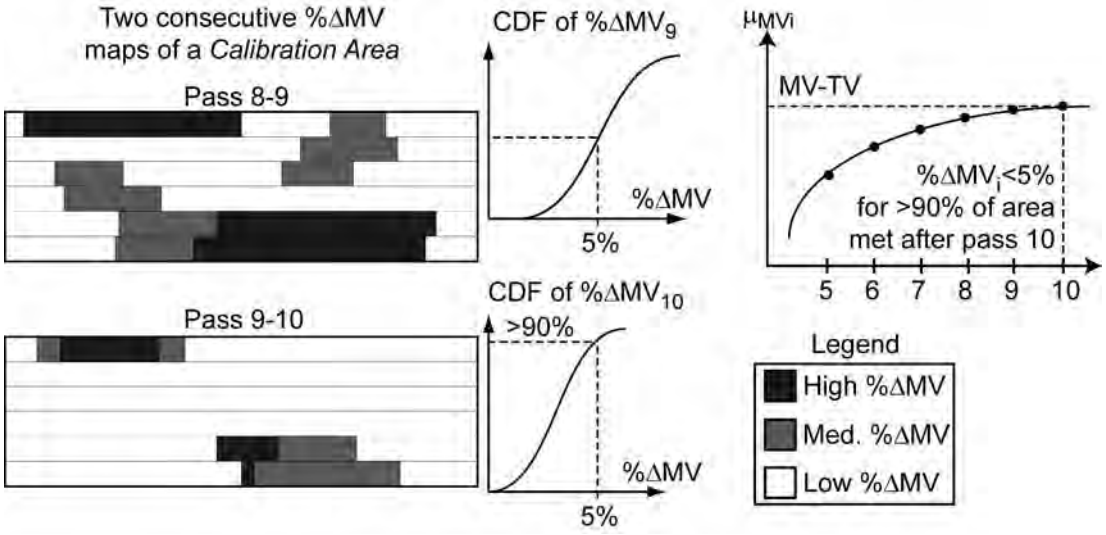

Figure 7.11. Determination of MV-TV via Option 3b.

7.8.3 Determination of MV-TV for QA Option 3c: Relating Roller MV to Lab-Determined Properties

In this approach the MV-TV is established through empirical correlation to laboratory-determined engineering properties (e.g., M_r) based on a preselected combination of moisture contents and dry unit weights. This option requires a significant investment of time to establish the MV-TV. It must be noted that performing laboratory resilient modulus tests is time consuming, which can potentially impact the application of this specification option if heterogeneous materials exist on a project.

Laboratory testing should be performed on samples prepared at preselected moisture-density combinations in accordance with standard protocols used by state agencies. For example, moisture contents may vary from w_{opt} – 4% to w_{opt} + 4% and dry unit weight from 90% to 110% of γ_{dmax} established from laboratory Proctor compaction (standard or modified) specified by the agency for QA. Using the test results, a multiple regression model is developed as a function of moisture and dry unit weight to predict the laboratory soil property values (Figure 7.12b). For stress-dependent M_r values, multiple regression relationships may be developed for a selected stress condition.

Compaction of the *Calibration Area* (selected per Section 7.4.7) is performed using variable moisture content (e.g., w_{opt} –4% to w_{opt} + 4%) and obtaining *Roller MVs* in parallel with in situ moisture and dry unit weight measurements from multiple passes (e.g., 1, 2, 4, 8, and 12). Using the *Spot-Test Measurement* data and corresponding *Roller MV* data, a multiple regression relationship is developed to predict *Roller MV* as a function of moisture and dry unit weight (similar to Option 3a; shown in Figure 7.12c using prediction limits). Using the multiple regression relationships from laboratory and field testing, laboratory soil properties are correlated to *Roller MVs* as shown in Figure 7.12a. An MV-TV can be determined based on a target laboratory soil property (QA-TV) from the linear regression relationship. Prediction intervals are employed as shown in Figure 7.12. The compaction method used for laboratory-prepared specimens can affect the laboratory-determined values, especially for fine-grained cohesive soils. Laboratory vibratory compaction is recommended for granular soils compacted using smooth drum rollers. Laboratory impact compaction is recommended for soils compacted using pad foot rollers.

7.9 Uniformity Criteria

Uniformity is recognized as an important component of quality compaction (e.g., Davis 1953, Sherman et al. 1966). Results from numerical studies indicate that considering average values in design may not capture actual performance (e.g. White et al. 2004, Griffiths et al. 2006). With the ability of real-time viewing of compaction data, roller-integrated measurement technology offers an opportunity to construct more uniform earthwork layers. Current CCC specifications address uniformity using percentage limits based on an MV-TV. The International Society for Soil Mechanics and Geotechnical Engineering (ISSMGE)/Austrian CCC earthwork specifications, for example, require that roller MVs in the production area should fall within 0.8 to 1.5 MIN-TV with a coefficient of variation < 20% (MIN-TV corresponds to the MV at 0.95 QA-TV established from calibration). Using a slightly different approach, the Minnesota Department of

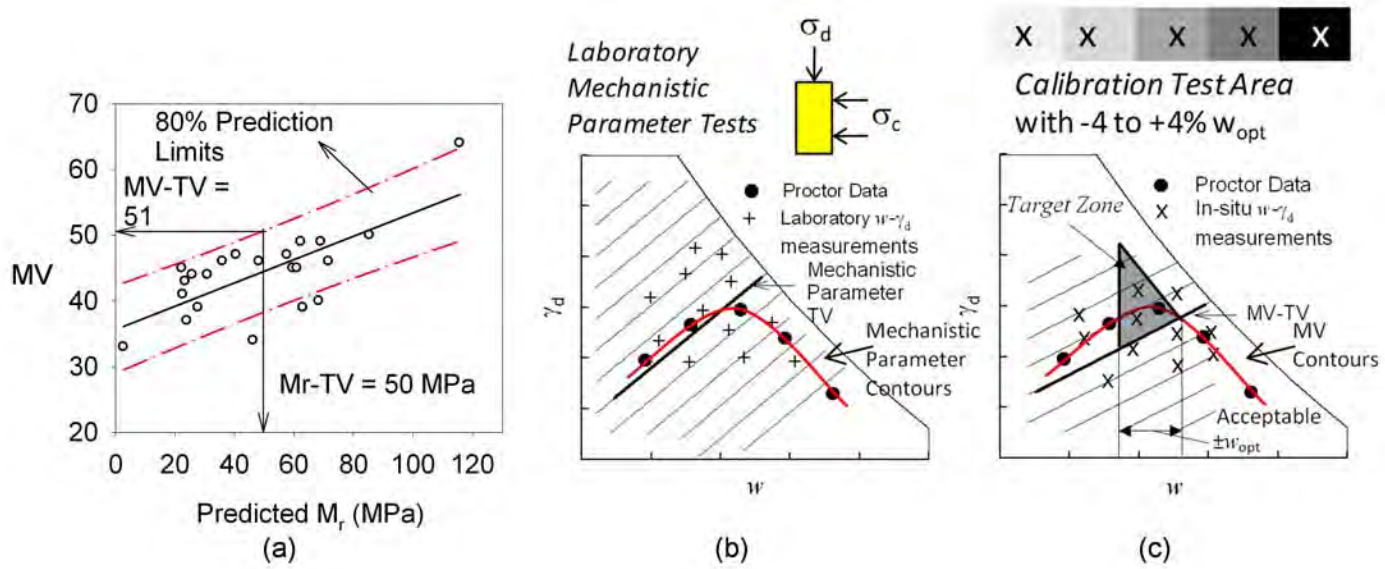

Figure 7.12. Determination of MV-TV via Option 3c.

Transportation (MnDOT) implemented a predetermined target percentage limits distribution criterion (Mn/DOT 2007) on a full-scale earthwork project in the state (White et al. 2007, 2008a, 2008b). The acceptance requirement was that at least 90% of roller MV data in the production area should fall within 90% to 120% of the MV-TV; none should be below 80% of the MV-TV; and if any are above 120%, a new MV-TV should be established.

If uniformity criteria are desired as part of the specification, the ISSMGE and Mn/DOT approaches described above can be implemented for specification Options 2 and 3. However, it must be realized that these approaches are limited to conditions where *Evaluation Sections* have similar spatial heterogeneity in compaction layer properties and support conditions to the *Calibration Area*. If not, achieving these uniformity targets is challenging. For such cases, information of underlying support conditions may help in evaluating compaction layer data and selecting representative *Calibration Areas*. Further, these approaches do not address uniformity from a spatial standpoint. More research is needed in relating uniformity to performance for a better understanding of the level of uniformity desired and how field operations can be improved to control nonuniformity.

An alternate approach to quantify uniformity is to use spatial statistics in combination with univariate statistics (mean and standard deviation; Brandl 2001, Vennapusa et al. 2009, Facas et al. 2010). Using spatial statistics requires developing semivariogram models using spatially referenced GPS coordinate measurements, which describe the spatial relationship in the measured roller MVs. The three main characteristics by which a semivariogram is often summarized are *range*, *sill*, and *nugget* (Isaaks & Srivastava 1989). Comparatively, a semivariogram with a lower *sill* and longer *range* represents reduced nonuniformity and improved spatial continuity. Vennapusa et al. (2009) describe an approach for using spatial statistics to target areas for compaction that results in improved spatial continuity and reduced nonuniformity.

CHAPTER 8

Case Study Evaluation of Specification Options

This chapter presents six case studies performed to illustrate implementation of the recommended quality assurance (QA) specification options detailed in Chapter 7 (see Table 8.1). These case studies were derived from field tests in Colorado, Florida, North Carolina, and Minnesota. The case studies presented here include granular subgrade (FL15, FL23, NC20), nongranular subgrade (MN10), granular subbase (CO34), and aggregate base materials (FL19). Additional case studies are presented in Appendix D. Multiple specification options were investigated as part of each case study to enable direct comparison of option strengths and limitations. Both successful and unsuccessful implementations are presented and discussed. Throughout this chapter, standardized terms from the Chapter 7 specification options are italicized and capitalized.

As summarized in Table 8.1, compaction QA acceptance testing was conducted by the project QA agents using criteria based on dry unit weight requirements (γ_d-TV), moisture requirements (*w*-TV), and/or static proof rolling (PR). For some case studies, comparisons with existing options are made. Table 8.1 summarizes whether each test bed passed (P) or failed (F) the existing contract specifications, if applicable. When appropriate, MV-TVs were established based on these same contract requirements.

8.1 Case Study I—Granular Subbase (TB CO34)

QA Specification Options 1, 2a, 2b, and 3a were evaluated on a 12-m (40-ft)-wide by approximately 300-m (1,000-ft)-long by 30-cm (12-in)-thick granular subbase *Evaluation Section* in Colorado (see Figure 8.1). The existing soil [A-4(3)] in this cut section was excavated. Four 30-cm (12-in)-thick lifts of granular subbase material (A-1-a) were placed and compacted jointly by the research team using the Dynapac intelligent compaction (IC) roller and by the contractor using typical vibratory and static equipment. This case study pertains to the fourth subbase layer. Contract QA specifications included γ_d-TV = 100% standard Proctor maximum dry unit weight [21.6 kN/m^3 (137.5 pcf) uncorrected for rock content] and *w*-TV = 3 ± 1% if the rock content (material retained on a #4 sieve) was less than 50%. Rock content exceeded 50% in this area; therefore, project QA was based solely on a static proof

Table 8.1. Summary of case studies presented.

		CCC-QA Options Evaluated[a]						Contract QA Pass/Fail[b]		
Test Bed	Soil (AASHTO)	1	2a	2b	3a	3b	3c	γ_d-TV	*w*-TV	PR
CO34	A-1-a	✓	✓	✓	✓	—	—	NR[c]	NR[c]	P[d]
FL15	A-3	✓	✓	✓	—	—	—	F	NS	NR
FL19	A-1-b	—	—	—	✓	—	—	P	NS	NS
FL23	A-1-b	✓	✓	✓	✓	✓	—	P	NS	NS
NC20	A-1-b	✓	—	—	✓	—	—	P	NS	P[d]
MN10	A-6(5)	—	—	—	—	—	✓	F	NS	NS

[a] ✓ evaluated; — not evaluated.
[b] Based on existing contract requirements for γ_d, *w*, and static proof roll (when required) and assessed by project QA agents; NS = not specified, NR= not required.
[c] Soil had >50% rock content; therefore, γ_d-TV and *w*-TV were requirements not enforced.
[d] Section passed, but remediation was required in small area(s).

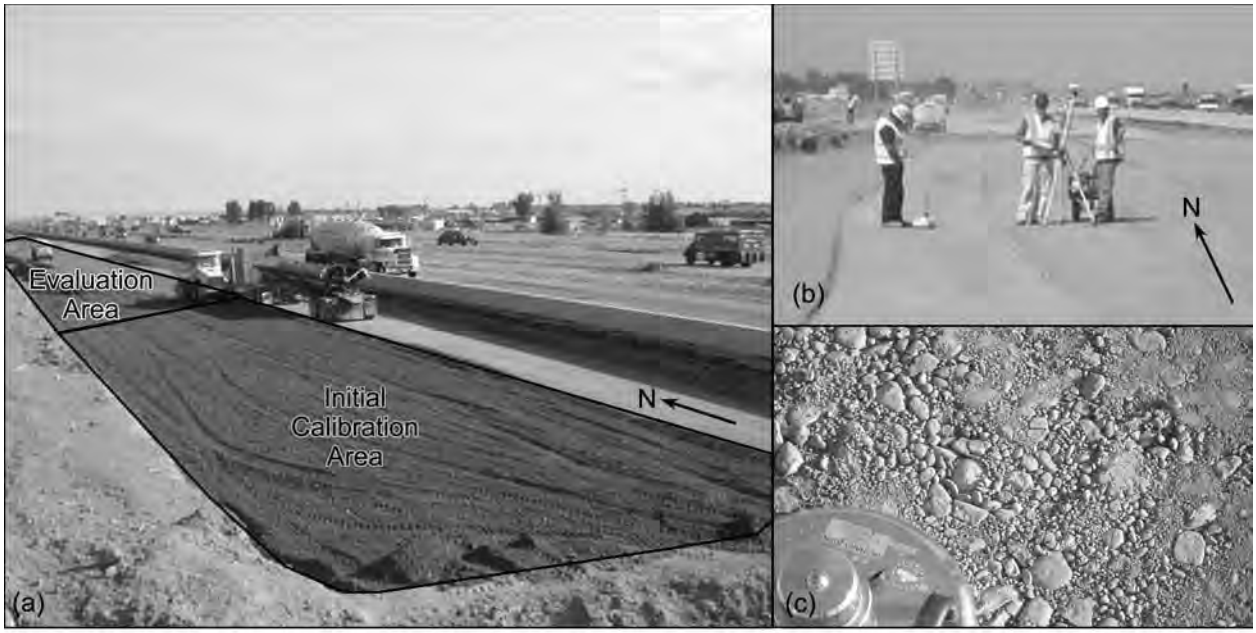

Test bed construction:
30 cm (12 in) lift of granular subbase material (A-1-a) placed atop ~90 cm (36 in) previously compacted subbase, no water conditioning performed

Measurement Pass Operating Parameters:
A = 0.9 mm (0.0035 in); f = 30 Hz;
v = 3.6 km/h (2.2 mph)

Evaluation Section compacted via the following Pass Sequence:
P1: A=2.1 mm (0.083 in), forward;
P2: A=0.9 mm (0.035 in), forward; P3: A=2.1 mm (0.083 in), reverse;
P4: A=0.9 mm (0.035 in), forward; P5: A=2.1 mm (0.083 in), reverse;
P6: A=0.9 mm (0.035 in), forward; P7: Static (A=0), reverse;
P8: A=0.9 mm (0.035 in), forward; P9: Static (A=0), reverse;
v=3.6 km/h (2.2 mph) for all passes, f=30 Hz for all vib. passes

Figure 8.1. Overview of TB CO34 summarizing construction and compaction of the test bed and showing (a) Evaluation Section and Calibration Area, (b) spot testing with the nuclear density gauge in the Calibration Area, and (c) the A-1-a subbase material.

roll. For this case study, the specification options were evaluated using the contract γ_d-TV.

The roadway alignment was transected by pipe crossings at approximately 300-m (1,000-ft) intervals and formed natural production earthwork sections. The contractor and QA agents informally treated these 300-m sections as independent QA units; therefore, the research team chose to use these natural sections as *Evaluation Section*s. The *Calibration Area* at the southern end of the *Evaluation Section* was believed to be representative of the *Evaluation Section* and was convenient given the south to north flow of haul trucks and earthwork material through the site (see Figure 8.1a). Spot-test measurements were performed with the nuclear gauge (γ_d, w), using a probe depth of 200 mm (8 in) and with the 300-mm (12-in)-diameter Zorn light weight deflectometer (LWD; $E_{LWD\text{-}Z3}$). Three to four LWD and two nuclear gauge tests were performed across the width of the drum lane and averaged to represent a single measurement for acceptance analysis. Each reported roller MV was determined by averaging over 1 m (3 ft) in the direction of roller travel.

The subbase material for the *Calibration Area* and *Evaluation Section* subbase layer was placed in one 30-cm (12-in)-thick lift. Logistically, the contractor placed material via side-dump trucks from south to north, beginning first in the *Calibration Area* and then the *Evaluation Section.* An area about 2 m (6 ft) wide on the east side was not filled to allow for some shoulder work. While the research team performed the Option 3a correlation analysis in the *Calibration Area*, the contractor placed and began compaction work in the *Evaluation Section.* After calibration was completed (about three hours), the research team compacted the remainder of the *Evaluation Section* according to the pass sequence summarized in Figure 8.1. Due to the contractor's schedule, further compaction was not possible, and the QA agent performed a

static proof roll test after pass 8. The *Evaluation Section* passed the static proof roll test despite very small areas with high clay content being identified for remediation, which involved scraping the clay material out with a motor grader. *Evaluation Section* roller MV data from pass 8 (MV_8) and spot-test measurement data obtained immediately after pass 8 are used to evaluate some of the options.

8.1.1 Acceptance Using Specification Option 1

Acceptance for Option 1 is based on achieving specified dry unit weight or relative compaction target values (γ_d-TV, RC-TV) in the weakest area(s) identified by the instrumented roller. The spot-test-based acceptance criteria should be determined by the appropriate agency and should be based on and modified as necessary per agency practice. Figure 8.2 presents the pass 8 MV data (MV_8) together with spot-test measurements performed immediately after pass 8. Three weakest areas were identified for nuclear gauge and LWD testing, as illustrated in Figure 8.2. All six spot-test measurements performed in these weakest areas failed to meet the γ_d-TV = 21.6 kN/m^3 (137.5 pcf) and RC-TV = 100% specified for this project (see Table 8.2). It can be argued, however, that requiring 100% relative compaction in the weakest areas is more stringent than the existing Colorado approach where test locations are randomly selected. For example, four of the six weakest areas would meet an RC-TV = 95% criteria. For this reason, individual agencies must carefully consider existing QA criteria and spot-testing practice when establishing acceptance criteria for Option 1.

An important premise behind Option 1 is that a positive correlation exists between roller MVs and spot-test measurements (i.e., low roller MVs correspond to low γ_d and high roller MVs correspond to high γ_d). Nine spot-test measurements were performed over a range of roller MVs to assess the relationship. Figure 8.2 shows that a reasonable correlation ($R^2 = 0.52$) exists between γ_d and the roller MV in the *Evaluation Section* and suggests that Option 1 is valid for this *Evaluation Section*. Conversely, an acceptable correlation was not evident from the roller MV versus $E_{LWD\text{-}Z3}$ data and would therefore call into question the validity of its use in Option 1. The difficulty obtaining a suitable roller MV-$E_{LWD\text{-}Z3}$ relationship is discussed later.

8.1.2 Acceptance Using Specification Option 2a

Acceptance for Option 2a is based on the percentage change in the mean MV $\%\Delta\mu_{MV_i}$ from consecutive passes over an *Evaluation Section*. Acceptance is met when $\%\Delta\mu_{MV_i}$ is less than the target percentage change (%Δ-TV = 5% for the case study presented here, similar to Austrian CCC specifications). Table 8.3 provides $\%\Delta\mu_{MV_i}$ for several passes over the *Evaluation Section*. The evaluation of $\%\Delta\mu_{MV_i}$ was performed on pass pairs 2-4, 4-6, and 6-8 because the intermediate passes (3, 5, 7) used higher-amplitude vibration (see pass sequence in Figure 8.1) or were static passes. Option 2a requires constant roller operating parameters for measurement passes. Per the %Δ-TV = 5% criterion, acceptance was met after pass 6.

8.1.3 Acceptance Using Specification Option 2b

Acceptance for Option 2b is based on the spatial percentage change in MV_i between consecutive passes $\%\Delta MV_i$ rather than the percentage change in mean MV of the entire *Evaluation Section* per Option 2a. Acceptance is met when $\%\Delta MV_i \leq$ %Δ-TV for a specified percentage of the *Evaluation Section* (%Area-TV). Per Section 7.5.3.1, the recommended %Δ-TV is two times the $\sigma_{\%\Delta MV}$ determined from repeatability testing (as described in Section 7.1.5.1) with a maximum %Δ-TV = 20%. However, higher %Δ-TV may be used at the discretion of the engineer of record. The $\sigma_{\%\Delta MV}$ = 12.5% for the CMV_D data, but the roller MV data were qualitatively repeatable. Therefore, %Δ-TV = 25% was set for this case study. The %Area-TV was set at 80%.

Figure 8.3 presents $\%\Delta MV_i$ data for passes 4, 5, and 6 ($\%\Delta MV_6$) and 6, 7, and 8 ($\%\Delta MV_8$), the last two *Measurement Pass* pairs over the *Evaluation Section*. The cumulative distributions of the $\%\Delta MV_i$ data are also shown. To compute $\%\Delta MV_i$, nearest neighbor interpolation was used to transform the MV_i data onto a fixed grid—the method currently used by most roller manufacturers. The process of transforming GPS-based roller MV data to a fixed grid is nontrivial and an area of ongoing research (e.g., see Facas et al. 2010). The cumulative distributions illustrate that roller MVs decreased by as much as 50% in some areas and increased by as much as 75% in others. These large changes are likely a manifestation of deviation in roller path and highlight one of the challenges with the gridding of MV data records. Figure 8.3 shows that the %Δ-TV = 25% was met for 81% of the *Evaluation Section* after pass 6, and therefore acceptance is met according to Option 2b. It should be noted that although the theory behind Option 2b is sound, it is limited practically by the difficulties associated with accurately transforming the MV data onto a fixed grid often with a *y*-scale resolution less than the 2-m-long drum length (see Chapter 3).

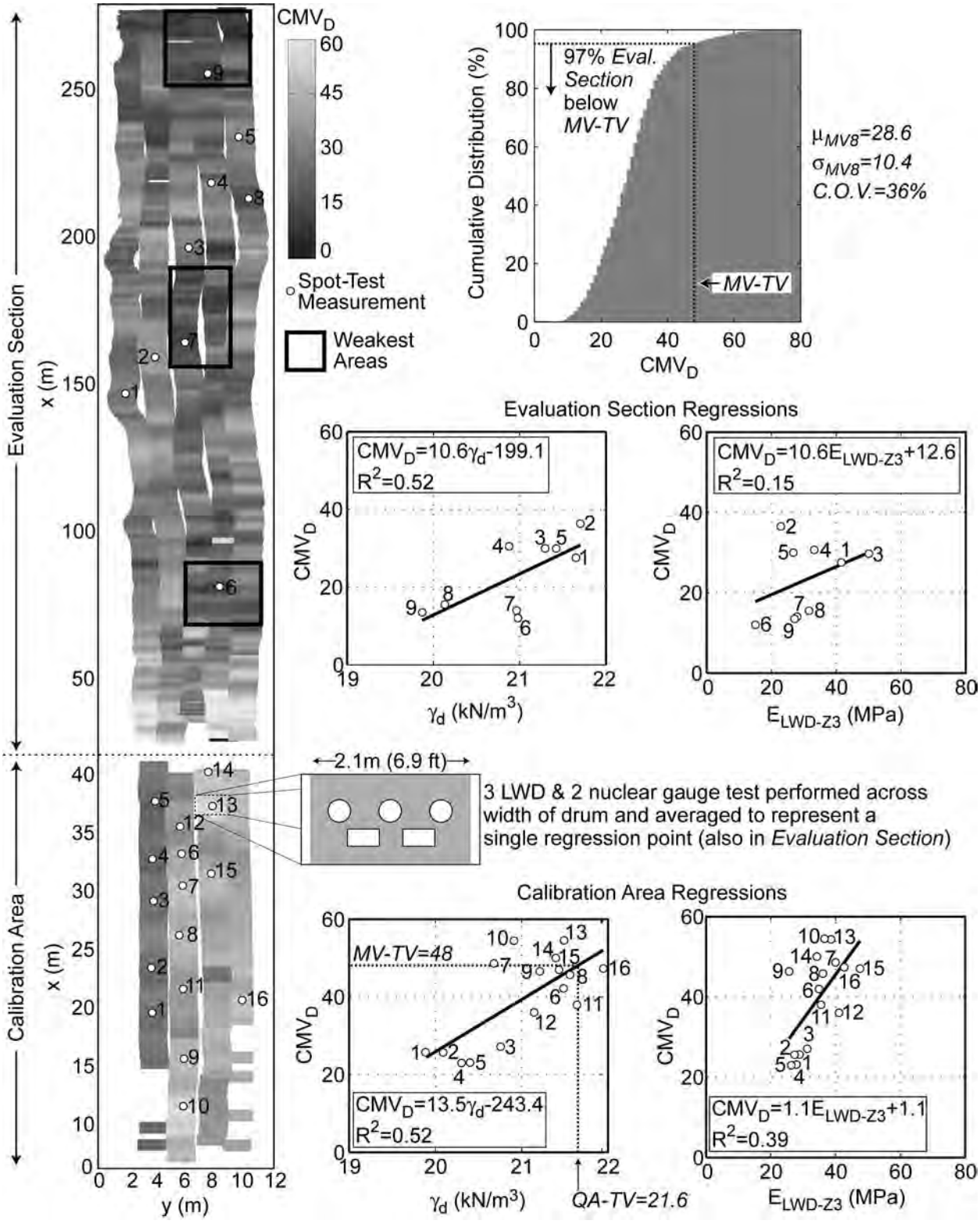

Figure 8.2. Roller MV maps of the Calibration Area and Evaluation Section, MV spot-test measurement correlations, and cumulative distribution of MV data after pass 8.

Table 8.2. Option 1: Spot-Test Measurements from weakest areas.

Weakest Area Location	γ_d (kN/m³) (pcf)	Relative Compaction[a]
6-1[b]	21.0 (134)	97.2%
6-2	21.0 (134)	97.2%
7-1	21.0 (134)	97.2%
7-2	20.9 (134)	96.7%
9-1	20.0 (127)	92.6%
9-2	19.8 (126)	91.7%

[a] Based on percentage of γ_d-TV = 21.6 kN/m³ (138 pcf).
[b] Reflects test 1 at position 6 in Figure 8.2.

Table 8.3. Summary of μ_{MV_i} and $\%\Delta\mu_{MV_i}$ from TB CO34.

Pass	μ_{MV_i}	$\%\Delta\mu_{MV_i}$
2	24.8	—
3	NA[a]	—
4	26.9	6.9%
5	NA[a]	—
6	28.1	4.1%
7	NA[b]	—
8	28.6	1.8%

[a] Pass was with high-amplitude vibration in reverse driving direction; MV data are not comparable to MV data from low- amplitude passes.
Pass was static; no MV data are available.

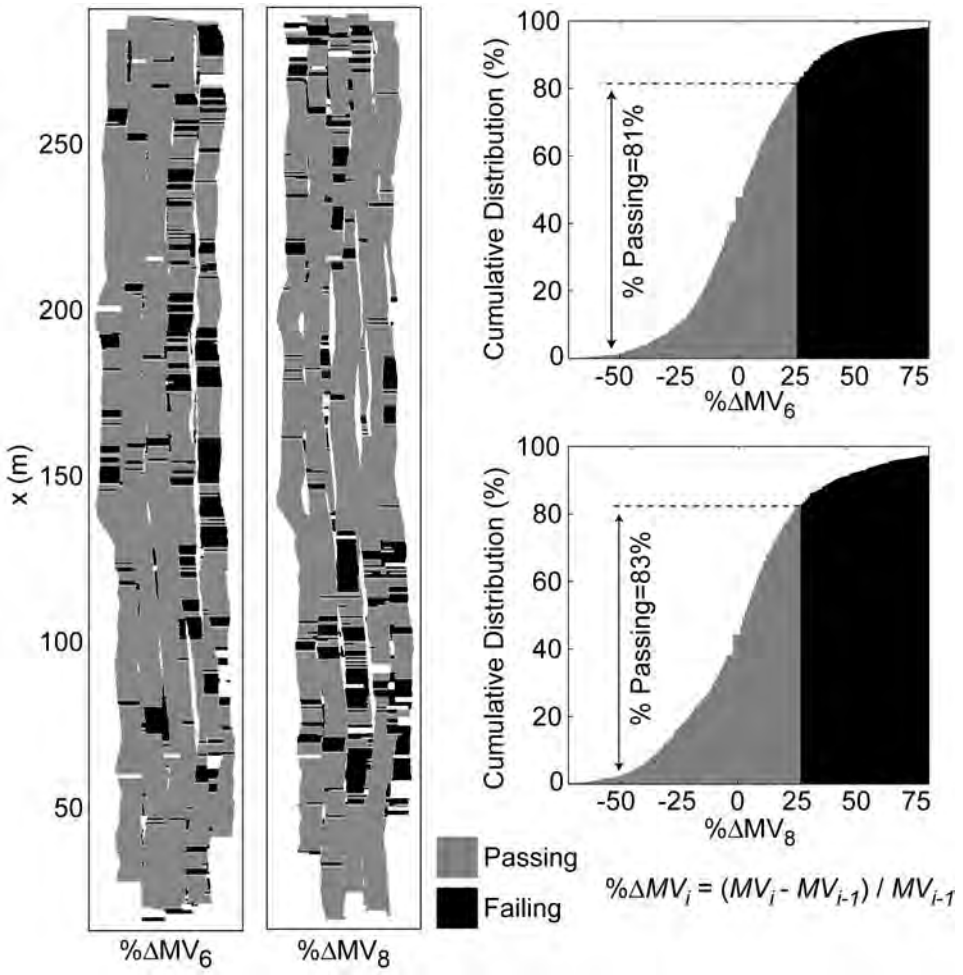

Figure 8.3. Percentage change in MV maps for passes 4, 5, and 6 ($\%\Delta MV_6$) and passes 6, 7, and 8 ($\%\Delta MV_8$) and cumulative distributions of percentage change showing percent of area meeting acceptance.

8.1.4 Acceptance Using Specification Option 3a

8.1.4.1 Initial Calibration

Option 3a requires calibration of roller MVs to spot-test measurements to determine an MV-TV. A *Calibration Area* was selected at the southern end of the *Evaluation Section* (Figure 8.1) and was compacted to provide low, medium, and full compaction states prior to measurement. Figure 8.2 shows MV data from a *Measurement Pass* over the *Calibration Area*. Spot testing was performed at five or six locations per compaction state. The resulting regression relationships are shown in Figure 8.2. A suitable correlation was found between CMV_D and γ_d ($R^2 = 0.52$) but not between CMV_D and $E_{LWD\text{-}Z3}$ ($R^2 = 0.39$). Based on the γ_d-TV = 21.6 kN/m^3 (138 pcf), the MV-TV = 48 (see Figure 8.2).

Beyond the influence of measurement depth mismatch between roller MVs and spot-test measurements, the poor MV-$E_{LWD\text{-}Z3}$ correlation is attributed to the high degree of local heterogeneity and the limitation of the LWD to reliably measure the stiffness of dry granular materials with rounded particles. The high degree of heterogeneity is illustrated by the spot-test measurements in Figure 8.4. The multiple data at each test location reflect the two moisture/density tests and three or four LWD tests performed across the drum lane as well as the range of roller MVs encountered in the 1 m (3 ft) of data averaged to represent a single point. Although γ_d exhibits little variation across the drum lane [<0.2 kN/m^3 (1.27 pcf)], the variation in $E_{LWD\text{-}Z3}$ measured across the drum width (3 to 20 MPa) approaches the entire range from low to high compaction states shown in Figure 8.2. The limitation of the LWD to measure the stiffness of dry granular materials with rounded particles is illustrated in Figure 8.2. Spot-test measurements 10 and 13 to 16 were from areas of high roller MV and high γ_d. However, the $E_{LWD\text{-}Z3}$ values are often less than the results from the medium MV areas and in the case of point 9 similar to the results from the low-MV areas.

8.1.4.2 Assessment of Evaluation Section

Acceptance for Option 3a is based on achieving the MV-TV over a specified percentage of the *Evaluation Section* (%Area-TV). In this case study, %Area-TV = 90% (similar to current German practice). Figure 8.2 shows MV_8 for the *Evaluation Section*. Pass 8 served as the final compaction pass and final *Measurement Pass* [$A = 0.9$ mm (0.035 in), $v = 3.6$ km/h (2.2 mph), $f = 30$ Hz]. The cumulative distribution of MV_8 data shows that only 3% of the *Evaluation Section* met the MV-TV; therefore, the *Evaluation Section* does not meet acceptance according to Option 3a.

One critical requirement of Option 3a is that the *Calibration Area* must be representative of the *Evaluation Section*. In

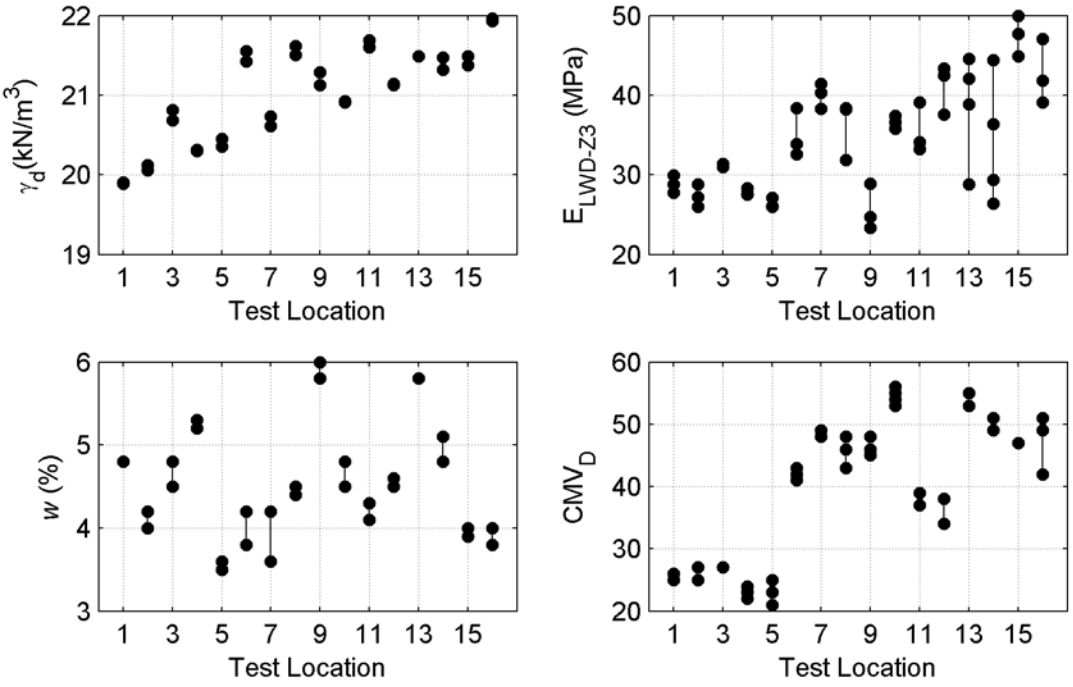

Figure 8.4. Variation in Spot-Test Measurements across the drum width and in roller MV along 1 m (3 ft) in the driving direction.

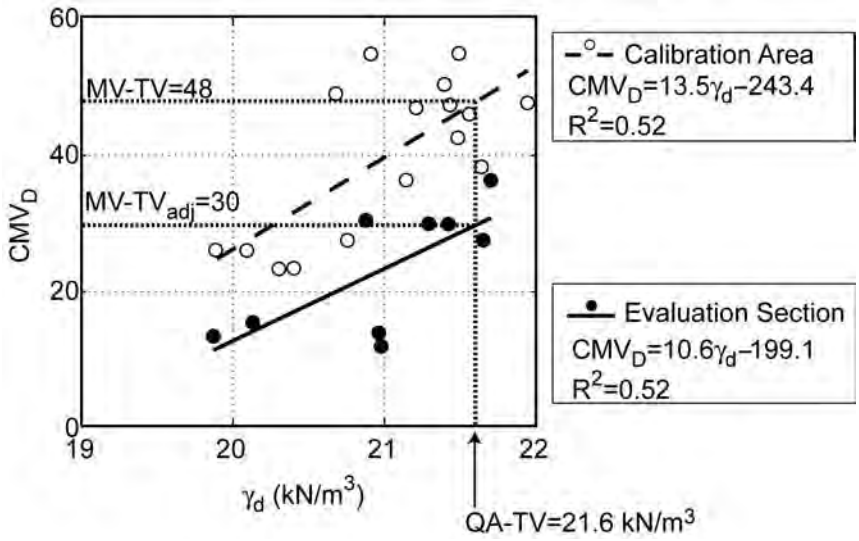

Figure 8.5. Comparison of Calibration Area and Evaluation Section MV-γ_d regression relationships.

retrospect this is an inappropriate *Calibration Area* for the *Evaluation Section*. Figure 8.5 shows a comparison of CMV-γ_d correlations from the *Calibration Area* and *Evaluation Section*, determined from the data presented in Figure 8.2. These correlations are clearly different. The *Calibration Area* is stiffer than the *Evaluation Section* (i.e., for a similar γ_d the roller MVs in the *Evaluation Section* were on average 50% of those measured in the *Calibration Area*). The higher roller MVs in the *Calibration Area* are likely due to the stiffer sublift material. Test bed CO34 represented the fourth 30-cm (12-in) lift of subbase material placed in this *Evaluation Section*. The previous three lifts were also compacted by the research team using the same general boundaries for the *Calibration Area* and *Evaluation Section*. This previous work resulted in the *Calibration Area* receiving additional roller passes (i.e., for research purposes), resulting in a stiffer subsurface in the *Calibration Area* than the rest of the *Evaluation Section*.

Acceptance of the *Evaluation Section* was reevaluated using the correlation from the *Evaluation Section*. Per the γ_d-TV = 21.6 kN/m^3 (137.5 pcf), the adjusted MV target value MV-TV_{adj} = 30. The cumulative distribution of MV_8 data shows that 43% of the *Evaluation Section* met the adjusted MV-TV. Per Option 3a, this *Evaluation Section* would still not meet acceptance.

8.1.5 Discussion

The *Evaluation Section* met project QA acceptance based on a static proof roll after pass 8 and provides some insight into the CCC-based QA Specification Options. Acceptance per Option 1 was not met after pass 8 (the last pass) if the standard spot-test-based criteria are used (i.e., RC-TV = 100%). Using this criterion, Option 1 imposes more stringent requirements than current randomized spot-testing criteria. In the case study presented here, acceptance was met when the RC-TV was relaxed to 92%. The existence of a positive CMV_D-γ_d correlation indicates that the principle of Option 1 is valid. Acceptance per Options 2a and 2b was met after pass 6. While it is not known for sure if the *Evaluation Section* would have passed the static proof roll test after pass 6, these results indicate that Options 2a and 2b, as evaluated here, would have resulted in a similar level of quality as current practice. Implementation of Option 3a was unsuccessful because the *Calibration Area* was not representative of the *Evaluation Section*. An acceptable CMV-γ_d correlation was found in the *Calibration Area*; however, this correlation was considerably different than that observed in the *Evaluation Section*.

Implementation of specification options presented a number of challenges. Construction traffic, particularly haul trucks moving through the earthwork area, often forced less than ideal *Rolling Patterns*. Truck traffic made it difficult to create uninterrupted and repeatable path *Evaluation Area* roller MV maps. Developing the required correlations in the *Calibration Area* required that the haul trucks (delivering material to the *Evaluation Section*) drive around the active earthwork. Contractors commonly utilize haul truck traffic to compact soil, and mandating that they remain off the freshly placed soil represents a significant change to current practice. Further, the pace of the production earthwork placement and compaction—deemed typical—clearly limits the time the research team was able to spend in the *Calibration*

Area. Including the time needed to construct the *Calibration Area*, the correlations were developed in approximately three to four hours, although a time frame of one to two hours would be more consistent with production schedules.

8.2 Case Study II—Stabilized Granular Subgrade (TB FL15)

Specification Options 1, 2a, and 2b were evaluated on a 12-m (40-ft)-wide by 60-m (200-ft)-long by 30-cm (12-in)-thick ash-stabilized sand subgrade *Evaluation Section* in Florida (see Figure 8.6). Due to site limitations, this *Evaluation Section* is smaller than typical. The stabilized subgrade consisted of 23 cm (9 in) of granular subgrade material (A-3) mixed with 7 cm (3 in) of bed ash (Figure 8.6c). Compaction was performed solely by the research team with the Sakai CCC roller and the pass sequence depicted in Figure 8.6. The case study presented here utilizes the $k_{s\text{-}CSM}$ MV computed from independent roller instrumentation (see Section 3.4). Nuclear gauge testing was conducted with a 200-mm (8-in) probe depth (γ_d, w), and LWD testing was conducted with a 300-mm (12-in)-plate-diameter Prima device ($E_{LWD\text{-}P3}$). Five LWD and three nuclear gauge measurements were performed across the width of the drum lane and averaged to represent γ_d and $E_{LWD\text{-}P3}$. Each reported roller MV was determined by averaging over 1 m (3 ft) in the direction of roller travel. Contract QA specifications included γ_d-TV = 98% modified Proctor maximum dry unit weight [γ_d-TV = 15.3 kN/m^3 (97.4 pcf), RC-TV = 98%). There were no QA requirements for moisture. The specification options were evaluated using the contractual γ_d-TV.

8.2.1 Acceptance Using Specification Option 1

Figure 8.7 shows the MV_{11} data map and the results of spot-test measurements performed in the roller-identified weakest areas immediately after the pass 11 *Measurement Pass* [A = 0.9 mm (0.035 in), v = 4.0 km/h (2.5 mph), f = 25 Hz)]. Two roller-identified weakest areas were selected for

Test bed construction:
30 cm (12 in) lift of ash-stabilized subgrade material (23 cm (9 in) of A-3 subgrade + 7 cm (3 in) of bed ash) placed atop previously compacted subgrade, mixed prior to compaction, no water conditioning performed

Test bed compacted via the following Pass Sequence:
P1: *A*=2.1 mm (0.083 in), forward; P2: *A*=0.9 mm (0.035 in), reverse;
P3: *A*=2.1 mm (0.083 in), forward; P4: *A*=0.9 mm (0.035 in), reverse;
P5: *A*=0.9 mm (0.035 in), forward; P6: Static (A=0), reverse;
P7: *A*=0.9 mm (0.035 in), forward; P8: Static (*A*=0), reverse;
P9: *A*=0.9 mm (0.035 in), forward; P10: Static (*A*=0), reverse;
P11: *A*=0.9 mm (0.035 in), forward; P12: Static (*A*=0), reverse;
v=4.0 km/h (2.5 mph) for all passes, *f*=25 Hz for all vib. passes

Figure 8.6. Overview of TB FL15 showing (a) a Measurement Pass, (b) spot testing with the nuclear density gauge, and (c) mixing the ash and soil.

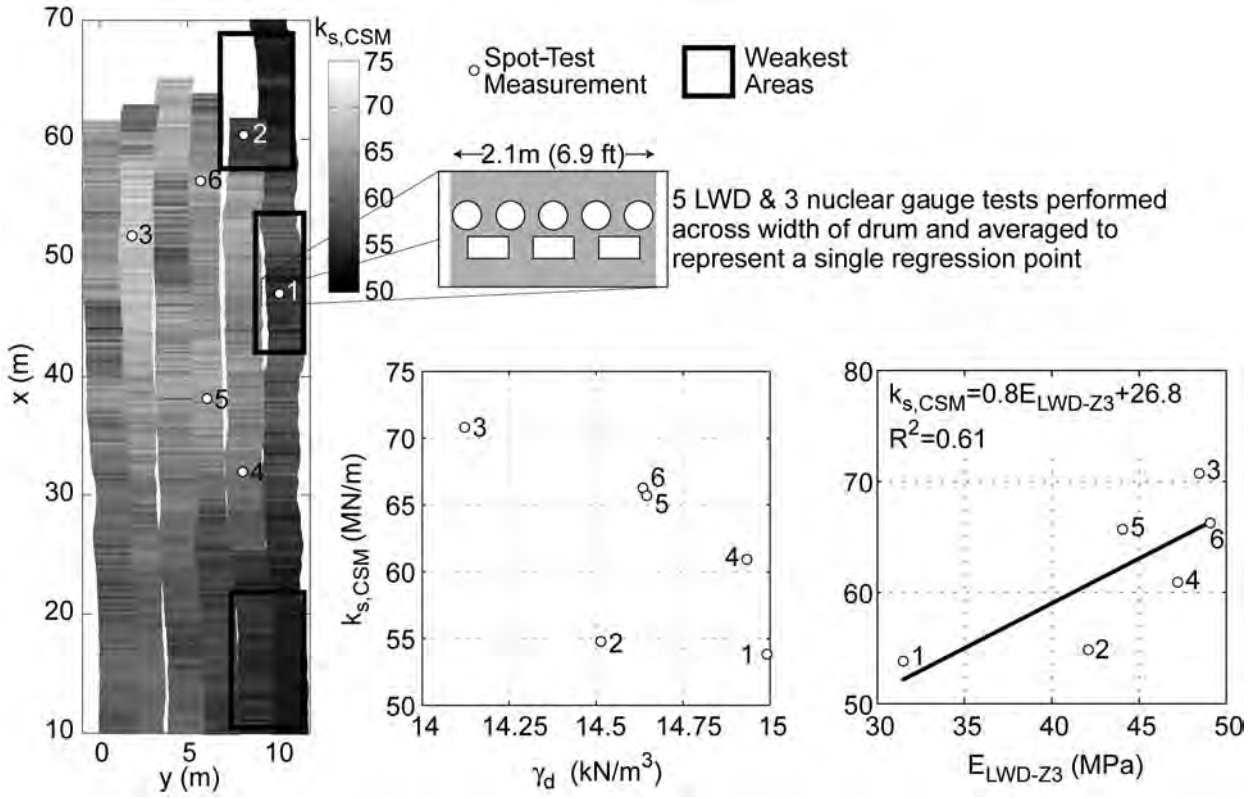

Figure 8.7. Spatial MV data obtained during the final Measurement Pass over TB FL15 and regression relationships between roller MV and Spot-Test Measurements.

spot testing. The third area was not tested due to time constraints. Table 8.4 shows that none of the six spots tested met the γ_d-TV or RC-TV; therefore, the *Evaluation Section* does not meet acceptance according to Option 1. Further compaction would have been required to meet acceptance based on current practice. Since the test bed was being constructed for research purposes, further compaction was not immediately pursued.

As with the results from TB CO34, it can be argued that requiring 98% relative compaction in the weakest areas is more stringent than the existing Florida approach in which test locations are randomly selected. For example, five of the six weakest areas would meet an RC-TV = 94% criteria. For this reason, individual agencies must carefully consider existing QA criteria and spot-testing practice when establishing acceptance criteria for Option 1. In addition, the fact that this area received 11 roller passes and was still not fully compacted according to Option 1 calls into question this particular γ_d-TV.

It is important to note that there is not a positive correlation between the roller MV and γ_d (Figure 8.7). This implies that the areas with low roller MVs do not necessarily correspond to areas with low density. This result implies that Option 1 should be used with caution, and a higher spot-test measurement frequency may be desired.

Table 8.4. Option 1: Spot-Test Measurements from weakest areas.

Location	γ_d (kN/m^3)	Relative Compaction[a]
1-1	15.2 (96.7)	97.4%
1-2	15.1 (96.1)	96.8%
1-3	14.7 (93.6)	94.2%
2-1	14.8 (94.2)	94.9%
2-2	14.8 (94.2)	94.9%
2-3	14.0 (89.1)	89.7%

[a]Based on maximum modified Proctor γ_d = 15.6 kN/m^3 (99.4 pcf).

8.2.2 Acceptance Using Specification Option 2a

Table 8.5 provides $\%\Delta\mu_{MV_i}$ for several consecutive passes (with constant operating parameters as listed above). Based on a %Δ-TV = 5%, the *Evaluation Section* meets acceptance after pass 9. Recall that the *Evaluation Section* had not met acceptance based on current practice after pass 11. This implies that Option 2a is less stringent than current practice for this *Evaluation Section.*

Table 8.5. Summary of μ_{MV_i} and $\%\Delta\mu_{MV_i}$ from TB FL15.

Pass	μ_{MV_i}	$\%\Delta\mu_{MV_i}$
5	50.8	—
6	NA[a]	—
7	56.8	11.7%
8	NA	—
9	58.5	3.0%
10	NA	—
11	59.9	2.4%

[a] Pass was static; no MV data are available.

8.2.3 Acceptance Using Specification Option 2b

The repeatability of $k_{s\text{-}CSM}$ at the Florida work site was determined to be 5% based on the procedure in Section 7.5.3.1; therefore, the Option 2b %Δ-TV was set equal to 10% for this case study. As with Case Study I, a %Area-TV = 80% was used. Figure 8.8 shows $\%\Delta MV_i$ for passes 9 and 11. The cumulative distributions of the $\%\Delta MV_i$ are also shown. Nearest neighbor interpolation was used to transform the data onto a fixed grid. As illustrated, 92% of the *Evaluation Section* met the %Δ-TV after pass 9. This percentage is greater than the %Area-TV, and therefore acceptance was met according to Option 2b after pass 9.

8.2.4 Discussion

As shown in Table 8.1, TB FL15 did not meet contract QA requirements for γ_d at the end of compaction. The test bed was constructed for research purposes, and further compaction (beyond 12 passes) was not immediately pursued. The *Evaluation Section* also failed to meet acceptance based on Option 1; however, it did meet acceptance based on Options 2a and 2b. These results imply that Options 2a and 2b may be less stringent than the other options and current practice. To

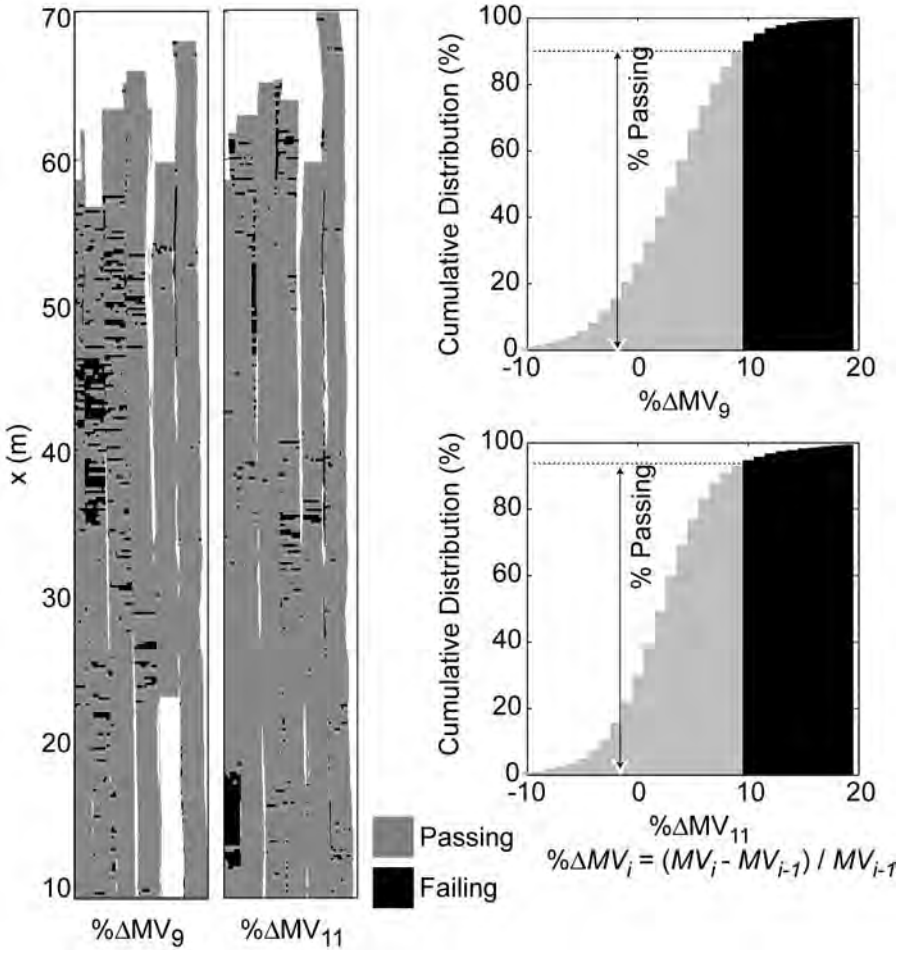

Figure 8.8. Percentage change in MV maps for passes 7, 8, and 9 ($\%\Delta MV_9$) and passes 9, 10, and 11 ($\%\Delta MV_{11}$) and cumulative distributions of percentage change showing percentage of area.

improve reliability, it may be desirable to implement Option 2a or 2b in conjunction with Option 1.

This case study also illustrated the importance of assessing whether or not a positive correlation exists between the roller MV and the spot-test measurements used for QA. Option 1 should be used with caution, and more spot-test measurements may be needed when an acceptable ($R^2 > 0.50$) positive correlation does not exist.

8.3 Case Study III—TB FL19 Aggregate Base

Construction of TB FL19 involved placing and compacting a nominal 0.15-m (0.50-ft)-thick aggregate base layer (AASHTO: A-1-b) over a compacted stabilized subgrade layer using the Dynapac smooth drum IC roller (with the CMV_D measurement system). Maximum dry unit weight (γ_{dmax}) and corresponding optimum moisture content (w_{opt}) per modified Proctor method (AASHTO T-180) were 18.2 kN/m³ (116.0 pcf) and 11.5%, respectively. Project specifications required that the base material be compacted to an RC-TV = 98% [γ_d-TV = 17.86 kN/m³ (113.70 pcf)]. No moisture control was required by the project specifications. To evaluate the influence of underlying support conditions on compaction layer roller CMV_D, the stabilized subgrade layer was mapped at nominal $A = 1.1$ mm (0.043 in), $f = 30$ Hz, and $v = 4.5$ km/h (2.8 mph) settings, prior to placing the base layer.

The *Evaluation Section* had plan dimensions of about 9.1 m × 275 m (30 ft × 917 ft). An approximate area of 2.4 m × 30 m (8 ft × 100 ft) at the southern end of the *Evaluation Section* was selected as the *Calibration Area* for Option 3a. The compaction layer fill material was placed using dump trucks, spread using a dozer, and leveled using a motor grader to the desired elevation. Compaction of the *Calibration Area* is described below. The *Evaluation Section* was compacted in manual mode using constant operation settings at nominal $A = 0.9$ mm (0.035 in), $f = 30$ Hz, and $v = 4.0$ to 4.5 km/h (2.5 to 2.8 mph). The *Evaluation Section* received uneven compaction from construction traffic during placing, spreading, and leveling operations. With the aid of the CMV_D map on the onboard computer, compaction efforts were focused in areas with low CMV_D. Compaction passes over the *Evaluation Section* varied from 6 to 15 roller passes. The compaction process was terminated when field observations indicated that additional compaction was not improving the CMV_D values. More details on the construction and testing procedures followed on this test bed are provided in Appendix D.

8.3.1 Acceptance Using Specification Option 3a

8.3.1.1 Calibration Area Testing and Analysis to Establish MV-TVs

After the material was placed and leveled, the *Calibration Area* was scarified to the bottom of the compaction layer using a motor grader. The test area was compacted with 13 roller passes at nominal $A = 0.9$ mm (0.035 in), $f = 30$ Hz, and $v = 4.0$ to 4.5 km/h (2.5 to 2.8 mph) settings. In situ moisture-density (using nuclear gauge), CBR (from DCP), and $E_{LWD\text{-}Z3}$ point measurements were obtained at five locations across the test strip with three measurements across the drum width at each test location (Figure 8.9). Moisture-density tests were conducted using a probe penetration depth of 150 mm (6 in). Point measurements were obtained after 1, 2, 3, 4, 8, and 12 roller passes.

Figure 8.10 shows spot-test measurements in comparison with the CMV_D. CMV_D data are shown as solid lines and point measurement as discrete points. Results show that both the CMV_D and in situ measurement values increased with increasing passes. Compaction growth for CMV_D and spot-test measurements are presented in Figure 8.11, with a hyperbolic fit to the average data. The curves indicate that, on average, the CMV_D, $E_{LWD\text{-}Z3}$, and γ_d measurements generally increased up to 12 roller passes. At 12 passes the required γ_d-TV (98% of T-180 γ_{dmax}) could not be reached as the material was, on average, 3% dry of w_{opt} (see Figure 8.12).

Figure 8.9. Calibration Area and Evaluation Section (TB FL19).

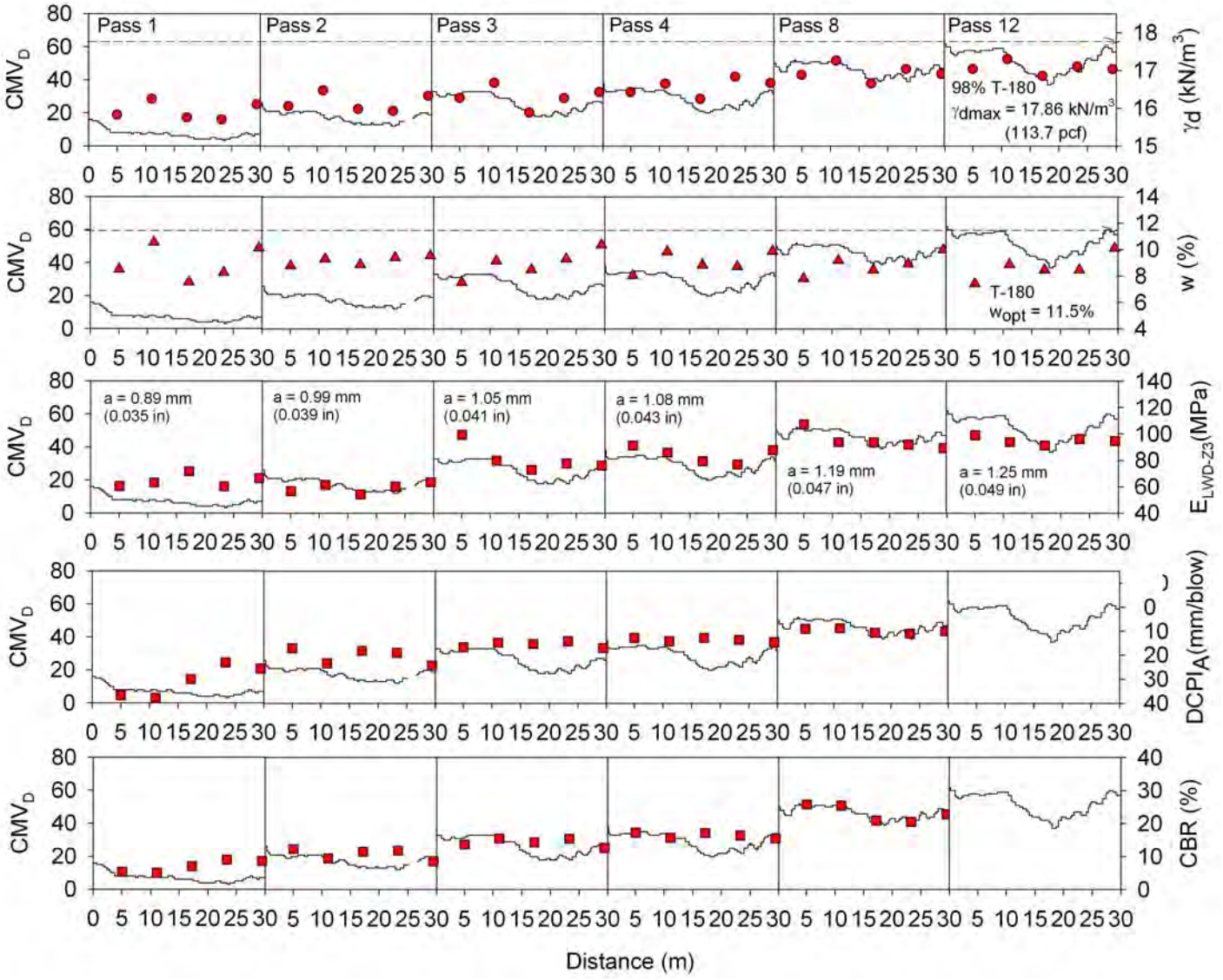

Figure 8.10. Roller MV (CMV_D) and in situ compaction measurement comparison for select roller passes from the calibration area.

Linear regression relationships between spot-test measurements and CMV_D were developed based on spatially nearest data (see Figure 8.13). Because the required γ_d-TV could not be achieved, the target values were selected from the field compaction curves for illustration purposes. As indicated in Figure 8.11, $E_{LWD\text{-}Z3}$ and γ_d corresponding to 98% of the hyperbolic curve asymptote were considered as QA-TVs [E_{LWD}-TV = 90 MPa and γ_d-TV = 16.80 kN/m³ (107 pcf)]. Using the *inverse regression* approach and an 80% upper prediction limit, MV-TV = 49 was established, corresponding to the E_{LWD}-TV and γ_d-TV. As described in Chapter 7, use of prediction limits in selecting the MV-TV accounts for the uncertainty in the relationships and can be used to increase the confidence in the estimated target value.

8.3.1.2 Assessment of Evaluation Section

Following compaction passes, the *Evaluation Section* was mapped using constant operation settings at nominal A = 0.9 mm (0.035 in), f = 30 Hz, and v = 4.0 to 4.5 km/h (2.5 to 2.8 mph). The CMV_D map and the frequency distribution of CMV_D from the *Evaluation Section* are presented in Figures 8.14 and 8.15, respectively. Using Specification Option 3a, approximately 32% of the area did not achieve the MV-TV, and therefore this *Evaluation Section* would not meet the acceptance requirements. An important finding is that the correlations between CMV_D and spot-test measurements in the *Evaluation Section* were not as defined as in the *Calibration Area* (Figure 8.14). As discussed below, the reason for scatter

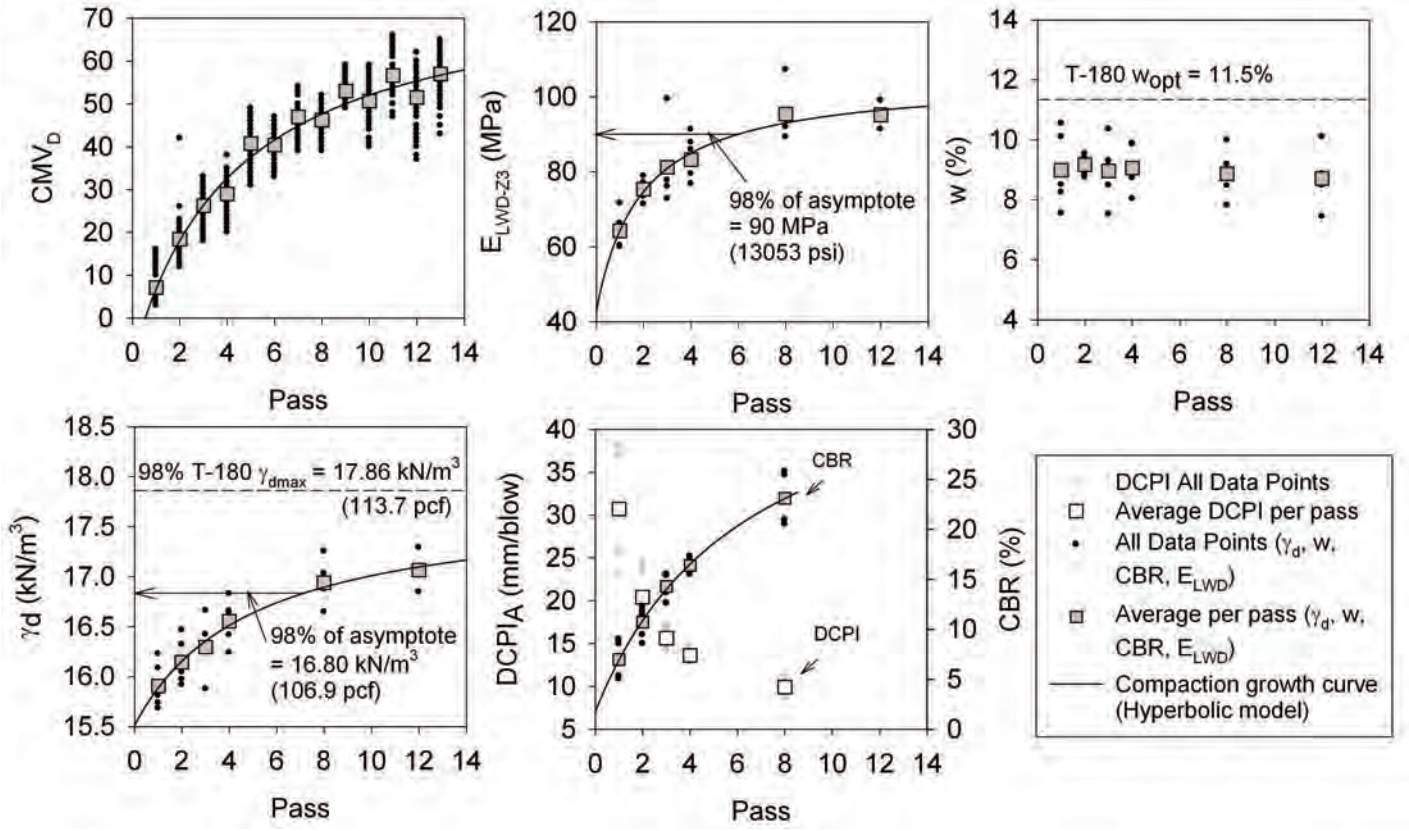

Figure 8.11. Compaction growth curves for roller MV (CMV_D) and spot-test measurements from the calibration strip (point measurements represent average of three measurements across the drum width).

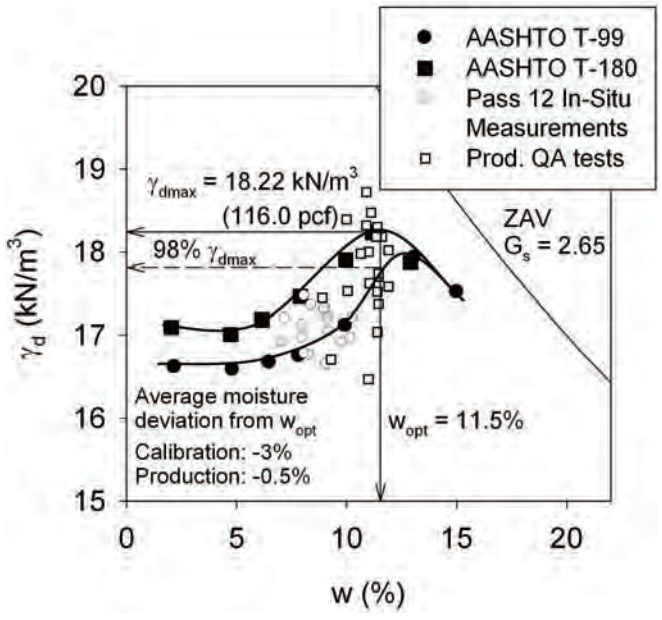

Figure 8.12. Comparison of laboratory Proctor compaction curves and in situ moisture and dry unit weight measurements.

in the *Evaluation Section* relationships is attributed to heterogeneity in the underlying layers.

In situ spot tests (γ_d and $E_{LWD\text{-}Z3}$) were performed at 23 test locations across the *Evaluation Area*, of which 12 locations consisted of areas with CMV_D < MV-TV. In situ spot tests and corresponding CMV_D comparison measurements (based on nearest point data) are compared with calibration regression relationships in Figure 8.14. Out of 23 spot tests performed in the *Evaluation Section*, eight $E_{LWD\text{-}Z3}$ and one γ_d test measurements failed to meet their respective QA-TVs. To further investigate the areas that met the γ_d-TV but not the E_{LWD}-TV requirement, DCP tests were conducted at five select test locations (8, 13, 19, 23, 25), extending into the stabilized subgrade layer to a depth of about 380 to 500 mm below the surface. CBR values were calculated from the DCP index values. To help interpret the CBR values, a target CBR = 21 was determined using a regression relationship obtained from calibration, corresponding to the MV-TV = 49 and 80% prediction interval (Figure 8.13). CBR profiles showed a zone (about 70 to 250 mm in thickness) of low CBR (< 21) in the stabilized subgrade layer at depths of about 190 to 300 mm (7.6 to 12.0 in) below the surface at test locations 8, 13, 15, 17,

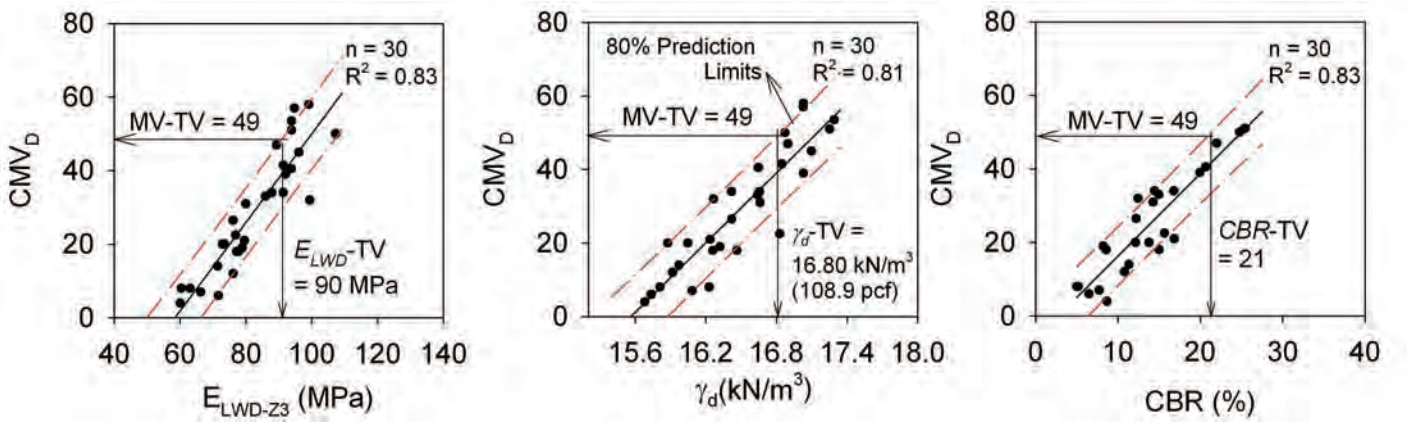

Figure 8.13. Simple regression relationships between roller MV (CMV_D) and Spot-Test Measurements with 80% prediction limits to establish MV-TVs (each test point represents an average of three spot-test measurements across the drum width).

19, 23, and 25 (see Figure 8.14). Low CMV_D and $E_{LWD\text{-}Z3}$ values at these test locations were likely influenced by these "weak" zones, while the compaction layer γ_d values were not, with the exception of test location 8. CBR profiles at two test locations (15 and 17) with CMV_D > MV-TV are also shown in Figure 8.14 for reference. These tests were terminated in the stabilized subgrade due to low penetration values [< 5 mm (0.198 in)/blow, which is about CBR > 48]. This example demonstrates how soft underlying layers affect CMV_D and how DCP testing can be used to identify these conditions and illustrates the importance of ensuring that the *Calibration Area* is representative of the *Evaluation Section*.

8.3.2 Implementation of Spatial Statistics for Nonuniformity Analysis

To demonstrate the approach of establishing nonuniformity criteria using spatial statistics, an experimental semivariogram of CMV_D from the *Calibration Area* was developed (Figure 8.15). A Gaussian theoretical model was fit to the experimental semivariogram with *sill* = 90, *range* = 7 m, and *nugget* = 0. The theoretical model was selected based on comparatively better least squares fit than other models (e.g., spherical, exponential), modified Cressie goodness of fit (Clark & Harper 2002), and cross-validation process (see Vennapusa et al. 2009 for full description of model fitting process). For acceptance using the *sill*-based nonuniformity criteria, an *Evaluation Section* with length equivalent to the *Calibration Area* should have *sill* values lower than the target *sill* (i.e., *sill* from the *Calibration Area*).

The CMV_D data from the *Evaluation Section* were evaluated for nonuniformity by plotting semivariograms for four select areas of length equal to the length of the calibration test area (~30 m). Only two of the four selected areas showed *sill* values < 90. It is clear that the *Evaluation Section* showed significantly greater spatial nonuniformity compared to the *Calibration Area*. This greater nonuniformity is attributed primarily to nonuniform conditions in the underlying stabilized subgrade layer, as shown in the stabilized subgrade CMV_D map (Figure 8.16) and previously verified with full-depth DCP index tests (Figure 8.14).

In short, the nonuniformity criteria established from the *Calibration Area* could not be met in the *Evaluation Section* due to the influence of heterogeneous underlying layer properties. Similar to the MV spot-test calibration analysis for Option 3a, it should be noted that this nonuniformity criterion is limited to conditions with *Evaluation Section* having similar spatial heterogeneity in underlying support conditions with respect to the *Calibration Area*. In this case study it was not. However, more research is needed in relating nonuniformity to performance for a better understanding of what level of uniformity is desired and how field operations can be improved to control nonuniformity.

8.3.3 Comparison to Existing German, ISSMGE, and Mn/DOT Specifications Acceptance Criteria

Comparison of acceptance using Specification Option 3a to the German, ISSMGE, and Mn/DOT acceptance criteria is presented in Figure 8.17. The German specifications (see Section 2.3.1) are very similar to Specification Option 3a, except the use of prediction limits is not specified. Acceptance requires that 90% of roller MVs in the *Evaluation Section* must exceed the MV-TV. As shown in Figure 8.17, the MV-TV from the linear regression relationship is 38. A frequency distribution plot indicates that 94% of the CMV_D is greater than the

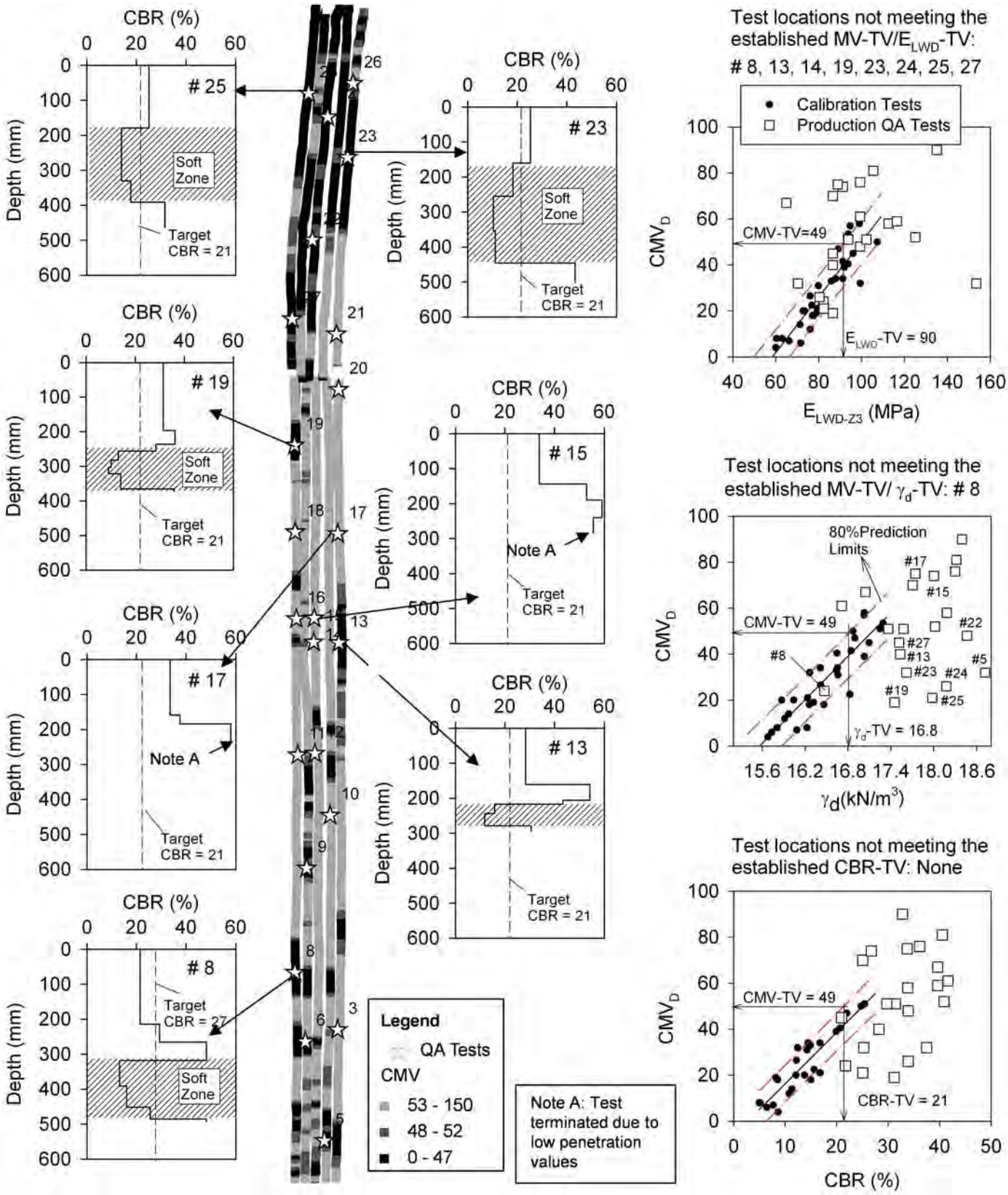

Figure 8.14. CMV$_D$ map of the Evaluation Section and CBR profiles at select locations.

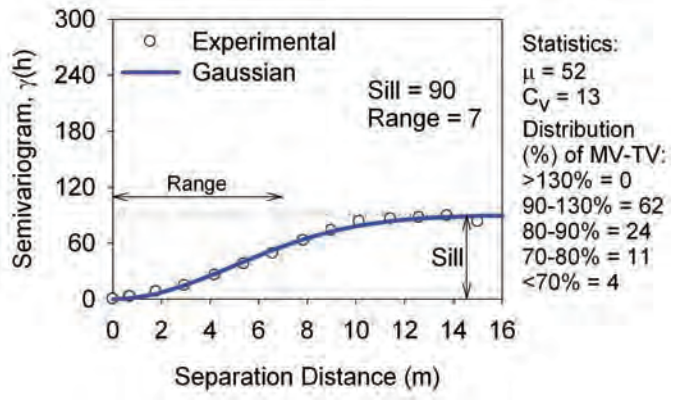

Figure 8.15. Semivarigoram, univariate statistics, and distribution of CMV_D from the Calibration Area.

MV-TV; therefore, the *Evaluation Section* does meet the German acceptance requirements.

ISSMGE specifications are described in Section 2.3.2. In brief, the mean TV in the *Evaluation Section* ME should be greater than ME-TV, all MVs within 0.8 MIN-TV, and MAX-TV with coefficients of variation (COVs) < 20%. Procedures for establishing ME-TV (~44), MIN-TV (~33), and MAX-TV (~50) are described in Figure 8.17. The frequency distribution plot of CMV_D data from the *Evaluation Area* indicates that ME = 56 and is greater than the ME-TV, but only about 63% of the data falls within 0.8 MIN-TV and MAX-TV. Therefore, the *Evaluation Area* does not meet acceptance. Further, the CMV_D COV was 27%, which exceeds the acceptance limit of 20%. The nonuniformity criteria were thus not achieved following the ISSMGE criteria, and reworking the *Evaluation Section* would be required.

Mn/DOT specifications are described in Section 2.3.4. In brief, the acceptance criterion calls for 90% of the roller MVs in the *Evaluation Section* to be within 90% to 130% of the MV-TV determined from the *Calibration Area.* The MV-TV (~53) determined using Mn/DOT procedure is shown in Figure 8.17. The CMV_D frequency distribution plot for the *Evaluation Section* showed that only 56% of the MVs are within the 90% to 130% range. Therefore, the Mn/DOT acceptance criterion was not achieved.

8.4 Case Study IV—TB FL23 Granular Subgrade

A *Calibration Area* (see test bed FL23 in Appendix D) was constructed prior to compaction in the *Evaluation Section.* Specification Options 1 and 2b do not require calibration, whereas calibration is required for Specification Option 3. QA for this project was based on achieving a target γ_d. For illustration purposes, an E_{LWD} target value was also selected for assessment of the *Evaluation Section* for Specification Option 3a. Compaction operations in the *Calibration Area* and *Evaluation Section* were performed with a Case IC roller with the k_s measurement system at constant settings, with nominal $A = 1.1$ mm (0.043 in), $f = 30$ Hz, and $v = 4.0$ km/h (2.5 mph). Moisture and dry unit weight tests (using nuclear gauge) were conducted using a probe penetration depth of about 150 mm (6 in), and LWD tests were conducted by excavating the loose surface sand to a depth of 50 to 75 mm (2 to 3 in) below the surface (see White et al. 2007).

Construction of TB FL23 involved scarifying the in-place embankment subgrade material (AASHTO: A-1-b) to a depth of 0.2 to 0.3 m (0.6 to 1.0 ft) below grade and compacting using the smooth drum Case IC roller. Maximum dry unit weight (γ_{dmax}) and corresponding optimum moisture content (w_{opt}) as determined by the standard Proctor method (AASHTO T-99) for the subgrade material were 15.9 kN/m^3 (101.2 pcf) and 8.3%, respectively. Project specifications required that the subgrade material be compacted to ≥ 95% standard Proctor γ_{dmax} [γ_d-TV = 15.11 kN/m^3 (96.2 pcf)]. Moisture control was not required by the project specifications. The *Evaluation Section* (FL23B) consisted of plan dimensions of about 12 m × 275 m (36 ft × 825 ft; see Figure 8.18). A lane located adjacent to the production test bed with material in a relatively loose and noncompacted state was arbitrarily selected for the *Calibration Area* (FL23A). The calibration test area was about 2.4 m × 60 m (7.2 ft × 180 ft).

8.4.1 Acceptance Using Specification Option 1

Acceptance for this option is based on achieving the γ_d-TV in roller-identified weakest areas, identified from the k_s data map of the *Evaluation Section.* In situ γ_d point measurements were conducted after pass 6 and focused in the weakest areas, where k_s < 23 MN/m. The tests results are summarized in a histogram plot shown in Figure 8.19. The relative compaction at these test measurements was between 97% and 109% of standard Proctor γ_{dmax}. Therefore, the *Evaluation Section* met the acceptance requirements of Specification Option 1 as well as current practice where testing is performed at discrete random locations.

8.4.2 Acceptance Using Specification Option 2a

This specification option requires evaluating the change in mean k_s ($\Delta\mu k_s$) with successive passes over the *Evaluation Section.* The *Evaluation Section* was compacted with six roller passes with constant roller operation settings as de-

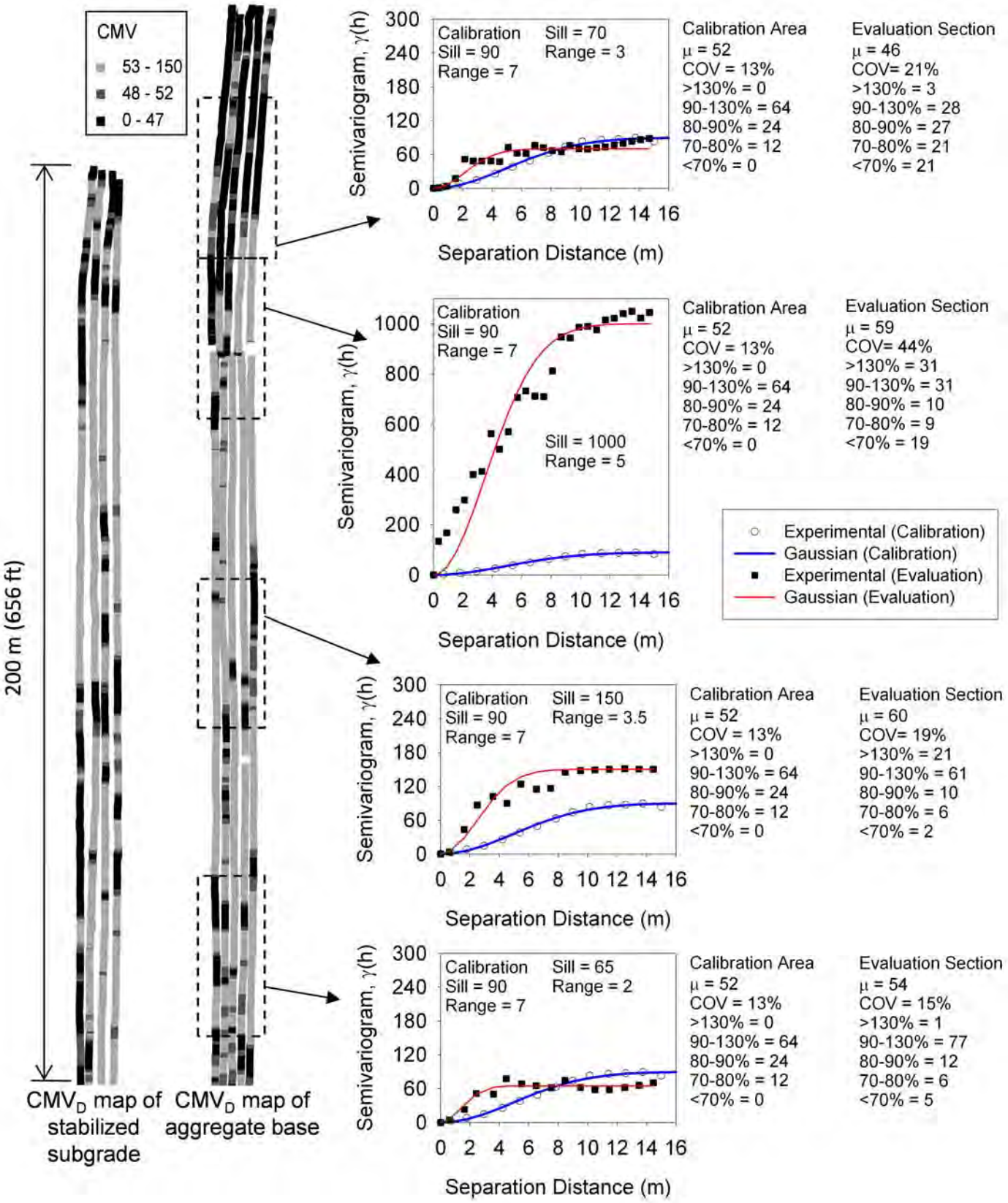

Figure 8.16. Uniformity-based acceptance criterion for Evaluation Section using spatial and univariate statistics.

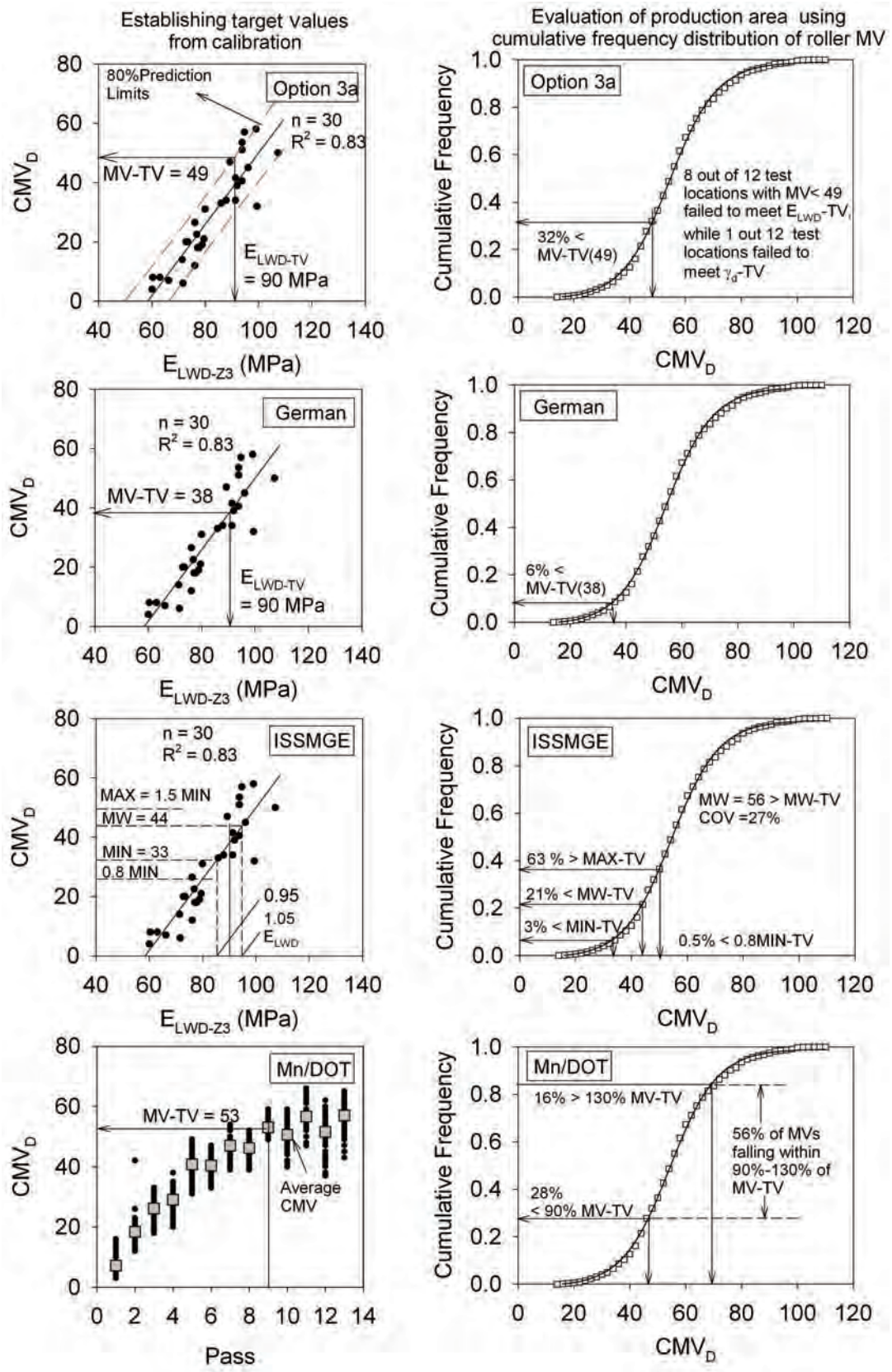

Figure 8.17. Evaluation of the Evaluation Section using Specification Option 3a in comparison to German, ISSMGE, and Mn/DOT acceptance criteria.

Figure 8.18. Calibration Area and Evaluation Section for TB FL23.

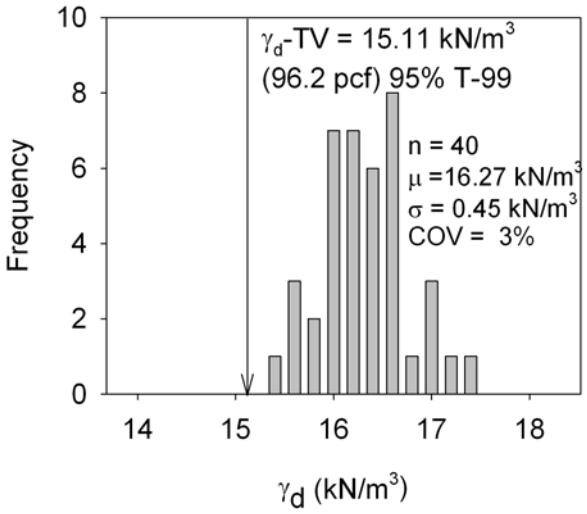

Figure 8.19. Histogram of QA test measurements in the Evaluation Section.

Table 8.6. Summary of Δk_s and $\Delta\mu k_s$ successive passes in the Evaluation Section.

Parameter	1	2	3	4	5	6
μk_s	16	20	20	21	20	20
$\Delta\mu k_s$	—	20	3	2	-2	2
Percent area $\Delta k_s \leq 5\%$	—	4	69	80	94	80

scribed above. As shown in Table 8.6, the target $\Delta\mu k_s$ of 5% was achieved after pass 3. Therefore, the *Evaluation Section* met the acceptance requirements of Specification Option 2a. No QA point measurements were obtained immediately after pass 3. QA measurements obtained after pass 6 are described in Figure 8.19, which indicated that all the measurements met the project's γ_d-TV per current practice.

8.4.3 Acceptance Using Specification Option 2b

This specification option requires evaluating the spatial percentage change in k_s (Δk_s) with successive passes over the *Evaluation Section*. To allow pass-to-pass comparison of the spatial k_s data, the data were placed on a fixed grid using kriging (see Figure 8.20). To perform the kriging, an omni-directional exponential variogram model was used and the data were assumed to be stationary. Fitting weights were not employed, and anisotropy was not considered. Average Δk_s and percent area with ≤ 5% Δk_s between successive passes is presented in Table 8.6. The target requirement of $\Delta k_s \leq 5\%$ over 90% of the area was met at pass 5. It is interesting to note that while the acceptance is met after pass 5, acceptance would not have been met after pass 6. This is possibly due to decompaction during pass 5 and subsequent recompaction during pass 6. Further, the kriged maps show two distinctly different compaction curves for areas 1 and 2, as highlighted in Figure 8.20, while the Δk_s curve was similar for the two areas. As discussed in the following section, these two areas contained different underlying layer conditions.

8.4.4 Acceptance Using Specification Option 3a

8.4.4.1 Initial Calibration

This specification option requires calibration of k_s to spot-test measurements from a *Calibration Area*. The selected *Calibration Area* was compacted with eight roller passes at constant machine operation settings. In situ γ_d and E_{LWD} point measurements were obtained at 10 locations across the *Calibration Area*. Tests were conducted after 1, 2, 4, and 8 roller passes. Linear regression relationships between γ_d, E_{LWD}, and k_s were developed based on spatially nearest data, as presented in Figure 8.21. Using the *inverse regression* approach and an 80% prediction interval, MV-TV = 23 MN/m was established, corresponding to the γ_d-TV. Moisture content was not a significant parameter in the regression analysis. To demonstrate the use of E_{LWD} as an alternate QA tool, E_{LWD}-TV = 28 MPa corresponding to the MV-TV and 80% prediction interval was established, as shown in Figure 8.21.

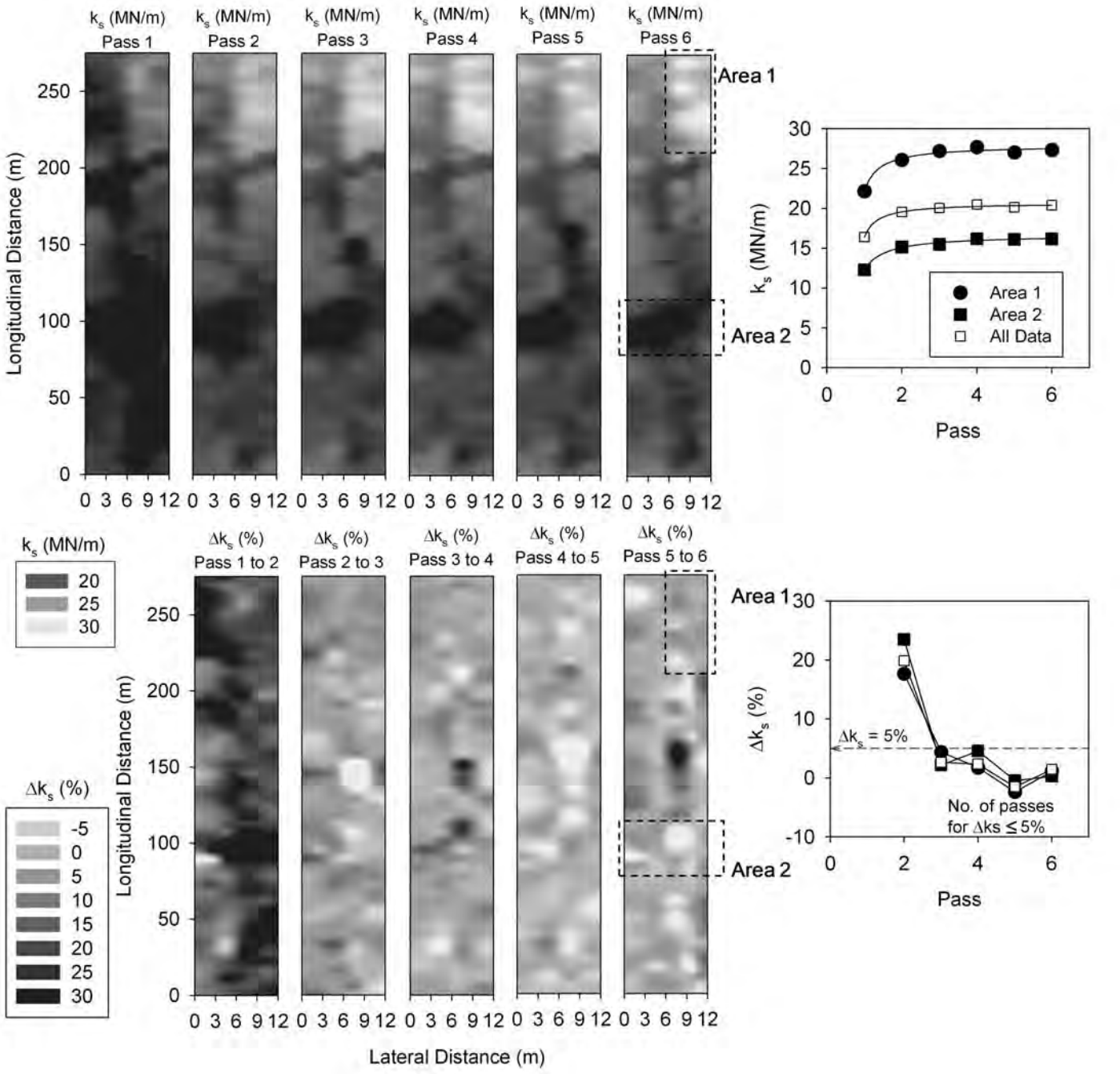

Figure 8.20. Kriged spatial maps of k_s from pass 1 to pass 6 and corresponding percent increase in roller k_s for each consecutive pass.

8.4.4.2 Assessment of Evaluation Section

After compaction operations in the *Evaluation Section*, the area was mapped using the same constant roller operation settings as in the *Calibration Area*. The k_s map of the *Evaluation Section* is shown in Figure 8.22. Acceptance using this option is based on achieving $k_s \geq$ MV-TV for a set percentage of the *Evaluation Section*, in this case 90% (similar to German practice). Analysis of the *Evaluation Section* showed only 20% of roller $k_s >$ MV-TV; therefore, the *Evaluation Section* does not meet acceptance per Option 3a.

In situ γ_d and E_{LWD} point measurements were obtained at 40 test locations, with 33 test locations in areas where $k_s <$ MV-TV. Spot-test measurements and corresponding k_s (based on

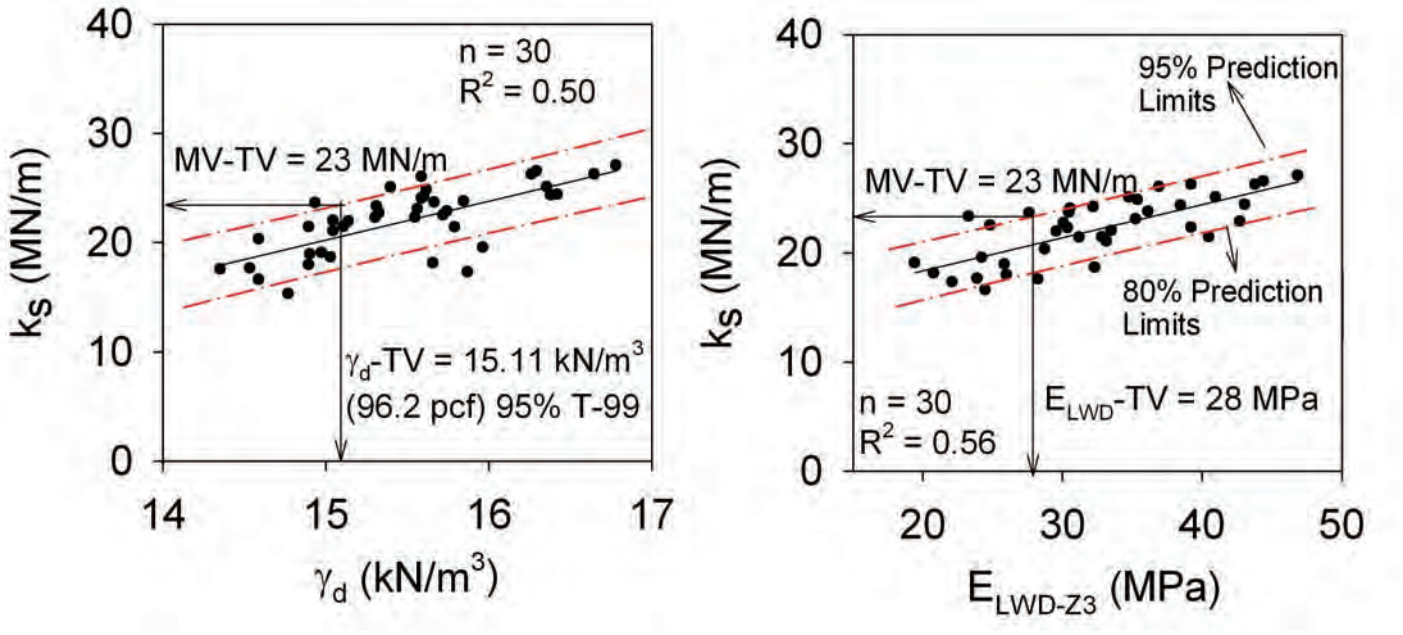

Figure 8.21. Linear regression relationships between spot-test measurements and k_s from the Calibration Area (TB FL23A).

nearest point data) are compared with calibration relationships in Figure 8.22. All of the γ_d measurements met the requirement with 97% to 109% of standard Proctor γ_{dmax} (see Figure 8.19). E_{LWD} at 12 of 40 locations failed to meet the E_{LWD}-TV. Inspection of Figure 8.22 reveals that the E_{LWD} data from the *Evaluation Section* generally follows the same trend as that from the *Calibration Area* and therefore for the selected *Calibration Area* appears appropriate for QA based on correlation to E_{LWD}-TV. However, the γ_d data from the *Evaluation Section* do not exhibit the same trend as that from the *Calibration Area,* and therefore the selected *Calibration Area* is not suitable for QA based on correlation to γ_d-TV. This illustrates a limitation of this calibration approach. Because of the lack of a suitable *Calibration Area*, it is not possible to comment here on how Option 3a compares to existing spot-test-based QA for this case.

To further investigate the locations that did not meet the E_{LWD}-TV, DCP tests were conducted at five select locations (10, 18, 24, 18, and 37) extending to about 500 mm below surface. DCP tests were also conducted at two locations where k_s > MV-TV (2 and 5) for comparison. CBR values were calculated from DCP index values following ASTM D6951. CBR profiles at the test locations are shown in Figure 8.22. At locations where E_{LWD} tests failed, CBR profiles showed lower underlying support conditions. CBR values at those locations were in the range of 5 to 12 from 100 to 400 mm (4 to 16 in) depth, which is low compared to locations 2 and 5, where the average CBR was > 25 from 100 to 400 mm (4 to 16 in) depth.

8.4.5 Acceptance Using Specification Option 3b

This specification option requires evaluating the change in k_s (Δk_s) between successive passes in *Calibration Area* to establish an MV-TV. Results obtained from the *Calibration Area* are presented in Table 8.7, with average Δk_s and percent area with ≤ 5% Δk_s between successive passes. The compaction growth curve for k_s, average Δk_s, and γ_d point measurements with a hyperbolic curve fit to the average data is presented in Figure 8.23. Five passes were required to achieve the requirement of $\Delta k_s \leq 5\%$ over 90% of the *Calibration Area.* The γ_d-TV was met at 9 of 10 test locations after four passes. The average k_s corresponding to pass 5 was MV-TV = 23 MN/m.

Acceptance using this option is based on *Evaluation Section* $k_s \geq$ MV-TV. A cumulative frequency distribution plot of *Evaluation Section* k_s is presented in Figure 8.24 and shows about 80% of $k_s <$ MV-TV. Note that this option mandates that the *Calibration Area* be representative of the larger *Evaluation Section*, which as shown earlier was not the case for this case study. Therefore, comparisons to existing practice should be treated with caution.

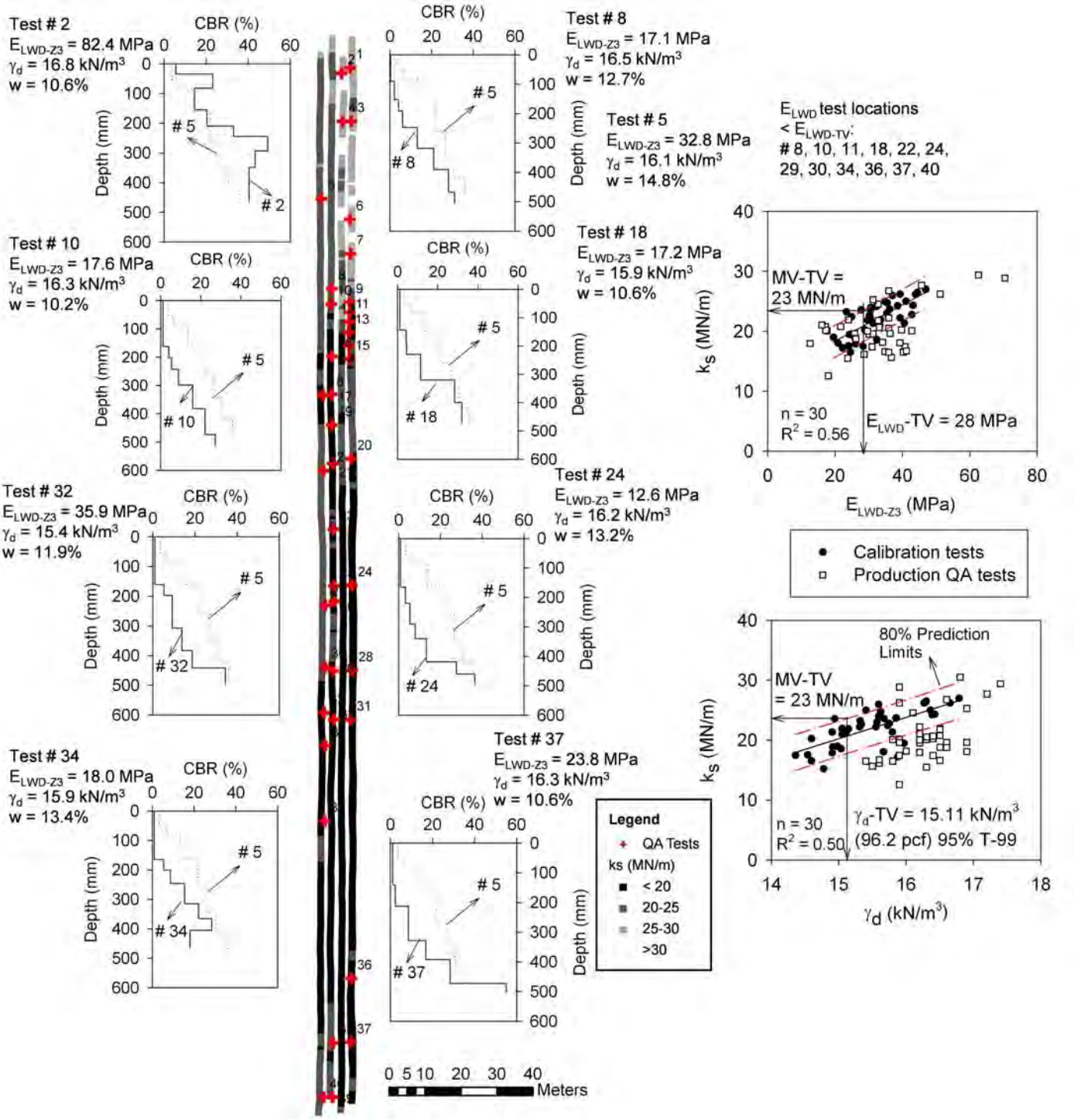

Figure 8.22. k_s map of the Evaluation Section, CBR profiles at select locations, and comparison of production test measurements with the established QA criteria.

Table 8.7. Δk_s from successive passes in the Calibration Area.

Δk_s	Pass 1 to 2	Pass 2 to 3	Pass 3 to 4	Pass 4 to 5	Pass 5 to 6	Pass 6 to 7	Pass 7 to 8
Average	20	5	4	-2	1	2	5
Percent area with ≤5%	0	52	75	94	87	89	59

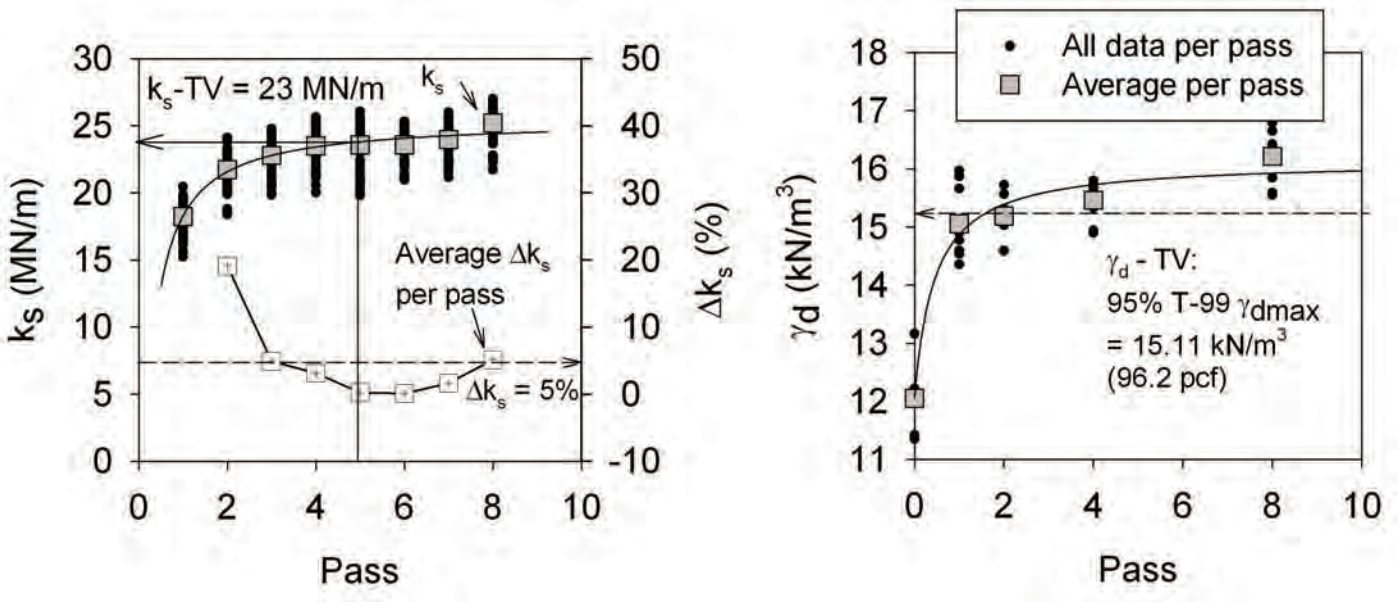

Figure 8.23. Compaction curves for k_s, Δk_s, and spot-test measurements.

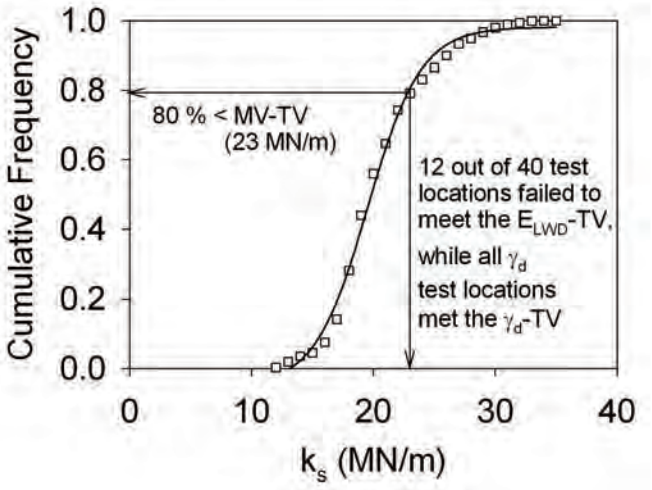

Figure 8.24. Cumulative frequency distribution plot of Evaluation Section k_s.

8.4.6 Comparison to German, ISSMGE, and Mn/DOT Specifications Acceptance Criteria

Acceptance criteria using the existing German, ISSMGE (2005), and Mn/DOT (2007) specifications are presented in Figure 8.25. Correlation between k_s and γ_d measurements is not recommended in the German specifications and therefore was not evaluated. E_{LWD} values were considered. As shown in Figure 8.25, 35% of the *Evaluation Section* met this requirement of MV-TV ≥ 21; therefore, the *Evaluation Section* does not meet acceptance.

Correlation between k_s and γ_d measurements is not recommended in ISSMGE specifications; therefore, E_{LWD} values were again considered. The *Evaluation Section* k_s shows that the mean k_s (ME = 20) is less than the ME-TV = 21, only 46% of the MVs are above the MIN-MV (k_s = 20), and approximately 15% of the data fall below the 0.8 MIN-TV (k_s = 16). Therefore, none of the acceptance criteria are met, and further compaction/reworking would be required. The coefficient of variation (COV = 19%) of k_s is within the acceptance limit of 20%.

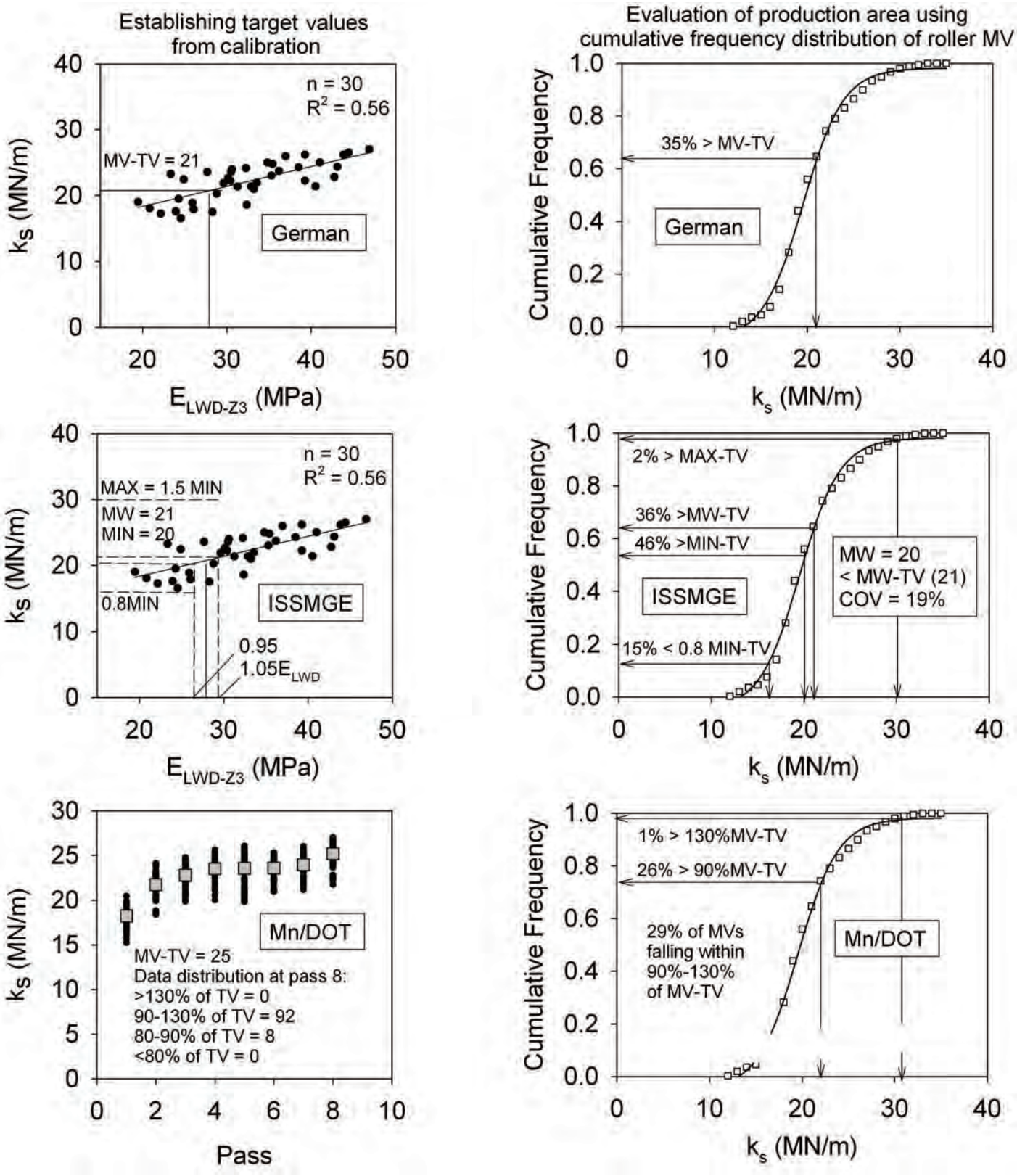

Figure 8.25. Acceptance using German, ISSMGE, and Mn/DOT specifications.

Using the Mn/DOT specification, MV-TV = 25 is established from the calibration data. The *Evaluation Section* k_s showed that only about 29% of the area is within 90% to 130% of MV-TV range. Therefore, the Mn/DOT criterion was not satisfied.

8.5 Case Study V—Granular Subgrade (TB NC20)

Specification Options 1 and 3a were evaluated on an 18-m (60-ft)-wide by 500-m (1,640-ft)-long granular subgrade *Evaluation Section* in North Carolina (see Figure 8.26). The silty sand subgrade material (A-2-4) was compacted by the contractor using typical vibratory equipment. The *Calibration Area* was full width [18 m (60 ft)] and occupied the northernmost 100 m (300 ft) of the *Evaluation Section*. A single *Measurement Pass* (i.e., a proof roll pass, i = pr) was performed with the Sakai CCC roller. *Spot-Test Measurements* were collected with the balloon density tester to a depth of 200 m (8 in) in the *Evaluation Section* and with the nuclear density gauge to a probe depth of 200 mm (8 in) in the *Calibration Area* and a Keros LWD with a 300-mm (12-in)-plate diameter ($E_{LWD\text{-}K3}$). The case study presented here utilizes the $k_{s\text{-}CSM}$ MV computed from independent roller instrumentation (see Section 3.4). Seven LWD and three nuclear gauge measurements were performed across the width of the drum and averaged to represent single γ_d and $E_{LWD\text{-}K3}$ measurements for regression analysis (i.e., in the *Calibration Area*). Each reported roller MV was determined by averaging over 1 m (3 ft) in the direction of roller travel.

The contract QA specifications included a γ_d-TV = 17.7 kN/m^3 (113 pcf) based on 95% standard Proctor maximum dry unit weight (RC-TV = 95%) and a static proof roll (see Figure 8.26b). There were no QA requirements for moisture. The project QA agent performed a static proof roll test over the *Evaluation Section* after option evaluation was completed. One isolated area with soft underlying clay layers did not pass proof roll and required remediation. The specification options were evaluated using the contractual RC-TV and an E_{LWD}-TV for Option 3a derived from the γ_d-TV (for illustration purposes).

8.5.1 Acceptance Using Specification Option 1

Figure 8.27 presents MV_{pr} data from the *Evaluation Section*. Spot-test measurements (γ_d) were performed in the roller-identified weakest areas. Results indicated relative compaction values of 100% and 102%, both exceeding the RC-TV = 95%. Therefore, the *Evaluation Section* met acceptance according to Option 1. The detailed calibration performed to evaluate Option 3a discussed below indicated that a positive

Figure 8.26. Overview of TB NC20 summarizing construction and compaction of the test bed and showing (a) a Measurement Pass and (b) static proof roll test.

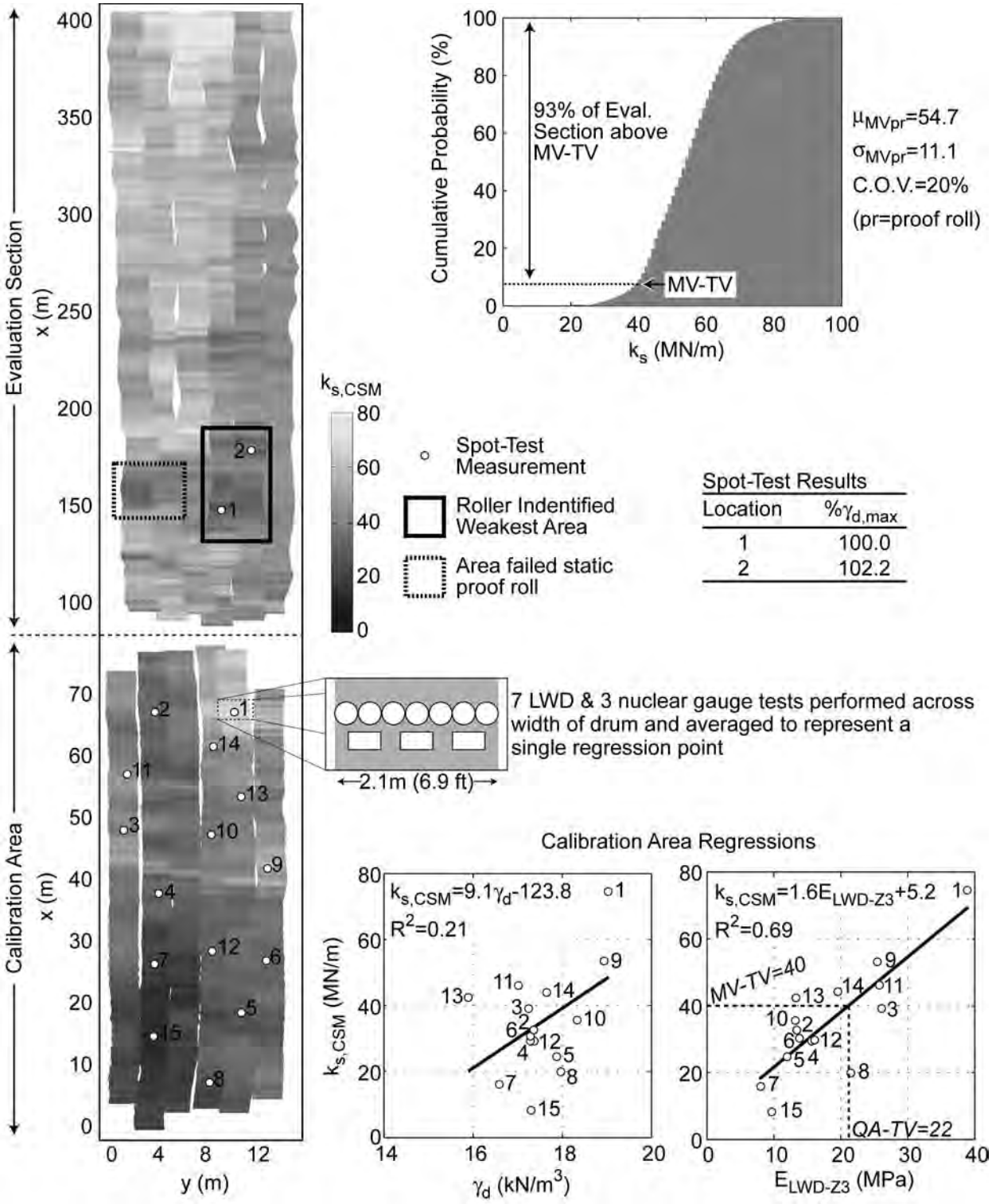

Figure 8.27. Roller MV maps of the Calibration Area and Evaluation Section, MV and spot-test measurement correlations and cumulative distribution of MV data.

correlation did exist between the roller MV and γ_d. However, this correlation was not acceptable ($R^2 = 0.21$), and in such cases Option 1 should be used with caution, and a higher number of spot-test measurements may be desirable.

A small area of the *Evaluation Section* that failed the static proof roll test (and therefore required remediation) is also shown in Figure 8.27. Due to time constraints, spot tests were not performed in this area. Conversely, the roller-identified weakest area passed the static proof roll test. The weak MV-γ_d correlation is one possible reason the roller-identified weakest area passed the static proof roll test while an area with slightly higher MVs failed.

8.5.2 Acceptance Using Specification Option 3a

8.5.2.1 Initial Calibration

Calibration of roller MVs to spot-test measurements was based on areas of low, medium, and high stiffness found within the *Measurement Pass* [A = 0.9 mm (0.035 in), v = 4.0 km/h (2.5 mph), f = 30 Hz] of the previously compacted *Calibration Area* at the northern end of the *Evaluation Section*. This is an alternative approach to creating discrete low, medium, and high compaction states. Four to five spot-test measurements were performed in low, medium, and high MV areas (see Figure 8.27). The resulting regression relationships are presented in Figure 8.27. A suitable correlation was not found between the roller MV and γ_d ($R^2 = 0.21$), and therefore Option 3a cannot be implemented. A good correlation was evident between the roller MV and $E_{\text{LWD-K3}}$ ($R^2 = 0.69$). For illustration, an $E_{\text{LWD-}K3}$-TV = 22 MPa was established based on the relationship observed between γ_d and $E_{\text{LWD-}K3}$ ($R^2 = 0.32$, graph not shown) and the γ_d-TV = 17.7 kN/m^3 (112.7 pcf). Based on $E_{\text{LWD-}K3}$-TV = 22 MPa, the resulting MV-TV = 40.

The difficulty in obtaining a good correlation between the roller MV and γ_d is likely due to sublift variability and measurement depth. For example, locations 14 and 15 exhibit significantly different roller MVs, yet their γ_d are the same. The roller MV at location 14 reflects stiffer sublift material compared to soft sublift conditions at location 15. The $E_{\text{LWD-}K3}$ from the 300-mm (12-in)-diameter LWD that measures to 30 to 60 cm (12 to 24 in) deep supports this (i.e., the $E_{\text{LWD-}K3}$ at location 14 is twice the $E_{\text{LWD-}K3}$ at location 15.

8.5.2.2 Assessment of Evaluation Section

Acceptance for Option 3a is based on achieving the MV-TV over a specified percentage of the *Evaluation Section* (%Area-TV). In this case study, %Area-TV = 90%, similar to German practice, and as determined above, MV-TV = 40. The MV map and cumulative distribution of MV data are shown in Figure 8.27. The cumulative distribution shows that 93% of the *Evaluation Section* met the MV-TV. Accordingly, the *Evaluation Section* met acceptance according to Option 3a based on the $E_{\text{LWD-}K3}$-TV.

8.5.3 Discussion

TB NC20 met contract QA requirements for γ_d and passed the static proof roll test (except in one small area). The *Evaluation Section* also met acceptance based on Option 1. However, the relationship between roller MVs and γ_d, while positive, was shown to be weak. Therefore, Option 1 should be employed with caution. Option 3a implementation was not valid, as a suitable correlation ($R^2 = 0.5$) was not found between the roller MV and γ_d. In such cases, Option 3a could not be used for QA. Other options such as 1 or 2a/2b or a combination of options would need to be pursued.

As in Case Study I, implementation of specification options presented a number of challenges. At the North Carolina site, haul trucks entered the *Evaluation Section* in reverse, deposited material, and then drove forward out of the area (see Figure 8.28). They did not drive through the project due to a geomembrane placed beneath the material. This often forced less than ideal roller pass patterns and created hazardous conditions for personnel performing spot-test measurements. Performing correlation studies in a designated full-width *Calibration Area* required a change in how the earthwork contractor placed material. To perform repeatable *Measurement Passes* in the *Evaluation Section*, the research team had to wait for the earthwork contractor to completely

Figure 8.28. Placing material (top) and performing spot-test measurements (bottom) in an active Evaluation Section at the North Carolina work site.

finish hauling and placing a section. In typical production compaction practice, roller compactors are used throughout the hauling, placing, and grading operation. Careful planning and cooperation between the contractor and QA agents are critical for successful implementation of CCC-based QA.

8.6 Case Study VI—MN10 Nongranular Subgrade

A test bed constructed as part of the MnROAD field testing program is presented herein as an approach to establish MV-TV relating to laboratory M_r values for Specification Option 3c and an approach to adjust the MV-TV for moisture content. Roller MV (E_{vib}) and spot-test measurements obtained from this test bed are described in Chapter 6 (Section 6.4.1). In brief, the test bed was constructed with a layer of nongranular subgrade material [AASHTO: A-6(5)] underlain by a relatively stiff and homogeneous subgrade layer. The subgrade layer was moisture conditioned w_{opt} by dividing the test bed into three sections to approximately -3%, 0%, and +3% of standard Proctor [maximum dry unit weight and optimum moisture content as determined by the standard Proctor method were 16.95 kN/m^3 (107.90 pcf) and 16.4%, respectively]. Compaction passes were performed using a pad foot Bomag IC roller, and in situ w-γ_d point measurements were obtained in parallel with the compaction process. The analysis and results presented below are for the purpose of illustrating the calibration approach for Option 3c. As such, detailed comparisons to current practice (i.e., γ_d spot-test-based QA) and other existing CCC specifications are not made and the assessment of an *Evaluation Section* is not pursued. Laboratory M_r tests were conducted on reconstituted laboratory-compacted specimens to develop w-γ_d-M_r relationships for the subgrade material. Test results are described in Section 6.4.1.

8.6.1 Relationship Between Roller MV and Spot-Test Measurements

Linear regression relationships between γ_d and E_{vib} were developed based on spatially nearest data, as presented in Figure 8.29(a). The regression relationship produced $R^2 = 0.37$. Multiple regression analysis was performed to incorporate the influence of moisture content in the relationship. The multiple regression relationship improved the correlations with $R^2_{adj} = 0.54$ [Figure 8.29(b)].

8.6.2 Establishing MV-TVs Based on Laboratory-Determined M_r Values for Specification Option 3c

The multiple regression relationship developed from laboratory testing was used to predict M_r values for the in situ w-γ_d point measurements. Since the laboratory relationship is valid only for the range of w-γ_d of the laboratory samples, the spot-test measurements close to the laboratory sample

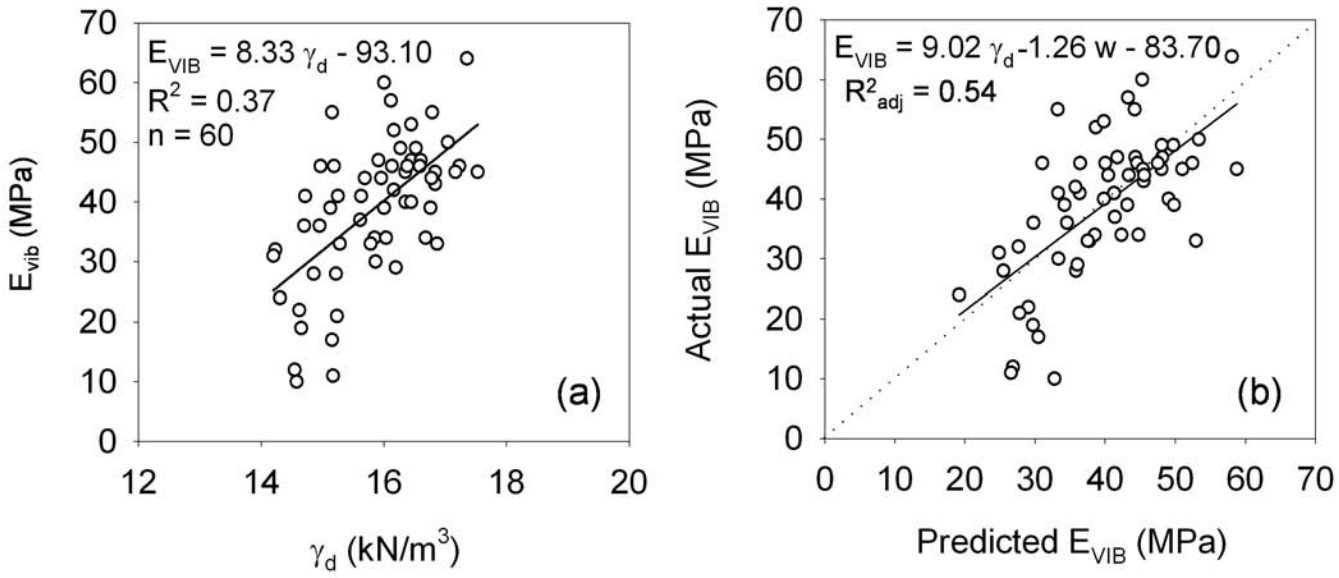

Figure 8.29. (a) Simple linear regression relationship between E_{vib} and γ_d and (b) multiple regression relationship between predicted and measured E_{vib}.

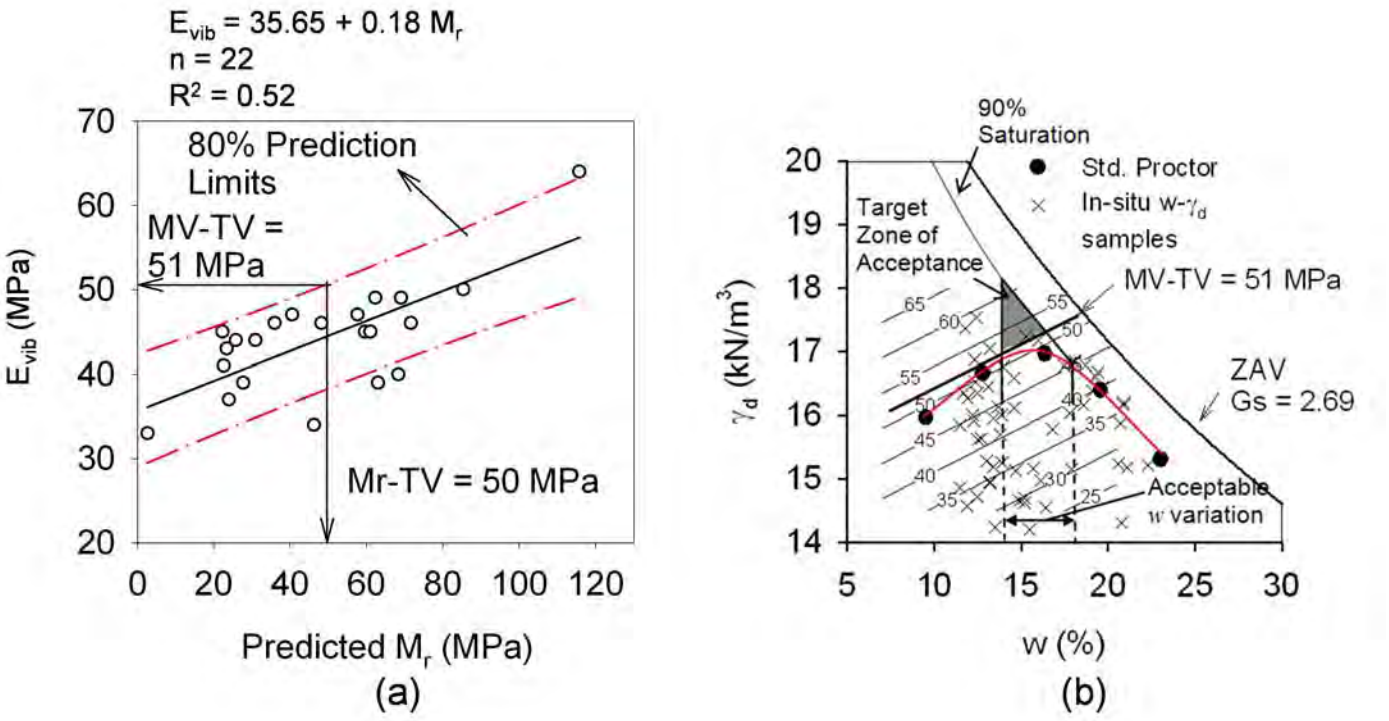

Figure 8.30. Relationship between laboratory (a) M_r and E_{vib} and (b) target zone of acceptance for Option 3c.

values were selected. Comparison of predicted M_r and E_{vib} for the selected data is presented in Figure 8.30(a), which showed a good correlation with $R^2 = 0.52$. For illustration purposes, a target M_r (M_r-TV) = 50 MPa was selected for establishing a roller MV-TV. Using the *inverse regression* approach and an 80% prediction interval, a roller MV-TV = 51 MPa was established for the M_r-TV.

Using the multiple regression relationship developed for roller E_{vib}, E_{vib} contours are plotted over a moisture–dry unit weight plot as presented in Figure 8.30(b) (see Section 6.4.1). Because the prediction equations were comprised of only linear terms, the E_{vib} contours are linear and parallel lines that decrease with increasing moisture. To select a target zone of acceptance, an area bounded by ±2 percent of w_{opt}, 90% saturation curve, and the MV-TV is highlighted in Figure 8.30b. For acceptance using Specification Option 3c, the production E_{vib} must be above the MV-TV and the QA test locations must have moisture contents within the zone of acceptance.

8.6.3 Adjustment of MV-TVs for Moisture Content

Data obtained from the above-described test bed is used to demonstrate the approach of adjusting the MV-TVs for moisture content. Using the multiple regression relationship developed for roller E_{vib}, E_{vib} contours are plotted over a moisture–dry unit weight plot as shown in Figure 8.31. The highlighted target zone is selected based on w_{opt} ±2% and 95% standard Proctor γ_{dmax}. High (MV-TV_1) and low (MV-TV_2) E_{vib} corresponding to low (w_1) and high (w_2) moisture contents, respectively, are selected. The equation to calculate MV-TV_{adj} is presented in Figure 8.31. This MV-TV adjustment can be used for Specification Options 3a, 3b, and 3c. Acceptance is based on QA test locations meeting the MV-TV_{adj}. Areas with E_{vib} > MV-TV_1 are considered as passed and those with E_{vib} < MV-TV_2 are considered as failed and need to be reworked for further QA testing.

8.7 Conclusions

The following conclusions can be drawn from the case studies presented in this chapter:

- Specification Option 1 requires minimal changes to typical current QA practices. Rather than selecting random points for spot-test measurements, QA inspectors use the roller MV data map to identify the weakest area(s). Depending on the number of weakest areas identified, the frequency of spot testing may increase compared to current practice. According to Option 1, if the roller-identified weakest area(s) meet acceptance, the rest of the *Evaluation Section* passes by association. However, given that testing locations are informed rather than random, requiring the weakest zones to meet 100% of the preexisting QA-TV may be

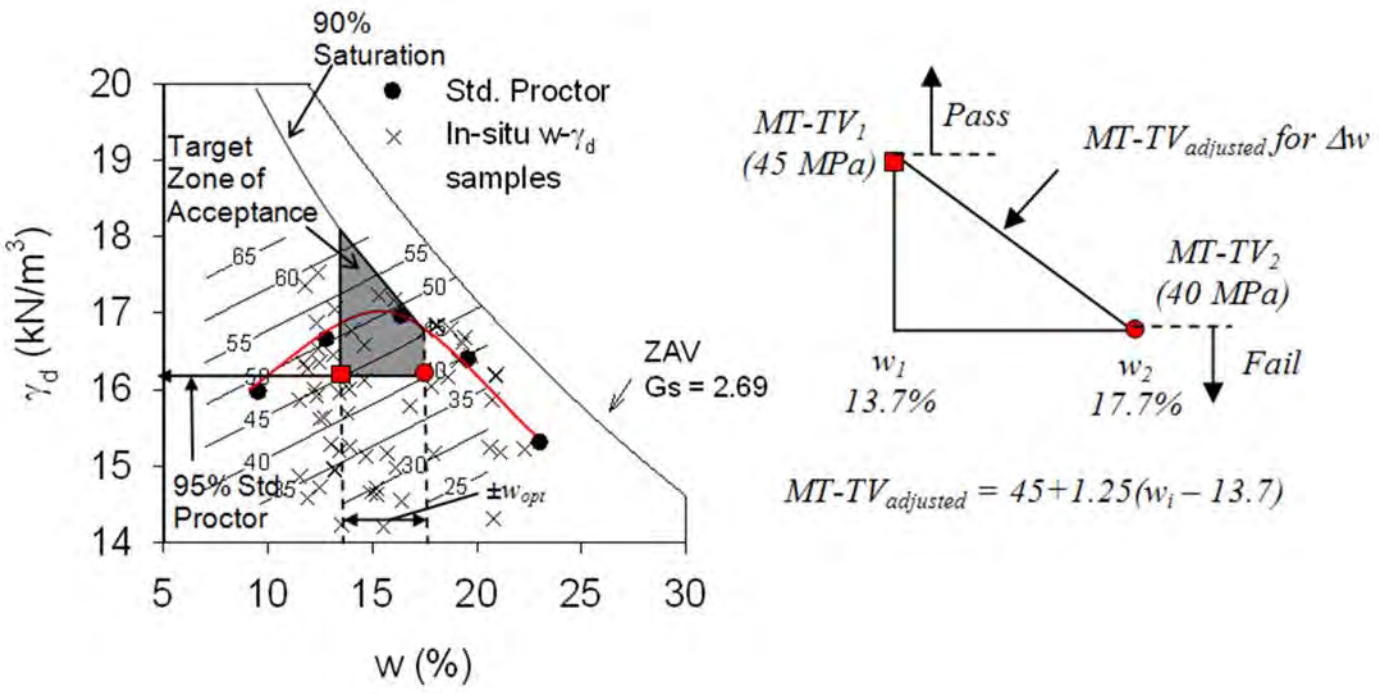

Figure 8.31. Moisture correction for E_{vib} target values.

more stringent than current random selection spot testing. Reducing the QA-TV may be more appropriate. In addition, an assumption underlying Option 1 is that the roller MV and spot-test measurement have an acceptable, positive correlation.

- Specification Options 2(a, b) and 3(a, b, c) require modification to current QA practices in that spot-test measurements do not form the basis for QA. Rather, acceptance is granted based on roller MVs. In Option 2a, acceptance is granted when the percentage change in the mean roller MV from pass to pass falls below a preset threshold. In the case studies presented here, Option 2a appeared to be less stringent than current practice, and it may be desirable to implement it in conjunction with Option 1 to improve reliability.
- Specification Option 2b uses the percentage change in spatial roller MV data as the basis for QA. One challenge associated with Option 2b is that the method of transforming roller MV data onto a fixed grid to allow spatial comparison is not trivial and reliable; proven methods do not yet exist. Based on the case studies here, Option 2b appears to be more stringent that current QA practices.
- One major challenge to successfully implementing Specification Option 3(a, b, c) is ensuring that the *Calibration Area* is representative of the *Evaluation Section*. Although using a roller MV data map of the *Evaluation Section* can aid in selecting an appropriate *Calibration Area*, this can be logistically challenging on a busy job site.
- Option 3(a, b, c) requires a significant initial investment of time and careful, detailed analysis. This analysis is more complex than that currently required for QA purposes, and it is easy to make errors. Accordingly, QA inspectors will need careful training to ensure they are familiar with both the roller MV systems and the analysis required for the various options.
- Construction traffic poses a challenge to implanting CCC-based QA. All of the options require careful, repeatable rolling patterns. However, construction traffic—particularly haul trucks moving through the earthwork area—often forces less than ideal roller pass patterns. Truck traffic often makes it difficult to create uninterrupted and repeatable *Evaluation Area* roller MV maps.
- Developing the required correlations (e.g., for Option 3a) necessitates that haul trucks remain outside the *Calibration Area* once material has been placed and spot-test measurements are being performed. However, it is common for contractors to utilize haul truck traffic to compact soil, and therefore truck drivers are accustomed to driving through an earthwork area. Similarly, it is not uncommon for haul trucks to enter the *Evaluation Section* in reverse, deposit their material, and then drive forward out of the area (see Figure 8.28). This often forces less

than ideal *Rolling Patterns* and creates hazardous conditions for personnel performing spot-test measurements. Performing correlation studies in a designated full-width *Calibration Area* requires a change in how the earthwork contractor places material. To perform repeatable *Measurement Passes* in the *Evaluation Section*, the research team had to wait for the earthwork contractor to completely finish hauling and placing a section. In typical production compaction practice, roller compactors are used throughout the hauling, placing, and grading operation. Careful planning and cooperation between the contractor and QA agents is critical for successful implementation of CCC-based QA.

- The pace of the production earthwork placement and compaction frequently limited the time the research team was able to spend in the *Calibration Area*. Including the time needed to construct the *Calibration Area*, the correlations were developed in approximately 3 to 4 hours, although a time frame of 1 to 2 hours or less would be more consistent with production schedules.

CHAPTER 9

Conclusions

9.1 Overview

NCHRP Project 21-09, "Intelligent Soil Compaction Systems," involved extensive field testing and analysis to better understand roller-integrated CCC and IC and to develop recommended specifications for the use of roller-integrated CCC in QA of soil and aggregate base material compaction. The quality of constructed earthwork materials is clearly critical to the performance of pavements. Roller-integrated measurement of soil properties holds significant promise in that it provides an effective tool to assess the quality of earthwork construction. The full or complete coverage capability of roller-integrated CCC is a significant improvement over current spot-test-based QA. The use of roller-integrated CCC enables state departments of transportation (DOTs) to enforce high expectations for earthwork quality. The successful implementation of roller-integrated CCC for earthwork QA will require high expectations as well as coordination and buy-in from DOTs and contractors. QA personnel and contractors will need proper training on the capabilities and use of roller-integrated CCC.

Intelligent compaction, currently implemented using automatic feedback control of vibration amplitude and sometimes frequency, is in its infancy and will likely evolve to incorporate numerous ways in which the process of compaction is improved and made more efficient. The capabilities and user-friendliness of onboard PCs and software will also likely improve significantly. Finally, the measurement systems, currently limited by the influence of operating parameters, local heterogeneity, and measurement depths that far exceed lift thickness, will continue to evolve to account for these factors.

True performance-based assessment of earthwork materials using roller-integrated CCC is within reach. The results presented here illustrate reasonably complex but deterministic soil behavior within the measurement volume of a vibrating roller. With further research, instrumented rollers will likely become capable of measuring the requisite layered earthwork properties to predict performance of pavement systems. The specific findings and conclusions from this study are summarized below in sections consistent with the presentation of the report.

9.2 Review of Literature and European CCC Specifications

Roller-integrated CCC has been used in European practice since the late 1970s, whereas IC technology has been available commercially only since the late 1990s. The initial research on roller-integrated measurement dates to the 1970s in Sweden with the development of the CMV by Geodynamik. Roller MVs have evolved over the past 30 years within the roller manufacturing community. There are currently a handful of proprietary vibration-based MVs in the market. When Geodynamik first introduced the compaction meter and CMV, vibration was implemented mechanically via a two-piece eccentric mass assembly (clamshell) within the drum. If rotated in one direction, the two eccentric masses would join together and provide maximum eccentric force or theoretical amplitude A. If operated in the reverse rotational direction, A would be a minimum. Automatic feedback control–based IC was made possible by the introduction of new drum technology in the 1990s. Bomag introduced the Variocontrol roller with counterrotating eccentric masses and servo-hydraulic control of the vertical component of eccentric force. Similarly, Ammann introduced the ACE roller with servo-hydraulic two-piece eccentric mass moment control and frequency control. Other manufacturers have followed suit. The integration of GPS-based positioning with roller-based measurement of soil properties, and the incorporation of user-friendly portable PCs with graphical software, has evolved over the past 5 to 10 years.

A considerable body of literature exists pertaining to roller vibration, roller-integrated measurement systems, roller modeling, and correlation of roller MVs to spot-test measurements. The modeling of vibratory roller-soil interaction has evolved with experimental studies of roller behavior. The initial assumptions about continuous drum/soil contact in the 1970s and 1980s gave way to experimental observation and lumped parameter modeling of partial loss of contact, chaotic drum jumping, and rocking mode in the 1990s and 2000s. Both experimental correlation studies and numerical investigations have shown that vibration-based roller MVs all track increases in soil stiffness/modulus effectively with the exception of CMV and CCV below values of approximately 8 to 10. Based on limited studies found in the literature, the measurement depth of roller MVs was found to vary from 0.6 to 1.0 m deep for 10-ton vibratory rollers to 0.8 to 1.5 m for 12- to 17-ton vibratory rollers. A commonly observed rule of thumb in the compaction community is that each 0.1 mm of amplitude A corresponds to 0.1 m of measurement depth. Owing to this measurement depth, a number of experimental studies have shown that roller MVs reflect the properties of both the compaction lift material and the sublift material. A number of studies have successfully correlated roller MVs to spot-test measurements. Given that roller vibration-based MVs reflect soil stiffness, roller MVs correlate well with PLT and LWD moduli. Successful correlations have been found between roller MVs and dry density.

Specifications for QA of earthwork compaction using roller-integrated CCC were first introduced in Austria (1990), Germany (1994), and Sweden (1994). Revisions to these original specifications have been made in each country. The International Society of Soil Mechanics and Geotechnical Engineering (ISSMGE) recently adopted the Austrian specifications for CCC. The Austrian/ISSMGE and German specifications each permit multiple options for using CCC in earthwork compaction QA. The most common and simplest approach (and the only approach permitted in Sweden) uses CCC to identify weak areas for evaluation via static PLT, LWD, or density spot testing. Acceptance is based on these weak areas meeting prerequisite PLT modulus, LWD modulus, or density requirements. The most advanced CCC-based QA specifications involve correlating roller MVs to PLT modulus, LWD modulus, or density in a defined calibration area. If a suitable correlation is found, a target roller MV is determined from the MV versus spot-test regression equation. Acceptance is based on comparison of roller MV data collected in a production area to the target roller MV. Based on a survey of European practice, the calibration approach is challenging to implement and requires a high level of on-site knowledge.

9.3 Fundamentals of Roller-Based Measurement Systems

A detailed investigation of numerous roller-based measurement systems was conducted to characterize the ground surface area represented by single-roller MVs, the spatial resolution in roller MV records, and uncertainty in roller MVs. Independent evaluation was performed to reproduce and validate numerous roller MVs using independent instrumentation. Extensive testing was performed to characterize the influence of roller operational parameters—namely, eccentric force amplitude, vibration frequency, roller speed, and forward versus reverse driving mode—on roller MVs. The objectives of these studies were to improve fundamental understanding of roller-based measurement systems and to provide guidance for roller-integrated CCC specifications.

Each vibration-based roller MV investigated—Ammann and Case/Ammann k_s, Bomag E_{vib}, Dynapac CMV_D, and Sakai CCV—provides a measure for an area of soil the width of the roller (2.1 m) by a spatial distance in the direction of travel that varies across MVs (0.06 to 1.0 m was observed). The reporting resolution of roller MVs varied from 0.2 to 1.0 m. To ensure full coverage with roller-integrated CCC, the spatial distance over which a single-roller MV is reported should equal the reporting resolution. The reporting spatial resolution should be no less than 10 times the GPS accuracy. Real-time kinematic (RTK) differential GPS (accuracy ~1 to 2 cm) is recommended for use with CCC and IC rollers. Assuming RTK accuracy, the spatial resolution of roller MVs should be no less than 0.25 m. The GPS-based position reporting of roller MVs exhibited errors of 0.4 to 1.5 m for the rollers and measurement systems investigated. This error was due to averaging of roller vibration data within each reported roller MV and to latency in onboard computation. A position-reporting procedure was developed and is recommended for roller-integrated CCC specifications (see Chapter 7).

A series of tests were performed with all rollers and roller MVs to characterize the uncertainty with which single-roller MVs should be reported. Repeatability testing of properly working CCC/IC rollers and roller measurement systems often revealed an uncertainty of ±10% (one standard deviation); that is, a repeated pass over the same area will yield individual roller MVs within ±10% of MVs from the previous pass. Repeatability testing plays an important role in verifying the proper working condition of a vibratory roller and/or roller measurement system. A repeatability testing procedure was successful in identifying when a roller or roller measurement system was faulty. Repeatability testing of pad foot measurement systems revealed single MV uncertainties of ±50% to 100%. A repeatability testing procedure was developed for CCC specifications and is further described in Chapter 7.

Roller MV uncertainty will influence the establishment of QA criteria for spatial differences in pass-to-pass roller MVs as described in Chapter 7.

Roller-integrated measurement of soil stiffness is not currently standardized (i.e., magnitude and rate of loading, etc.). With CCC and IC rollers, measurement occurs during roller operation, and roller operation parameters can vary considerably. Field testing was performed to characterize the influence of various operational parameters on roller MVs and to determine if these influences are predictable and therefore could be accounted for. Field testing revealed that the influence of the magnitude of eccentric force (or theoretical drum vibration amplitude A) on roller MVs varies widely. From low to high A vibration on the same material, roller MVs were found to change by as much as 100%. The amplitude dependence of roller MVs was not determinate and not predictable. Roller MVs were found to increase, decrease, or remain the same with increasing A depending on the soil and layering conditions. The mechanics-based understanding of this is discussed in Section 9.4. Due to the unpredictability in A dependence, a fixed-vibration amplitude is recommended for roller-integrated CCC.

Evaluation of travel speed dependence on roller MVs produced mixed results. CCV and CMV_D were found to decrease noticeably with an increase in roller speed. The influence of roller speed on E_{vib} was inconclusive within the uncertainty of the measurement approach and the limited data collected. Roller MVs were found to be mildly dependent on forward- versus reverse-driving modes. Roller MVs differed by 2% to 13% in forward- versus reverse-driving mode. Given that typical compaction work involves forward- and reverse-driving sequences, there is considerable benefit to employing roller MVs in both forward and reverse modes. Forward and reverse mode measurement can be considered; however, site-specific calibration is required to characterize and verify the relationship between forward-measuring and reverse-measuring roller MVs.

The vibration-based roller MVs investigated—Ammann and Case/Ammann k_s, Bomag E_{vib}, Dynapac CMV_D, and Sakai CCV—correlate well with each other over the range of soft to stiff soil conditions investigated in this study. CCV and CMV were relatively insensitive to changes in soil stiffness below values of about 8 to 10, consistent with findings in the literature (see Chapter 2). Many of the roller MVs employed by manufacturers were validated using independent instrumentation and implementation of published roller MV algorithms. This dispels the "black box" mentality that would inhibit implementation within the engineering community.

Local soil heterogeneity perpendicular to the direction of roller travel has a significant influence on roller MVs. Due to the nature of drum instrumentation, roller MVs are directionally dependent on heterogeneous soil. Bidirectional roller MVs were found to vary by 100% due to transverse soil stiffness variability. This was confirmed by LWD testing across the drum lanes. As a result, spot testing should be conducted across the drum lane when correlating to roller MVs, and great care should be used when performing spatial statistical analysis of pass-to-pass data maps in the presence of heterogeneity.

9.4 Relationship Between Roller-Measured Stiffness and In-Ground Response

To better characterize what roller MVs reflect and to build a framework for performance-based assessment of earthwork properties using roller-based measurements, a series of test beds were constructed with in-ground instrumentation to capture in situ stress-strain-modulus behavior. Numerous vertically homogeneous embankments and layered subgrade, subbase, and base test beds were instrumented with stress and strain sensors at multiple levels to capture in situ behavior during static and vibratory roller passes. This aspect of the study sought to explain, from a mechanics-based perspective, the vibration amplitude dependence of roller MVs, characterize measurement depth of the instrumented roller, and determine how current roller MVs are related to in situ soil response in vertically homogeneous and layered structures.

Roller MVs measure to depths considerably greater than typical compaction lifts. For the vertically homogeneous embankment conditions and the 11- to 15-ton smooth drum vibratory rollers used in this study, the volume of soil reflected in a roller MV is cylindrically shaped, extending to 0.8 to 1.2 m deep and 0.2 to 0.3 m in front of and behind the drum. Drum/soil contact widths range from 0.1 to 0.3 m and decrease as soil stiffness increases. For vertically homogeneous embankment situations, the measurement depth of roller MVs is controlled by the relative decay of roller-induced cyclic stress and strain and is reached when values have decayed to 10% of their peak. The measurement depth was mildly influenced by vibration amplitude; that is, a 0.1-mm increase in A yielded about a 3.0-cm increase in measurement depth. This is significantly different than the 0.1-mm and 10.0-cm rule of thumb found in the literature. Roller MVs are a composite reflection of typical base, subbase, and subgrade structures with surface-to-top-of-subgrade thickness of less than approximately 1 m. The contribution of each layer to the roller MV is influenced by layer thickness, relative stiffness of the layers, vibration amplitude, and drum/soil interaction issues (contact area, dynamics). The contribution of sublift materials to roller MVs can be significant.

In situ stress-strain-modulus measurements at depths to 1 m beneath the roller revealed highly nonlinear modulus be-

havior within the bulb of soil reflected in roller MVs. In base, subbase, and subgrade structures, modulus varies widely from layer to layer and within layers. Modulus values increased by a factor of 2 with depth in vertically homogeneous embankment test beds. In situ modulus is strongly influenced by vibratory loading. A change in vibration amplitude from low to high created a twofold change in modulus. Numerical simulation of roller-soil interaction using modulus function parameters for cohesive and cohesionless soils revealed significant variations of the modulus field beneath the roller. Plane strain conditions exist under the center of the drum and do not exist under the drum edges. As a result, the soil under the drum center responds stiffer than the soil under the edge. The nonlinear modulus behavior and three-dimensional nature of soil behavior beneath the drum must be considered in the extraction of performance-related parameters from roller-based measurements.

The amplitude (A) dependence of roller MVs—particularly stiffness measures such as E_{vib} and k_s—is a result of stress-dependent soil modulus, layer interaction, and drum/soil contact mechanics. For vertically homogeneous embankment conditions, the nature of the MV-A dependence (i.e., positive, negative, or neutral) depends on the modulus function parameters of the soil. Granular soils that are governed by mean effective stress-induced hardening may generally exhibit a positive roller MV-A dependence (i.e., an increase in A yields an increase in roller MV). Conversely, cohesive soils governed by shear stress–induced softening may generally exhibit a negative roller MV-A dependence (i.e., an increase in A yields a decrease in roller MV). The roller MV-A dependence of layered structures is more complex and is influenced by stress-dependent soil modulus (modulus function parameters), layer thickness, relative stiffness of layers, and drum/soil interaction issues. Both positive and negative roller MV-A dependence is possible, even within the same material. The roller MV-A relationship is site dependent and cannot be predicted a priori.

Roller MVs were found to be insensitive to the compaction of thin lifts [e.g., 15 cm (6 in)] of stiff base material placed directly over a soft subsurface. Roller MVs were sensitive to compaction of 30-cm lifts of the same stiff material over soft subgrade. The sensitivity of roller MVs to compaction of thin lifts improves as the modulus ratio of the overlying to underlying layers decreases, and roller MVs were sensitive to compaction of 15-cm lifts of base material placed atop similar base material. These results imply that CCC-based QA of thin base layers atop softer subgrade may be unreliable.

Levels of vibratory roller-induced deviator stress were found to be considerably greater than those used in laboratory M_r testing, whereas levels of confining stress were considerably less. Even during low excitation force associated with finishing passes and proof rolling of compacted soil, estimated deviator stresses q from $z = 0$ to 0.5 m (0 to 1.6 ft) in clayey sand were up to three times greater than the maximum q values used for laboratory M_r testing of subgrade soils. Similarly, estimated q values in crushed-rock base course were up to 2.5 times greater than the maximum q used for laboratory M_r testing of base materials. For $z > 0.5$ m, field and maximum laboratory q values were reasonably similar. Conversely, values of p observed in the field were approximately 0.3 to 0.5 of those used during laboratory M_r testing.

The extraction of mechanistic material parameters using roller-based measurements for performance-based specifications consistent with mechanistic-empirical-based design (e.g., AASHTO 2007 Pavement Design Guide) is possible but challenging. The extraction of appropriate parameters must account for the three-dimensional nature of the roller/soil interaction, the influence of layers, the nonlinear modulus of each involved material, and the dynamics of the drum/soil interaction.

9.5 Evaluation of Automatic Feedback Control–Based Intelligent Compaction

Current technology for IC involves *sensing* via measurement of vibration-based parameters and *adapting* via AFC of excitation force amplitude (Ammann, Bomag, Case/Ammann, Dynapac) and in some cases excitation frequency (Ammann, Case/Ammann). At a minimum level, each manufacturer controls the vertical excitation force amplitude to prevent unstable "jump" mode vibration of the roller (see Section 2.1.2). When the measurement system senses jump mode, the vertical excitation amplitude is decreased until the measurement system indicates stable vibration. Jump mode may persist even at the lowest vibration amplitude setting. This level of AFC is aimed at protecting the roller from accelerated wear and the operator from chaotic response of the roller. Bomag, Ammann, and Case/Ammann use additional AFC in an attempt to improve compaction and uniformity. Bomag controls the vertical excitation amplitude based on the relationship of the current roller MV to a limit MV. The vertical excitation is maximized within one of five levels chosen by the operator and is decreased if MV is greater than or equal to the limit MV. Ammann and Case/Ammann control the excitation amplitude and frequency to maintain one of three levels of force transmitted to the soil.

The principles of AFC-based IC were investigated using the Bomag Variocontrol and Ammann ACE systems. Repeated passes were performed with both IC rollers over mixed material test beds exhibiting significant longitudinal variability in ground stiffness (soft to stiff). Both constant amplitude mode and AFC mode were used for comparison. A comparison of low- and high-amplitude constant amplitude passes revealed

areas of positive MV-*A* dependence (MVs increased with increasing *A*) and negative MV-*A* dependence (MVs decreased with increasing *A*). The dependence of roller MVs on *A* can provide a misleading record of soil stiffness when operating in AFC mode. The positive and negative MV-*A* dependence was observed during testing and resulted in an artificial and misleading level of variability in recorded soil stiffness. In addition, the roller MV-*A* dependence can falsely trigger AFC changes in *A*. This is particularly problematic when roller MVs hover around a target or limit MV. The response distance of AFC tested was found to be approximately 1 m (3 ft), indicating that rollers in AFC mode can respond to relatively local changes in soil conditions.

The influence of AFC-based IC on compaction efficiency and uniformity was investigated on granular base material. Two granular base test beds were prepared side by side and compacted with a Bomag Variocontrol system in AFC and constant amplitude modes, respectively. Spot-test measurements were obtained at several intermediate compaction passes to assess compaction efficiency and uniformity. Compaction curves built from spot-test measurement averages revealed similar trends in both test beds with no noticeable difference. The COVs of spot-test measurements were similar after pass 8 for the two test beds, indicating no discernable difference in uniformity. A comparison of COVs from roller MVs recorded during constant amplitude final passes on each test bed showed no difference in uniformity. AFC-based IC did not produce greater compaction or improved uniformity compared to constant amplitude mode compaction for these test bed conditions.

9.6 Relationship Between Roller Measurement Values and Spot-Test Measurements

Implementation of roller-integrated CCC into earthwork specifications requires an understanding of relationships between roller MVs and spot-test measurements. A comprehensive evaluation of five roller-integrated MVs (i.e., MDP, CMV_D, E_{vib}, k_s, CCV) and 17 different soils was performed. The soils are grouped into three material groups: nongranular subgrade, granular subgrade, and granular subbase/base materials. Roller MVs were obtained from smooth drum and pad foot drum rollers on 60 controlled test beds. The test beds varied in material types, moisture content, and underlying layer support conditions. Roller MVs were obtained for different amplitude, frequency, and speed settings. A variety of conventional and mechanistic related in situ test measurements [i.e., dry unit weight, CBR, LWD modulus, PLT modulus] and laboratory M_r test measurements were used in correlation analyses to MVs. The objectives were to (1) investigate simple linear relationships between roller MVs and various in situ point measurements, (2) identify key factors that influence these relationships, and (3) evaluate multiple regression relationships that consider variations in soil conditions and machine operation settings.

The results indicated that correlations are possible to dry unit weight, modulus, and CBR with simple linear regression analysis on test beds with homogeneous and relatively stiff underlying layer support conditions and MVs obtained under constant operation settings. A summary of typical ranges of R^2 values for modulus, CBR, and dry unit weight measurements for the three referenced material groups is provided in Table 9.1. The wide range in resulting R^2 values is attributed to various factors, including sublift heterogeneity, moisture content variation, narrow range of measurements, transverse heterogeneity, and variation in machine operating parameters. High variability in soil properties across the drum width and soil moisture content contributes to scatter in relationships. Averaging measurements across the drum width and incorporating moisture content into multiple regression analysis, when statistically significant, can help mitigate the scatter to some extent. Relatively constant machine operation settings are critical for calibration strips (i.e., constant amplitude, frequency, and speed), and correlations are generally better for low-amplitude settings [e.g., 0.7 to 1.1 mm (0.028 to 0.043 in)].

The influence of some of these factors (i.e., soil moisture content, compaction layer lift thickness, underlying layer properties, and machine operation settings) was statistically analyzed using multiple regression analysis. A summary of typical ranges of R^2_{adj} (adjusted for the number of model parameters) values for modulus, CBR, and dry unit weight measurements for the three referenced material groups from multiple regression analysis is provided in Table 9.2. Where heterogeneous conditions were evident below the compaction layer, the underlying layer properties (MVs and spot-test measurements) were often found to be statistically significant in the multiple regression model. Regression relationships improved by incorporating the underlying layer properties. Where compaction layer properties were strongly correlated with the underlying layer properties, the compaction layer

Table 9.1. Typical range of R^2 values for simple linear regression analysis.

Material	Modulus	CBR	γ_d
Nongranular subgrade	0.1–0.7	0.1–0.7	0.0–0.6
Granular subgrade	0.3–0.7	0.0–0.4	0.1–0.5
Granular subbase/base	0.2–0.8	0.0–0.6	0.0–0.5

Table 9.2. Typical range of R^2_{adj} values for multiple linear regression analysis

Material	γ_d	Modulus	CBR
Nongranular subgrade	0.6–0.8	0.2–0.6	0.3–0.7
Granular subgrade	—	0.5–0.7	—
Granular subbase/base	0.4–0.8	0.6–0.9	0.4–0.8

point measurements were not statistically significant in the analysis.

Moisture content was found to be significant for two nongranular subgrade layer test beds and one granular base layer test bed. Generally, moisture content was not statistically significant in the regression analysis for most of the test bed studies. Factors contributing to this observation are (1) moisture content did not vary enough over the length of the test strip; (2) spot-test measurements typically only measure moisture content to about 75 mm (3 in) below the surface, while the measurement depth of the roller is much greater; and (3) when correlating with elastic modulus-based spot-test measurements using multiple regression analysis, moisture content is co-linear (i.e., highly correlated to in situ measurement). Amplitude variation was statistically significant for all cases where minimum amplitude variation of ±0.30 mm was present in the data.

An approach to empirically relate laboratory-determined M_r for a selected stress condition and roller MVs was presented. The M_r values were predicted for in situ w-γ_d measurements using a w-γ_d-M_r relationship developed from laboratory testing. Similar to other in situ point measurements, the relationships were possible for compaction layer material underlain by homogeneous and relatively stiff support conditions. Heterogeneous supporting layer conditions affected these relationships, and the relationships improved by including parameter values that represent the underlying layer conditions through multiple regression analysis.

9.7 Recommended Specification Options for Earthwork Compaction QA Using Roller-Integrated Continuous Compaction Control

Based on a thorough critique of European specifications and practice, a review of previous research, and the findings from the research conducted for this project, recommended specification options for QA of subgrade, subbase, and aggregate base course compaction using roller-integrated continuous CCC were developed. Six viable QA options are proposed to accommodate the diverse site conditions and agency needs observed across the United States. Many of the recommended options were inspired by current European specifications (summarized in Chapter 2). Additional recommended options stem from the research findings presented in this report. The six recommended QA specification options are summarized in Table 9.3 and Figure 9.1. Options are numbered 1, 2a, 2b, 3a, 3b, and 3c and are distinguished by three principal categories. In Option 1, CCC is used to assist in QA, but acceptance is based on spot-test measurements. Acceptance of Options 2a and 2b is based on roller MVs, but initial calibration of roller MV to spot-test measurements is not required. Acceptance of Options 3a, 3b, and 3c is based on achieving a MV-TV determined via various initial calibration techniques. Method-based approaches, such as using GPS positioning and documentation to record the pass sequence, are also viable approaches. Because they do not utilize roller MVs, their implementation is straightforward and not presented here. None of the recommended options constitute performance-based specifications. Further research is required to implement, for example, the findings from Chapter 4 into viable performance-based specifications that can be implemented in practice.

The recommended specification options prohibit the use of automatic feedback control IC during QA due to the influence that roller operating parameters have on roller MVs. Automatic feedback control IC may be used during compaction operations. The proposed specification is applicable to cohesive and cohesionless soils and aggregate base materials. However, as shown in this study, current roller MVs are less reliable on cohesive soils, and particular attention must be given to soil moisture content. Vibratory and nonvibratory-based roller MVs that can be correlated to soil properties (e.g., density, stiffness, shear strength) are permitted. Each of the recommended specification options can be adopted as the sole method for QA. Alternatively, two or more options can be combined to increase reliability. Uniformity criteria can be added to any of these options.

A number of important issues regarding roller-integrated CCC specifications are detailed in Chapter 7 and are worth highlighting here. The implementation of roller-integrated CCC for earthwork QA requires knowledgeable field personnel. QA personnel must be familiar with the aspects of CCC and IC described in this report and with the CCC and IC equipment on the job site. The specifications require close collaboration between the QA personnel and the contractor (i.e., roller operator). To this end, roller operators must understand the various aspects of measurement passes, roller operating parameters, driving patterns, and so forth, as well as the documentation systems of CCC/IC rollers.

Table 9.3. Summary of roller-integrated CCC specification options.

Roller-Integrated CCC QA Option	Target Measurement Value (MV-TV)	Acceptance Criteria
Option 1: Spot testing of roller-informed weakest area(s)	Not required	Spot-test measurements in roller-identified weakest area(s) satisfy contract spot-test measurement requirements (QA-TV)
Option 2a: Monitoring percentage change in mean MV	Not required	Achieving ≤ 5% change in mean MV between consecutive roller passes
Option 2b: Monitoring spatial percentage change (%Δ) in MVs	Not required	Achieving the %Δ-TV between consecutive passes over a defined percentage of an evaluation section
Option 3a: Empirically relating MVs to spot-test measurements	Based on correlation of MV to spot-test measurement: MV-TV = MV corresponding to contract QA-TV [a]	Achieving MV-TV over a set percentage of an evaluation section
Option 3b: Compaction curve based on MVs	MV-TV = mean MV when the increase in pass-to-pass mean MV in a calibration area ≤5%	
Option 3c: Empirically relating MVs to lab-determined properties (e.g., M_r)	Based on correlation of MV to lab soil property: MV-TV = MV corresponding to contract QA-TV[b]	

[a] Assumption is that QA-TV is spot-test-based measurement of density, modulus, etc.
[b] For example, a QA-TV based on M_r.

Acceptance testing for all specification options is performed on evaluation sections. Proper selection of evaluation sections that exhibit consistently distributed heterogeneity (or homogeneity) in both the longitudinal and transverse directions is critical to successful implementation of CCC specifications. Because roller MVs reflect both the compaction lift and sublift properties, it is also critical that the selected calibration area (for Option 3) exhibit the same degree of heterogeneity as the evaluation section.

Instrumented rollers used for CCC-based QA must meet minimum performance criteria. The documentation system must display and record roller MVs and their three-dimensional GPS position, vibration amplitude and frequency, and travel speed. Data must be easily accessible via the onboard computer and easily exportable for postprocessing and record keeping. Onboard computers should perform basic statistical analyses of roller MV data and operational parameters. The instrumented roller must demonstrate a minimum level of repeatability and reporting position accuracy.

9.8 Implementation of Specification Options: Case Studies

The recommended specification options were implemented during field testing in Colorado, Florida, North Carolina, and Minnesota. The case studies presented included compaction and roller-integrated CCC QA of granular subgrade, nongranular subgrade, granular subbase, and aggregate base material. Multiple specification options were investigated as part of each case study, thus enabling the direct comparison of option strengths and limitations. Compaction QA acceptance testing was conducted by the project QA personnel using criteria based on dry density requirements (γ_d-TV), moisture requirements (w-TV), and/or static proof rolling. For some case studies, comparisons with existing QA approaches were made.

Implementation of the recommended specifications allowed a direct comparison of roller-based CCC options with each other and with existing (i.e., random spot-test driven) QA practice. Specification Option 1 requires minimal changes to typical existing QA practices. Rather than selecting random points for spot testing, QA inspectors use the roller MV data map to identify the weakest area(s). Depending on the number of weakest areas identified, the frequency of spot testing may be increased compared to current practice. According to Option 1, if the roller-identified weakest area(s) meet acceptance, the rest of the evaluation section meets acceptance. However, given that testing locations are informed rather than random, requiring the weakest zones to meet 100% of the preexisting QA-TV may be more stringent than current random selection spot testing. Reducing the QA-TV may be more appropriate.

Specification Options 2(a, b) and 3(a, b, c) require modification to current QA practices in that spot-test measurements do not form the basis for QA. Rather, acceptance is granted based on roller MVs. In Option 2a, acceptance is granted when the percentage change in the mean roller MV from pass to pass falls below a preset threshold. In the case studies presented, Option 2a appeared to be less stringent than current practice. It may be desirable to implement Option 2a in conjunction

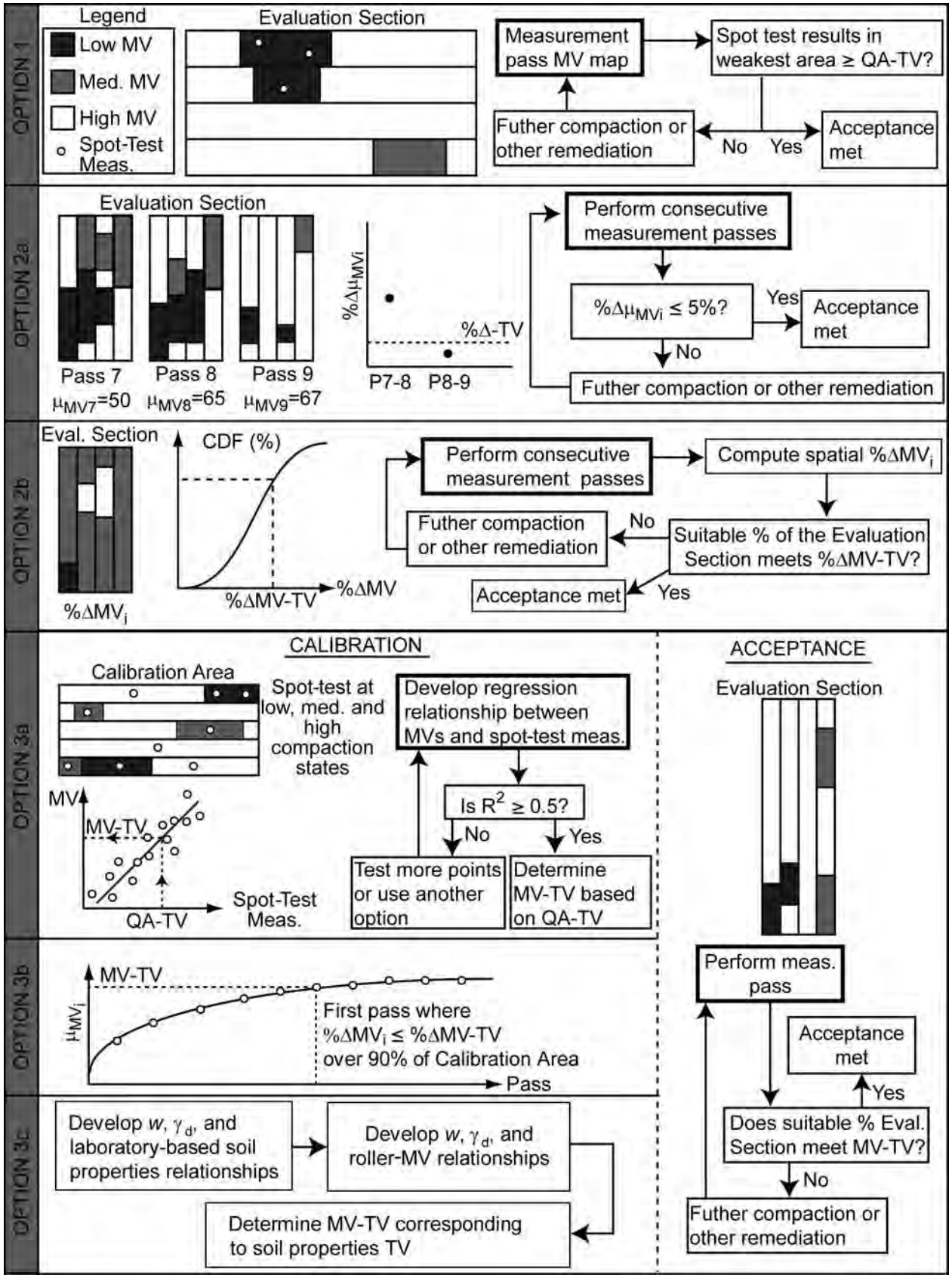

Figure 9.1. Summary of roller-integrated CCC specification options.

with Option 1 to improve reliability. Similarly, specification Option 2b uses the percentage change in spatial roller MV data as the basis for QA. One challenge associated with Option 2b is that the method of transforming roller MV data onto a fixed grid to allow spatial comparison is not trivial and reliable, and practical methods do not yet exist.

One major challenge to successfully implementing Specification Option 3(a, b, or c) is ensuring that the calibration area is representative of the evaluation section. Although using a roller MV data map of the evaluation section can aid in selecting an appropriate calibration area, this can be logistically challenging on a busy job site. Option 3(a, b, and c) requires a significant initial investment of time and careful, detailed analysis. This analysis is more complex than that currently required for QA, and it is easy to make errors. Accordingly, QA inspectors will need careful training to ensure that they are familiar with both the roller MV systems and the analysis required for the various options.

Construction traffic poses a challenge to implementing CCC-based QA. All of the options require careful, repeatable rolling patterns. Construction traffic, particularly haul trucks moving through the earthwork area, forced less than ideal roller pass patterns. Truck traffic often made it difficult to create uninterrupted and repeatable evaluation section roller MV maps. Developing the required correlations requires that haul trucks remain outside the calibration area once material has been placed and spot-test measurements are being performed. However, it is common for contractors to utilize haul truck traffic to compact soil. Similarly, it is not uncommon for haul trucks to enter the evaluation section in reverse, deposit their material, and then drive forward out of the area. This forces less than ideal roller pass patterns and creates hazardous conditions for personnel performing spot-test measurements.

Performing correlation studies in a designated full-width calibration area requires a change in how the earthwork contractor places material. To perform repeatable measurement passes in the evaluation section, the research team had to wait for the earthwork contractor to completely finish hauling and placing material in a section. The pace of the production earthwork placement and compaction frequently limited the time the research team was able to spend in the calibration area. Including the time needed to construct the calibration area, the correlations were developed in approximately 3 to 4 hours, although a time frame of 1 to 2 hours or less would be more consistent with production schedules. In typical production compaction practice, roller compactors are used throughout the hauling, placing, and grading operation. Careful planning and cooperation between the contractor and QA personnel, together with modifications in work flow, are critical for successful implementation of CCC-based QA.

References

Adam, D. (1996). "Flächendeckende Dynamische Verdichtungskontrolle (FDVK) mit Vibrationswalzen (Continuous Compaction Control with Vibratory Rollers)." Institut für Grundbau und Bodenmechanik, Dissertation, Technische Universität Wien.

Adam, D. (2007). "Roller Integrated Continuous Compaction Control (CCC) Technical Contractual Provisions & Recommendations." *Design and Construction of Pavements and Rail Tracks: Geotechnical Aspects and Processed Materials*, A.G. Correia, Y. Momoya, and F. Tatsuoka, eds., Taylor & Francis Group, London, UK, pp. 111–138.

Adam, D., and F. Kopf. (2004). "Operational Devices for Compaction Optimization and Quality Control (Continuous Compaction Control & Light Falling Weight Device)." *Proceedings of the International Seminar on Geotechnics in Pavement and Railway Design and Construction*, Athens, Greece, pp. 97–106.

Anderegg, R. (1998). "Nichtlineare Schwingungen bei dynamischen Bodenverdichtern (Nonlinear Vibrations with Dynamic Soil Compactors)." Dissertation. Diss. ETH Nr. 12419, Eidgenössische Technische Hochschule, Zürich.

Anderegg, R., and K. Kaufmann. (2004). "Intelligent Compaction with Vibratory Rollers." *Transportation Research Record 1868,* Transportation Research Board, Washington, D.C., pp. 124–134.

Anderson, D.G., and R.D. Woods. (1975). "Comparison of Field and Laboratory Shear Modulus." *Proceedings, In Situ Measurement of Soil Properties,*Vol. I, ASCE, Raleigh, N.C., pp. 69–92.

Andrei, D., M.W. Witczak, C.W. Schwartz, and J. Uzan. (2004). "Harmonized Resilient Modulus Test Method for Unbound Pavement Materials." *Journal of Transportation Research Record,* No. 1874, Transportation Research Board, Washington, D.C., pp. 29–37.

Bekker, M. G. (1969). *Introduction to Terrain-Vehicle Systems.* University of Michigan Press, Ann Arbor.

Brandl, H., and D. Adam. (1997). "Sophisticated Continuous Compaction Control of Soils and Granular Materials." *Proceedings 14th International Conference on Soil Mechanics and Foundation Engineering.* Hamburg, Germany, pp. 1–6.

Brandl, H., and D. Adam. (2000). "Flächendeckende Dynamische Verdichtungskontrolle (FDVK) mit Vibrationswalzen—Grundlagenforschung und praktische Anwendung (Continuous Compaction Control with Vibratory Rollers—Basic Research and Practical Application)." Schriftenreihe der Straßenforschung Heft 506, Forschungsvorhaben Nr. 3.147, Bundesministerium für Wirtschaftliche Angelegenheiten, Wien.

Brandl, H. (2001). "Compaction of Soil and Other Granular Material-Interactions." *Geotechnics for Roads, Rail Tracks and Earth Structures*, A.A. Balkema Publishers, Lisse/Abington/Exton (Pa)/Tokyo.

Brandl, H., F. Kopf, and D. Adam. (2005). "Continuous Compaction Control (CCC) with Differently Excited Rollers." Schriftenreihe der Straßenforschung Heft 553, Forschungsvorhaben Nr. 3.176, Bundesministerium für Verkehr, Innovation und Technologie, Wien.

Bräu, G., K. Hartman, and G. Pelz. (2004). "Flächendeckende Prufung der Verdichtung (FDVK)—Baupraktische Umsetzung und verfahrens-bezogene Verdichtungsanforderungen (CCC Testing of Compaction—Implementation in Construction Practice and Procedure-Related Compaction Specifications)." Lehrstuhl und Prüfamt für Grundbau, Bodenmechanik und Felsmechanik der Technischen Universitat München, Heft 897, München.

Clark, I., and W. Harper. (2002). *Practical Geostatistics 2000.* Ecosse North America LLC, Columbus, Ohio.

D'Appolonia, D.J., R.V. Whitman, and E.D'Appolonia. (1969). "Sand Compaction with Vibratory Rollers." *Journal of Soil Mechanics & Foundations Division*, ASCE, Vol. 95, pp. 263–284.

Daleiden, J.F., B.M. Killingsworth, A.L. Simpson, and R.A. Zamora. (1994). "Analysis of Procedures for Establishing In Situ Subgrade Moduli." *Transportation Research Record,* Vol. 1462, pp. 102–107.

Davis, F.J. (1953). "Quality Control of Earth Embankments." *Proceedings 3rd International Conference on Soil Mechanics and Foundation Engineering*, Vol. I, August 16–27, Zurich.

Dynatest. (2004). *Keros Portable FWD—Instruction Manual for Use and Maintenance.* Issue No. 010704, Denmark.

Facas, N.W., and M.A. Mooney. (2010). "Position Reporting of Data from Intelligent Compaction Rollers." *Journal of Testing and Evaluation*, ASTM, Vol. 38, No. 1, 1-6.

Facas, N.W., M.A. Mooney, and R. Furrer. (2010). "Anisotropy in the Spatial Distribution of Roller-Measured Soil Stiffness." *International Journal of Geomechanics*, ASCE, Vol. 10, No. 4, 129-135.

Floss, R., N. Gruber, and J. Obermayer. (1983). "A Dynamical Test Method for Continuous Compaction Control." *Proceedings 8th European Conference on Soil Mechanics and Foundation Engineering,* H. G. Rathmayer and K. Saari, eds., May, Helsinki, pp. 25–30.

Floss, R., G. Bräu, M. Gahbauer, N. Gruber, and J. Obermayer. (1991). "Dynamische Verdichtungsprüfung bei Erd-und Straßenbauten (Dynamic Compaction Testing in Earth and Road Construction)." Prüfamt für Grundbau, Boden-und Felsmechanik Technische Universität München, Heft 612. München.

Forssblad, L. (1980). "Compaction Meter on Vibrating Rollers for Improved Compaction Control." *Proceedings of the International Conference on Compaction*, Vol. II, Paris, pp. 541–546.

Freund, R., R. Littell, and L. Creighton. (2003). *Regression Using JMP®.* SAS Institute and Wiley, Cary, NC.

Grabe, J. (1994). "Spatial Variation of Soil Stiffness: Spectral Density Approach." *Soil Dynamics and Earthquake Engineering*, Vol. 13, Great Britain, pp. 25–29.

Griffiths, D.V., G.A. Fenton, and N. Manoharan. (2006). "Undrained Bearing Capacity of Two-Strip Footings on Spatially Random Soil." *International Journal of Geomech*anics, Vol. 6, No. 6, pp. 421–427.

Hartman, K. (2002). "Untersuchung zur Prognose von Anforderungswerten an die Beschleunigungsmesswerte der FDVK—Methode (Research Towards Prediction of Specification Values (Measurement Values) of CCC Methods Based on the Acceleration Measurement Values)." Dissertation. Lehrsthul und Prüfamt für Grundbau, Bodenmechanick und Felsmechanick der Technischen Universität München, Schriftenreihe Heft 34, München.

Isaaks, E.H., and R.M. Srivastava. (1989). *An Introduction to Applied Geostatistics.* Oxford University Press, New York.

Ishihara, K. (1996). *Soil Behavior in Earthquake Geotechnics.* Clarendon Press, Oxford.

ISSMGE. (2005). *Roller-Integrated Continuous Compaction Control (CCC), Technical Contractual Provisions—Recommendations.* International Society for Soil Mechanics and Geotechnical Engineering: Geotechnics for Pavements in Transportation Infrastructure.

Kopf, F., and P. Erdmann. (2005). "Numerische Untersuchunsen der Flachendecker Dynamischer Verdichtungskontrolle (Numerical Analysis of Continuous Compaction Control)." Osterreichische Ingenieus-und Architekten-Zeitschrift (OIAZ), Vol. 150, No. 4–5, pp. 126–143.

Kröber, W. (1988). "Untersuchung der Dynamischen Vorgäge bei der Vibrationsverdichtung von Böden (Analysis of Dynamic Operation During the Vibrational Compaction of Soil)." Dissertation. Lehrstuhl und Prufamt fur Grundbau, Bodenmechanik und Felsmechanik der Technischen Universität, Munchen, Schriftenreihe Heft 11, Munchen.

Kröber, W., R. Floss, and W. Wallrath. (2001). "Dynamic Soil Stiffness as Quality Criterion for Soil Compaction." *Geotechnics for Roads, Rail Tracks and Earth Structures.* A.A. Balkema Publishers, Lisse/Abingdon/Exton (Pa)/Tokyo.

Lundberg, G. (1939). "Elastische Berührung Zweier Halbräume (Elastic Contact Between Two Half Spaces)." *Forschung auf dem Gebiete des Ingenieurwesens*, Vol. 10, pp. 201–211, Göteborg.

Machet, J.M. (1980). "Compactor-Mounted Control Devices." *Proceedings, International Conference on Compaction*, Vol. II, Paris, pp. 577–581.

Mn/DOT Specification 2106. (2007). "Excavation and Embankment—Quality Compaction by IC, LWD, & Test Rolling (Pilot Specification for Embankment Grading Materials)." Minnesota Department of Transportation, 11 pp.

Mooney, M. A., P. B. Gorman, E. Farouk, J. N. Gonzalez, and A. S. Akanda (2003). "Exploring Vibration Based Intelligent Soil Compaction." *Oklahoma Department of Transportation.* Project No. 2146, Final Report, 250 pp.

Mooney, M.A., P.B. Gorman, and J.N. Gonzalez. (2005). "Vibration Based Health Monitoring During Earthwork Construction." *Journal of Structural Health Monitoring*, Vol. 2, No. 4, pp. 137–152.

Mooney, M.A., and D. Adam. (2007). "Vibratory Roller Integrated Measurement of Earthwork Compaction: An Overview." *Proceedings FMGM2007—International Symposium on Field Measurements in Geomechanics*, September 24-27, Boston.

Mooney, M.A., and R.V. Rinehart. (2007). "Field Monitoring of Roller Vibration During Compaction of Subgrade Soil." *Journal of Geotechnical and Geoenvironmental Engineering*, ASCE, Vol. 133, No. 3, pp. 257–265.

Mooney, M. A., and P. K. Miller. (2008). "Analysis of Light Falling Weight Deflectometer Test Based on In-Situ Stress and Strain Response." *Journal of Geotechnical and Geoenvironmental Engineering*, ASCE, Vol. 135, No. 2, pp. 199–208.

Mooney, M.A., and R.V. Rinehart. (2009). "In-Situ Soil Response to Vibratory Loading and Its Relationship to Roller-Measured Soil Stiffness." *Journal of Geotechnical and Geoenvironmental Engineering*, ASCE, Vol. 135, No. 8, pp. 1022–1031.

Nazarian, S., J. Rojas, R. Pezo, D. Yuan, I. Abdallah, and T. Scullion, T. (1998). "Relating Laboratory and Field Moduli of Texas Base Materials." *Transportation Research Record,* 1639, pp. 1–11.

Odemark, N. (1949). "Investigations as to the elastic properties of soils and design of pavements according to the theory of elasticity." *Statens Väginstitut, Mitteilung No. 77*, Stockholm, Sweden.

Ott, R.L., and M. Longnecker. (2001). *An Introduction to Statistical Methods and Data Analysis,* 5th Ed., Wadsworth Group, Pacific Grove, Calif.

Petersen, L. (2005). *Continuous Compaction Control MnROAD Demonstration.* Final report submitted to Mn/DOT, Report No. MN/RC-2005-07.

Petersen, D., M. Erickson, R. Roberson, and J. Siekmeier. (2007). "Intelligent Soil Compaction: Geostatistical Data Analysis and Construction Specifications." Transportation Research Board 86th Annual Meeting, Washington, D.C., Paper #07-2858, CD-ROM.

Ping, W.V., M. Leonard, Z. Yang, and S. Putcha. (2002). "Laboratory Simulation of Field Compaction Characteristics on Sandy Soils." *Transportation Research Record,* Vol. 1808, pp. 84–95.

Preisig, M., R. Noesberger, M. Caprez, P. Amann, and R. Anderegg. (2006). *Flächendeckende Verdichtungskontrolle (FDVK) mittels bodenmechanischer Materialkenngrössen (Continuous Compaction Control Based on Geotechnical Parameters)*, Report VSS 2000/353, Institute for Geotechnik, Federal Institute of Technology ETH, Zurich.

Quibel, A. (1980). "Le comportement vibratoire: Trait d'union entre le choix des parameters et l'efficacite des rouleaux vibrants (The Vibratory Behavior: Interactions Between Vibration Parameters and the Effectiveness of Vibratory Rollers)." *Proceedings of the International Conference on Compaction, Session VII Compaction Equipment, ENPC, LCPC*, Paris.

Rahman, F., M. Hossain, M. Hunt, and S. Romanoschi. (2008). "Soil Stiffness Evaluation for Compaction Control of Cohesionless Embankments." *Geotechnical Testing Journal*, Vol. 31, No. 5, pp. 1–10.

Rinehart, R.V., M.A. Mooney, and J.R. Berger. (2008). "In-Ground Stress-Strain Beneath Center and Edge of Vibratory Roller Compactor." *Advances in Transportation Geotechnics: Proceedings 1st International Conference on Transportation Geotechnics*, Nottingham, U.K., Aug. 25–27, pp. 737–741.

Rinehart, R.V., and M.A. Mooney. (2008). "Instrumentation of a Roller Compactor to Monitor Vibration Behavior During Earthwork Compaction." *Automation in Construction*, No. 17, pp. 144–150.

Rinehart, R.V., J.R. Berger, and M.A. Mooney. (2009). "Comparison of Stress States and Paths: Vibratory Roller Measures Soil Stiffness and Resilient Modulus Testing." *Transportation Research Record 2116, 8-15.*

Rinehart, R.V., and M.A. Mooney. (2009a). "Measurement of Roller Compactor Induced Triaxial Soil Stresses and Strains." *Geotechnical Testing Journal*, ASTM, Vol. 32, No. 4, pp. 347–357.

Rinehart, R.V., and M.A. Mooney. (2009b). "Measurement Depth of Vibratory Roller-Measured Soil Stiffness." *Geotechnique*, Vol. 59, No. 7, pp. 609–619.

Rodhe, G.T., and T. Scullion. (1990). *MODULUS 4.0: Expansion and Validation of the MODULUS Backcalculation System.* Research Report 1123-3, Texas Transportation Institute, Texas A&M University, College Station.

Samaras, A.A., R. Lamm, and J. Treiterer. (1991). "Application of Continuous Dynamic Compaction Control for Earthworks in Railroad Construction." *Transportation Research Record,* Vol. 1309, pp. 42–46.

Santha, B.L. (1994). "Resilient Modulus of Subgrade Soils: Comparison of Two Constitutive Equations." *Transportation Research Record,* Vol. 1462, pp. 79–90.

Scherocman, J., S. Rakowski, and K. Uchiyama. (2007). "Intelligent Compaction, Does It Exist?" *Proceedings of the Annual Conference—Canadian Technical Asphalt Association*, No. 52, pp. 373–398.

Sherman, G.B., R.O. Watkings, and R. Prysock. (1966). *A Statistical Analysis of Embankment Compaction.* California Department of Public Works, Division of Highways, Sacramento.

Thompson, M.J., and D.J. White. (2007). "Field Calibration and Spatial Analysis of Compaction Monitoring Technology Measurements." *Transportation Research Record,* Vol. 2004, pp. 69–79.

Thompson, M., D. White, H. Gieselman, and J. Siekmeier. (2008). "Variable Feedback Control Intelligent Compaction to Evaluate Subgrade and Granular Pavement Layers—Field Study at Minnesota US 14." Transportation Research Board 87th Annual Meeting, Washington, D.C., Paper #08-0275, CD-ROM.

Thompson, M., and D. White. (2008). "Estimating Compaction of Cohesive Soils from Machine Drive Power." *Journal of Geotechnical and Geoenvironmental Engineering,* ASCE, Vol. 134, No. 12, pp. 1771–1777.

Thurner, H., and Å. Sandström. (1980). "A New Device for Instant Compaction Control." *Proceedings of the International Conference on Compaction*, Vol. II, Paris.

Timoshenko, S.P., and J.N. Goodier. (1951). *Theory of Elasticity*. McGraw-Hill, New York.

Ting, T.C.T. (1996). *Anisotropic Elasticity*. Oxford University Press, New York.

Uzan, J. (1985). "Characterization of Granular Materials." *Transportation Research Record*, Vol. 1022, pp. 52–59.

Van Susante, P.J., and M.A. Mooney. (2008). "Capturing Vibratory Roller Compactor Behavior Through Lumped Parameter Modeling." *Journal of Engineering Mechanics*, ASCE, Vol. 134, No. 8, pp. 684–693.

Vennapusa, P., and D.J. White. (2009). "Comparison of Light Weight Deflectometer Measurements for Pavement Foundation Materials." *Geotechnical Testing Journal*, Vol. 32, No. 3, pp. 239–251.

Vennapusa, P., D. J. White, and M. Morris. (2009). "Geostatistical Analysis of Spatially Referenced Roller-Integrated Compaction Measurements." *Journal of Geotechnical and Geoenvironmental Engineering*, ASCE, Vol. 136, No. 6, 813-822.

White, D.J., T. Rupnow, and H. Ceylan. (2004). "Influence of Subgrade/Subbase Nonuniformity on Pavement Performance." *Proceedings, Geo-Trans 2004—Geotechnical Engineering for Transportation Projects*, Geotechnical Special Publication No. 126, ASCE, pp. 1058–1065.

White, D.J., M.D. Morris, and M.J. Thompson. (2006). "Power-Based Compaction Monitoring Using Vibratory Pad Foot Roller." *Proceedings of GeoCongress 2006: Geotechnical Engineering in the Information Technology Age*, February, Atlanta, CD-ROM.

White, D., and M. Thompson. (2008). "Relationships Between In Situ and Roller-Integrated Compaction Measurements for Granular Soils." *Journal of Geotechnical and Geoenvironmental Engineering*, ASCE, Vol. 134, No. 12, pp. 1763–1770.

White, D., M. Thompson, and P. Vennapusa. (2007). *Field Validation of Intelligent Compaction Monitoring Technology for Unbound Materials.* Report No. MN/RC 2007-10, Minnesota Department of Transportation, St. Paul, MN.

White, D., M. Thompson, and P. Vennapusa. (2008a). *Field Validation of Intelligent Compaction Monitoring Technology for Unbound Material.* Minnesota Department of Transportation, St. Paul, pp. 123–164.

White, D., M. Thompson, P. Vennapusa, and J. Siekmeier. (2008b). "Implementing Intelligent Compaction Specifications on Minnesota TH64: Synopsis of Measurement Values, Data Management and Geostatistical Analysis." *Transportation Research Record 2045, 1-9.*

White, D., P. Vennapusa, and H. Gieselman, H. (2008c). "Roller-Integrated Compaction Monitoring Technology: Field Evaluation, Spatial Visualization, and Specifications." *Proceedings, 12th International Conference of the International Association for Computer Methods and Advances in Geomechanics (IACMAG),* October 1–6, Goa, India.

Witczak, M.W., and J. Uzan. (1988). *The Universal Airport Design System, Report I of IV: Granular Material Characterization.* Department of Civil Engineering, University of Maryland, College Park.

Yoo, T.S., and E.T. Selig. (1979). "Dynamics of Vibratory-Roller Compaction." *Journal of the Geotechnical Engineering Division*, ASCE, Vol. 105, No. GT10, pp. 1211–1231.

Yoo, T.S., and E.T. Selig. (1980). "New Concepts for Vibratory Compaction of Soil." *Proceedings of the International Conference on Compaction, Vol. II*, Paris.

Zorn, G. (2003). *Operating Manual: Light Drop Weight Tester ZFG2000.* Stendal, Germany.

Glossary

Abbreviations and Acronyms

AASHTO	American Association of State Highway and Transportation Officials
ACE	Ammann Compaction Expert
AFC	Automatic Feedback Control
ASTM	American Society for Testing and Materials
BCM	Bomag Compaction Meter
BV	Bouncing Value
CBR	California Bearing Ratio
CCC	Continuous Compaction Control
CCV	Continuous Compaction Value (reported by Sakai)
CIV	Clegg Impact Value
CMV	Compaction Meter Value
CO	Colorado
COV	Coefficient of Variation
CSM	Colorado School of Mines
DCA	Dynapac Compaction Analyzer
DCO	Dynapac Compaction Optimizer
DCP	Dynamic Cone Penetrometer
DGPS	Differential Global Positioning System
DOT	Department of Transportation
E	East
EPC	Earth Pressure Cell
F	Fail
FL	Florida
FWD	Falling Weight Deflectometer
GIS	Geographic Information System
GPS	Global Positioning System
IC	Intelligent Compaction
ISSMGE	International Society for Soil Mechanics and Geotechnical Engineering
LVDT	Linear Voltage Displacement Transducer
LWD	Light Weight Deflectometer
MD	Maryland
MDP	Machine Drive Power (Caterpillar MV)
M-E	Mechanistic-Empirical
MN	Minnesota
Mn/DOT	Minnesota Department of Transportation
MV	Measurement Value
N	North
NC	North Carolina
NCHRP	National Cooperative Highway Research Program
NF	North Forward
NMEA	National Marine Electronics Association
P	Pass
PC	Personal Computer
PD	Pad-foot Drum
PJK	A specific GPS data format
PLT	Plate Load Test
PR	Proof Roll
QA	Quality Assurance
QC	Quality Control
RMV	Resonance Meter Value
RTK	Real-Time Kinematic
S	South
SD	Smooth Drum
SF	South Forward
ST	Shelby Tube
TB	Test Bed
TV	Target Value
USB	Universal Serial Bus
USCS	Unified Soil Classification System
W	West
WGS	World Geodetic System

Symbols (English)

a	Machine acceleration (used in MDP calculation)
A	Theoretical vibration amplitude, $m_0 e_0 / m_d$
A_{max}	Maximum eccentric force levels
A_Ω	Frequency domain amplitude
$A_{2\Omega}$	2nd harmonic of the vertical drum acceleration frequency domain amplitude
b	Drum-soil contact width
b	Machine internal loss coefficients used in MDP calculation
b	Regression coefficient
c	Constant used to calculate CMV (usually 300)
CCV_{CSM}	Continuous Compaction Value computed by CSM
$CIV_{4.5\text{-kg}}$	Clegg Impact Value using 4.5-kg drop weight
$CIV_{20\text{-kg}}$	Clegg Impact Value using 20-kg drop weight
CMV_C	Compaction Meter Value reported by Caterpillar
CMV_D	Compaction Meter Value reported by Dynapac
CMV_{CSM}	Compaction Meter Value computed by CSM
COV	Coefficient of variation
E	Young's modulus (E-modulus)
E_{FWD}	Modulus from FWD
$E_{FWD\text{-}D3}$	Modulus from Dyntest FWD device with 300-mm plate
E_{LWD}	General modulus from LWD
$E_{LWD\text{-}K2}$	Modulus from Keros LWD device with 200-mm plate
$E_{LWD\text{-}K3}$	Modulus from Keros LWD device with 300-mm plate
$E_{LWD\text{-}P3}$	Modulus from Prima LWD device with 300-mm plate
$E_{LWD\text{-}Z2}$	Modulus from Zorn LWD device with 200-mm plate
$E_{LWD\text{-}Z3}$	Modulus from Zorn LWD device with 300-mm plate
E_{LWD}-TV	LWD modulus target value
E_{vib}	Vibration modulus, reported by Bomag
E_{V1}	E-modulus from the first loading loop in the static plate load test
E_{V2}	E-modulus from the second loading loop in the static plate load test
f	Roller excitation frequency (Hz)
f	Shape factor
F_{ecc}	Eccentric force, $m_0 e_0 \Omega^2$
F_{ev}	Vertical component of F_{ecc}
f_{GPS}	Frequency of GPS data
f_{MV}	Frequency of MVs to onboard computer
f_{report}	Frequency of reported MVs
F_s	Force transmitted to soil (also called drum/soil contact force)
$F_{s(max)}$	Maximum contact force setting
$F(t)$	Centrifugal force
g	Acceleration of gravity
H	Layer thickness
H_c	Critical value of layer thickness corresponding to the roller measurement depth
k_1-k_3	Coefficients for stress-dependent soil modulus model
k_s	Soil stiffness reported by Ammann (also called k_B in European figures and literature)
$k_{s\text{-}CSM}$	Soil stiffness calculated from independent instrumentation
k_{SSG}	Stiffness from soil stiffness gauge
K	Coefficient of lateral earth pressure
M	Vertical dynamic deformation modulus
m	Machine internal loss coefficients used in MDP calculation
m	Slope of loading line in p'-q space
MAX-TV	Maximum arget value
m_d	Mass of roller drum
ME	Mean MV
ME-TV	ME target value
M_{e1}	Equivalent to E_{V2}
M_{e2}	Equivalent to E_{V1}
m_f	Mass of roller frame
MIN-TV	Minimum target value
M_L	Tangent modulus of the loading portion of the in situ σ_z-ε_z curve
M_r	Resilient modulus
M_r-TV	Target M_r
M_S	Secant modulus from zero in situ σ_z-ε_z through the point of maximum ε_z
MV_i	MV for pass i
MV-TV	Measurement value target value
$m_o e_o$	Eccentric mass moment
n	Number of observations
p	Number of regression parameters
p	Mean normal stress
p_a	Atmospheric pressure
P_a	Atmospheric pressure
P_g	Gross power (used in MDP calculation)
q	Deviator stress
r	Correlation coefficient
R	Drum radius
R	EPC stress registration ratio
R^2	Correlation coefficient

R^2_{adj}	Adjusted R^2
RC-TV	Relative compaction target value
t_{MV}	Time window over which one MV is collected
v	Roller speed
V	Roller velocity (used in MDP calculation)
VIF	Variance inflation factors
W	Roller weight (used in MDP calculation)
w	Soil moisture content
w_{opt}	Optimum moisture content
w-TV	Moisture TV
x	Position coordinate of moving drum
x_{error}	Horizontal position accuracy
x_{MV}	Spatial window in x direction over which one MV is collected
y	Location in y direction
y_{MV}	Spatial window in y direction over which one MV is collected
z	Spatial coordinate (elevation)
z_d	Vertical drum displacement
z_d	Vertical drum acceleration
$z_{d(max)}$	Maximum vertical drum displacement
z_{error}	Vertical position accuracy
%Δ	Percentage change
$\%\Delta MV_i$	Percentage difference in MV between pass i and i-1
%Δ-TV	Percentage change target value
%Area-TV	Percentage area target value

Symbols (Greek)

α	Point measurement value
α	Vector angle
β	Underlying layer roller MV
Δk_s	Spatial percent change in k_s
Δx	Spatial resolution of MVs in x direction
Δy	Spatial resolution of MVs in y direction
$\Delta\mu k_s$	Change in mean k_s
ε_p	Plastic strain
ε_x	Normal strain in the x direction
ε_y	Normal strain in the y direction
ε_z	Normal strain in the z direction
$\varepsilon_{z,max}$	Maximum value ε_z profile with depth (at or near the surface)
$\varepsilon_{z,peak}$	Maximum value of ε_z recorded by an in situ sensor (when roller is directly over sensor)
ϕ	Phase lag between F_{ecc} and z_d
γ	Lift thickness
γ_d	Soil dry unit weight
γ_d-TV	Dry unit weight requirement
γ_{dmax}	Maximum dry unit weight
$\gamma(h)$	Semi-variogram function
μ	Mean value
ν	Poisson's ratio
θ	Slope angle (used in MDP calculation)
θ	Sum of principal stresses, or bulk stress
θ	Angle between two eccentric masses
σ	Standard deviation
$\sigma_{1\text{-}3}$	Principal stresses
σ_c	Confining stress
σ_d	Deviator stress
σ_x	Normal total stress in the x direction
σ_y	Normal total stress in the y direction
σ_z	Normal total stress in the z direction
$\sigma_{z,peak}$	Maximum value of σ_z recorded by an in situ sensor (when roller is directly over sensor)
$\sigma_{z,max}$	Maximum value σ_z profile with depth (at or near the surface)
$\sigma_{\%\Delta MV}$	Standard deviation of percentage difference
τ_{oct}	Octahedral shear stress
Ω	Roller excitation frequency (rad/s)
μk_s	Mean k_s
μ_{MV_i}	Mean MV for pass i
$\mu_{\%\Delta MV}$	Mean of percentage difference
$\%\Delta\mu_{MV_i}$	Percentage change in the mean MV for pass i

Appendixes A Through D

Appendixes to the contractor's final report for NCHRP Project 21-09 are not published herein but are available on the TRB website at http://www.trb.org/Main/Blurbs/164279.aspx. The appendix titles are the following:

- Appendix A: Supplement to Chapter 1
- Appendix B: Supplement to Chapter 3
- Appendix C: Supplement to Chapter 6
- Appendix D: Supplement to Chapter 8

Abbreviations and acronyms used without definitions in TRB publications:

AAAE	American Association of Airport Executives
AASHO	American Association of State Highway Officials
AASHTO	American Association of State Highway and Transportation Officials
ACI–NA	Airports Council International–North America
ACRP	Airport Cooperative Research Program
ADA	Americans with Disabilities Act
APTA	American Public Transportation Association
ASCE	American Society of Civil Engineers
ASME	American Society of Mechanical Engineers
ASTM	American Society for Testing and Materials
ATA	Air Transport Association
ATA	American Trucking Associations
CTAA	Community Transportation Association of America
CTBSSP	Commercial Truck and Bus Safety Synthesis Program
DHS	Department of Homeland Security
DOE	Department of Energy
EPA	Environmental Protection Agency
FAA	Federal Aviation Administration
FHWA	Federal Highway Administration
FMCSA	Federal Motor Carrier Safety Administration
FRA	Federal Railroad Administration
FTA	Federal Transit Administration
HMCRP	Hazardous Materials Cooperative Research Program
IEEE	Institute of Electrical and Electronics Engineers
ISTEA	Intermodal Surface Transportation Efficiency Act of 1991
ITE	Institute of Transportation Engineers
NASA	National Aeronautics and Space Administration
NASAO	National Association of State Aviation Officials
NCFRP	National Cooperative Freight Research Program
NCHRP	National Cooperative Highway Research Program
NHTSA	National Highway Traffic Safety Administration
NTSB	National Transportation Safety Board
PHMSA	Pipeline and Hazardous Materials Safety Administration
RITA	Research and Innovative Technology Administration
SAE	Society of Automotive Engineers
SAFETEA-LU	Safe, Accountable, Flexible, Efficient Transportation Equity Act: A Legacy for Users (2005)
TCRP	Transit Cooperative Research Program
TEA-21	Transportation Equity Act for the 21st Century (1998)
TRB	Transportation Research Board
TSA	Transportation Security Administration
U.S.DOT	United States Department of Transportation